Modelling plasma cell differentiation to risk stratify secondary antibody deficiencies for immunoglobulin replacement therapy

Eleanor O'Callaghan

Submitted in accordance with the requirements for the Degree of Doctor of Philosophy

The University of Leeds

Faculty of Medicine and Health

January 2025

Declaration

The candidate confirms that the work submitted is her own and that appropriate credit has been given where reference has been made to the work of others.

This copy has been supplied on the understanding that it is copyright material and that no quotation from the thesis may be published without proper acknowledgement.

The right of Eleanor O'Callaghan to be identified as Author of this work has been asserted by her in accordance with the Copyright, Designs and Patents Act 1988.

Acknowledgments

Firstly, I extend my deepest gratitude to my supervisors, Professor Sinisa Savic and Dr Gina Doody, for their unwavering guidance, invaluable support, and for giving me the opportunity to be part of such fascinating research. Their mentorship has been pivotal throughout my PhD journey. I am also grateful to CSL for their funding, without which this research would not have been possible.

A special thanks to the entire Doody/Tooze lab group for fostering a collaborative and inspiring environment. The insightful discussions, suggestions during lab meetings, and journal clubs have been incredibly helpful. I am especially thankful to Sophie Stephenson for her expertise in B-cell differentiation and her generous willingness to dedicate so much time to guide me. Her patience and kindness have made challenging moments much more manageable. To the rest of the group, thank you not only for your scientific input but also for becoming such great friends during this journey.

I would also like to express heartfelt thanks to my family - my mum, dad, brother, and grandad - whose encouragement and belief in me gave me the strength to move to Leeds and pursue this PhD. To my partner Ollie, thank you for your endless pep talks and for always reminding me to believe in myself.

Lastly, I dedicate this work to my late Momma, who inspired my passion for immunology – her memory and influence are at the heart of everything I do and hope to achieve in the future.

Abstract

B-cells of patients with secondary and primary antibody deficiency often exhibit defects in maturation, activation, or survival, which may lead to impaired immune responses after SARS-CoV-2 vaccination. These defects contribute to vaccine non-responsiveness in some patients. The underlying mechanisms and the feasibility of pre-vaccination risk stratification remain unclear. To investigate B-cell intrinsic differentiation capacities in a heterogeneous cohort of vaccine-responding and non-responding antibody-deficient patients, an *in vitro* plasma cell differentiation model has been utilised. Such an approach may also be useful in assessing their suitability for immunoglobulin replacement therapy (IgRT).

B-cells from participants enrolled in the COV-AD study, taken after their fourth SARS-CoV-2 vaccine dose, were isolated and induced to differentiate into plasma cells. B-cell functionality at critical differentiation stages was assessed using flow cytometry, ELISA, BCR analysis, and RNA sequencing. The study revealed distinct differences in B-cell differentiation between vaccine responders and non-responders. Non-responders (n=15) and a subset of responders (n=10/35) exhibited significantly reduced or absent expression of the BAFF-R survival receptor. Immunoglobulin heavy chain sequencing showed no significant differences in BCR profiles between responders and non-responders. Both patient groups displayed reduced intracellular and secreted IgG and IgA expression compared to healthy controls.

Atypical B-cell differentiation profiles in antibody deficient patients, particularly reduced BAFF-R expression, may underpin impaired SARS-CoV-2 vaccine responses. The identification of BAFF-R as a critical survival receptor emphasises its potential as a biomarker for risk stratification. Integrating BAFF-R profiling into clinical workflows could help identify patients at risk of poor immune outcomes, enabling tailored therapeutic interventions. Refining this *in vitro* plasma cell differentiation model to allow for faster assessments, focusing on BAFF-R levels and other key markers, will enhance its feasibility as a practical tool for pre-IgRT risk stratification in clinical settings.

Table of Contents

Table of Contents

Table of Figures

Chapter 1

Chapter 2

Chapter 3

Chapter 4

Chapter 5

Chapter 6

Table of tables

Chapter 1

Chapter 2

Chapter 4

Chapter 5

Chapter 1- Introduction

1.1 Humoral immunity: protection provided by B-cells

Immune responses can largely be classified into two categories: innate and acquired. Whilst overlaps between the two exist, it is generally true that innate responses account for the initial, rapid, and non-specific response to antigen that recognise pattern/danger recognition receptors and primarily act through phagocytosis. Conversely, acquired immunity involves a slower, highly specific response that develops overtime and relies on lymphocyte activation and the formation of immunological memory for long-term protection.

Humoral immunity is deemed the highly specific acquired or adaptive response to antigen and relies on T and B lymphocytes to destroy extracellular microorganisms through the production of antibodies (Marshall *et al.,* 2018). T and B-cells are constantly generated in the bone marrow (BM). Whilst precursor T cells migrate to the thymus following successful BM generation, B-cells complete maturation in secondary lymphoid tissues (i.e. lymph nodes, spleen and tonsils). Prior to exiting the bone marrow, developing B-cells undergo highly regulated processes that sequentially trigger B-cell receptor (BCR) assembly, expression and signalling to result in functional B-cell production (Cano and Lopera, 2013).

The BM niche is highly specialised. The proximity of stromal cells to developing immunocytes elicits the formation of adhesive contacts and provides cytokines and chemokines required for early differentiation and proliferation (Carsetti, 2000). This environment enables haemopoietic stem cells (HSCs) to differentiate into myeloid

progenitor cells (MPPs) or lymphoid progenitor cells (LPCs), whereby the latter may give rise to lymphocytes such as pro-B-cells (Figure 1.1).

1.2 Introducing diversity

A successful adaptive immune response requires the generation of a diverse array of antigen receptors. In B-cells, such diversity is attributed to three regulated processes known as V (D) J recombination, somatic hypermutation (SHM) and class switch recombination (CSR) (Chi, Li and Qui, 2020).

1.2.1 V (D) J recombination

It is at the pro-B-cell stage in the BM that B-cell progenitors undergo rearrangement of their immunoglobulin heavy chain (IgH) genes via the process of V (D) J recombination. This mechanism encompasses the multiple variable (V), diversity (D) and joining (J) gene segments within the IgH locus (Nguyen *et al.,* 2016), and involves double-stranded DNA breaks being made and subsequently repaired. The initial step in V (D) J recombination is the recognition of specific recombination signal sequences (RSSs) located at the boundaries of the V, D and J gene segments within the IgH locus by a recombinase complex consisting of the recombination-activating gene (RAG-1 and RAG-2) enzymes (Schatz, Oettinger and Baltimore, 1989; Oettinger *et al.,* 1990). The binding of the RAG complex to DNA triggers a conformational change to RSS sites, resulting in discrete DNA single-stranded breaks between each coding region and its RSS. This initial DNA breakage creates a 3'-OH group that facilitates a transesterification reaction to generate hairpins via the formation of double stranded breaks between the V, D and J segments that flank RSS sites (Bassing, Swat and Alt., 2002; Christie, Fijen and Rothenberg, 2022).

Following successful cleavage, other proteins in the recombinase complex trigger the subsequent double-stranded break repair (DSBR) process via nonhomologous end joining (NHEJ), which is an inexact process that aids further diversification. In NHEJ, exposed DNA ends are recognised by the Ku protein which itself interacts with the DNA-dependent protein kinase catalytic subunit to form a holoenzyme that scaffolds other reparation proteins (Fell and Schild-Poulter 2015; Yue *et al.,* 2020). The recruitment of other scaffolding proteins results in the bridging of DNA ends via the process of synapsis (Graham, Walter and Loparo 2016). DNA ends are then ligated, and the process of V(D)J recombination is complete (Figure 1.2).

Successful heavy chain production enforces allelic exclusion, a process resulting in the recognition of a single antigen via the expression of only one allele, and triggers μ chain expression to denote pre-B-cell production (Alt *et al*., 1984; Murphy, Weaver and Janeway, 2017). μ expression intersects with lambda-5 and VpreB to form a surrogate light chain in a transient complex called the pre-BCR that signals via Ig-α/β and Btk (Tsubata and Reth, 1999; Winkler and Mårtensson., 2018). Signalling results in development of large pre-B-cells which are capable of proliferation. At this stage, surrogate light chain expression is downregulated and the μ heavy chain is expressed in the cytoplasm. This results in RAG1/2 recombinase re-expression that triggers light-chain gene rearrangement. Successful light-chain gene assembly results in an immature B-cell, with an intact BCR, that expresses IgM at the cell surface (Collins and Watson, 2018; Sims *et al.,* 2005). Immature B-cells can migrate to secondary lymphoid organs for additional maturation and differentiation.

The additional incorporation of immunological diversity through CSR and SHM is introduced later in B-cell differentiation and will be discussed in section 1.4.1.

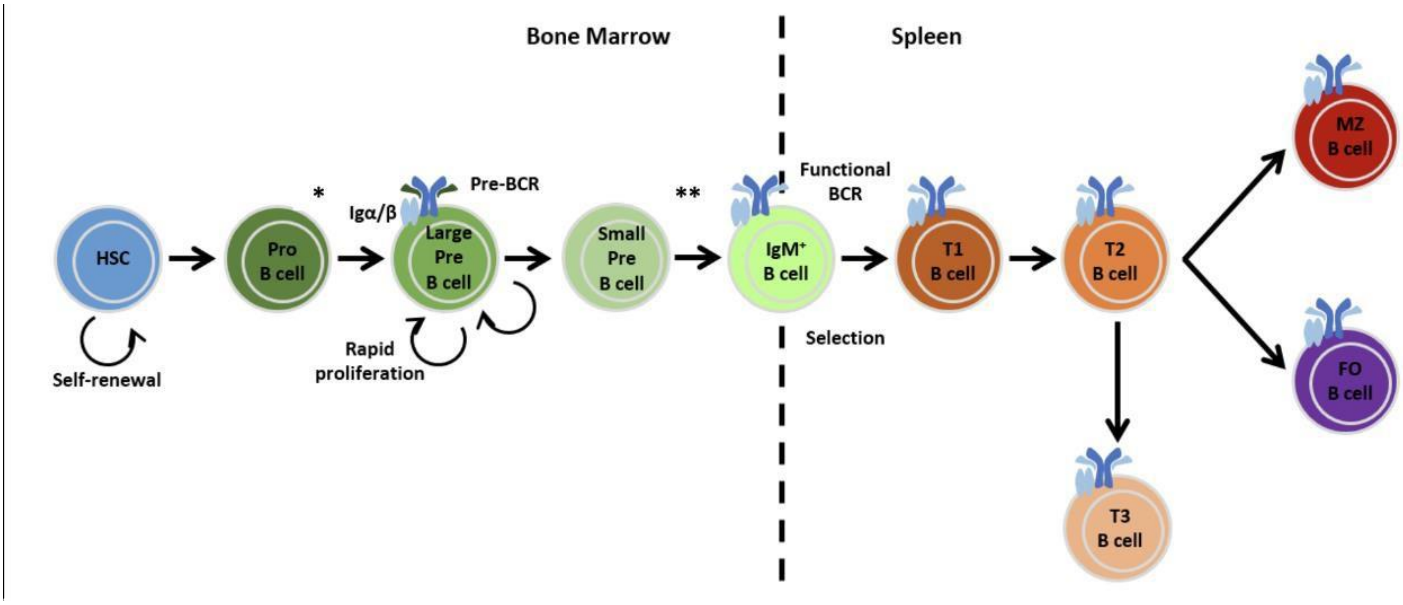

Figure 1.1: B-cell development and subsets. B-cells develop in the bone marrow (BM) from haematopoietic stem cells (HSCs), capable of developing into pro-B-cells and subsequent large pre-B-cells via V-DJ recombination to generate functional heavy chain. Following large pre-B-cell formation, the heavy chain complexes with the surrogate light changes and drives pre-BCR formation to elicit rapid proliferation and differentiation into small pre-B-cells. Pre-B-cells experience light chain rearrangement, which is successfully denoted by a functional BCR and surface IgM expression. Immature B-cells may then exit the BM for additional differentiation that give rise to mature follicular (FO), marginal zone (MZ) B-cells or anergic B-cells. HSC, hematopoietic stem cell; BCR, B-cell receptor; T1 and T2, transitional B-cells; MZ, marginal zone; FO, follicular; T3, anergic B-cells. * Denotes where heavy chain rearrangement occurs, and ** marks where light chain rearrangement occurs. Figure adapted from Rebecca Newman, 2021.

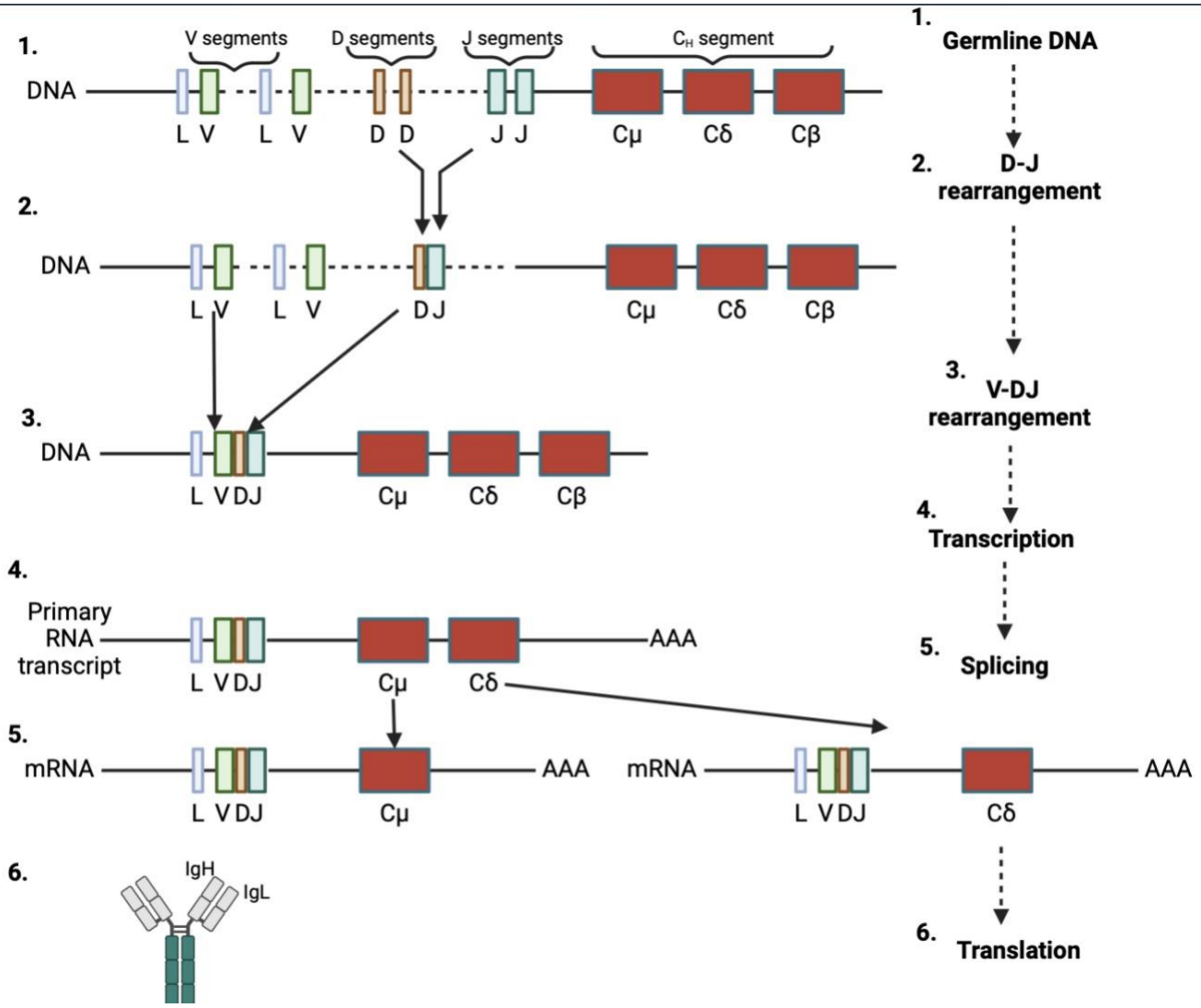

Figure 1.2: Simplified schematic of heavy chain immunoglobulin (IgH) V (D) J recombination. The diversity (D) and joining (J) gene segment join followed by the joining of the variable (V) region. The heavy-chain C-segment (C_H) is encoded for by several exons which are additionally spliced (in addition to the leader, L, sequence) during heavy-chain recombination. Following translation, the L sequence is removed and disulfide bonds linking the polypeptide chains are formed.

1.3 B-cell differentiation into antigen-secreting cells

The binding of antigen to the BCR initiates B-cell proliferation and differentiation into short-lived or long-lived plasma cells (PCs), which both secrete antibodies or memory B-cells that facilitate an immune response to reinfection. The factors determining a PC versus memory cell fate are largely elusive, but it is postulated that expression of the master transcription factor, IRF-4/BLIMP1, facilitates PC generation (Nutt *et al.,* 2011), and higher expression of transcription factors such as Bach2 could facilitate memory B-cell fate (Shinnakasu *et al.,* 2016). Another observation is that B-cells with lower antigen affinity tend to become memory and have fewer mutations than PCs, hence could be generated earlier (Taylor, Pape and Jenkins, 2012).

Before reaching maturity, B-cells undergo several transitional stages, starting as immature B-cells in the bone marrow. These immature cells migrate to the spleen, where they pass through transitional stages (T1 and T2), distinguishable through surface phenotype and functional characteristics, before becoming mature but naive B-cells (Chung *et al.,* 2003). At this stage, naive B-cells have not yet encountered their specific antigen but maintain functional BCRs and can respond to antigens upon activation (Chung *et al.,* 2003). It is these mature, naive B-cells, rather than their immature counterparts, that can differentiate into antibody-secreting cells (ASCs) upon antigen encounter.

B lymphocyte activation is either T cell-dependent (TD) or T cell-independent (TI). In both cases, secondary lymphoid tissue migration occurs and usually involve signalling from antigen binding to the BCR, although some TI reactions are initiated by pathogen-associated molecular patterns (PAMPs). (Cano *et al.,* 2013). However, a secondary signal is additionally needed to trigger antibody production in TD responses (Jeurissen, Ceuppens and Bossuyt, 2004).

1.3.1 T-cell dependent and independent responses

Secondary signalling required for TD responses derives from CD4+ T helper cells. The recognition of antigen by naive B-cells triggers antigen internalisation (Yuseff *et al.,* 2013). Subsequent processing and presentation using a major histocompatibility complex II (MHC II) occurs, which enables antigen recognition by antigen-specific CD4+ T follicular helper cells that thereafter become activated (Parker., 1993, Yuseff *et al.,* 2013; Akkaya *et al.,* 2019). Activated CD4+ T cells express CD40L, which binds to CD40 on B-cells, in addition to various interleukins (ILs) that strongly trigger B-cell activation (Figure 1.3) (Parker, 1993; Elgueta *et al.,* 2009).

TI responses are characteristic for marginal zone and a subset of follicular B-cells, occurring independently of T-cell help and therefore tending to be more rapid (Figure 1.3) (Cerutti, Cols and Puga, 2013). TI responses occur when BCRs interact directly with pathogens possessing repetitive epitope units, such as lipopolysaccharides. This enables multiple BCR cross-linking to provide an initial activation signal. Direct interaction is also mediated (independently or collectively with BCRs) by innate immune receptors, such as cell surface and intracellular toll-like receptors (TLRs) which primarily recognise microbial membrane components (e.g. lipids, lipoproteins and proteins and bacterial/viral nuclei acid derivatives, respectively (Kawasaki and Kawai, 2014).

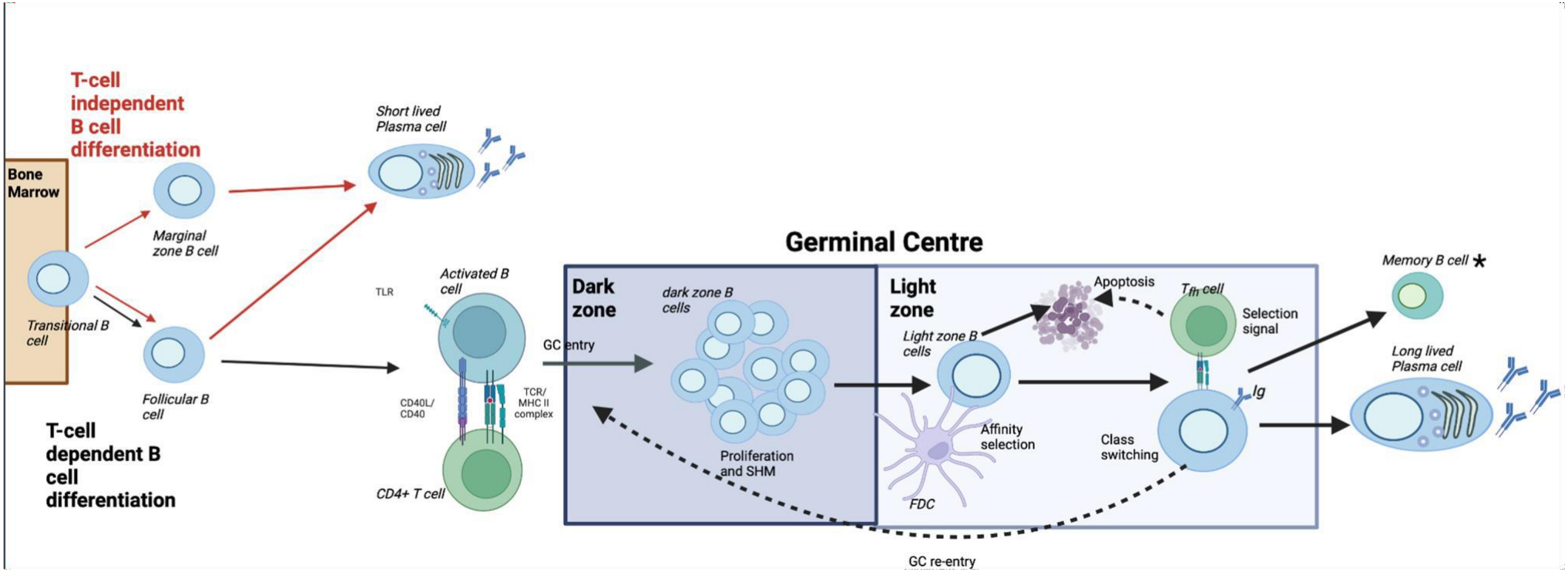

Figure 1.3: T -cell dependent and independent B-cell differentiation. In T-cell independent B-cell differentiation, transitional B-cells exit the bone marrow and differentiate into either marginal zone B-cells or follicular B-cells (T-cell independent pathway is indicated by red arrows). B-cells may then receive direct stimulation to drive short-lived plasma cell generation. In T-cell dependent B-cell differentiation (indicated by black arrows), transitional B-cells exit the bone marrow and differentiate into follicular B-cells that may receive CD4+ T cell CD40-L stimulation. Cells may then enter the dark zone of germinal centres, where proliferation and somatic hypermutation (SHM) occur. Cells may progress to the germinal centre light zone, where cells are subject to affinity maturation to determine whether apoptosis or differentiation-progression occurs. Selected cells undergo class switching and can mature into memory B-cells or plasma cells.

1.3.2 Germinal centre reactions

The initial antigen/BCR binding stage shared by both TD and TI responses facilitates rapid B-cell proliferation and differentiation into transient plasmablasts. This occurs via the extrafollicular response. B-cells activated by a TD response can also initiate a germinal centre (GC), an anatomical structure within secondary lymphoid organs whereby processes that alter the immunoglobulin molecule, such as class switch recombination (CSR) and somatic hypermutation (SHM), occur (Pone *et al.,* 2012). CSR relates to the changing of the constant immunoglobulin region, downstream of the hypervariable VDJ segment of B-cell immunoglobulin genes, from Cμ to Cγ, Cε or Cα (Honjo, Kinoshita and Muramatsu, 2002). This recombinational event enables an isotypic switch in B-cells from producing IgM to IgG, IgE or IgA whist maintaining synonymous antigen specificity that is determined by the variable region (Pone *et al.,* 2012; Nutt *et al.,* 2015). The resultant class-switched isotype is determined by cytokines that can work synergistically to stimulate or suppress a particular immunoglobulin class, thus creating a complex microenvironment tailored to combat specific antigens (Chaudhuri and Alt, 2004) (Table 1.1).

Cytokine	**Immunoglobulin isotype**	**Reference**
IL-4	IgE, IgG1	Snapper, Finkelman and Paul, 1988
IL-5	IgA	Harriman *et al.,* 1998 Murray *et al.,* 1987
IL-6	IgG3, IgG1	Dienz *et al.,* 2009
TGF-b	IgA	Borsutzky *et al.,* 2004
IFN-g	IgG2, IgG3	Snapper *et al.,* 1992 Inoue *et al.,* 1995

Table 1.1: Immunoglobulin isotype generation and cytokine expression. The generation of specific immunoglobulin isotypes is largely attributed to the expression of specific cytokines.

1.3.3 Immunoglobulin classes

Each immunoglobulin class has unique properties and functions tailored to the required immune response. IgM is the initial antibody produced during B-cell development, hence the additional mechanism resulting in immunoglobulin diversity (i.e. somatic hypermutation) infrequently occur in the initial response to antigen. Thus, IgM antibodies enable low- affinity IgM-expressing B-cells, or natural antibodies, to rapidly respond to various antigens (Schroeder and Cavacini, 2010) (Figure 1.4). IgM is expressed in its monomeric form on the surface of naïve B-cell where it acts as an antigen receptor. IgM also exists in secreted form as a large multimer whereby single IgM units are linked by disulphide bonds. Secreted IgM is effective in microbe agglutination and activation of the compliment system due to its pentameric structure (Schroeder and Cavacini, 2010).

Membranous IgD can be co-expressed with IgM to engage in BCR signalling (Geisberger, Lamers and Achatz, 2006), however the role of circulating IgD is less clear. Nonetheless, it has been postulated that its functions include assisting in mucosal immune surveillance by providing mucosal-reactive IgD antibodies to myeloid effector cells (Figure 1.4) (Gutzeit, Chen and Cerutti, 2018).

IgG is the most abundant and long-lasting antibody class and can be sub-classified in humans, based on relative abundance, as either: IgG1 (most abundant), IgG2, IgG3 and IgG4 (least abundant). Each IgG subclass has differences in the constant region, which itself elicits different effector functions including complement activation, antibody-dependent cellular cytotoxicity and phagocytosis (Figure 1.4) (Vidarsson, Dekkers and Rispens, 2014).

IgA exists in two forms (IgA1 and IgA2) and can be found as a monomer in serum or as a dimer with a J chain and secretory component in mucosal secretions (Figure 1.4). The imperative role of IgA in mucosal immunity is evidenced in its abundance at mucosal surfaces such as the respiratory, gastrointestinal and genitourinary tracts (De Sousa-Pereira and Woof, 2019).

IgE is found at the lowest concentration of all immunoglobulin classes, and its functions correspond to hypersensitivity, allergy and parasitic infections (Figure 2.4). Such responses are attributed to interaction with high-affinity FcεRI receptors on mast cells and basophils, triggering the release of histamines and other allergy-related immune mediators (Schroeder and Cavacini, 2010).

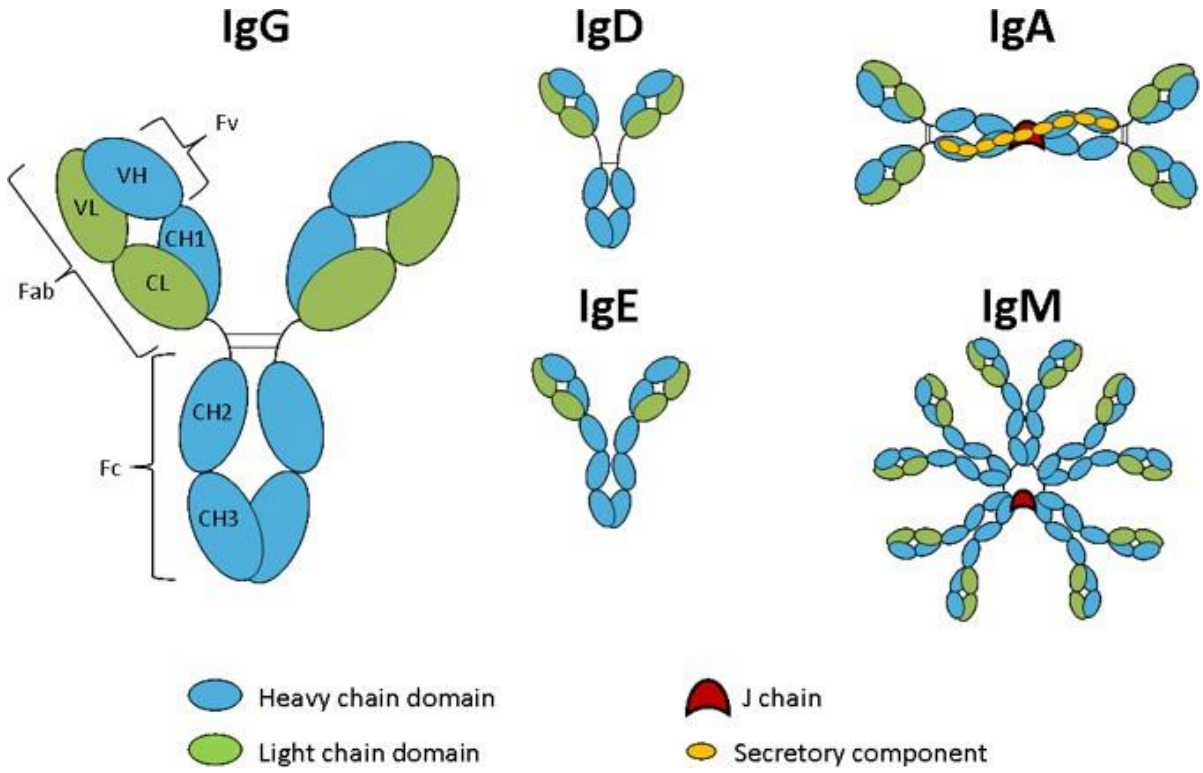

Fig 1.4: Immunoglobulin isotypes. Schematic representation of IgG, IgD, IgA, IgE and IgM immunoglobulin isotypes in mammals. Fab, fragment-antigen binding regions; Fv, variable region; Fc, fragment crystallisable region; VL, variable light chain; CL, constant light chain; VH, variable heavy chain; CH (1-3), constant heavy chain. Taken from Absolute Antibody, 2018.

The last mechanism by which immunoglobulin diversity can occur is secondary to antigen exposure through the process of SHM in the GC dark zone (DZ) (Schroeder and Cavacini, 2010) SHM involves the incorporation of point mutations into the variable regions of immunoglobulin genes, resulting in an improved affinity (Figure 1.3) (Chi, Li and Qui, 2020).

Both CSR and SHM are mediated by enzymes such as activation-induced cytidine deaminase (AID) (Muramatsu *et al.,* 2000; Kuraoka *et al.,* 2011). AID is expressed in activated GC B-cells (Revy *et al*., 2000), and facilitates alteration of immunoglobulin

constant regions and antibody diversity by binding to the DNA locus at VDJ segments to deaminate cytidine to uracil, thereby introducing DNA double strand breaks (DSBs) (Papavasiliou and Schatz 2002; Revy *et al.,* 2000; Muramatsu *et al.,* 2000). DSBs result in base substitutions that are inherited by all B-cell progeny, generating clonal BCR variants. While these variants contribute to antigen-driven selection, B-cell survival is promoted through activation of transcriptional pathways such as the nuclear factor-kappa B (NF-κB) pathway (LeBien and Tedder 2008; Guldenpfennig *et al.,* 2023), rather than as a direct consequence of DSBs.

Clonal variants produce terminally-differentiated PCs capable of secreting high-affinity antibodies, alongside a pool of long-lived memory B-cells poised for rapid recall responses (Akkaya and Kwak, 2019). Following SHM in the DZ, B-cell progeny relocate to the light zone (LZ), where they undergo stringent selection. In this compartment, B-cells compete for antigen displayed on the surface of follicular dendritic cells (DCs), capturing antigen via their mutated BCRs and presented processed peptides on MHC class II molecules to T-follicular helper cells (Stebegg *et al.,* 2018). The extent of T cell help a B-cell receives is determined by the affinity of its BCR, with higher-affinity clones capturing more antigen, presenting greater levels of peptide–MHC complexes, and in turn securing increased survival and proliferative signals via CD40–CD40L interactions and cytokines such as IL-21. This facilitates the preferential selection of high-affinity clones for continued participation in the GC response, while low-affinity variants are eliminated via apoptosis (De Silva and Klein, 2015) (Figure 1.3).
In a subset of selected B-cells, this interaction promotes further affinity maturation by initiating additional cycles of proliferation, SHM and selection. Positively selected LZ B-cells are instructed to either differentiate into memory B-cells or PCs, or to recirculate to the DZ for further rounds of mutation. This process is coordinated by a network of transcriptional regulators, with MYC and the NF-κB subunit REL playing essential roles in maintaining GC integrity and permitting DZ re-entry of antigen-selected B-cells. The termination of the GC reaction and commitment to terminal differentiation is tightly controlled by both transcriptional and post-transcriptional mechanisms, ensuring that only B-cells with sufficiently high-affinity receptors contribute to long-lived humoral immunity (De Silva and Klein, 2015).

1.4 Plasma cell transcription factors

B-cell differentiation is a complex and highly regulated process involving significant changes in antibody surface markers and transcription factors that facilitate the determination of B-cell fate (Roth *et al*., 2013) (Table 1.2 and Figure 1.5). Important surface markers used to define B-cell differentiation stages include CD19, CD20, CD27, CD38 and CD138 (Table 1.2), all of which have important functions in B-cell differentiation.

Surface marker	**Function**	**B-cell subset where marker is primarily expressed**	**Reference**
CD19	B-cell lineage marker Co-receptor for BCR that decreases activation threshold, allowing direct and indirect recruitment of downstream kinases (e.g. Ras, Abl, Btk)	Naïve (+) Activated (++) Plasmablast (+) Plasma cell (+/-) Memory	Zhou *et al.,* 1992 Wang, Wei and Liu, 2012
CD20	-Regulates differentiation and cell cycle progression -Involved in calcium signalling	Naïve (++) Activated (++) Memory	Tedder and Engel, 1994

CD27	-Often used to distinguish memory from naïve B-cell subsets -Signalling can activate NFkB pathway	Activation (+/-) Plasmablast	Tangye *et al.,* 1998 Klein *et al.,* 1998
CD38	-Ubiquitous in most cells -An ADP-hydrolase with function in calcium signalling -Signalling transduction	Plasmablast (+) Plasma cell (++)	Takasawa *et al.,* 1993 States, Walseth and Lee, 1992 Lee, 2006
CD138	-Mediates plasma cell adhesion to bone marrow extracellular matrix -Enhances plasma cell survival	Plasma cell (+)	Sanderson *et al.,* 1992 McCarron *et al.,* 2017

Table 1.2: **B-cell markers**. B-cell markers CD19, CD20, CD27, CD38 and CD138 expression can be used to study B-cell differentiation.

All B-cells highly express the transcription factor Paired Box 5 (PAX5), which plays a crucial role in promoting lineage commitment and maintaining the B-cell state by suppressing genes associated with terminal differentiation (Nutt *et al.,* 1999; Schebesta *et al.,* 2007; Cobaleda *et al.,* 2007). Within GCs, the decision to differentiate into antigen-secreting memory B-cells or PCs is governed by a network of transcriptional regulators (De Silva and Klein, 2015). A key factor in sustaining the GC phenotype is B-cell lymphoma 6 (BCL6), which is highly expressed in GC B-cells and functions to suppress PC differentiation by repressing the expression of B-lymphocyte induced maturation protein 1 (BLIMP1) (Reljić *et al.,* 2000; Shaffer *et al.,* 2002).

As B-cells commit to terminal differentiation, PAX5 and BCL6 expression is progressively downregulated (Carotta *et al.,* 2006), permitting BLIMP1 activation (Calame, Lin and Tunyaplin, 2003). BLIMP1 acts as a master regulator of PC fate by repressing genes involved in cell proliferation, DNA synthesis and B-cell antigen presentation (Shaffer *et al.,* 2002). This transition is further supported by interferon regulatory factor 4 (IRF4), which is

induced following PAX5 repression and promotes BLIMP1 expression while inhibiting BCL6 in a dose-dependent manner (Carotta *et al.,* 2014; Ochiai *et al.,* 2013). In parallel, X-box binding protein 1 (XBP1) is upregulated downstream of BLIMP1, initiating the unfolded protein response (UPR) to accommodate the high secretory demands of antibody-producing PCs (Reimold *et al.,* 2001; Minnich *et al.,* 2016).

Together, these regulatory pathways ensure that only B-cells with appropriately high-affinity antigen receptors are permitted to exit the GC reaction and contribute to long-lived humoral immunity, maintaining a balance between differentiation and self-renewal while safeguarding against dysregulated responses that could lead to autoimmunity or immunodeficiency (De Silva and Klein, 2015).

1.5 Plasma cell survival niches and their role in antibody production

Long-lived PCs (LLPC), distinguishable from short-lived PCs (SLPC), are critical in providing long-term and sustained antibody production. The ability of LLPCs to survive for extended periods of time is not intrinsic to the PC itself but rather accounted for by their high dependence to migrate, localise and respond to specialised microenvironments known as PC survival niches that are primarily located in the BM, spleen and inflamed tissues (Lightman *et al.,* 2019). Within these niches, PCs receive survival signals (e.g. IL-6, APRIL) and through interactions with stromal cells, DCs, and other components of the niche environment (Lindquist *et al.,* 2019).

The environment within these niches is highly competitive due to limited availability of space and resources. Only the LLPCs capable of effectively migrating to and establishing themselves within these niches can persist. This competitive nature ensures that only the most functionally capable PCs are maintained, contributing to the quality and effectiveness of the antibody-mediated immune response. Without the continuous access of survival signals and supportive interactions, LLPCs cannot sustain themselves and will undergo apoptosis (Simons and Karin, 2024). The removal of unfit PCs is a critical regulatory mechanism that prevents the accumulation of dysfunctional or unnecessary PCs.

Recent work challenges the strict dependence of LLPCs on specialised survival niches and suggests that their longevity is largely governed by intrinsic cellular programmes, including immunoglobulin isotype and metabolic state. Notably, tissue-resident PCs were found to be inherently long-lived across multiple organs, with their gene expression signatures shaped by both developmental cues and local tissue environments. This paradigm shift implies that while survival niches may support or modulate LLPC function, they are not strictly required for sustaining long-term PC survival (Tellier *et al.,* 2024).

Nonetheless, the formation, maintenance, and function of these niches remain important for optimising LLPC survival and function. Disruptions to niche integrity can still reduce the efficiency of PC support, potentially leading to diminished antibody levels (Unger *et al.,* 2014). Given the complexity of PC niches and the

broader process of B-cell differentiation, impairments in these systems (i.e. intrinsic or extrinsic) can contribute to immune dysregulation, as evidenced in antibody deficiency disorders.

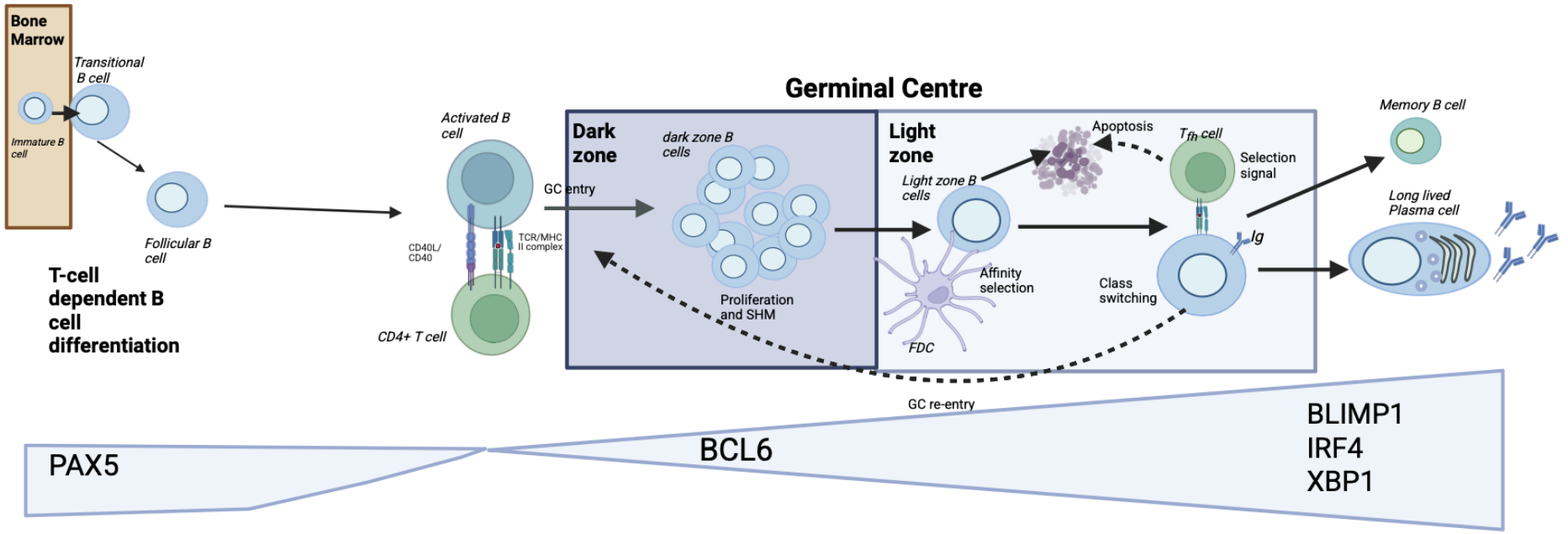

Figure 1.5: T-cell dependent B-cell differentiation is facilitated by alterations in transcription factor expression. Immature B-cells highly express PAX5 and BCL6. As B-cells become activated, PAX5 and BCL6 are inhibited whilst BLIMP1, IRF4 and XBP1 expression gradually increase to facilitate B-cell differentiation. PAX5, Paired Box 5; BCL6, B-Cell Lymphoma 6; IRF4, Interferon Regulatory Factor 4; BLIMP1, B-Lymphocyte Induced Maturation Protein1; XBP1, X-Box Binding Protein 1.

1.6 Antibody deficiency

Antibody deficiencies correspond with increased infection susceptibility, attributed to a loss of or failed immunoglobulin function (Duraisingham *et al.,* 2014). Deficiencies are either primary (PAD) or secondary (SAD) in nature and can have variable impact on immunoglobulin profiles depending on the precise genetic defect (Herriot and Sewell, 2008). Before reviewing PADs and SADs individually, general immunodeficiency disorders will be the focus, most notably in its primary form.

1.6.1 Primary immunodeficiencies

Primary immunodeficiencies (PIDs) or inborn errors or immunity (IEI) represent a large, heterogenous group of inherited disorders affecting immune responses that may present as: increased susceptibility to infections; autoimmunity; autoinflammatory diseases; allergy; BM failure; and/or malignancy. (Demirdağ and Gupta, 2021; Tangye *et al.,* 2022). PIDs are estimated to have a documented prevalence of around 1 in 1,000 to 1 in 5,000 worldwide, although it is likely that high amounts of unrecorded cases exist. (Tangye *et al.,* 2020; Meyts *et al.,* 2020). The high incidence of unrecorded cases is thought to be attributable to four factors: underutilisation of next-generation sequencing, incomplete penetrance (partial or no presentable disease), manifestation to organs other than blood and lymphatic system and the role of somatic mutations that can present in adulthood (Akalu and Bogunovic, 2023).

The mechanism by which PID results in disease is dependent on both the nature of the variants and its inheritance (Figure 1.6). Monoallelic variants are heterozygous, attributed to one allele carrying the variant and eliciting disease through haploinsufficiency, negative dominance or gain-of-function (GOF). Biallelic variants are homozygous or compound heterozygous, occurring if both alleles are variant-carriers (Heyne *et al.,* 2023) and result in autosomal recessive disease through: loss of expression, loss of function (LOF), GOF or neomorphic mutations. Biallelic variants may also result in X-linked recessive traits due to LOF or GOF variants (Tangye *et al.,* 2022).

To date, there are 485 confirmed IEI (Yu, 2023). According to the most up-to-date IEI classification, IEI are categorised into 10 groups: combined immunodeficiencies, combined immunodeficiencies with syndromic features, predominantly antibody deficiencies, diseases of immune dysregulation, congenital defects of phagocytes, defects in intrinsic and innate immunity, autoinflammatory diseases, complement deficiencies, BM failure and phenocopies of IEI. The latter refers to conditions that mimic the clinical features of inherited IEIs but arise from non-genetic causes, such as SHM or autoantibodies that disrupt normal immune function (Tangye *et al.,* 2020).

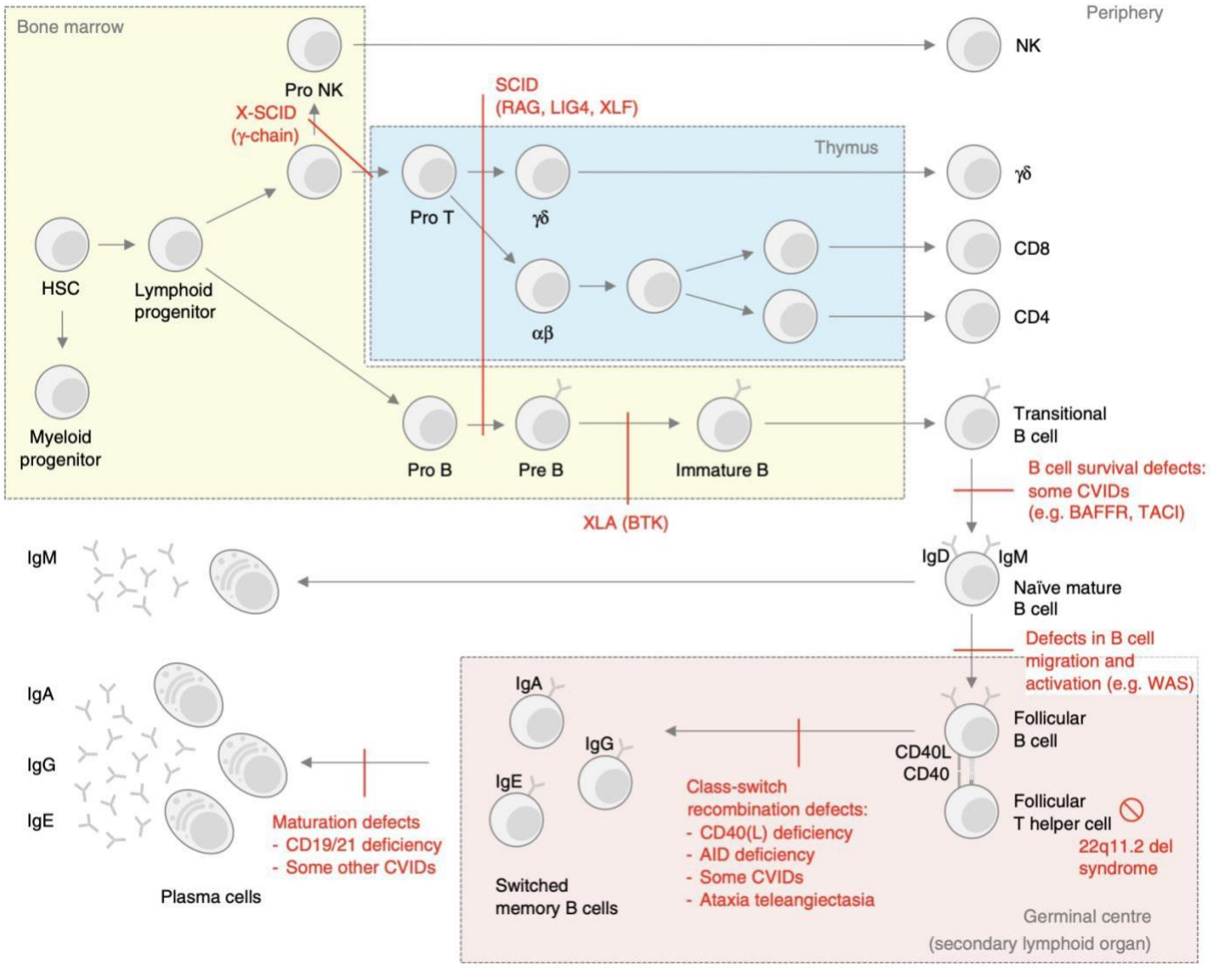

Figure 1.6: Lymphocyte development and genetic origins of various primary immunodeficiencies. B-cell development starts in the bone marrow and continues maturation in the thymus (T-cells) and secondary lymphoid organs (B-cells). Examples of primary immunodeficiency are shown in red. Figure taken from Ghraichy *et al.,* 2018.

1.6.2 Primary antibody deficiencies

The most prevalent category of IEI are PADs, which arise due to genetic factors impairing antibody production, maturation and/or function (Durandy, A, Kracher, S and Fischer, A, 2013). Over 17 PADs have been documented, attributed to numerous different genetic defects (European Society of Immunodeficiencies, 2024). PAD presentation is not apparent at birth due to the protective neonatal ability of maternal antibodies, however as the effectiveness of these antibodies declines clinical presentations may arise commonly in the form of frequent infections with encapsulated bacteria (e.g. Streptococcus pneumoniae, Haemophilus influenzae type b) (Ballow, 2002). Despite this, however, around 95% of PAD patients show no clinical presentation until after the age of six years (Wood, 2009). Upon referral, regardless of age, most PAD patients are diagnosed by serum IgG levels of < 3 g/l ; IgA levels of < 0.1 g/l or (rarely) IgM levels of < 0.25 g/l in combination with severe/recurrent/unusual infections (Wood, 2009).

The antibody impairment resulting in PAD may be B-cell-intrinsic, although impairments may originate from other immune cell lineages (Durandy, A, Kracher, S and Fischer, A, 2013), such as T cells and innate immune cells. Regardless of the cell origin, patients experience infectious and non-infectious (including autoimmunity and malignancies) manifestations (Demirdağ and Gupta, 2021) that can range in severity. More than 50% of PAD diagnoses can be accounted for by common variable immunodeficiency (CVID), a heterogenous condition that tends to have an adult-onset presentation and affects around 1 in 25,000-50,000 of the population (Gereige and Maglione, 2019).

1.6.3 Common variable immunodeficiency

The current consensus of a CVID is largely ill-defined due to the extent of its heterogeneity and multifactorial aetiology whereby the genetic basis in most patients is never determined (Ameratunga *et al.,* 2014). It is due to this undefinable genetic defect that patients diagnosed with CVID are not considered to have an IEI but rather have a CVID-like disorder secondary to an IEI (Ameratunga *et al.,* 2023).

The initial CVID diagnosis can be made when patients experience: 'a marked decrease of serum IgG and a marked decrease of at least one of the isotypes IgM or IgA and fulfils all the following criteria: 1. Onset of immunodeficiency at greater than 2 years of age 2. Absent isohaemagglutinins and/or poor response to vaccines 3. Defined causes of hypogammaglobinaemia have been excluded according to a list of differential diagnosis' (Bonilla *et al.,* 2016). Thus, hypogammaglobinaemia is the shared outcome of a wide spectrum of immunoregulatory defects amongst CVID patients.

The heterogeneity of CVID and its clinical manifestations suggests for a subgrouping system. Whilst all CVID patients display infection-associated manifestations, patients can be grouped based on whether they have additional inflammatory and/or autoimmune conditions secondary to the CVID (Cunningham-Rundles, 2012). Patients with secondary manifestations represent the majority of CVID cases and have additional complications that increase the risk of mortality and reduced quality of life (Resnick *et al.,* 2012). The most prevalent secondary manifestation amongst CVID patients is stable or progressive interstitial lung disease (ILD) which manifests comparably to benign lymphoproliferative lung pathology and can develop in the presence of IgRT (i.e. ILD is not the result of bronchiectasis or pneumonia in patients) (Maglione *et al.,* 2019). The underlying mechanisms driving the autoimmune and lymphoproliferative conditions, such as ILD, in certain CVID patients remains elusive but has been postulated to be attributed to alterations in pathways affecting B-cell activation and/or survival (Maglione *et al.,* 2019).

Patients with CVID have also been grouped based on phenotypes assessed through flow cytometry (Table 1.3), predominantly to determine levels of circulating memory B-cells and isotype-switched memory B-cells (Ruschel and Vaqar, 2023). However,

this classification approach is not routinely used to aid CVID diagnosis (Ruschel and Vaqar, 2023), and subgroups have not been concretely linked to clinical manifestation.

Classification system	Definition	Reference
Freiburg	Patients classified into two groups: **I** those with switched memory B-cells below 0.4% and **II** those with normal numbers of switched memory-B-cells. Type I can further be subdivided into group **1a** (>20% $CD21^{low}$ B-cells) and group **Ib** (<20% $CD21^{low}$ B-cells)	Warnatz *et al*., 2002
Paris	Patients classified into three groups: **MB0** have <11% CD27+ B-cells. **MB1** have <8% class-switched memory B-cells. **MB2** are those that are neither MB0 or MB1	Piqueras *et al*., 2003
EUROclass	Classified as: **group B-** which have ≤1% B-cells or **group B+** which have >1%. Group B+ further divided into **smB-** with ≤2% switched memory B-cells and group **smB+** with >2% switched memory B-cells. Patients are additionally characterised based on percentages of transitional B-cells and based on expansion of $CD21^{low}$ B-cells within CD19+ B-cells	Wehr *et al*., 2008
B-cell patterns	CVID patients are divided into five patterns based on B-cell subset. **Pattern 1**: decreased numbers of transitional B-cells with reduced memory B-cell numbers. **Pattern 2:** reduced transitional B-cells and reduced naïve mature marginal zone-like and memory B-cells. **Pattern 3**: reduced marginal zone-like and memory B-cells. **Pattern 4:** decreased memory B-cells only. **Pattern 5:** normal marginal zone-like and memory B-cells and reduced plasmablast numbers	Driessen *et al*., 2011

Table 1.3: Published classification systems for common variable immunodeficiency (CVID).

1.6.4 Secondary antibody deficiency

Conversely to PADs, SADs occur due to one or more extrinsic factors (i.e. chronic infection, malignant disease, malnutrition or immunosuppressive drugs), with a variable spectrum of infection susceptibility/severity and primarily implicate IgA and IgG (Herriot and Sewell, 2008). The severe infection risk presented to SAD patients was particularly apparent in the recent coronavirus disease 2019 (COVID-19) pandemic, whereby SAD individuals had worse outcomes than those with PADs (Shields *et al.,* 2021). It is plausible that outcomes for SAD patients may have reduced severity, such as seen with COVID19, if mechanisms and treatment approaches were better understood.

The most common cause of SAD is haematological malignancies, namely chronic lymphocytic leukaemia (CLL) whereby up to 85% of patients experience symptomatic SAD corresponding to disease-related and iatrogenic immunological dysfunction of both innate and adaptive immune responses (Srivastasa and Wood 2016; Dhalla *et al.,* 2014; Jolles *et al.,* 2021). Patients experience marked hypogammaglobinaemia involving IgM, IgG and IgA likely corresponding to reduced PC numbers and functional suppression (Forconi and Moss, 2015). A proposed mechanism for PC functional suppression is through increased numbers of B- and T-regulatory cells (Breg; Treg, respectively), whereby CLL B-cells are proposed to have phenotypic similarities with Bregs (e.g. soluble IL10 production post stimulation) and there is an increased formation of Tregs after interaction with the CLL cells (DiLillo *et al*., 2012; Jak *et al*., 2009). Another proposed source of hypogammaglobinaemia is the observed CD95L (FasL) expression of CLL B-cells, whereby interaction with CD95(Fas) expressed on CD4+ T cells may trigger CD4+ T cell apoptosis (Tinhofer *et al.,* 1995; Sampalo and Brieva, 2002).

Whilst the spectrum and severity of SAD infections is highly variable, correlations have been made between patient age/comorbidities and infection severity. In the case of CLL, SAD-related infections contribute to 25-50% of deaths amongst patients (Hamblin and Hamblin, 2008).

The risk of acquiring SAD is additionally and increasingly elevated in patients administered immunosuppressive treatments such as the small molecule Bruton Tyrosine Kinase (BTK) inhibitor, ibrutinib (Varughese *et al.,* 2018). Ibrutinib impairs downstream signalling of malignant B-cells since BTK is a key mediator of B-cell signalling and is required for B-cell growth, proliferation and survival (Paydas, 2019). Rituximab is another therapeutic agent used in lymphoproliferative and autoimmune conditions to target CD20+ B-cells for killing through induced complement activation and cell- mediated cytotoxicity (Smith, 2003).

Whilst small molecule inhibitors and monoclonal antibodies such as ibrutinib and rituximab damage malignant B- cells (i.e. CLL B-cells), this effect directly translates to normal B-cells (Paydas, 2019; Smith *et al.,* 2003) resulting in B-cell phenotypic and functional impairments that increase susceptibility to infection. Thus, it is critical that patients taking immunosuppressive medication are carefully and regularly monitored during and after treatment cessation.

The manifestation of SADs as hypogammaglobinaemia or as functional or subclass immunoglobulin deficiencies with normal total IgG (Srivastava and Wood, 2016) means diagnosis and treatment are often delayed. This is particularly true since many patients remain asymptomatic despite their elevated risk of serious infection (Srivastava and Wood, 2016).

In suspected SAD patients, immunoglobulin levels are typically assessed using different methodologies following administration of a pneumococcal capsular polysaccharide vaccination: normal adult IgG, IgA and IgM levels should be 6.0-16.0 g/L, 0.8-3.0 g/L and 0.4-2.5 g/L, respectively (Oxford University Hospitals NHS Trust, n.d.). In cases where patients are unable to mount at least a 2-fold increase in antibody levels or have serum IgG levels less than 4 g/L, and are experiencing recurrent bacterial infection, an antibody deficiency diagnosis can be made (European Medicines Agency, 2019).

1.7 Treatment for antibody deficiencies

Treatment approaches for PADs and SADs, including CVID, predominantly aim on managing symptoms and reducing infection risk. As such, antibiotics such as macrolides are the most common first-line treatment approach in antibody deficiency (in some instances, dependent on the deficiency, anti-virals or anti-fungals may be used) which tend to be used prophylactically (Immunodeficiency. 2023; NHS England, 2018; Agostini *et al.,* 2016; Oscier *et al.,* 2012; Srivastava and Wood, 2016). The efficacy of prophylactic antibiotics in PAD has been evidenced in clinical trials, such as low dose azithromycin in PAD which was evidenced to provide various benefits including a reduced risk of hospitalisation and improved quality of life (Milito *et al.,* 2019). However, the ever-present risk of antimicrobial resistant infection can be elevated (Ballow, 2023) in some patients on long-term prophylactic antibiotics which suggests for alternative and/or additional treatment approaches.

1.7.1 Immunoglobulin replacement therapy

Unresponsive patients may be considered suitable candidates for a 12-month IgG immunoglobulin replacement therapy (IgRT) trial period (Agostini *et al.,* 2016; Jolles *et al*. 2017) following assessment of possible comorbidities and potential adverse effects (Ammann *et al.,* 2016; Stiehm, 2013). The primary goal of IgRT in SAD/PAD patients is to achieve sufficient levels of passive IgG to enable pathogen opsonisation and neutralisation, which is achieved by low-dose replacement therapy. IgRT can also be beneficial in the setting of autoimmune and inflammatory diseases, whereby higher dosage facilitates additional immunomodulatory effects (e.g. neutralisation of autoantibodies, reducing inflammatory cytokine secretion) (Sil *et al.,* 2024; Bayry *et al.,* 2023). In addition to dosage alternations, the frequency of administration should be individualised based on: disease severity, clinical presentation, response to treatment and potential side effects.

It is generally accepted that PADs are better characterised in the context of IgRT, with an overall proven IgRT success and safety rate (defined by lower incidence of severe infection following and during treatment) and better-defined clinical parameters (Mallick *et al.,* 2021; Jolles *et al.,* 2017). High degree of PAD IgRT understanding and success is likely attributed to the more routine nature of studying PAD pathophysiological mechanisms compared to with SADs (Duraisingham *et al.,* 2014). Hence, PAD treatment approaches can be more targeted. This could suggest that a greater understanding of individual SAD pathophysiological mechanisms, complimenting current approaches, could assist in formulating better treatment algorithms to improve IgRT success in SAD. The same is likely applicable to more heterogenous PADs, including CVID, where understanding disease and subsequent treatment approaches should be individualised/personalised.

In the context of IgRT in SAD, clinical trials evidence its benefits in certain patients, most notably with CLL (Griffiths *et al.,* 1989; Sklenar *et al.,* 1993; Jurlander *et al.,* 1994; Chapel *et al.,* 1994; Boughton *et al.,* 1995, Molica *et al.,* 1996; Vacca *et al.,* 2018; Legendre *et al.,* 2020). However, such studies also make apparent the fact that SAD IgRT treatment is often incorrectly used and frequently ineffective, possibly due to lack of accurate quantitative evidence guiding physicians (i.e. use of antibody concentration tests only) (Jolles *et al.,* 2017; Legendre *et al.,* 2020; Jolles *et al.,* 2021). This unclarity results in a high degree of treatment subjectivity amongst physicians and immunologists in the context of patient selection, clinical endpoints, treatment duration and especially in terms of selecting biomarkers deemed appropriate for monitoring patient status/treatment response (Na *et al.,* 2019; Bonet *et al.,* 2020). This may contribute to worsening of preexisting SADs (Legendre *et al.,* 2020) in addition to having economic implications (Beaute *et al.,* 2010; Sun *et al.,* 2022).

Treating both PADs and SADs with IgRT has limitations, most notably in the difficulty to personalise therapy to individual patients. In a select few instances where a causative genetic mutation is well characterised, genetic editing has a potential and curative use, thus being the ultimate form of personalised treatment. This is achieved

using haematopoietic stem cell transplantation to deliver stem cells with added or edited versions of the faulty gene resulting in the deficiency (Kohn and Kohn, 2021). Ongoing advancements in gene editing technologies are being achieved, but immense challenges and limited applicability to the majority of PADs/SADs render it very limited. This may indicate that correctly using and improving IgRT is a more economical, feasible and widely beneficial treatment approach for most antibody deficient patients.

Collectively, IgRT has become a keystone of treating PADs and SADs alike. However, there is an apparent need for a more personalised approach to IgRT treatment based on a culmination of clinical and laboratory-based information. This raises questions concerning the possibility of combining laboratory and clinical information to determine future infection and mortality risks amongst individual patients. Such information may facilitate the identification of patients more likely to benefit from IgRT in addition to paving way for a more tailored approach to IgRT.

1.8 COVID19 and antibody deficiency

The global COVID19 pandemic caused by a novel coronavirus SARS-CoV-2 affected more than 630 million people and resulted in 6.5 million deaths worldwide (Milota, Smetanova and Bartunkova, 2023) Poorer outcomes were predominantly associated with older age, chronic lung and cardiovascular disease and lymphopenia (Public Health England, 2020). Patients on haemodialysis were also at particular risk during the first wave, with a case-fatality rate of 23%, likely attributed to their inability to adhere to shielding guidelines (Kular *et al.,* 2020). Immunodeficient, notably antibody deficient, patients were additionally vulnerable to poorer outcomes, which was particularly true in combination with the predominantly associated risk-factors. The detriment of COVID19 in the context of immunodeficiency was evidenced in the fact that 1 in 4 individuals with immunodeficiency who contracted SARS-CoV-2 virus died during the initial wave (Shields *et al.,* 2021). Hence, the urgency to identify and

better understand why discrepancies in PAD and SAD patient responses to COVID19 infection occurred, in addition to whether such discrepancies extended to vaccine responses, became critical.

1.9 Genetics of vaccine responses

Discrepancies in responses to numerous vaccines amongst individuals is widely accepted and various studies link genetics to vaccine responses, such as correlating specific human leukocyte antigen (HLA) alleles to vaccine-induced immunity notably in the context of rubella and measles (Oysyannikova *et al.,* 2014; Jacobson *et al.,* 2011). Genetics have also been associated with severe immune outcomes following vaccines, including patients with accelerated ageing of immune cells (Liu *et al.,* 2023) or those with defects in IFN immunity resulting in severe illness following yellow fever or measles mumps and rubella (MMR) vaccination (Hernandez *et al.,* 2019).

In relation to COVID19 vaccination, vulnerability and discrepancies in responses were evidenced in the observational cohort trial T cells, antibodies and vaccine efficacy in SARS-CoV-2 (OCTAVE) study, whereby 12% of immune vulnerable patients failed to make an antibody and T cell response following vaccination. Amongst the 12%, vaccine failure rates were highest in: ANCA-associated vasculitis patients on rituximab, solid-organ transplant recipients, haemodialysis patients on immunosuppressive therapy and patients undergoing chimeric antigen receptor (CAR-T) therapy (Barnes *et al.,* 2023). The study also identified that a decreased magnitude of both serological and T cell response was associated with severe disease, evidencing the cooperative need for both arms of the immune system (Barnes *et al.,* 2023).

1.10 COVAD study

With over 250 worldwide interventional studies on COVID, understanding COVID19 was and remains an integral part of scientific research (Immunodeficiency UK, 2023). The COVID19- in patients with antibody deficiency (COVAD) study is a multi-site study from the United Kingdom, encompassing both SADs and PAD cases that are unresponsive to pneumococcal vaccine (i.e. candidates for IgRT), with three primary aims: '(i) determine the prevalence of asymptomatic and symptomatic SARS-CoV-2 infection in patients with primary and secondary antibody deficiency, (ii) determine how frequently SARS-CoV-2 viral persistence occurs in patients with primary and secondary antibody deficiency and (iii) characterise the immune response of these patients following SARS-CoV-2 infection and vaccination'. Given the recognised reduced ability of some antibody deficient patients in responding to other vaccinations (Shields *et al.,* 2022a; Shields *et al.,* 2022b), it was of paramount importance to understand if and why such response discrepancy translated to COVID19 vaccinations. Categorising patients with impaired vaccine responses would identify those requiring additional strategies such as prophylactic monoclonal antibodies. This was particularly important given the elevated risk of fatality amongst SAD/PAD patients (Shields *et al.,* 2021; Shields *et al.,* 2022a; Shields *et al.,* 2022c).

Initial data from the COVAD study evidenced that, despite the large heterogeneity, 76% of PAD/SAD patients were able to make an antibody response following three vaccine doses (Shields *et al.,* 2022a). The ability to elicit antibody response termed these patients as responders and those unable as non-responders. Initial data suggested that clinical history (e.g. patients with bronchiectasis, splenomegaly, liver disease and those on steroids and immunosuppressive medication) and accelerated immune-ageing correlated with non-response (Shields *et al.,* 2022a). However, potential functional pathway defects that could be governing a vaccine response versus non-response in patients remains an imperative question in the study which could facilitate the identification of predictive biomarkers in a SARS-CoV-2 setting and beyond.

1.11 Aims and Objectives

1.11.1 *In vitro* long-lived plasma cell differentiation modelling of antibody deficiencies

Due to the rarity and difficulty of accessing/harvesting human PCs, detailed analysis of B-cell differentiation is challenging. The *in vitro* differentiation model of long-lived human plasma cells previously established by the Doody-Tooze laboratory is a unique culture system enabling direct and detailed manipulation and analysis at each stage of human long-lived PC differentiation (Cocco *et al.,* 2012; Stephenson *et al.,* 2019; Stephenson *et al.,* 2021). Thus far, the system has successfully been utilised to study primary immunodeficiency in patients (Wu *et al.,* 2021; Spegarova *et al.,* 2020; Walker *et al*., 2023), facilitating analysis of genetic cell-autonomous antibody production impairments/failures.

The model conditions include the isolation of human B-cells from peripheral blood, followed by either TLR or CD40L and F(ab')2 anti IgG/M/A stimulation. Additional proliferative signals are initially provided by IL2 and IL21, then subsequently the acquisition of mature PC phenotype is promoted by the inclusion of IL6 and APRIL/IFN- α /TGF- β for long-term culture into PCs (Cocco *et al.,* 2012; Stephenson *et al.,* 2019; Stephenson *et al.,* 2022). Immunophenotypes of differentiating cells can thereafter be studied using flow cytometry. Immunoglobulin secretion can be detected by enzyme-linked immunosorbent assays (ELISA) and extracted RNA can be analysed.

Based on the *in vitro* B-cell differentiation model, this investigation will be the first to report a detailed study on potential pathway defects that could be governing a SARS-CoV-2 vaccine response versus non-response in patients with antibody deficiency. It will enable the characterisation of B-cell phenotypes in a heterogenous population of PAD and SAD patients, potentially paving the way for future diagnostic and treatment approaches.

1.11.2 Project aims

1. Replicate the *in vitro* B-cell differentiation model under different stimulatory conditions and in different B-cell subtypes.
2. Assess the feasibility of using the *in vitro* system on a heterogenous group of primary and secondary antibody deficient patients and make any optimisation steps as required prior to analysis on patient samples.
3. Relative to healthy controls, analyse and compare phenotypic, secretory, BCR repertoire and gene expression data in a cohort of SARS-CoV-2 vaccine responding and vaccine non-responding patients with antibody deficiency using the *in vitro* PC differentiation model.

Chapter 2- Methods

2.1 Healthy donors and patient samples

Peripheral blood was obtained from healthy donors with their informed consent. Patient PBMCs were derived from peripheral blood samples collected from participants with various primary and secondary antibody deficiencies enrolled in the COV-AD study (Shields *et al.,* 2021; Shields *et al.,* 2022a; Shields *et al.,* 2022b), across multiple immunology centres nationwide. Samples were collected up to 28 days following the third or fourth dose of the SARS-CoV-2 vaccination. Additional details on patient recruitment and sample collection methods can be found in previously published reports (Shields *et al.,* 2021; Shields *et al.,* 2022a; Shields *et al.,* 2022b). Ethical approval was granted by London-Dulwich Research Ethics Committee (21/LO/0162).

2.2 In vitro differentiation of long-lived PCs

2.2.1 Human peripheral blood mononuclear cells (PBMCs) isolation

An equal ratio of blood and phosphate buffered saline (PBS) were mixed and added to lymphoprep (1 volume lymphoprep: 2 volume blood/PBS mix). Contents were centrifuged at 1150 RCF for 20 mins at room temperature (RT) (acceleration 5, brake 0), and PBMCs were removed and transferred to a fresh tube containing 10 mL cold PBS. The volume was made up to 50 mL with PBS, and the tube was centrifuged at 650 RCF for 15 mins at 4^{o}C. PBS was thereafter removed, and cells were washed with 15 mL ice-cold MACS buffer (PBS, 0.5% BSA), and 10 µL was removed for

counting using a haemocytometer and trypan blue exclusion before centrifugation at 450 RCF at 4°C.

2.2.2 Magnetic cell labelling and separation of B-cells

A memory isolation kit for a maximum of 1 x 10^8 cells was used to select for B cells (reagent quantities were doubled when PBMC count exceeded 1x10^8). The cell pellet was resuspended in 400 µL cold MACS buffer, and 100 µL B cell Biotin-Antibody cocktail (cocktail of biotin-conjugated monoclonal antibodies against CD2, CD3, CD4, CD14, CD15, CD16, CD34, CD56, CD61, CD235a and FcεRIα) was added and incubated for 20 minutes at 4°C. An additional 300 µL cold MACS buffer and 200 µL of Anti-Biotin MicroBeads (MicroBeads conjugated to monoclonal anti-biotin antibodies) were added, mixed and subject to a further 30-minute incubation period at 4°C. Cells were then washed using 10 mL MACS buffer, and centrifuged for 10 minutes at 450 RCF. Cell pellets were resuspended in 1 mL MACS.

To achieve a pool of negatively selected total B-cells, an LD column (Miltenyi) was placed in the magnetic field of a suitable MACS separator. The column was equilibrated with 2 mL cold MACS buffer, followed by the addition of the cell suspension. Supernatant containing unlabelled cells was collected in a fresh tube, and the column was washed with 2x 1mL MACS buffer. Cells were then counted, washed with buffer and centrifuged at 450 RCF for 5 minutes and resuspended at 5x10^5 cells/mL in IMDM + 10% FBS media.

2.2.3 Anti-CD27 depletion for naïve B-cell isolation

To separate naïve and memory B-cell populations, following the above steps for isolation of total B cells, cells were centrifuged at 450 RCF for 10 minutes and resuspended in 500 µL MACs buffer. 100 µL anti-CD27 MicroBeads were added and cells were incubated for 15 mins at 4^{o}C. Contents were washed in 10 mL MACs, centrifuged at 450 RCF for 10 minutes and resuspended in 500 µL MACs buffer. The cell suspension was applied to an MS column (Miltenyi), with collected flowthrough containing naïve cells. Magnetically labelled memory B-cells were flushed out and collected in a separate tube. Both naïve and memory fractions were resuspended in IMDM containing 10% heat-inactivated foetal bovine serum (HIFBS) in preparation for commencing B cell differentiation.

2.3 Culture conditions

2.3.1 Preparation of irradiated CD40L-L cells for B-cell co-culture

Murine fibroblasts transfected with human CD40L (CD40L-L cells) were irradiated in advance at 50Gy for 50 minutes in a gamma irradiator and stored at -80^{o}C (Banchereau *et al.,* 1991). These feeder cells provide membrane-bound CD40L, mimicking T-cell help to promote B-cell activation, proliferation and differentiation. When required, 1x10^{6} of irradiated human CD40L cells were thawed and added to 10 mL IMDM complete media + 10% HIFBS and then centrifuged at 450 RCF for 5 minutes. Cells were then resuspended in 12 mL of fresh IMDM + 10% HIFBS media, and either 500 µL per well of a 24-well plate or 250 µL per well of a 48-well plate (dependent on anticipated B-cell counts) were seeded 24 hours in advance at 37^{o}C and 5% CO_2.

2.3.2 Culture conditions used during B-cell differentiation

The culture conditions for various stages of B-cell differentiation are as follows (Figure 1.4), and a comprehensive list of reagents can be found in Table 2.1:

Day 0: Cells were either directly stimulated with the TLR7/8 agonist R848 (1 µg/mL) + hIL2, (20 U/mL), hIL21 (50 ng/mL) and F(ab')$_2$ goat anti-human IgM/G/A (10 µg/mL) in IMDM, or CD40L-L growth medium was replaced with fresh IMDM + hIL2, (20 U/mL), hIL21 (50 ng/mL) and F(ab')$_2$ goat anti-human IgM/G/A (10 µg/mL). Cells

were then resuspended at 2.5 x 10^5 cells/mL in IMDM, and 500 µL or 250 µL was plated to each well of a 24-well or 48-well plate, respectively.

Day 3*:* Activated B cells were counted before reseeding at 1x10^5 cells/mL of fresh IMDM + 10% HIFBS supplemented with amino acid solution (1:50) and Lipid Mixture 1 (1:200) + hIL2 (20 U/mL), hIL-21 (50 ng/mL).

Day 6*:* Plasmablasts (PB) were counted before reseeding at 1x10^6 cells/mL of fresh IMDM + 10% HIFBS supplemented with amino acid solution (1:50) and Lipid Mixture 1 (1:200) + hIL21 (10ng/mL), hIL6 (10 ng/mL) and APRIL (100ng/mL).

Day 13*:* Day 13 marked the differentiation end-point, hence PCs were counted and all remaining cells were used for downstream analysis.

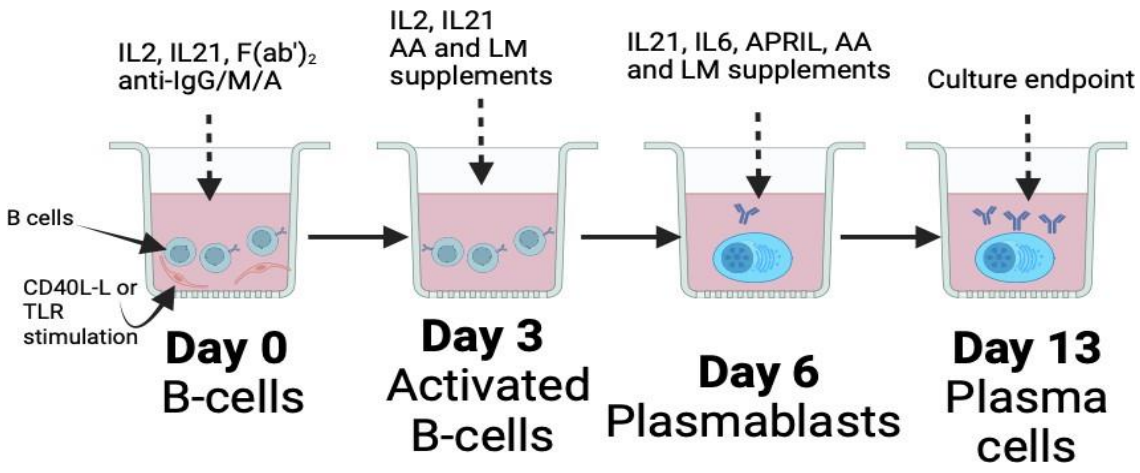

Figure 2.1: *In vitro* B-cell differentiation culture conditions. Isolated B-cells at day 0 are activated by CD40L or TLR agonist (i.e. R848) with F(ab')$_2$ anti-IgG/M/A. Corresponding stages of differentiation relative to the days are indicated, and cytokines/media requirements at each stage are stated above. Samples for flow cytometry, ELISA, BCR repertoire and RNA analysis are taken at the different stages. APRIL, a proliferation-inducing ligand; AA, amino acid; LM, lipid media.

Name	Company	Catalogue Number
hIL-2	Miltenyi Biotec	130-097-746
hIL-21	PeproTech	200-21
hIL-6	PeproTech	200-06
Goat anti-human F(ab')$_2$ (anti-IgG/M/A)	Stratech Scientific Ltd	109-006-064
R848 (Resiquimod)	Invivogen	144875-48-9
APRIL (TNFSF13)	R&D Systems Biotechne	5860-AP-010
Heat-inactivated foetal bovine serum (HIFBS)	Invitrogen	10270106
Lymphoprep	Allere Limited	11114547
IMDM	Invitrogen	31980048
MACS Rinsing Solution	Miltenyi	130-091-376
PBS tablets	Sigma	P4417
Human Memory B cell isolation kit	Miltenyi	130-393-546
LD columns	Miltenyi	130-042-901
Lipid mix	Sigma	L0288
Amino acids	Sigma	M550
Transwell for 24 well plate	Corning	CLS3464-48EA
Transwell for 48 well plate	Corning	CLS3548-100EA

Table 2.1: Table of cytokines and other reagents used for *in vitro* B-cell differentiation.

2.4 Flow Cytometry staining

Markers of B cell differentiation was assessed using surface and intracellular flow cytometry staining. Cells were washed with PBS and centrifuged at 450 RCF for 5 minutes at RT. Live/dead fixable Zombie UV stain (BioLegend, 423107) was diluted in PBS (1:1000) and 100 µL was transferred and resuspended in FACS tubes. Tubes were incubated in the dark at RT for 15 minutes and washed with 2 mL of MACS buffer before centrifugation at 450 RCF for 5 minutes at RT. For intracellular staining, cells were fixed with 4% paraformaldehyde and stored at 4^{o}C until required. For surface staining, cells were resuspended in 25 µL of 2X blocking buffer (93.3 µL MACS buffer, 16.6 µL hIgG, 50 µL normal mouse serum) and incubated at 4^{o}C for 15 minutes. 10 µL of master mix was added (Table 2.2) and tubes were incubated in the fridge for 20 minutes. Cells were washed with 2 mL MACS buffer before centrifugation at 450 RCF for 5 mins at 4 ^{o}C and fixed with 4% paraformaldehyde and stored at 4^{o}C.

Prior to analysis on the flow cytometer, intracellular immunoglobulin staining required additional centrifugation followed by: wash with 1x permeabilisation buffer (10x saponin buffer diluted with PBS), 15-minute RT incubation in the dark, addition of IgG, IgM and IgA antibodies (Table 2.3), further 30 minute incubation, wash with permeabilisation buffer and resuspension in PBS. Data was collected on a Beckman Coulter's Cytoflex LX analyser. Manuel haemocytomer slides or CountBright beads (Invitrogen) were used for absolute cell number analysis. Post-collection analysis was performed using FlowJo (BD Biosciences) and gating followed the strategy outlined in Figure 2.2.

Antibody	Fluorochrome	Laser	µL per sample	Supplier	Catalogue number
CD19	PE	Yellow/green	0.4	Thermo Fisher Scientific (Life Technologies)	MA119646
CD20	eFluor V450	Violet	2.5	Thermo Fisher Scientific (Life Technologies)	48-0209-42
CD27	FITC	Blue	2	BD Biosciences	555440
CD38	PE-Cy7	Yellow/green	0.5	BD Biosciences	335825
CD138	APC	Red	0.4	Miltenyi Biotec	130-127-977

Table 2.2: Master mix I surface staining antibodies used for surface flow cytometry immunophenotyping.

Antibody	Fluorochrome	Laser	µL per sample	Supplier	Catalogue number
IgM	APC	Red	20	BD Biosciences	561010
IgG	FITC	Blue	20	BD Biosciences	555786
IgA	VioBlue	Violet	2.5	Miltenyi Biotec	130-113-479

Table 2.3: Staining antibodies used for intracellular flow cytometry immunophenotyping.

2.4.1 Gating strategy for flow cytometry

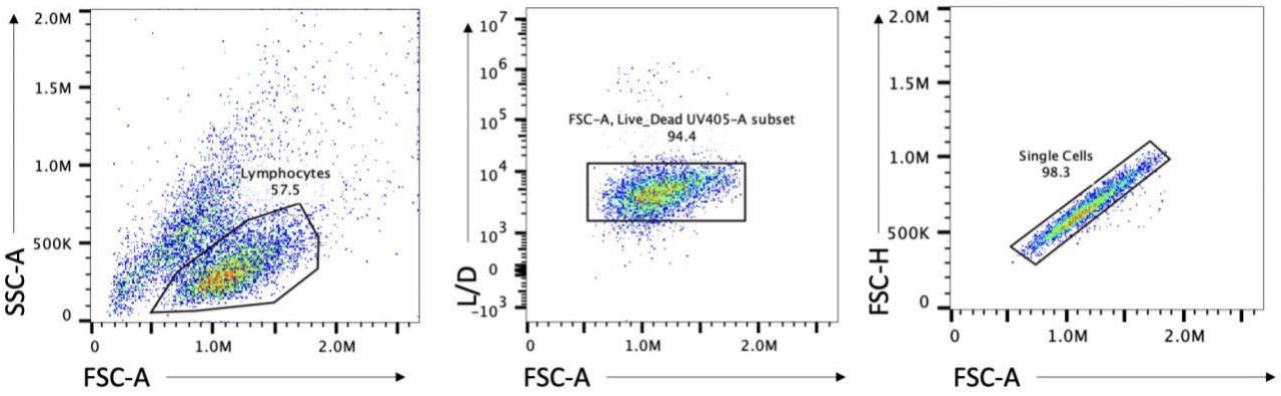

Figure 2.2: Gating strategy for immunophenotype analysis. B cells were first gated based on forward vs side scatter. Live-dead determination was deduced using UV Zombie staining, which was plotted against area. Doublets were then excluded by plotting area against width.

2.5 IgM, IgG and IgA ELISA

Tissue culture supernatants were collected and frozen on days 6 and 13 for the analysis of secreted IgG, IgM and IgA using sandwich ELISAs. ELISAs were performed according to the manufacturer's instructions. 96 well plates (ThermoFisher, 10547915) were coated with 100 µL of affinity purified goat-anti-human IgM (Bethyl Laboratories, A80-100A), IgG (Bethyl Laboratories, A80-104A) or IgA (Bethyl Laboratories, A80-102A) antibody diluted in coating buffer (Table 2.4) for 1 hour at RT (See Table 2.5 for sample plate layout). Antibody solution was thereafter removed and washed 5 times using ELISA wash solution (Table 2.4). 200 µL of blocking solution (Table 2.4) was added to each well and incubated at RT for an hour to prevent non-specific binding. Blocking solution was removed and the wash step was repeated. Standards (Bethyl Laboratories, RS10-110) were diluted in

sample diluent solution (10 µL:4.4 mL for IgM, 5 µL: 22 mL for IgG and 10 µL:14.4 mL for IgA) and serially diluted to facilitate the generation of a standard curve on analysis. Samples were diluted to a concentration predicted to fall within the standards' range (1:100, 1:200 and 1:400). 100 µL of each standard/sample was added to the appropriate well in duplicates and incubated for 1 hour at RT (see Table 2.5 for example plate layout). Plates were washed 5 times with wash solution and 100 µL of horseradish peroxidase (HRP)-conjugated detection antibody (Bethyl Laboratories, A80-100P for IgM; Bethyl Laboratories, A80-104) for IgG; Bethyl Laboratories, A80-102P for IgA) (1:100,000 dilution for IgM, 1:200,000 for IgG and 1:150,000 for IgA) was added to each well and incubated for 1 hour at RT. Plates were washed 5 times with wash solution and 100 µL of TMB substrate (ThermoFisher, E102) was added to each well and incubated for up to 15 minutes in the dark. Reactions were stopped using 100 µL of stop solution Table 2.4), and concentrations were quantified using a plate reader (Cytation 5, BioTek) and analysed using GraphPad Prism 10.

Buffer name	**Components**
Coating buffer	0.05M Carbonate-bicarbonate, pH 9.6
Wash solution	50mM Tris, 0.14M NaCl, 0.05% Tween20, pH 8.0
Blocking solution	50mM Tris, 0.14M NaCl, 1% BSA, pH 8.0
Enzyme substrate	TMB (3,3'5,5'-tetramethylbenzenzidine)
Stop solution	0.18M H_2SO_4

Table 2.4: Buffers used in IgM, IgG and IgA ELISA analysis.

	1	2	3	4	5	6	7	8	9	10	11	12
A	1000 →		S1, 1:100 →									
B	500 →		S1, 1:200 →									
C	250 →		S1, 1:400 →									
D	125 →		S2, 1:100 →									
E	62.5 →		S2, 1:200 →									
F	31.25 →		S2, 1:400 →									
G	15.6 →											
H	0 →											

Table 2.5: Example ELISA plate layout. Standard were serially diluted in duplicates in columns 1 and 2. Samples (e.g. S1, S2) were added to plates in duplicates under different dilutions whereby concentrations were predicted to fall within the standards' range.

2.6 RNA extraction and analysis

2.6.1 RNA purification from cell suspension

Cells were lysed in 800 µL cold Trizol® (Invitrogen, 15596018) and stored at -20ºC until needed. When required, cells were thawed and 160µL of chloroform was added and tubes were inverted. Lysed cells were then centrifuged at 12000 RCF for 15 minutes at 4ºC to produce three separate layers and the top aqueous layer containing RNA was carefully transferred to a new tube. 15 µL of RNAse free glycogen (Invitrogen, AM9510) and 0.4 mL of isopropyl was added to facilitate RNA precipitation. Contents were vigorously shaken and incubated for 10 minutes at RT. Samples were centrifuged at 12000 RCF for 10 minutes at 4ºC to precipitate a pellet. Pellets were washed/resuspended in 1 mL of 75% ethanol three times and air-dried. RNA was dissolved in 30-45µL nuclease-free dH_20 and incubated for 10 minutes at 55ºC.

2.6.2 RNA clean-up

DNA contaminants were removed from RNA using a DNA-free kit (Invitrogen, AM19060). 4 µL of 10X DNAse buffer and 1 µL DNAse I enzyme was then added to samples and incubated for 1 hour at 37ºC. Next, 5 or 6 µL of inactivation reagent (code) was added and incubated for 2 minutes at RT. Samples were centrifuged at 10000 RCF for 1.5 minutes and supernatants were transferred to fresh tubes and concentration/purity was quantified using a Nanodrop™ (Thermofisher).

2.6.3 RNA to cDNA conversion

cDNA synthesis was performed using GoScipt™ Reverse Transcription System (Promega, A5001). The reaction mix (Table 2.6) was made up to a total volume of 5 µL with nuclease-free dH_20 and incubated at 70°C for 5 minutes, immediately placed on ice and briefly centrifuged. Next, a reverse reaction mix was made (Table 2.7), and the samples were run at the programme specified in Table 2.8 and stored at -20°C until required for downstream analysis.

Reagent	**Amount**
RNA sample (up to 5 ug)	Variable
Random primers	0.5 µL
Oligos (dT)	0.5 µL
Nuclease-free H_20	Up to 5 µL
Total volume	**5 µL**

Table 2.6: Reaction mixture for cDNA synthesis.

Reagent	**Volume per samples**
5X Reaction buffer	4 µL
$MgCl_2$	1.5 µL
PCR nucleotide mix	1 µL
Reverse Transcriptase	1 µL
RNasin	1 µL
Nuclease-free H_2O	6.5 µL
RNA template	5 µL
Total final volume	**20 µL**

Table 2.7: Reverse reaction mixture.

Step	Time (minutes)	Temperature (ºC)
Anneal	5	25
Extend	60	42
Reverse Transcriptase inactivation	15	70

Table 2.8: cDNA synthesis PCR programme.

2.6.4 RNA analysis

Raw RNA sequencing data were obtained as FASTQ files following sequencing by Novogene. Initial processing involved trimming reads to remove low-quality bases and adapter sequences using Cutadapt (Martin, 2011). Initial quality control (QC) of the trimmed reads was then performed using FastQC (Cock *et al.,* 2010), to evaluate read quality, adapter contamination and GC content.

High-quality reads were aligned to the human reference genome GRCh38.p13 using the STAR aligner (Dobin *et al.,* 2012). Gene-level quantification was then performed with FeatureCounts (Liao *et al.,* 2013) to generate raw count data for downstream analysis.

Differential gene expression analysis was conducted using the DESeq2 package in RStudio (Love et al., 2014) to generate lists of differentially expressed genes (DEGs), which were then functionally annotated using Enrichr (Chen *et al.,* 2013). These analyses were performed by Dr Leon Chang (Figure 2.3). Visualisation of DEGs was performed using ggplot2 (https://ggplot2.tidyverse.org) and Apptyper (https://appyters.maayanlab.cloud/#/).

Differentially expressed genes identified using DESeq2 were defined based on a threshold of adjusted *p*-value <0.01, corrected for multiple testing using Benjamini-Hochberg adjustment (Benjamini and Hochberg, 1995; Chang, 2023).

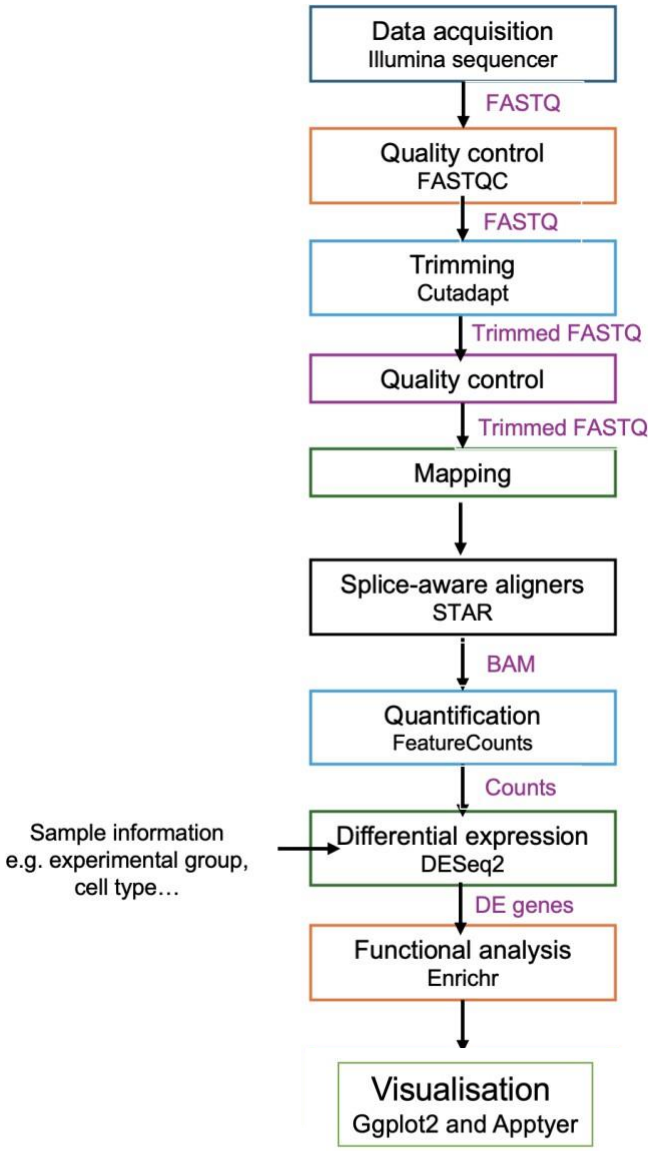

Figure 2.3: RNA sequencing data analysis workflow. A schematic outlining the key steps involved in RNA sequencing data analysis pipeline. RNA analysis was performed by Dr Leon Chang.

2.7 BCR repertoire

2.7.1 First Round PCR Amplification

For the analysis of the B-cell receptor (BCR) repertoire, primers for amplifying the immunoglobulin heavy chain (IgH) variable (V) and joining (J) regions were designed following the guidelines outlined by the BIOMED-2 Concerted Action framework (Van Dongen *et al.,* 2003). Primer sets used for amplification included a mix of VHN forward primers and a single JHN reverse primer (Table 2.9).

Primers	**Sequence (5' to 3')**	**Temperature (°C)**
JHN	GTCTCGTGGGCTCGGAGATGTGTATAAGAGACAGCTTACCTGAGGAGACGGTGACC	65
VhL 1/7 N	TCGTCGGCAGCGTCAGATGTGTATAAGAGACAGCTCACCATGGACTGSAYYTGGAG	65
VhL 2 N	TCGTCGGCAGCGTCAGATGTGTATAAGAGACAGATGGACAYACTTTGYTMCACRCTCC	65
VhL3a N	TCGTCGGCAGCGTCAGATGTGTATAAGAGACAGATGGARTTKGGGCTKWGCTGGGTTT	65
VhL3b N	TCGTCGGCAGCGTCAGATGTGTATAAGAGACAGGGCTGAGCTGGGTTTTCCTTGTTGC	65
VhL4 N	TCGTCGGCAGCGTCAGATGTGTATAAGAGACAGCTGTGGTTCTTYCTBCTSCTGGTGG	65
VhL5 N	TCGTCGGCAGCGTCAGATGTGTATAAGAGACAGCCTCCTCCTRGCTRTTCTCCAAG	65
VhL6 N	TCGTCGGCAGCGTCAGATGTGTATAAGAGACAGCTGTCTCCTTCCTCATCTTCCTGCC	65

Table 2.9: VDJ region PCR amplification primers.

Immunoglobulin heavy chain variable regions (IgVH) were amplified using a first round of PCR, whereby each reaction consisted of a PCR reaction mixture (Table 2.10 and each primer was at a concentration of 16.7 µM. cDNA synthesised from Chapter 2.6.3 were used to prepare the PCR reaction mix. Thermal cycling was performed under the following conditions:

1. Initial denaturation at 98°C for 10 seconds
2. 30-35 cycles of:
   - 98°C for 1 second
   - 65°C for 5 seconds
   - 72°C for 10 seconds
3. Final extension at 72°C for 1 minute

Reagent	**Volume per samples**
2X Phusion Flash Master Mix	10 µL
V_hN primer mix	0.24 µL
J_hN primer	0.4 µL
Genomic DNA (cDNA template)	100 ng
Nuclease-free H_2O	Up to 20 µL
Total final volume	**20 µL**

Table 2.10: PCR reaction mixture.

2.7.2 Gel extraction of desired PCR product

On completion of the PCR reaction, samples were separated on a 2% agarose gel containing ethidium bromide and ran at 130V for 50 minutes in 1X TBE. Appropriate IgH bands were visualised and excised under UV light. The excised gel slices were purified using the New England Biolabs Monarch DNA Gel Extraction Kit® (T1020L), whereby each excised band was placed in a fresh Eppendorf tube and weighed. A calculated amount of dissolving buffer was added to individual samples, based on the relative weight of each sample. Samples were incubated at 50^{o}C for 10 minutes, inverting the sample regularly. Samples were then loaded into column/collection tubes and spun at 16,000 RCF for 1 minute. Columns were washed with 200 µL DNA Wash Buffer, spun at 16,000 RCF for 1 minute (X2 times) and transferred to fresh Eppendorf tubes. DNA was then eluted using 8 µL of Elution Buffer and incubated for 1 minute RT. Columns were spun at 16,000 RCF for 1 minute and eluted samples were stored at -20^{o}C overnight in preparation for the second round of amplification.

2.7.3 Second Round Amplification and Library Preparation

The purified amplicons of interest were used as templates for the second round of amplification to prepare the libraries for high-throughput sequencing. Indexing was performed using Nextera^{TM}Index Kit (Ilumina, 15055294), whereby unique N and S primer pairs were used to differentiate between samples (Table 2.11). A mixture, including the Nextera^{TM} primers, was prepared (Table 2.12) and added to tubes of a PCR strip.

Primers	Sequence (5' to 3')
N701	15031852 B/ ID2058125-N701
N702	15031842 B/ ID2084610-N702
N703	15031843 B/ ID2710848-N703
N704	15031844 B/ ID2687742-N704
N705	15031845 B/ ID2089169-N705
N706	15031846 B/ ID2735728-N706
N707	15031847 B/ ID2067272-N707
N708	15031848 B/ ID2058125-N708
N709	15031849 B/ ID2056188-N709
N710	15031850 B/ ID2065323-N710
N711	15031851 B/ ID2669677-N711
N712	15031852 B/ ID2749067-N712
S502	15031903 C/ ID2727120-S502
S503	15031904 C/ ID2717638-S503
S504	15031905 C/ ID2045733-S504
S505	15031906 C/ ID2658597-S505
S506	15031907 C/ ID2766519-S506
S507	15031908 C/ ID2667222-S507
S508	15031909 C/ ID2039842-S508
S517	15049978 A/ ID2035610-S517

Table 2.11: Nextera™ indexing primers.

Reagent	Volume per sample
2X Phusion Flash Master Mix	12 µL
Post Gel Extraction Template	8 µL
Nextera N primer	2 µL
Nextera S primer	2 µL
Total final volume	**24 µL**

Table 2.12: Nextera™ indexing reaction mixture.

The PCR strip reaction was run on the following programme:

1. 98°C for 1 second
2. 72°C for 10 seconds
3. Repeated 1-2 times for 10 cycles

2.7.4 Bead Purification of indexed PCR products

Indexed samples were purified using AMPure XP beads (Beckman Coulter, A63880) to remove unincorporated primers, primer dimers and other contaminants. A calculated volume of Bead Reagent (PCR reaction volume X 1.8) was added to each sample, mixed by pipetting 10 times and incubated for 5 minutes at RT. The PCR strip was placed on a magnet for separation to occur, as indicated by the beads clearing the solution. Keeping the PCR strip on the magnet, the clear solution was aspirated and washed twice with 150 µL of 70% ethanol. The PCR strip was removed from the magnet and 40 µL of elution buffer was added to each sample, mixed by pipetting 10 times and incubated at RT for 2 minutes. The PCR strip was re-inserted onto the magnet for 1-2 minutes to allow for the dissociation of the beads

from the solution. Elutes were transferred to fresh Eppendorf tubes and stored at -20ºC until ready to be sent for sequencing.

2.7.5 Concentration Determination

The concentration of double-stranded DNA (dsDNA) for sequencing was measured using the Quant-iT™ dsDNA BR Assay Kit (Invitrogen, Q33267). In a 96-well non-sterile plate, 10 µL of each Quant-iT 1X dsDNA BR standard and each sample were loaded in duplicate. 200 µL of Quant-iT 1X dsDNA working solution was added to each well and mixed thoroughly by pipetting. The plate was incubated for 2 minutes at RT and fluorescence was measured using a Cytation 5 plate reader to determine dsDNA concentrations. Equal amounts of each sample were pooled into a maximum total volume of 15 µL and prepared for sequencing. Prior to sequencing, dsDNA purity was quantified using a Nanodrop™ (Thermofisher).

2.7.8 High-throughput sequencing and BCR repertoire analysis

Libraries were sent for Illumina sequencing to capture BCR repertoire. Two FASTQ files, R1 and R2, were generated per sample and processed using the MiXCR software (v3.0, MiLaboratory), which is an immunoinformatic tool for analysing high-throughput sequencing data of BCRs. The pipeline included several steps (Figure 2.4):

1. **Data preprocessing**: Raw sequencing reads were imported into MiXCR to automatically handle quality filtering, read alignment and extraction of BCR regions.
2. **Alignment and clonotype identification**: MiXCR was run using the BIOMED-2 present for heavy chain to perform alignment and identify V(D)J segments. The software aligned reads to the IMGT® database and identified

clonal sequences based on CDR3 regions. This step ensured precise identification of V, D and J segments in the BCR repertoire.

3. **Post-Processing and data generation**: Following alignment, a post-analysis step was performed in MiXCR to generate a comprehensive JSON file containing information on clonotype, CDR3 regions and V (D) J gene usage. For visualisation of V and J gene combinations, CIRCOS plots were created using the online generator (https://mk.bcgsc.ca/tableviewer/visualize/), providing a graphical representation of gene segment relationships.
4. **Clonotype analysis and visualisation**: The output data from MiXCR were imported into the Immunarch package (v0.6.5) in R for further clonotype analysis, such as clonotype frequency, rare clonal proportion, relative clonal abundance and the distribution of CDR3 length.

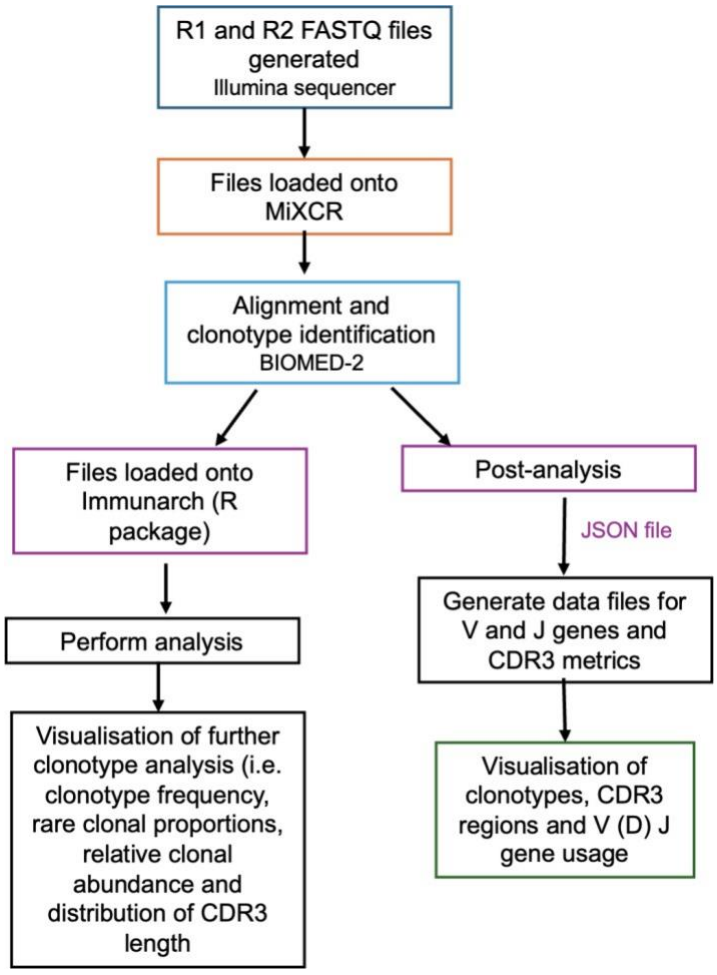

Figure 2.4: BCR repertoire sequencing data analysis workflow. A schematic outlining the key steps involved in BCR repertoire sequencing data analysis pipeline.

Chapter 3 - Establishing conditions for robust analysis of *in vitro* B-cell differentiation

3.1 Introduction

The immunophenotype of differentiating B-cells in healthy donors was first determined at different time points up to and including D13, according to the protocol previously established by the group (Cocco *et al.,* 2012; Stephenson *et al.,* 2019; Stephenson *et al.,* 2021). At day 0, PMBCs were isolated and provided with optimum $F(ab')_2$ anti-IgG/M/A and CD40L stimulation, as outlined in Figure 1.4, to mimic *in vitro* TD B-cell differentiation. Alternatively, stimulation was elicited by the TLR7 agonist, R848, to mimic TI B-cell differentiation. Flow cytometry and ELISA analysis was performed at critical differentiation stages (i.e. days 0, 3, 6 and 13) to study: surface marker changes, intracellular and secreted immunoglobulin expression. The initial establishment of the working *in vitro* model would provide insight into potential approaches to optimise the protocol for use in AD patients. Hence, the initial aim of establishing the published *in vitro* model under different conditions will be addressed in this chapter.

3.2 In vitro differentiation of isolated human B-cells using TD conditions

Following B-cell isolation from PBMCs obtained from 50 mL fresh healthy control (HC) blood (Cocco *et al.,* 2012; Stephenson *et al.,* 2019; Stephenson *et al.,* 2021) outlined in Chapter 2.3, the purity of undifferentiated B-cell phenotypes were determined using flow cytometry. As denoted by CD19+CD20+ expression, B-cell purity at day 0 (D0) was 99.7% and cells were overall CD19+CD20+CD38^{lo}CD138-, as expected for undifferentiated, unactivated B-cells (Sanz *et al.,* 2019). TD activated cells at D3 were CD19+CD20+CD27-CD38^{hi}CD138-, and plasmablast differentiation became apparent at D6 when CD20 expression began decreasing and CD27 expression increased, giving a CD19+CD20-CD27+CD38^{hi}CD138- phenotype. The large increase in CD138+ B-cells by D13 suggests 56% of cells are maturing into LLPCs (CD19+CD20-CD27+CD38^{hi}CD138+) (Figure 3.1). This differentiating D0-D13 phenotypic trend was observed amongst differentiation series from additional and independent HCs (Figure 3.2).

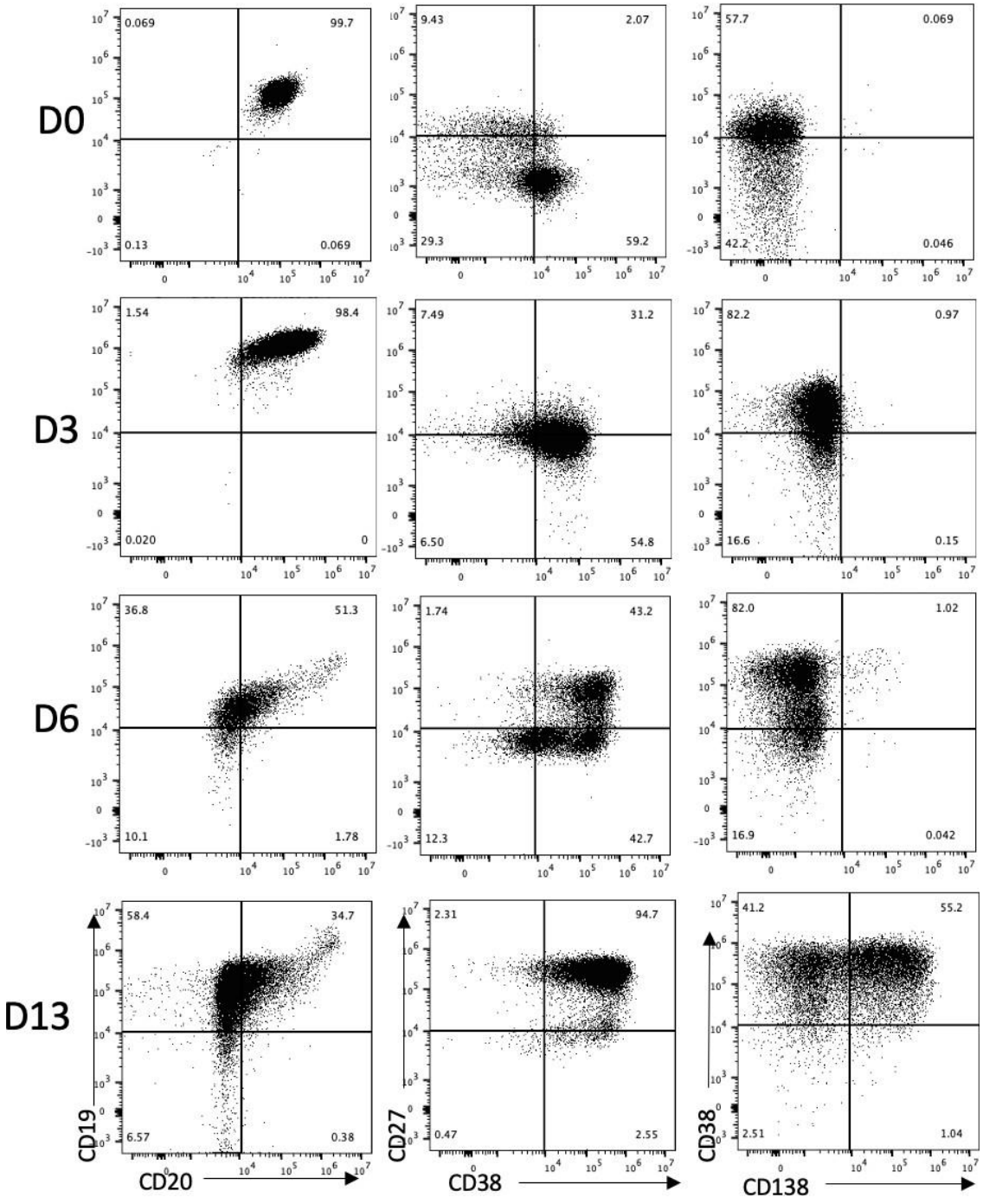

Figure 3.1: Surface immunophenotype of *in vitro* differentiated B-cells between days 0 and 13 stimulated with TD conditions. Total B-cells were isolated from healthy donor peripheral blood and stimulated with F(ab')2 anti-IgG/M/A and CD40L at day 0. Cytokines and supplements were added at specific time points: day 0: IL-2, IL-21; day 3: IL-2, IL-21, lipid media, amino acids (AA**);** day 6: IL-6, IL-21, APRIL, lipid media, AA. Surface staining was determined on days 0, 3, 6 and 13 for the study of plasma cell differentiation. Representative data is shown for one donor.

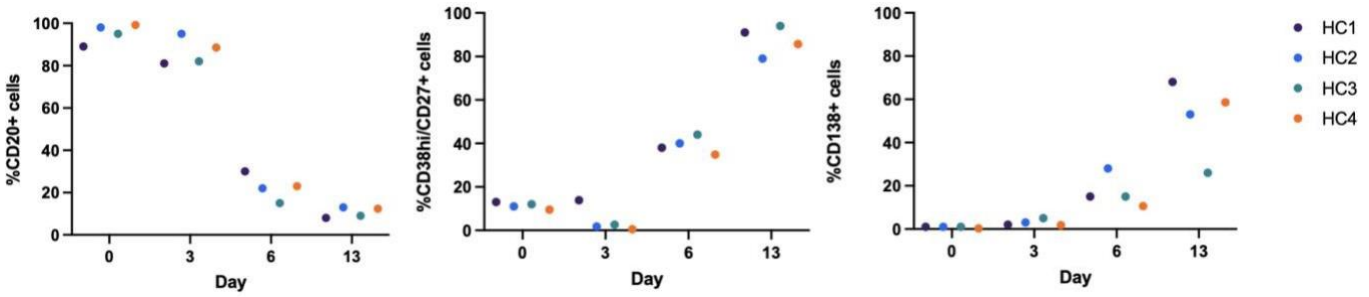

Figure 3.2: Phenotypic profiles of healthy control B-cells denoting the relative percentages of CD20+; CD38^{hi}CD27+ and CD138+ B-cells between days 0 and 13 stimulated with TD conditions. Total B-cells were isolated from representative healthy control (HC1) and additional control (HC2, HC3 and HC4) peripheral blood and stimulated with F(ab')$_2$ anti-IgG/M/A and CD40L at day 0. Surface staining was determined on days 0, 3, 6 and 13 (D0-13) for the study of plasma cell differentiation. Each plot represents the percentage of cells expressing the stated CD marker. Independent differentiations are represented by different colours.

Intracellular immunoglobulin phenotypes (IgG, IgM, and IgA) were also analysed to study B-cell differentiation *in vitro*, as abnormalities in immunoglobulin expression at various stages of B-cell development may be observed in patients. Consistent with the characteristics of undifferentiated, non-class-switched B-cells, 75.91% of unstimulated cells at D0 expressed IgM, while IgG and IgA levels were minimal. As differentiation progressed, the percentage of IgM+ cells decreased between D3 and D13, while IgG and IgA expression steadily increased (Figure 3.3). These trends in intracellular IgM, IgG, and IgA were consistently observed across multiple independent HCs (Figure 3.4) and are characteristic of B-cell differentiation. This pattern may reflect immunoglobulin class switching, the preferential survival or expansion of switched B-cells, or the outgrowth of switched PCs. Furthermore, these findings support the notion that LLPCs predominantly express IgG and IgA.

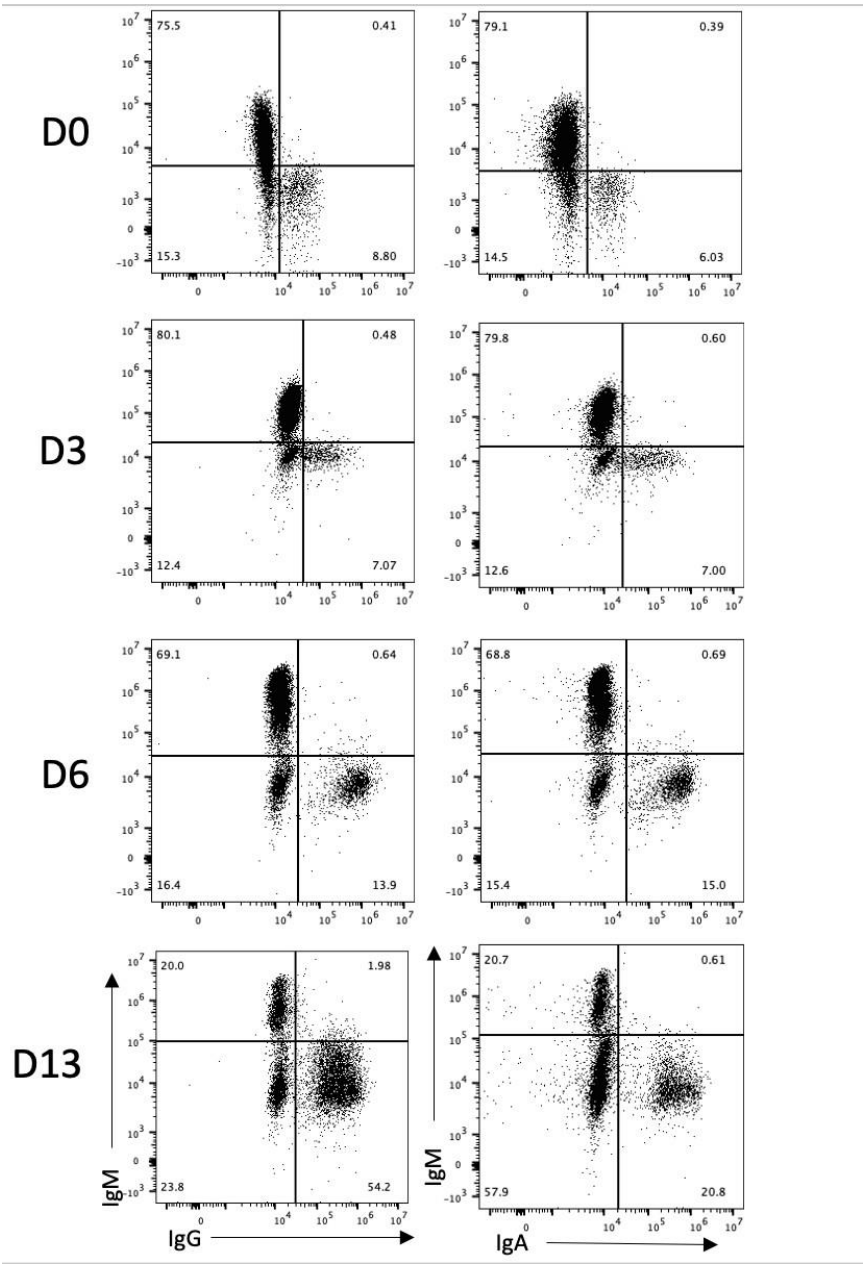

Figure 3.3: Intracellular immunophenotype of *in vitro* differentiated B-cells between days 0 and 13 stimulated with TD conditions. Total B-cells were isolated from healthy donor peripheral blood and stimulated with F(ab')$_2$ anti-IgG/M/A and CD40L at day 0. Cytokines and supplements were added at specific time points: day 0: IL-2, IL-21; day 3: IL-2, IL-21, lipid media, amino acids (AA**);** day 6: IL-6, IL-21, APRIL, lipid media, AA. In parallel with surface marker evaluation, intracellular immunoglobulin staining was determined on days 0, 3, 6 and 13 (D0-13). Representative data is shown for one donor.

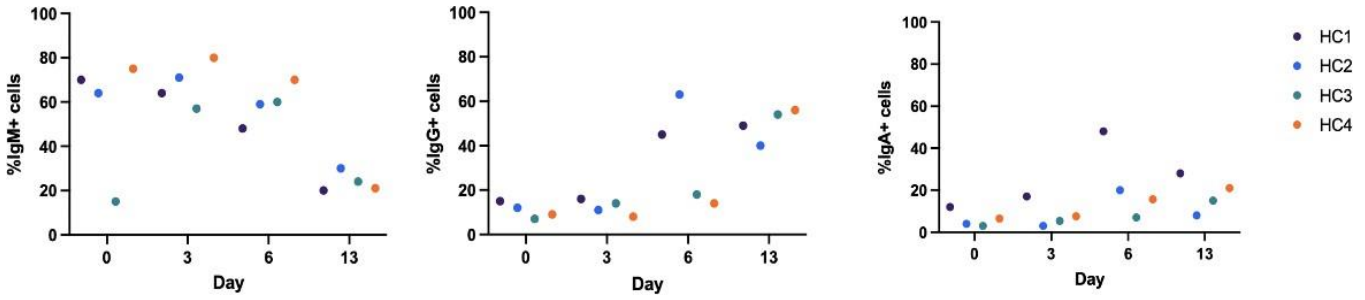

Figure 3.4: Intracellular immunoglobulin profiles of healthy control B-cells denoting the relative percentages of IgM+; IgG+ and IgA+ B-cells between days 0 and 13 stimulated with TD conditions. Total B-cells were isolated from representative healthy control (HC1) and additional control (HC2, HC3 and HC4) peripheral blood samples and stimulated with $F(ab')_2$ anti-IgG/M/A and CD40L at day 0. Cytokines and supplements were added at specific time points: day 0: IL-2, IL-21; day 3: IL-2, IL-21, lipid media, amino acids (AA**);** day 6: IL-6, IL-21, APRIL, lipid media, AA. Surface staining was determined on days 0, 3, 6 and 13 (D0-13). Each plot represents the percentage of cells expressing the stated immunoglobulin.

As an additional readout for B-cell differentiation into antibody-secreting cells, supernatants were collected on D6 and D13, and IgG, IgM, and IgA concentrations were analysed using ELISA. Similar to the immunophenotypic results denoted by flow cytometry, IgG and IgA concentrations gradually increased as B-cells differentiated into PCs by D13. Contrary to intracellular IgM, secreted IgM concentrations either remained constant or steadily increased by D13 in representative and additional HCs (n=4), likely reflecting the active production and release of IgM over the 6-day culture period, even as intracellular levels decrease due to class-switching to IgG and IgA (Figure 3.5). These results support the successful generation of immunoglobulin-secreting PCs from healthy B-cells, with features consistent with being LLPCs (Cocco *et al.,* 2012).

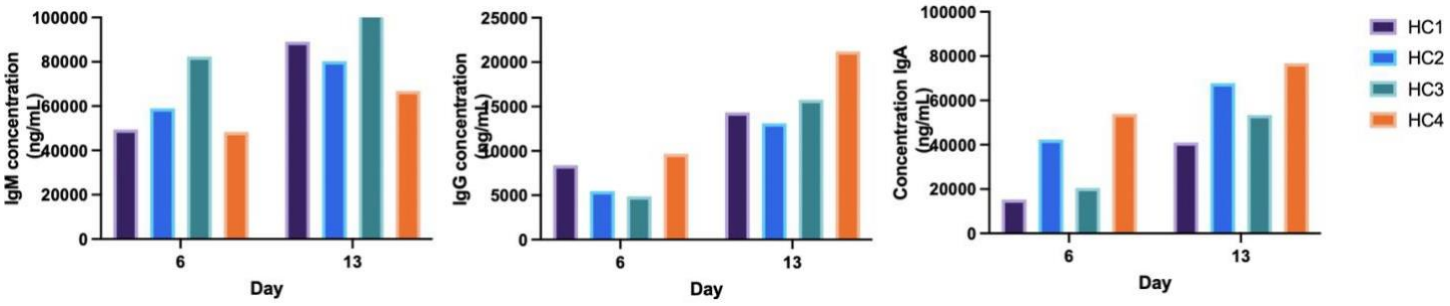

Figure 3.5: Quantification of IgM, IgG and IgA concentrations at days 6 and 13 following CD40L stimulation. Supernatants were collected at the specified time points and analysed using specific ELISA quantification kits as per the manufacturer's protocol. Values were normalised against respective control ELISA standards. Data is shown for the representative healthy control (HC1) and from three additional independent healthy controls (HC2, HC3 and HC4). Values are based on the average of three separate dilutions per sample.

B-cell counts were initially quantified using a haemocytometer, with CountBright absolute counting beads employed for time points beyond D6 (Figure 3.6). By D3, only a slight increase in cell numbers was observed, likely due to a balance between early activation-driven proliferation and significant cell death, which may have masked the extend of proliferation at this stage. By D6, as cells acquired a plasmablast phenotype, proliferation rates appeared to increase more noticeably, potentially reflecting both an increase in proliferation and a relative reduction in cell death compared to earlier timepoints. However, as differentiation progressed, proliferation sharply declined, and the transition to the PC state was accompanied by extensive cell death, contributing to the subsequent reduction in cell numbers (Figure 3.6). Ultimately, only a small population of LLPCs persisted, shaped by both continued selective survival and ongoing cell loss.

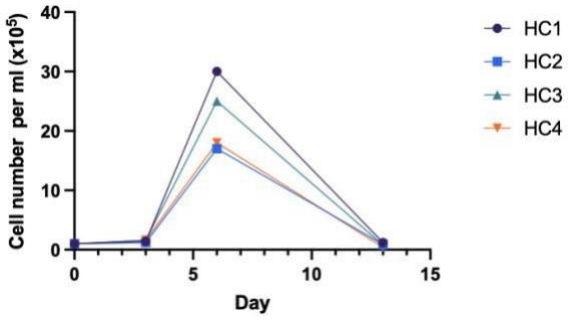

Figure 3.6: B-cell counts at days 0, 3, 6 and 13 following TD stimulation. Cell counts were determined manually using a haemocytometer from days 0-3 and using flow cytometry CountBright absolute counting beads at later time points. Data is shown for the representative healthy control (HC1) and from three additional healthy controls (HC2, HC3 and HC4).

3.3 *In vitro* differentiation of isolated human B-cells using TI conditions

Antibody deficiencies can affect both TI and TD B-cell stimulation, making it essential to study both conditions for a comprehensive understanding of disease mechanisms. The next objective was to mimic TI stimulation, using the TLR7 agonist R848. Optimal TI activation was achieved using 1 µg/mL R848 in combination with $F(ab')_2$ anti-IgG/M/A to facilitate BCR cross-linking (Ono *et al.,* 1996; Shrimpton *et al.,* 2020; Xie *et al.,* 2021). To allow direct comparison, R848-stimulated cells were analysed alongside TD CD40L-stimulated cells from the same HC blood sample.

R848-stimulated B-cell differentiation followed similar surface expression patterns to those observed with CD40L stimulation, demonstrating that both conditions can effectively trigger B-cell differentiation. In both cases, CD19 and CD20 levels gradually declined, while CD27 and CD38 expression progressively increased from D0 to D13. CD138 expression showed the greatest upregulation between D6 and D13 (Figure 3.7), regardless of the stimulation method.

However, R848 stimulation exhibited typical TI responses, such as the accelerated expansion of CD27+ memory cells and a faster overall rate of B-cell differentiation compared to TD CD40L stimulation (Figure 3.7). This faster differentiation is characteristic of TI responses, which are known to proceed more rapidly as they do not require T-cell help, relying instead on direct activation via TLRs or BCR cross-linking (Vos *et al.,* 2000). This acceleration under R848 was most evident on D6 and D13, where higher percentages of $CD38^{hi}CD138+$ PCs were observed (Figure 3.7). The same trend was observed in independent healthy controls, following the same experimental procedure (Figure 3.8).

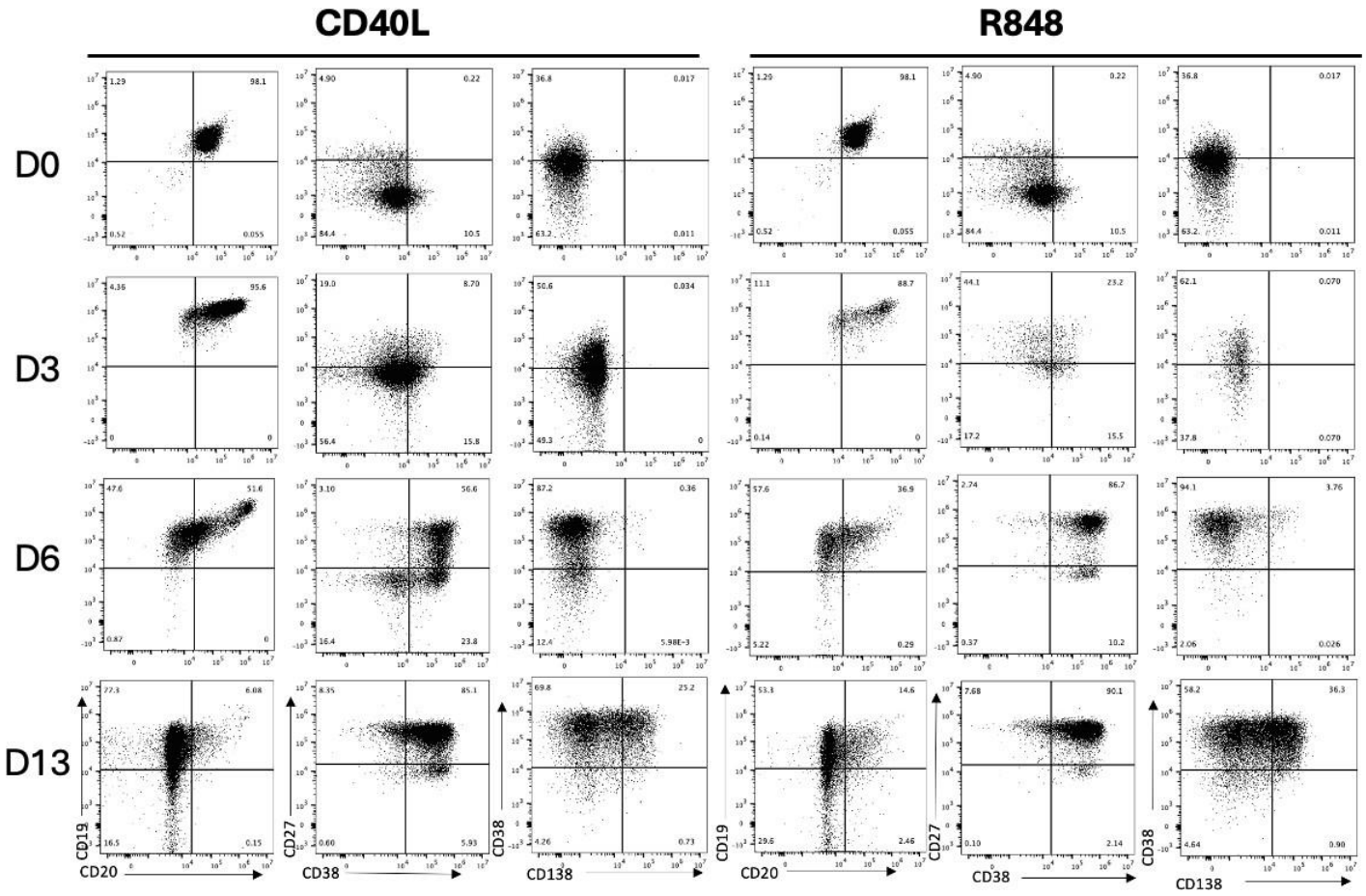

Figure 3.7: Surface immunophenotype of *in vitro* differentiated B-cells between days 0 and 13 stimulated either TI CD40L or TI R848 conditions. Total B-cells were isolated from healthy donor peripheral blood and stimulated with $F(ab')_2$ anti-IgG/M/A and either CD40 or 1ug/mL R848 at day 0. Cytokines and supplements were added at specific time points: day 0: IL-2, IL-21; day 3: IL-2, IL-21, lipid media, amino acids (AA**);** day 6: IL-6, IL-21, APRIL, lipid media, AA. Surface staining was determined on days 0, 3, 6 and 13 (D0-13). Representative data is shown for one donor.

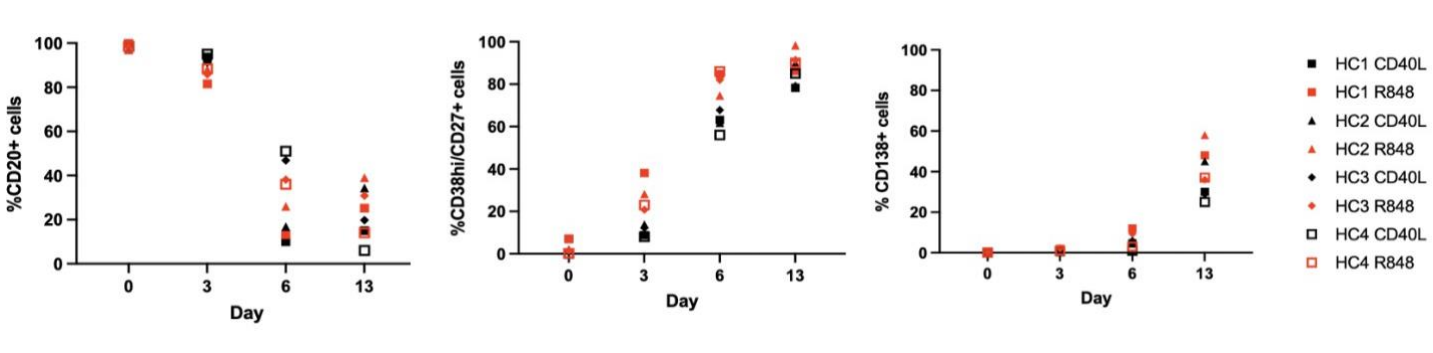

Figure 3.8: Phenotypic profiles of healthy control B-cells denoting the relative percentages of CD20+; CD38^{hi}CD27+ and CD138+ B-cells between days 0 and 13 stimulated either with TD CD40L or TI R848 conditions. Total B-cells were isolated from representative healthy control (HC1) and three additional healthy control (HC2, HC3 and HC4) peripheral blood samples and stimulated with F(ab')$_2$ anti-IgG/M/A and CD40L at day 0. Cytokines and supplements were added at specific time points: day 0: IL-2, IL-21; day 3: IL-2, IL-21, lipid media, amino acids (AA**);** day 6: IL-6, IL-21, APRIL, lipid media, AA. Surface staining was determined on days 0, 3, 6 and 13. Each plot represents the percentage of cells expressing the stated CD marker. Black denotes CD40L stimulated B-cells and red denoted R848 stimulated B-cells. Independent differentiation is represented by different shapes.

Intracellular immunoglobulin expression under both stimulatory conditions was generally similar; however, notable differences in the relative proportions of cells expressing particular immunoglobulins emerged following B-cell stimulation with either CD40L or R848. Both conditions exhibited the highest percentage of IgM expressing cells at D0-3, which subsequently declined. The percentages of IgG+ and IgA+ cells gradually increased by D13, indicating ongoing differentiation and class switching. Differences in the relative percentages of immunoglobulin isotypes were observed, including elevated percentages of IgM expressing cells under CD40L stimulation compared to R848 at all time points, as well as increased numbers of IgG expressing cells under R848 stimulation. The fraction of IgA+ cells remained comparable under both conditions, although it was notably higher at D13 in CD40L-stimulated cells (Figure 3.9). While subtle variations among different HCs were observed, the overall trend in intracellular immunoglobulin expression was consistent across all HCs studied (Figure 3.10). Any differences reflected the accelerated differentiation typically observed under TI conditions.

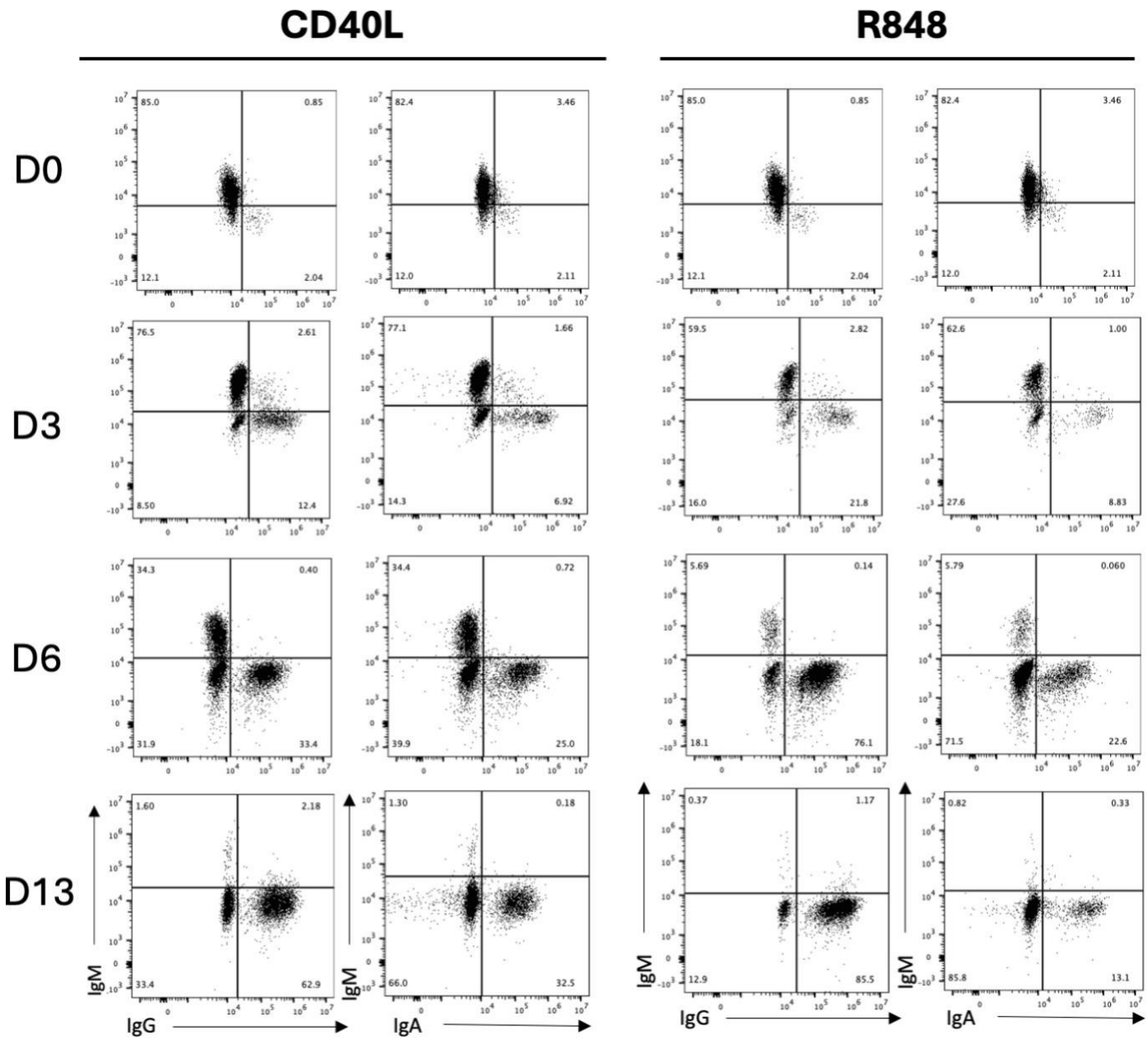

Figure 3.9: Intracellular immunophenotype of *in vitro* differentiated B-cells between days 0 and 13 stimulated with either TD CD40L or TI R848 conditions. Total B-cells were isolated from healthy donor peripheral blood and stimulated with F(ab')$_2$ anti-IgG/M/A and either CD40L or the TLR7 agonist, R848 at day 0. Cytokines and supplements were added at specific time points: day 0: IL-2, IL-21; day 3: IL-2, IL-21, lipid media, amino acids (AA**);** day 6: IL-6, IL-21, APRIL, lipid media, AA. Intracellular immunoglobulin staining was determined on days 0, 3, 6 and 13 (D0-13). Representative data is shown for one donor.

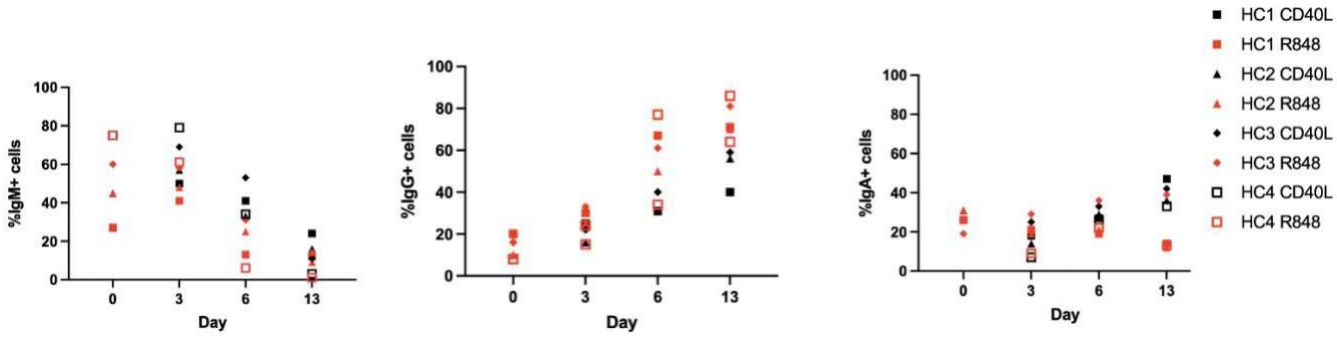

Figure 3.10: Intracellular immunoglobulin profiles of healthy control B-cells denoting the relative percentages of IgM+; IgG and IgA+ B-cells between days 0 and 13 stimulated with either TD CD40L or TI R848 conditions. Total B-cells were isolated from representative healthy control (HC1) and three additional healthy control (HC2, HC3 and HC4) peripheral blood samples and stimulated with $F(ab')_2$ anti-IgG/M/A and CD40L at day 0. Cytokines and supplements were added at specific time points: day 0: IL-2, IL-21; day 3: IL-2, IL-21, lipid media, amino acids (AA**);** day 6: IL-6, IL-21, APRIL, lipid media, AA. Surface staining was determined on days 0, 3, 6 and 13. Each plot represents the percentage of cells expressing the stated immunoglobulin. Black denotes CD40L stimulated B-cells and red denoted R848 stimulated B-cells. Independent differentiation is represented by different shapes.

Results from ELISA analyses of the representative HC revealed comparable patterns of IgG, IgM, and IgA concentrations between the two stimulation conditions. However, all isotypes exhibited slightly lower levels at D13 under R848 stimulation (Figure 3.11), likely due to differences in activation pathways and the efficiency of PC differentiation, as TI responses may not facilitate optimal antibody secretion as effectively as TD pathways (Cascalho and Platt, 2021). Nevertheless, the increased secretion of all immunoglobulin isotypes at D13 underscores the ability of the *in vitro* system to generate functional PCs under both TI and TD mimicking conditions.

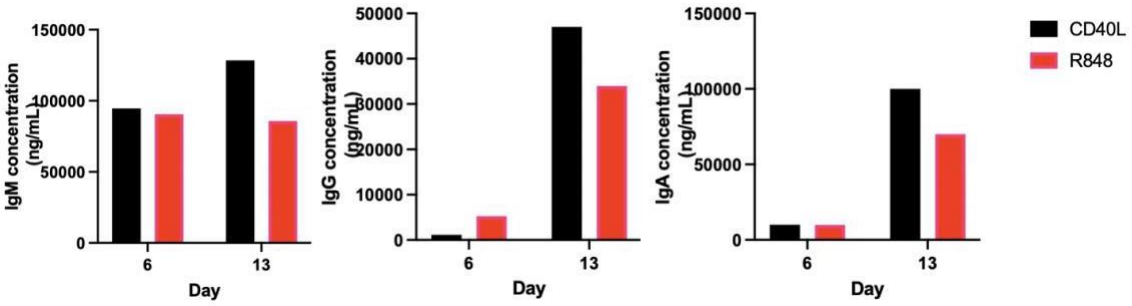

Figure 3.11: Quantification of IgM, IgG and IgA concentrations at days 6 and 13 following TD CD40L or TI R848 stimulation. Supernatants were collected at the specified time points and analysed using specific ELISA quantification kits as per the manufacturer's protocol. Values were normalised against respective control ELISA standards. Representative data is shown for one donor, and values are based on the average of three separate dilutions per sample.

Cells stimulated with either CD40L or R848 exhibited similar proliferation patterns on days 0, 3, 6, and 13. However, CD40L-mediated stimulation resulted in an average 9.2-fold increase in proliferation, compared to a 4.7-fold increase observed with R848-induced stimulation. This data aligns with previous research indicating superior proliferation under CD40L conditions, particularly between days 3 and 6 (Shrimpton *et al.,* 2020). Following this peak, cell numbers declined under both stimulation conditions, eventually stabilising at a low plateau around day 13, with only a small population of LLPCs managing to persist (Figure 3.12).

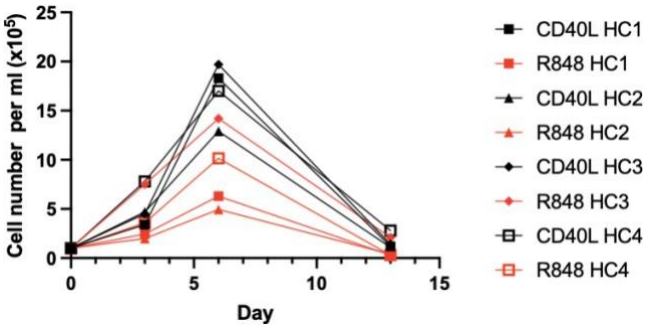

Figure 3.12: B-cell counts at days 3, 6 and 13 following TD CD40L or TI R848 stimulation. Cell counts were determined manually using a haemocytometer on D0-3 and using flow cytometry CountBright absolute counting beads at later time points. Data is shown for the representative healthy control (HC1) and from three additional healthy controls (HC2, HC3 and HC4).

3.4 *In vitro* B-cell differentiation in fractioned naïve versus memory populations

In cases where immunodeficient patients have impairments/deficiencies specifically affecting B naïve or memory cell populations, fraction-specific assays should be performed to ensure patients and control cell inputs are similar. Hence, CD40L + $F(ab')_2$ anti-IgG/M/A differentiation assays of fractioned healthy donor naïve or memory populations was reproduced using methods outlined in Chapter 2.2.3.

The overall phenotypes of fractioned naïve and memory populations from D0 to D13 in both representative and additional HCs evidenced a typical differentiation marker phenotypic progression, similar to Figures 3.1 and 3.7. However, differences between the naïve versus memory cell fractioned were seen across HCs.

Prior to stimulation at D0 in the representative HC, both fractions exhibited purity levels exceeding 98%. The unstimulated CD27+ expression was around 57% higher in memory versus naïve B-cell populations, which is indicative of a memory B-cell phenotype. While elevated CD27+ expression in memory cells was consistently observed at all time points, the relative percentages of CD27+ cells increased in both fractions by D13, ultimately becoming similar as PCs developed. Although $CD38^{hi}$ expression was higher in naive cells at D0, the accelerated $CD38^{hi}$ expression in memory cells surpassed that of naive populations thereafter (Figure 3.13).

Data from the other HCs also indicated a slightly elevated percentage of $CD38^{hi}$CD138+ PCs at days 6 and 13 in the memory fractions (Figure 3.14). Consistent with published literature, these findings suggest that accelerated differentiation may occur more readily in memory populations compared to naive populations (Arpin and Liu, 1997; Tangye *et al.,* 2003).

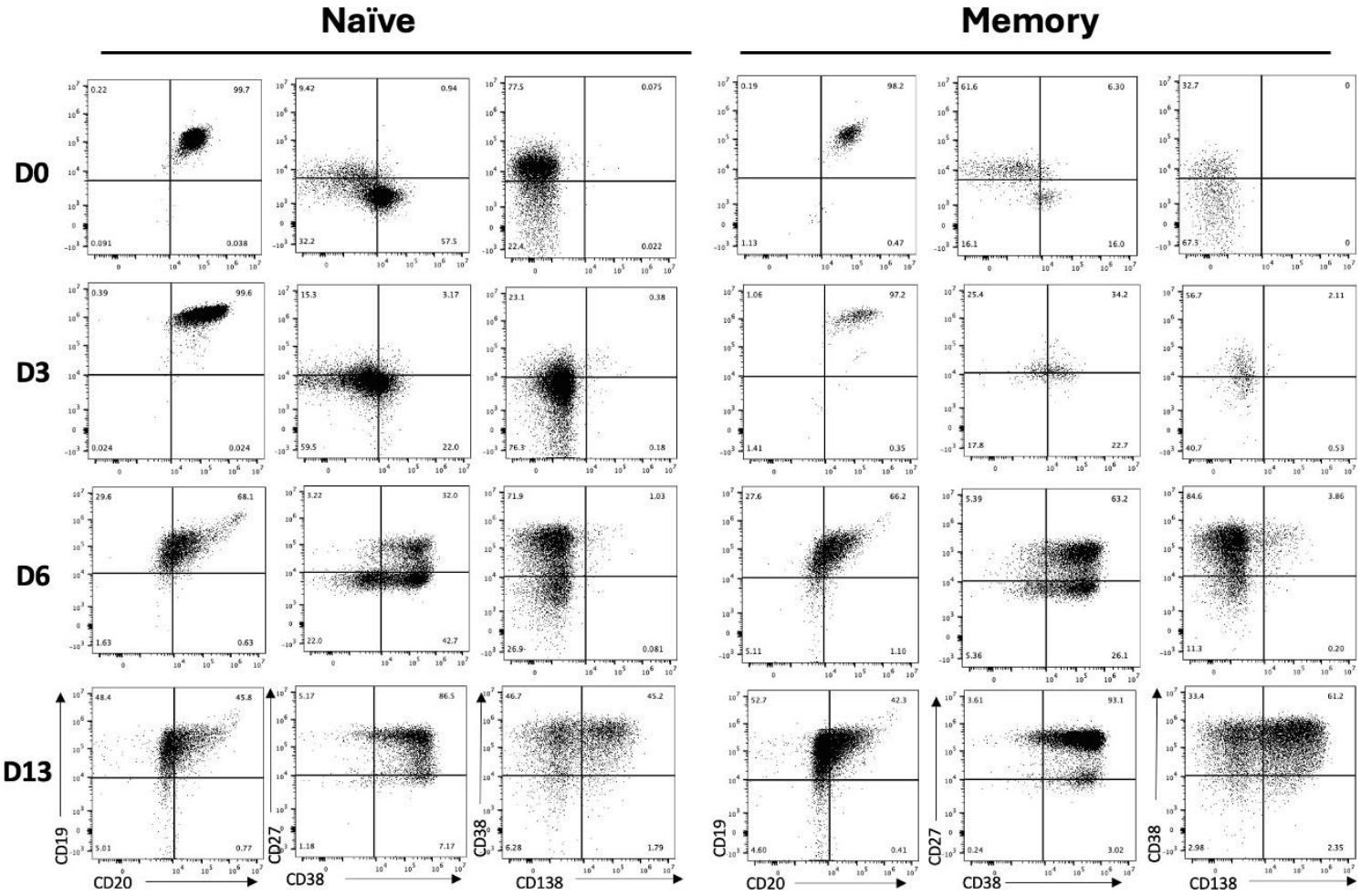

Figure 3.13: Surface immunophenotype of *in vitro* differentiated B naïve and B memory cells between days 0 and 13 stimulated with TD CD40L conditions. Total B-cells were isolated from healthy donor peripheral blood and stimulated with F(ab')$_2$ anti-IgG/M/A and CD40L at day 0. Cytokines and supplements were added at specific time points: day 0: IL-2, IL-21; day 3: IL-2, IL-21, lipid media, amino acids (AA**);** day 6: IL-6, IL-21, APRIL, lipid media, AA. Surface staining was determined on days 0, 3, 6 and 13 (D0-13). Representative data is shown for one donor.

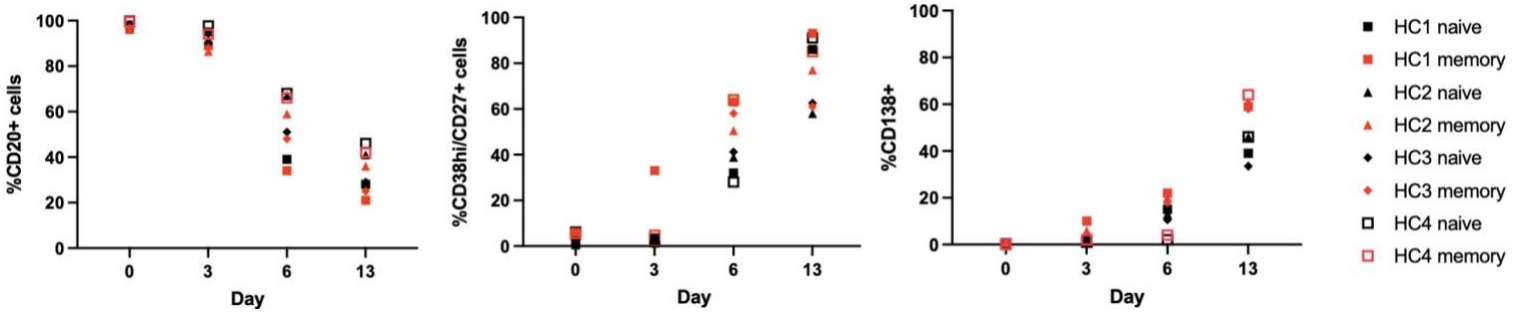

Figure 3.14: Phenotypic profiles of healthy control B-cells denoting the relative percentages of CD20+; CD38^{hi}CD27+ and CD138+ B-cells between days 0 and 13 in naïve versus memory B-cell fractions. Total B-cells were isolated from representative healthy control (HC1) and three additional healthy control (HC2, HC3 and HC4) peripheral blood samples and stimulated with F(ab')$_2$ anti-IgG/M/A and CD40L at day 0. Cytokines and supplements were added at specific time points: day 0: IL-2, IL-21; day 3: IL-2, IL-21, lipid media, amino acids (AA**);** day 6: IL-6, IL-21, APRIL, lipid media, AA. Surface staining was determined on days 0, 3, 6 and 13. Each plot represents the percentage of cells expressing the stated CD marker. Black denotes naïve B-cell fractions and red denotes memory B-cell fractions. Independent differentiation is represented by different shapes.

Intracellular immunoglobulin expression profiles showed similar trends across HCs, with a consistent decrease in IgM and a corresponding increase in IgG and IgA that aligned with the profiles depicted in previous figures. However, notable differences emerged between the naive and memory populations.

Specifically, IgM expression was higher in the naive fractions from days 0 to 6 compared to their memory counterparts, though these differences diminished by D13. Both fractions exhibited a progressive increase in IgG+ levels, with memory populations consistently demonstrating higher expression across all time points examined. In the representative control, IgA expression was consistently higher in memory fractions across all time points; however, by day 13, levels equilibrated to closely resemble those in naive populations (Figure 3.15). This pattern was also observed in the other controls (Figure 3.16).

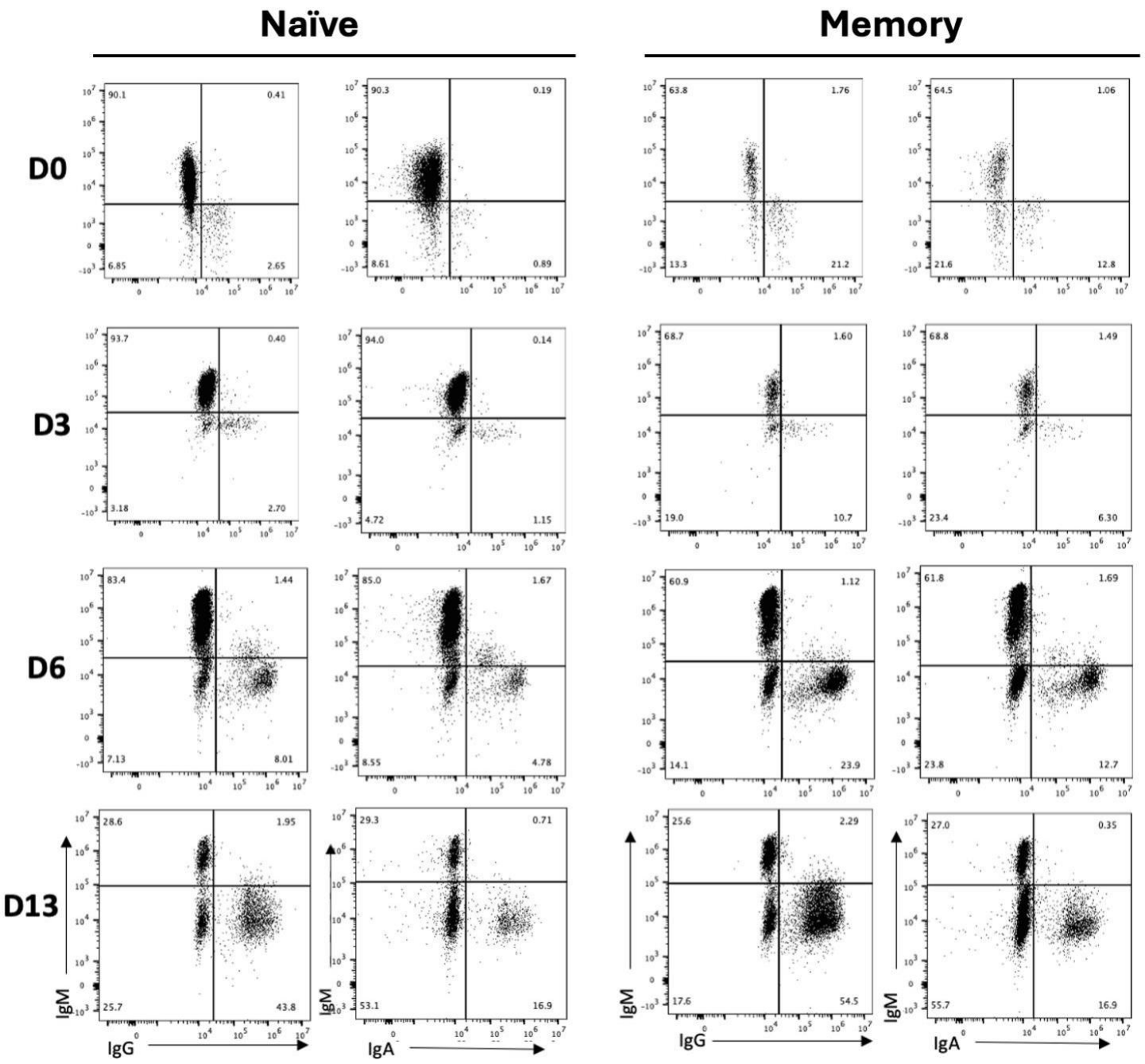

Figure 3.15: Intracellular immunophenotype of *in vitro* differentiated B naïve and B memory cells between days 0 and 13 stimulated with TD CD40L conditions. Total B-cells were isolated from healthy donor peripheral blood and stimulated with F(ab')$_2$ anti-IgG/M/A and CD40L at day 0. Cytokines and supplements were added at specific time points: day 0: IL-2, IL-21; day 3: IL-2, IL-21, lipid media, amino acids (AA)**;** day 6: IL-6, IL-21, APRIL, lipid media, AA. Surface staining was determined on days 0, 3, 6 and 13 (D0-13). Representative data is shown for one donor.

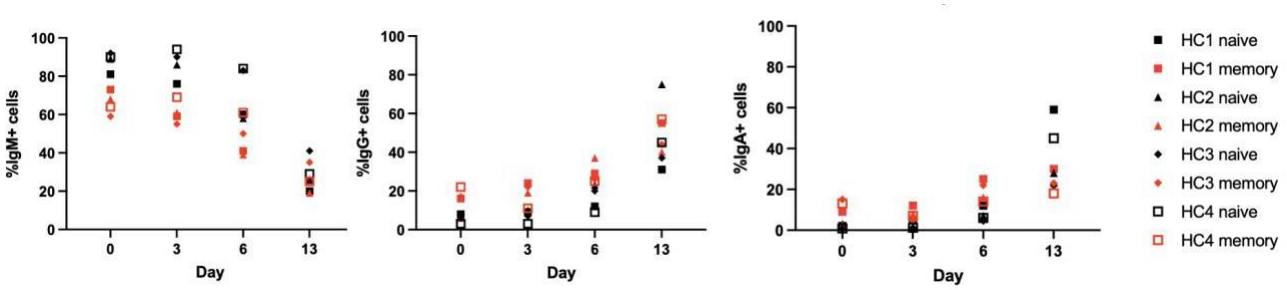

Figure 3.16: Intracellular immunoglobulin profiles of healthy control B-cells denoting the relative percentages of IgM+; IgG+ and IgA+ cells between days 0 and 13 in naïve versus memory B-cell starting fractions. Fractionated B-cells were isolated from representative healthy control (HC1) and three additional healthy control (HC2, HC3 and HC4) peripheral blood samples and stimulated with F(ab')2 anti-IgG/M/A and CD40L at day 0. Cytokines and supplements were added at specific time points: day 0: IL-2, IL-21; day 3: IL-2, IL-21, lipid media, amino acids (AA**);** day 6: IL-6, IL-21, APRIL, lipid media, AA. Surface staining was determined on days 0, 3, 6 and 13. Each plot represents the percentage of cells expressing the stated immunoglobulin. Black denotes naïve B-cell fractions and red denotes memory B-cell fractions. Independent differentiation is represented by different shapes.

In the representative HC, the relative secretion of all immunoglobulin isotypes increased from days 6 to 13 as both populations underwent differentiation (Figure 3.17). While differences in immunoglobulin secretion became evident by D13, they were minimal across the various fractions. Notably, IgG concentrations were elevated in the memory cells, reflecting the accelerated generation of antibody-secreting CD138+ PCs relative to naïve counterparts observed in Figure 3.13. In contrast, variations in IgM and IgA secretion were less pronounced (Figure 3.17), preventing any definitive conclusions regarding these isotypes.

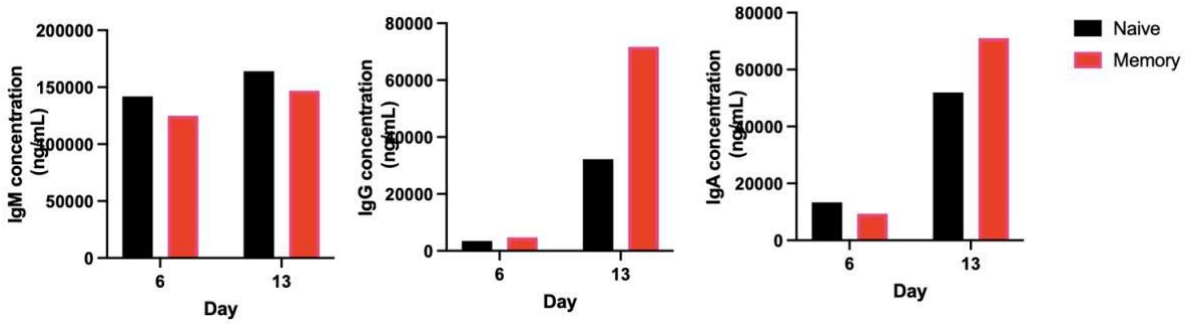

Figure 3.17: Quantification of IgM, IgG and IgA concentrations at days 6 and 13 in naïve versus memory B-cell fractions. Supernatants were collected at the specified time points and analysed using specific ELISA quantification kits as per the manufacturer's protocol. Values were normalised against respective control ELISA standards. Representative data is shown for one donor, and values are based on the average of three separate dilutions per sample.

The cell numbers of both naïve and memory populations remained stable and exhibited a similar proliferation pattern from days 0 to 13. Although both fractions in all HCs demonstrated increased proliferation from days 3 to 6, memory populations from HC4 proliferated two-fold more than their naïve counterparts. In contrast, HC3 showed reduced proliferation in the memory population compared to the naïve cells (Figure 3.18). These observed differences likely reflect individual donor variability.

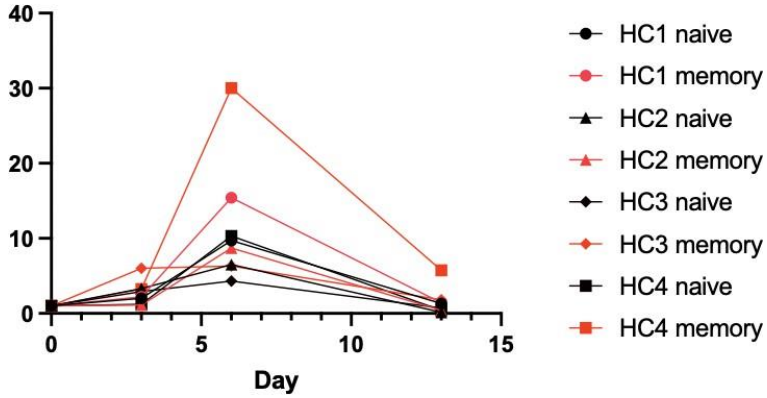

Figure 3.18: B-cell counts at days 0, 3, 6 and 13 in naïve versus memory B-cell fractions. Cell counts were determined manually using a haemocytometer on D0-3 and using flow cytometry CountBright absolute counting beads at later time points. Data is shown for the representative healthy control (HC1) and from three additional healthy controls (HC2, HC3 and HC4).

3.5 Discussion

The chapter provides preliminary data concerning *in vitro* B-cell differentiation in HCs under various conditions, which would allow the establishment of a system for modelling and analysing PC differentiation in antibody-deficient individuals.

Complimentary with previous data, CD40L stimulation elicited the normal phenotypic progression of HC B-cells into PCs by D13 (Cocco *et al.,* 2012; Stephenson *et al.,* 2019; Stephenson *et al.,* 2022), as assessed using surface markers in multiple independent donor B-cell differentiations.

Intracellular and secretory IgG, IgM, and IgA expression supported the group's previous findings, especially highlighting IgG secretion as a hallmark of LLPCs (Cocco *et al*., 2012). IgA, which is highly expressed in mucosal PCs (Pabst, 2012), was analysed for its potential relevance in studying antibody deficiencies, particularly in SADs. Low IgA levels can pose a severe infection risk in SAD cases where IgM does not adequately compensate, especially in CLL cases (Pabst and Slack, 20; Jolles *et al*., 2021). The *in vitro* model has also illustrated reduced IgA expression in elderly samples, linking age-related IgA decline to mucosal vulnerability and potential implications for antibody deficiencies (Xie *et al.,* 2021).

Results shown here demonstrated that, in HCs, intracellular and secretory IgA levels increased from D0 to D13, albeit to a lesser degree than IgG. It is possible that IgA expression would continue increasing at timepoints beyond D13, as previous studies have reported that most IgA+ PCs are indeed long-lived regardless of their residential tissue (Wilmore *et al.,* 2021), and that IgA concentrations may peak three weeks after viral infection exposure (Sterlin *et al.,* 2020). However, D13 is the culture end-point in all differentiations, since any differences in: differentiation, immunoglobulin expression/secretion and cell numbers (with regards to patient samples) would become apparent by D13 as timepoints beyond tend to be LLPC maintenance stages (Cocco *et al.,* 2012; Stephenson *et al.,* 2019; Stephenson *et al.,* 2021). Hence, it is more meaningful to utilise all D13 cells for analysis than maintain the PC pool.

Preliminary data shown here additionally modelled B-cells in TD CD40L versus TI R848 conditions. Phenotypes were overall highly similar between B-cells stimulated with CD40L and R848, although minor differences were observed. One such difference was the accelerated expansion of CD27+ memory cells under TI conditions. In agreement with current literature (Simchoni and Cunningham-Rundles., 2015), this data reflects the elevated responsiveness to TLR7 stimulation of memory compared to naïve cells which itself is due to increased memory B-cell TLR7/9 expression (Bernasconi *et al.,* 2003). Another notable difference between stimulation under the different conditions was the somewhat quicker differentiation rate observed under R848 versus CD40L stimulation. Together with the accelerated expansion of memory B-cells seen with R848 compared to CD40L, this data supports the primed ability of memory B-cells to rapidly respond to pathogens and thus generate a quicker immune response (Good and Tangye, 2007).

However, intracellular data was somewhat surprising. Firstly, the percentage of IgM+ cells was higher under CD40L compared to R848 stimulation. This is contradictory to the literature (Poeck *et al.,* 2004; Simchoni and Cunningham-Rundles., 2015) which evidences greater IgM positivity with TLR stimulation in favour of the characteristically rapid TD response.

Secondly, flow cytometry data evidenced higher percentages of IgG+ cells under R848 conditions at all timepoints, when it was expected that TD conditions would elicit a longer-lasting IgG expression that generated more IgG+ cells than TI conditions. Despite this, ELISA results demonstrated little difference in IgG secretion between the two conditions. To this respect, the *in vitro* system can robustly model both TI and TD generation of antigen secreting B-cells.

Preliminary evidence comparing CD40L versus R848 B-cell differentiation suggests that the generation of an immune response is quicker under TI conditions, yet higher proliferation/cell counts observed under CD40L stimulation could reflect a stronger and longer-lasting response that is more capable of differentiating both memory and naïve populations in comparison to R848 stimulation (Simchoni and Cunningham-Rundles., 2015). Hence, TI responses elicit a faster immune response due to rapid and more transient differentiation of memory B-cells that are less persistent than TD responses. Studying both TD CD40L and TI R848 B-cell stimulation will be

important in the context of antibody deficiency, since a deficiency could primarily affect the functioning of proteins critical for one of the two stimulatory conditions (e.g. a deficiency affecting CD40/CD40L interaction). This may have different outcomes on the other stimulatory pathway which could, in turn, either: remain function, also be impaired or even over-compensate in a pathological manner to exacerbate a condition.

The independent differentiation of fractioned control naïve and memory populations is important when studying antibody deficient patients whereby only one of the two B-cell subtypes might be affected, since it limits the risk of cell count bias. Results obtained in these experiments, whereby PCs were generated at quicker rates amongst memory B-cells, and that memory B-cell populations had higher levels of IgG+ cells compared to naïve cells which themselves appeared more IgM+. Such findings support the literature (Deenick *et al.,* 2013), and observed memory versus naïve B-cell differences likely reflect the reduced activation threshold and subsequent ability of responding more rapidly to stimulation (i.e. accelerated differentiation) with memory B-cells. Similar to reasons discussed for R848 stimulation, quicker memory B-cell responses are partly due to their enhanced ability to respond to co-stimulatory signals (i.e. higher TLR expression), in addition to other factors including: earlier recruitment to cell division relative to naïve cells (Macalla *et al.,* 2005), higher CD80 and CD86 expression to facilitate T-helper cell assistance (Liu *et al.,* 1995; Tangye *et al.,* 1998; Ellyard *et al.,* 2004; Good *et al.,* 2009), differences in downstream BCR signalling pathways (Moens *et al.,* 2016) and the lower expression of genes negatively regulating cell cycle entry (Good and Tangye, 2007; Horikawa *et al.,* 2007; Deenick *et al.,* 2013).

Proliferation capacities of both fractions were overall similar from D0-13 across donors, whereby there is a rapid expansion of memory versus naïve B-cells at D6.

Collectively, this chapter establishes the B-cell differentiation model under various conditions as previously described by the group. Whilst this system robustly models B-cell differentiation in healthy cells, there is a need to optimise the protocol for suboptimal conditions and likely caveats that may occur when studying the B-cells of

patients with antibody deficiency. Hence, the next chapter will discuss protocol optimisation.

Chapter 4 – Optimising the *in vitro* B-cell differentiation system in healthy donors for application to COV-AD patient samples

4.1 Introduction

Data discussed thus far provides a fundamental basis of differentiating fresh healthy donor B-cells under different conditions using the established *in vitro* model system. Perhaps the most apparent caveat in these experiments, in the context of patients, is the practicality of obtaining the high PBMC and isolated B-cell counts achieved when starting with around 50 mL of fresh blood from HCs. Low starting B-cell numbers in patients could be the result of sample scarcity, use for multiple immunological assays, long-term storage/freezing or directly due to the defect(s). This is particularly true for the COV-AD study (Chapter 1.10), whereby PBMCs from a heterogenous cohort of primary and secondary antibody-deficient SARS-CoV-2 vaccine-responders and non-responders have been stored. Harnessing the B-cell differentiation assay may prove invaluable in the analysis of patient-specific B-cell responses and possible reasons for variable vaccine responses. However, the inevitability of low cell counts may hinder analysis, since the lower-limits of B-cell numbers for successful *in vitro* differentiation have not yet been studied.

4.2 *In vitro* B-cell differentiation using limited starting cell counts

It is yet to be determined whether low starting B-cell counts can be used with confidence when performing the B-cell differentiation assay. Accordingly, the next objective was to determine the potential for LLPC differentiation from low starting B-cell numbers in healthy donors and identify potential approaches to optimise the

culture system to maximise B-cell differentiation in the very low starting B-cell counts that would likely be seen in patient samples.

To initially compare the differentiation potential of varying starting B-cell numbers, 30 mL of fresh blood was obtained from HCs and separated into: 15 mL, 10 mL and 5 mL. Relative to the reduced cell numbers, the *in vitro* culture followed the same protocol outlined in chapter 2.2 with the same ratio of B-cells to the TD stimuli (Cocco *et al.,* 2012; Stephenson *et al.,* 2019; Stephenson *et al.,* 2021), however three independent (i.e. 15 mL vs 10 mL vs 5 mL) experiments were being run in parallel to establish the possibility of successful LLPC generation when starting with low B-cell counts and identify any divergences in differentiation and proliferation (Figure 4.1). Isolated PBMC and B-cell numbers per mL from three experimental repeats can be seen in Table 4.1.

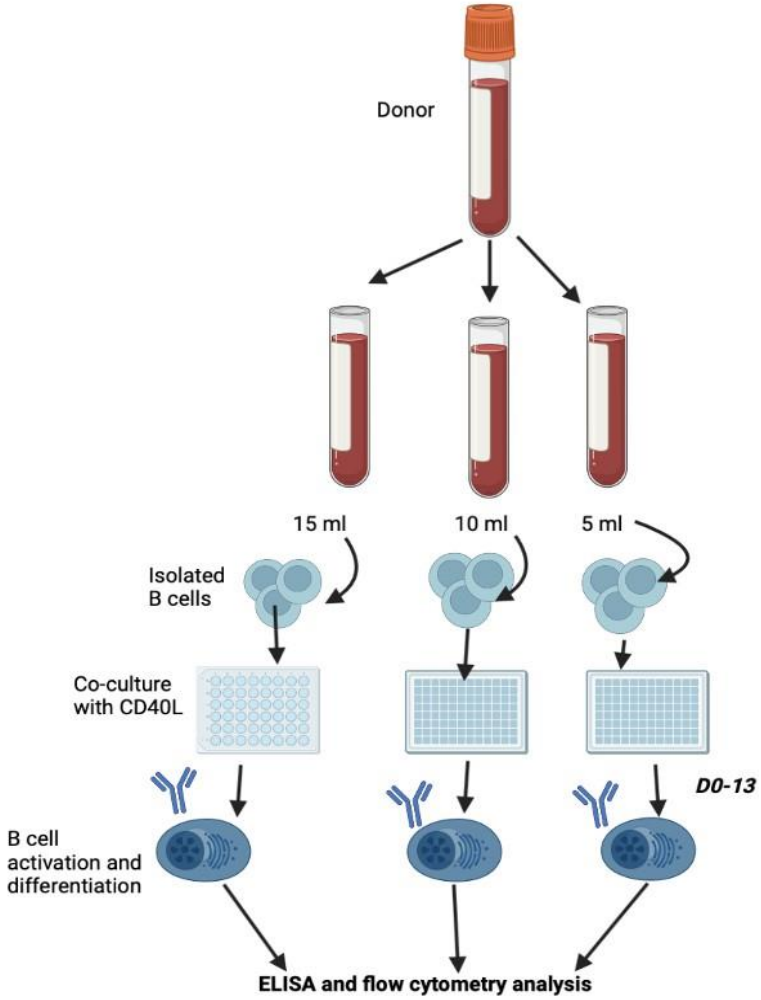

Figure 4.1: Experimental workflow for the analysis of low starting B-cell counts. 30 mL of blood was collected from a representative healthy control (HC) and divided into 15 mL, 10 mL and 5 mL samples. B- cells were isolated and co-cultured with TD conditions, as described in methods (Chapter 2.3). Samples were analysed at day 0, 6 and 13 (D0, D6 and D13) to assess the effect of working with low starting B- cell numbers.

PBMCs

A

	15 ml	10 ml	5ml
HC1	2.46×10^5	1.6×10^5	0.85×10^5
HC2	2×10^5	1.55×10^5	1.1×10^5
HC3	3.7×10^5	2.4×10^5	1.15×10^5

B-cells

B

	15 ml	10 ml	5ml
HC1	1.35×10^5	0.35×10^5	0.25×10^5
HC2	1.05×10^5	1.35×10^5	0.8×10^5
HC3	3.5×10^5	1.3×10^5	1.0×10^5

Table 4.1: **Cell counts.** Starting PBMC (**a**) and B-cell (**b**) numbers per mL in three different healthy controls (HC1, HC2 and HC3) from either 15 mL, 10 mL or 5 mL fresh blood. *In vitro* culture followed the same experimental protocol outline in chapter 2.3, with adjustments made relative to the reduced cell numbers.

The purity of all three starting blood amounts from the representative control (HC1) was >95% and D0 phenotypes were similar. D3 flow cytometry samples were to be omitted in this and all subsequent experiments to preserve as many cells as possible. Slight variations in the relative percentages of CD20+, $CD38^{hi}CD27+$ and CD138+ cells between the different starting amounts were observed, such as the retention of CD19+CD20+ expression in the 5 mL sample compared to 15 mL and 10 mL. Despite minor discrepancies in relative expression percentages, phenotypes were highly comparable across timepoints in the representative HC whereby characteristic progression into PC was observed (Figure 4.2). The same was true in the additional HC replicate experiments, although limited D6 cell counts in all conditions with one HC rendered analysis to D13 not possible (Figure 4.3).

Intracellular staining in the representative control showed variability in the relative percentages of IgM+, IgG+, and IgA+ cells across different time points, with distinct trends observed in response to different starting cell numbers (Figure 4.4). Notably, IgG+ cell percentages decreased progressively from 15 mL to 10 mL to 5 mL starting conditions, a trend that was consistent across both donors analysed to D13 (Figure 4.5). In contrast, IgA+ cell percentages showed a slight increase as the starting cell number decreased, suggesting a potential shift in differentiation dynamics when fewer cells were present. These findings indicate that initial cell numbers may influence the balance of IgG and IgA differentiation. Assessing a third donor, if sufficient cells had been available, would have been valuable to determine whether these trends were reproducible. Nonetheless, the staining patterns confirm that B-cells could successfully differentiate into antibody-secreting PCs across all conditions, despite variations in starting cell number (Figure 4.5).

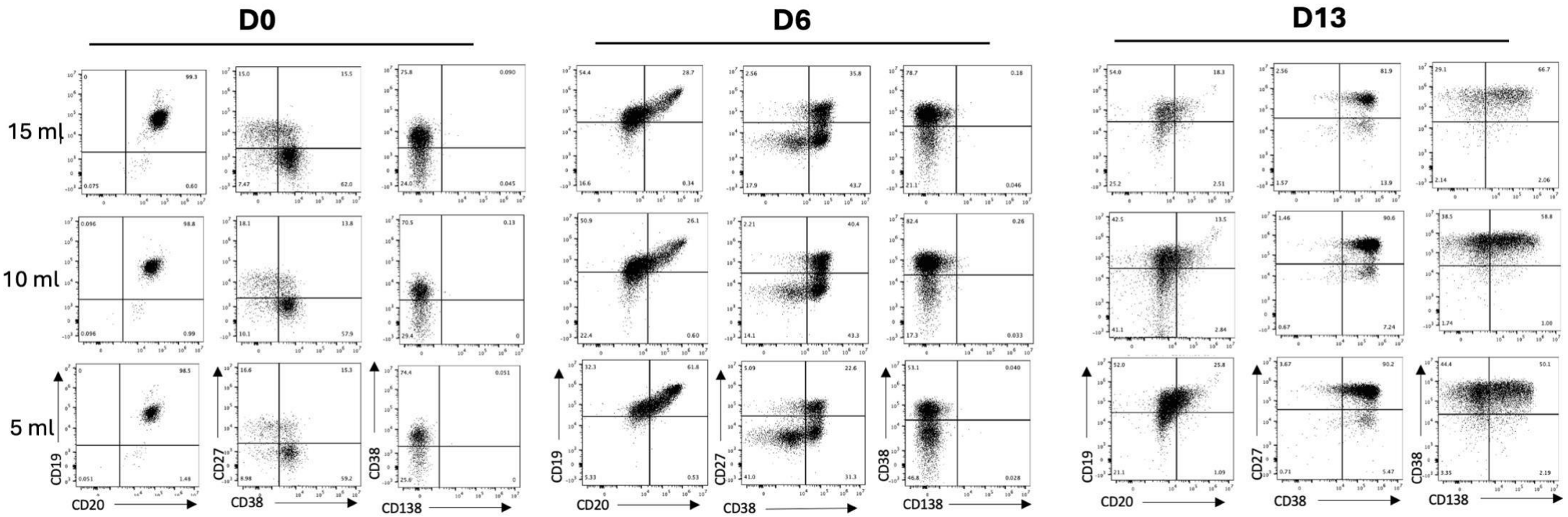

Figure 4.2: Surface immunophenotype at days 0, 6 and 13 of *in vitro* differentiated B-cells generated from either 15 mL, 10 mL or 5 mL stimulated with TD conditions. Total B-cells from 15, 10 and 5 mL were isolated from one healthy control (HC1) peripheral blood obtained and stimulated with $F(ab')_2$ anti-IgG/M/A and CD40L at day 0. Cytokines and supplements were added at specific time points: day 0: IL-2, IL-21; day 3: IL-2, IL-21, lipid media, amino acids (AA**);** day 6: IL-6, IL-21, APRIL, lipid media, AA. Surface staining was determined on days 0, 6 and 13 (D0-13). Representative data is shown for one donor.

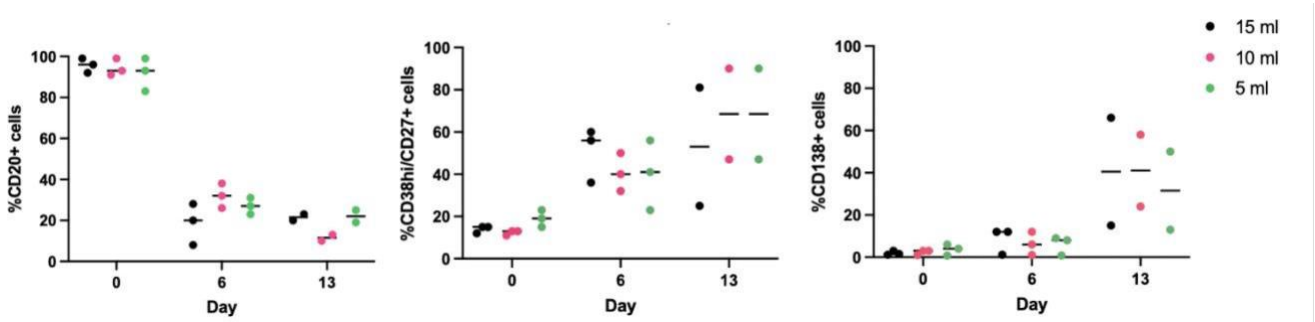

Figure 4.3: Phenotypic profiles of healthy control B-cells (HC1, HC2 and HC3) denoting the relative percentages of CD20+; CD38^{hi}CD27+ and CD138+ B-cells between days 0 and 13 generated from either 15 mL, 10 mL or 5 mL stimulated with TD conditions. Total B-cells were isolated from healthy control (HC1, HC2 and HC3, as indicated by the number of dots per sample) peripheral blood and stimulated with F(ab')$_2$ anti-IgG/M/A and CD40L at day 0. Surface staining was determined on days 0, 6 and 13. Each plot represents the percentage of cells in each donor (n=3) expressing the stated CD marker and each colour represents a different starting amount of blood. Note that limited day 6 cell counts in all conditions with one HC rendered analysis to D13 not possible.

Measurement of IgM, G and A secretion showed progressive increase in all isotypes from day 6-13 (Figure 4.6). Whilst values of all immunoglobulin isotypes appear slightly elevated at 10 mL, this is likely attributed to slight cell culture-related variation, such as the possibility of achieving an optimal cell density and nutrient availability for immunoglobulin secretion at this amount.

With regards to cell number, all starting volumes exhibited typical B-cell expansion patterns, with cell counts increasing to D6 and thereafter rapidly declining by D13. While the 15 mL starting volume demonstrated overall higher total cell numbers compared to the other starting volumes, the differences between the starting amounts were only noticeable at D0 and D6 (Figure 4.7) and were not striking. This suggests that, although the starting amounts showed some variation, all volumes were capable of supporting differentiation. The observed trend indicates that the balance between proliferation and apoptosis may be slightly more favorable for survival in the higher starting volumes, but overall, the differences were relatively modest.

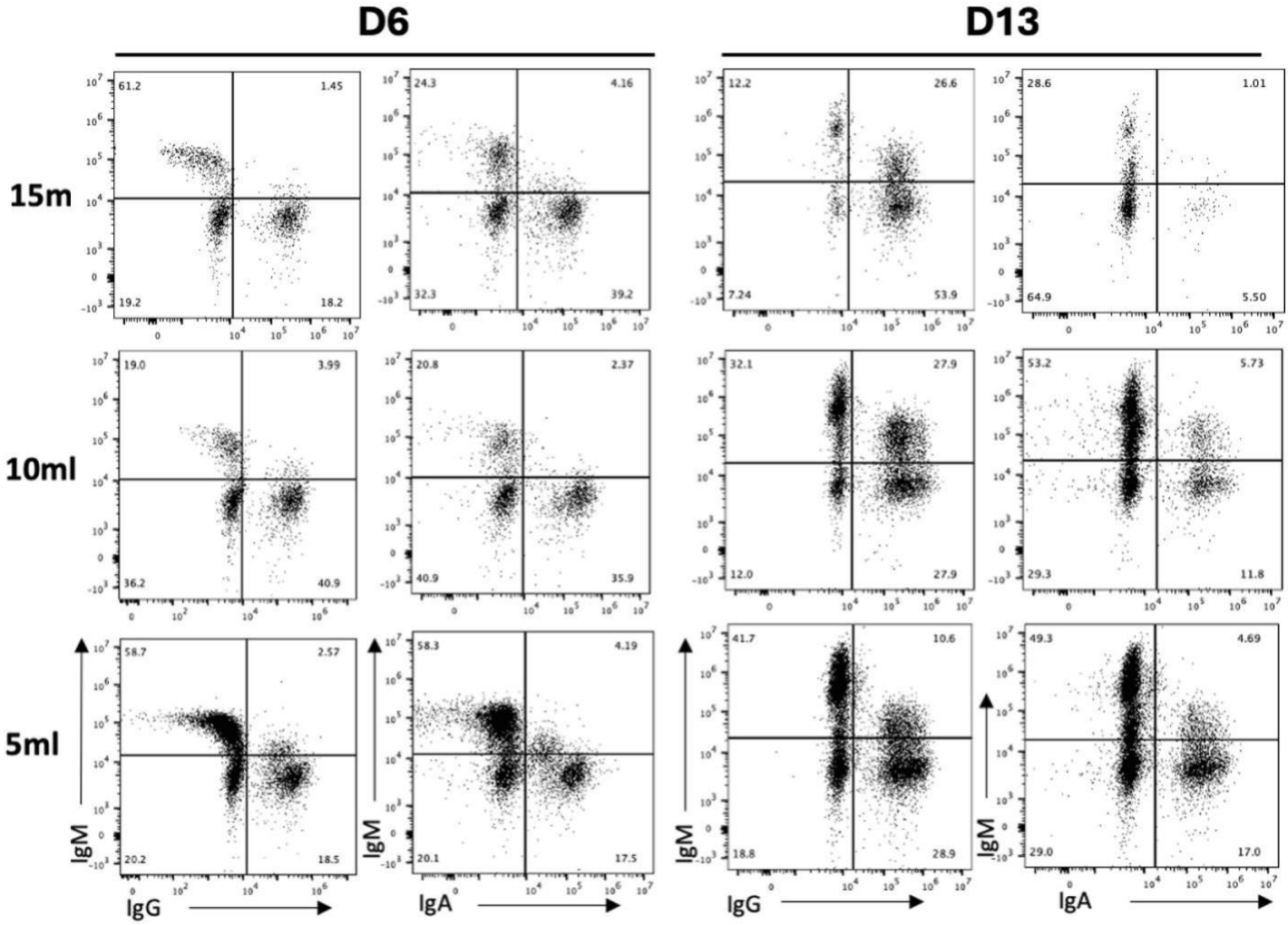

Figure 4.4: Intracellular immunophenotype of *in vitro* differentiated B-cells generated from either 15 mL, 10 mL or 5 mL stimulated with TD conditions. Total B-cells from 15, 10 and 5 mL were isolated from healthy control (HC1) peripheral blood obtained from the same donor and stimulated with $F(ab')_2$ anti-IgG/M/A and CD40L at day 0. Cytokines and supplements were added at specific time points: day 0: IL-2, IL-21; day 3: IL-2, IL-21, lipid media, amino acids (AA**);** day 6: IL-6, IL-21, APRIL, lipid media, AA. Intracellular staining was determined on days 6 and 13 (D6-13).

Representative data is shown for one donor.

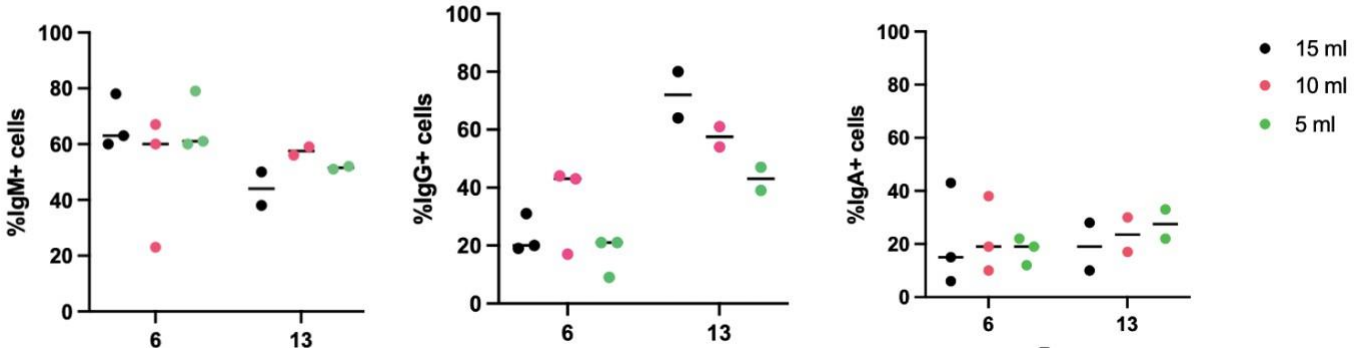

Figure 4.5: Intracellular immunoglobulin profiles of healthy control B-cells (HC1, HC2 and HC3) denoting the relative percentages of IgM+; IgG+ and IgA+ B-cells between days 0 and 13 generated from either 15 mL, 10 mL or 5 mL stimulated with TD conditions. Total B-cells were isolated from healthy donor peripheral blood and stimulated with $F(ab')_2$ anti-IgG/M/A and CD40L at day 0. Cytokines and supplements were added at specific time points: day 0: IL-2, IL-21; day 3: IL-2, IL-21, lipid media, amino acids (AA**);** day 6: IL-6, IL-21, APRIL, lipid media, AA. Intracellular staining was determined on days 6 and 13. Each plot represents the percentage of cells in each donor (n=3) expressing the stated immunoglobulin and each colour represents a different starting amount of blood. Note that limited day 6 cell counts in all conditions with one HC rendered analysis to D13 not possible.

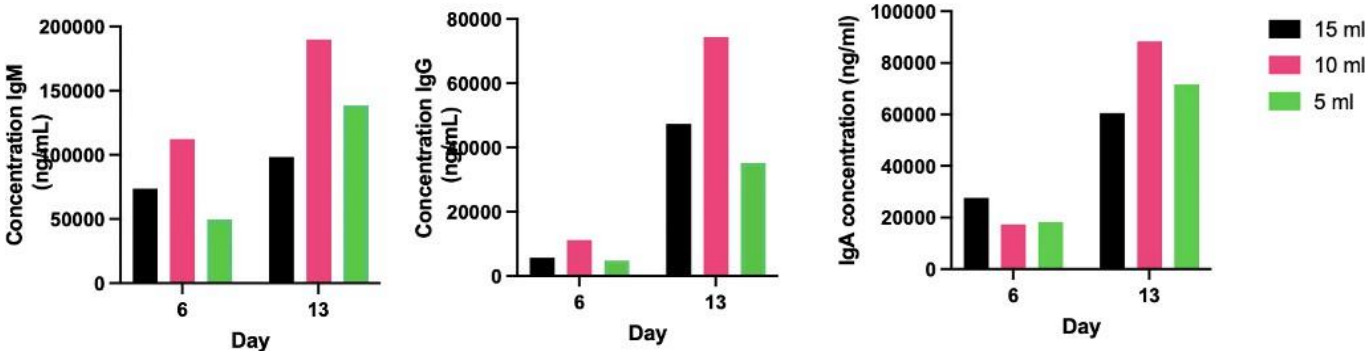

Figure 4.6: Quantification of IgM, IgG, IgA concentrations at days 6 and 13 in the representative healthy control (HC1) generated from either 15 mL, 10 mL or 5 mL under TD stimulation using CD40L of total B-cells. Supernatants from healthy control 1 were collected at the specified time points and analysed using specific ELISA quantification kits as per the manufacturer's protocol. Values were normalised against respective control ELISA standards. Representative data is shown for one donor, and values are based on the average of three separate dilutions per sample.

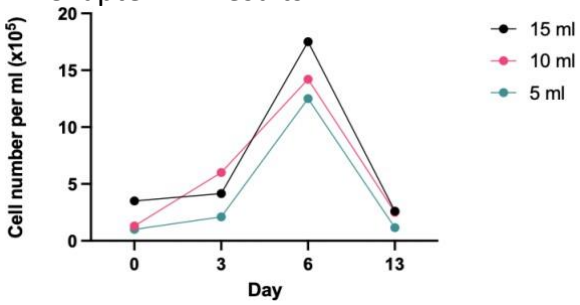

Figure 4.7: B-cell counts at days 0, 6 and 13 in the representative healthy control generated from either 15 mL, 10 mL or 5 mL under TD stimulation using CD40L of total B-cells. Cell counts were determined manually using a haemocytometer on D0-3 and using flow cytometry CountBright absolute counting beads at later time points. Data is shown for the representative healthy control (HC1).

In vitro data generated from B-cell differentiations starting with limited cell numbers demonstrates the potential and characteristic comparability of generating functional LLPCs, regardless of reduced PBMC counts. This data is promising for the potential translatability of patient samples to the *in vitro* system, even with lower starting cell numbers. However, a potential caveat highlighted by the data is the possible reduced ability for B-cell survival by the D13 timepoint, particularly in differentiations with lower starting cell counts. Given that patient cell numbers are anticipated to be much lower than those used in these experiments, this poses a challenge for obtaining sufficient numbers of samples at various timepoints for analysis. Enhancing B-cell survival through the addition of a survival factor, such as BAFF, early in B-cell differentiation may improve survival to the D13 LLPC stage and optimize the differentiation process (Marsman *et al.,* 2022).

4.3 Optimisation of *in vitro* B-cell differentiation with BAFF

The TNF family B-cell activation factor (BAFF) is a B-cell-specific survival factor that binds to the BAFF-receptor, transmembrane activator and calcium-modulating and cyclophilin ligand interactor (TACI) and (to a lower affinity) B-cell maturation antigen (BCMA) (Schneider., 2005). Engagement of BAFF with the BAFF-R induces PAX5 modulation and enhanced BCR signalling, which in turn elicits the upregulation of CD19 expression (Wang *et al.,* 2012). BAFF has been evidenced to increase B-cell survival in both mice and humans (Rolink *et al.,* 2002; Avery *et al.,* 2003; Marsman *et al.,* 2022) under various *in vitro* conditions. It could, therefore, be possible that the incorporation of BAFF into the established B-cell differentiation system could elevate B-cell numbers at D6-13 which would facilitate analyses.

The initial experimental aim was to compare the differences, if any, with versus without the incorporation of BAFF (AdipoGen, AF-40B-0112-3010) into the model system. 50 mL of blood was obtained from a HC and B-cells were isolated as per the protocol (Chapter 2.2). At the co-stimulation step, equal amounts of cells were split into three separate differentiation conditions. Condition 1 was treated with $F(ab')_2$, IL2, IL21 and BAFF at D0; condition 2 was treated with $F(ab')_2$, IL2 and IL21 at D0 with BAFF being added at D3 and condition 3 followed the normal protocol (Cocco *et al.,* 2012; Stephenson *et al.,* 2019; Stephenson *et al.,* 2021) without any addition of BAFF. In instances where BAFF was added, a concentration of 100 ng/mL was used (Figure 4.8), demonstrating the upper range recommended for robust B-cell activation and differentiation (Thien *et al.,* 2004). Experimental procedures were otherwise equivalent to the described protocol (chapter 2.2)

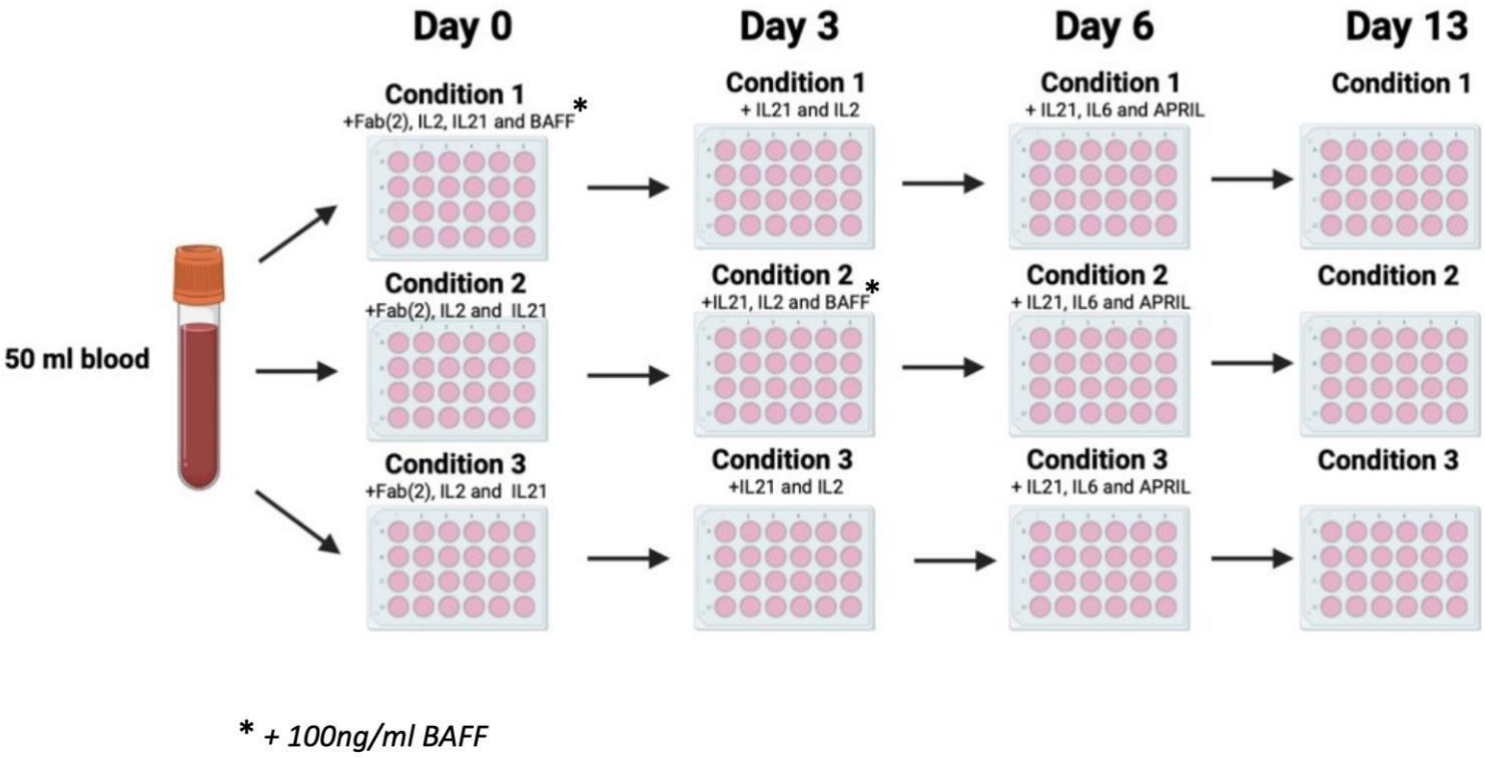

Figure 4.8: Experimental setup for the evaluation of the temporal effects of B-cell activation factor (BAFF) on B-cell activation and differentiation. Total B-cells were isolated from a healthy control and the impact of BAFF addition at day 0 versus day 3 of culture, relative to no addition, was assessed.

In all instances hereafter, BAFF-R surface marker (BD Biosciences, 564817) was used in replacement for CD20, and summary CD marker plots will include CD19+BAFF-R+ expression. This is both to confirm an initial pure B-cell population (i.e. both are typically highly expressed amongst pre-activated peripheral B-cells) as well as provide further clues on BAFF physiology. At D0, the phenotype of the representative control (HC1) evidenced a pure CD19+/BAFF-R+ B-cell population with a donor-specific anomaly of having high CD27+ expression prior to activation. By D6, cells stimulated with D3 BAFF appeared to lose BAFF-R expression to a higher degree than without BAFF or with D0 BAFF, although these differences were not observed thereafter. The expression of all other phenotypic markers in the representative HC were highly similar otherwise (Figure 4.9). Despite minor donor-specific discrepancies, all other HC replicates demonstrated highly comparable phenotypes, despite the addition of BAFF at any timepoint (Figure 4.10).

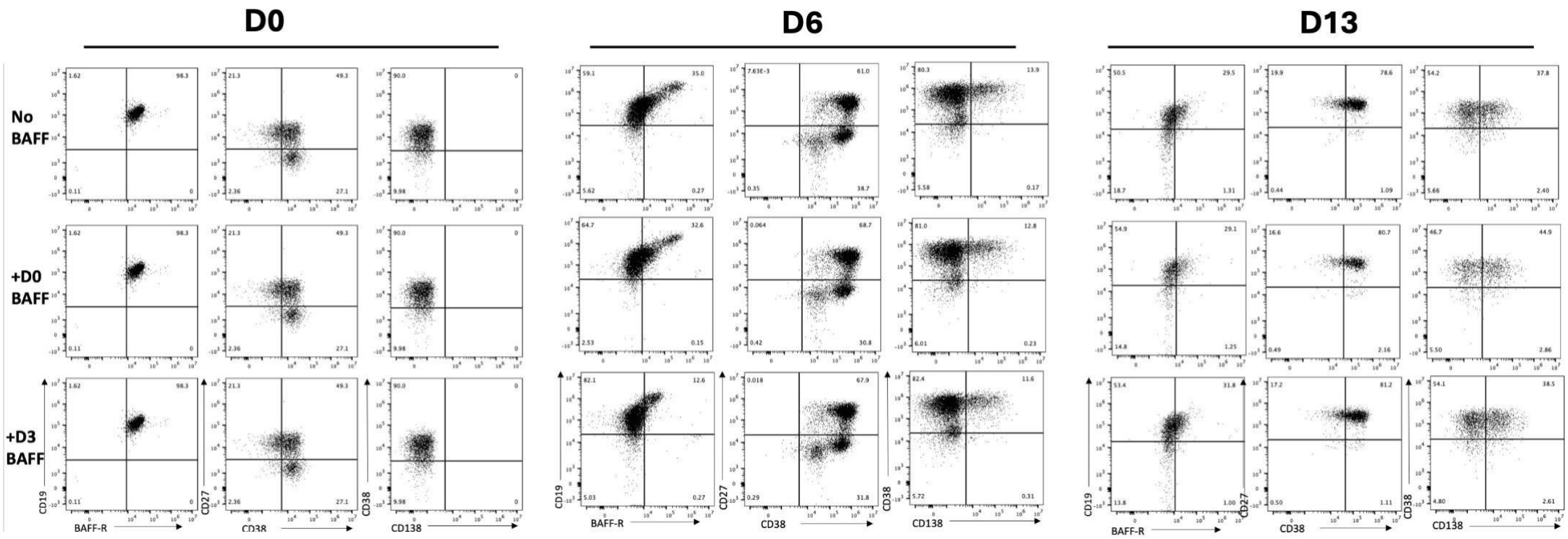

Figure 4.9: Surface immunophenotype at days 0, 6 and 13 of *in vitro* differentiated B-cells stimulated with TD conditions either in the absence of BAFF or with the addition of BAFF at day 0 (D0) or day 3 (D3). Total B-cells were isolated from 50 mL of healthy donor peripheral blood obtained from the same donor and stimulated with F(ab')$_2$ anti-IgG/M/A and CD40L at day 0. Cytokines and supplements were added at specific time points: day 0: IL-2, IL-21; day 3: IL-2, IL-21, lipid media, amino acids (AA**);** day 6: IL-6, IL-21, APRIL, lipid media, AA. Isolated B-cells were equally split into three conditions: No BAFF, BAFF added at day 0 or BAFF added at day 3. Surface staining was determined on days 0, 6 and 13 (D0-13). Representative data is shown for one donor.

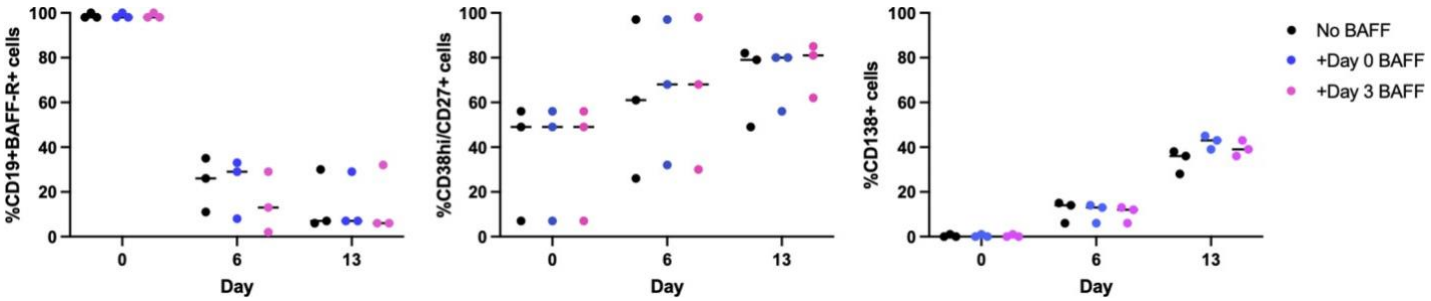

Figure 4.10: Phenotypic profiles of healthy control B-cells (HC1, HC2 and HC3) denoting the relative percentages of CD19+BAFF-R+; CD38^{hi}CD27+ and CD138+ B-cells between days 0 and 13 during the differentiation assay in no BAFF, day 0 or day 3 +BAFF conditions. Total B-cells were isolated from healthy control (n=3, as indicated by the number of dots per sample) peripheral blood and stimulated with F(ab')$_2$ anti-IgG/M/A and CD40L at day 0. Cytokines and supplements were added at specific time points: day 0: IL-2, IL-21; day 3: IL-2, IL-21, lipid media, amino acids (AA**);** day 6: IL-6, IL-21, APRIL, lipid media, AA. Surface staining was determined on days 0, 6 and 13. Each plot represents the percentage of cells expressing the stated CD marker and each colour represents different culture conditions.

Similarly, in HC1, intracellular immunoglobulin expression followed the expected patterns of isotype switching, with similar profiles observed regardless of the addition of BAFF (Figure 4.11). This consistency was also seen across additional controls, despite some variability in relative expression percentages between donors (Figure 4.12). Secreted immunoglobulin in HC1 displayed comparable levels between conditions, though the highest relative secretion was seen in the + day 3 BAFF condition (Figure 4.13). Despite this, both intracellular and secreted immunoglobulin data suggest that BAFF does not significantly alter immunoglobulin expression levels, highlighting its limited effect on overall immunoglobulin production.

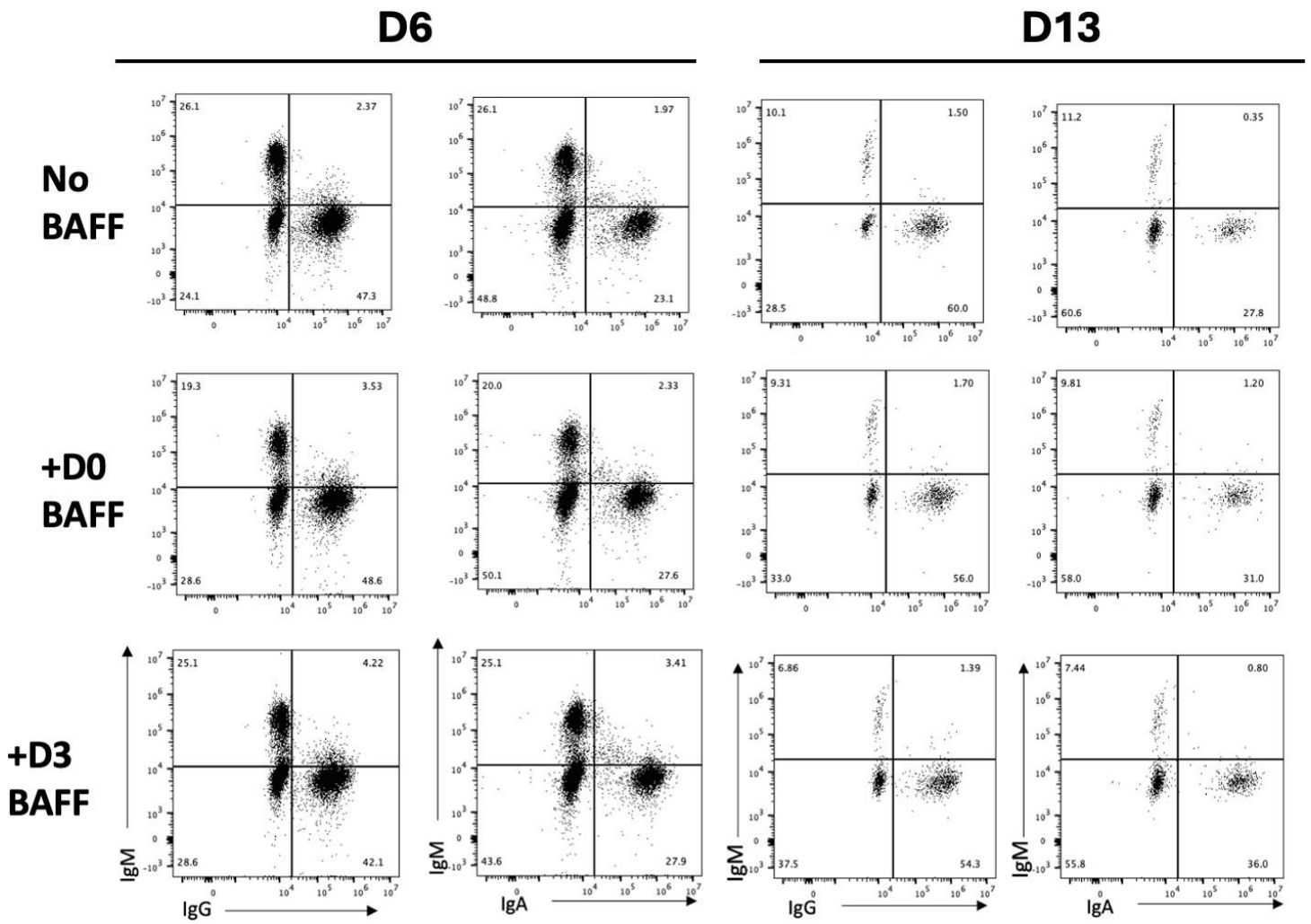

Figure 4.11: Intracellular immunophenotype at days 6 and 13 of *in vitro* differentiated B-cells stimulated with TD conditions either in the absence of BAFF or with the addition of BAFF at day 0 (D0) or day 3 (D3). Total B-cells were isolated from 50 mL of healthy donor peripheral blood obtained from the same blood donor and stimulated with F(ab')$_2$ anti-IgG/M/A and CD40L at day 0. Cytokines and supplements were added at specific time points: day 0: IL-2, IL-21; day 3: IL-2, IL-21, lipid media, amino acids (AA**);** day 6: IL-6, IL-21, APRIL, lipid media, AA. Isolated B-cells were equally split into three conditions: No BAFF, BAFF added at day 0 or BAFF added at day 3. Intracellular staining was determined on days 6 and 13 (D6-13). Representative data is shown for one donor.

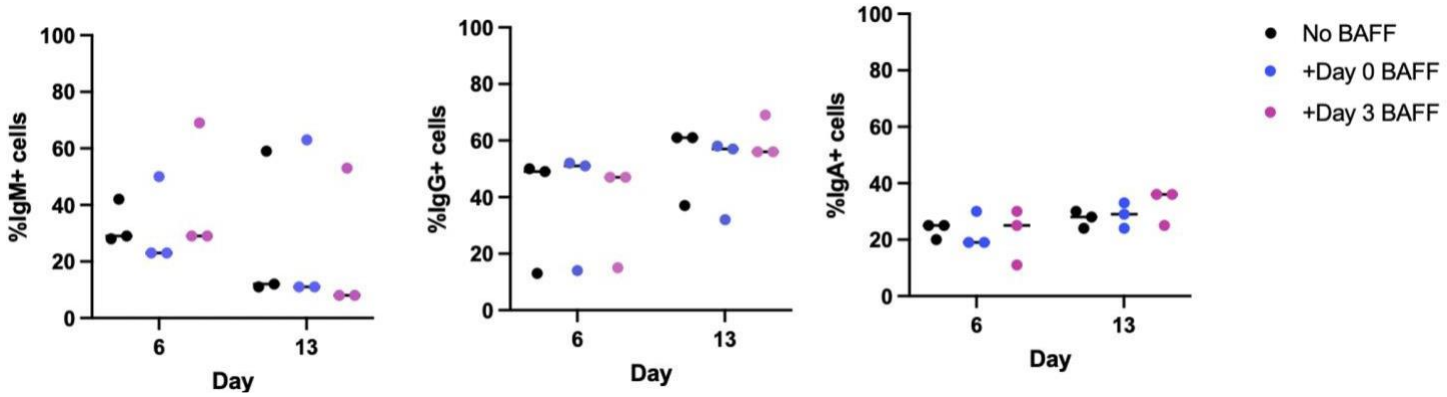

Figure 4.12: Intracellular immunoglobin profiles of healthy control B-cells (HC1, HC2 and HC3) denoting the relative percentages of IgM+; IgG+ and IgA+ B-cells between days 0 and 13 during the differentiation assay in no BAFF, day 0 or day 3 +BAFF conditions. Total B-cells were isolated from healthy control (n=3, as indicated by the number of dots per sample) peripheral blood and stimulated with F(ab')$_2$ anti-IgG/M/A and CD40L at day 0. Cytokines and supplements were added at specific time points: day 0: IL-2, IL-21; day 3: IL-2, IL-21, lipid media, amino acids (AA**);** day 6: IL-6, IL-21, APRIL, lipid media, AA. Intracellular staining was determined on days 0, 6 and 13. Each plot represents the percentage of cells expressing the stated immunoglobulin and each colour represents different culture conditions.

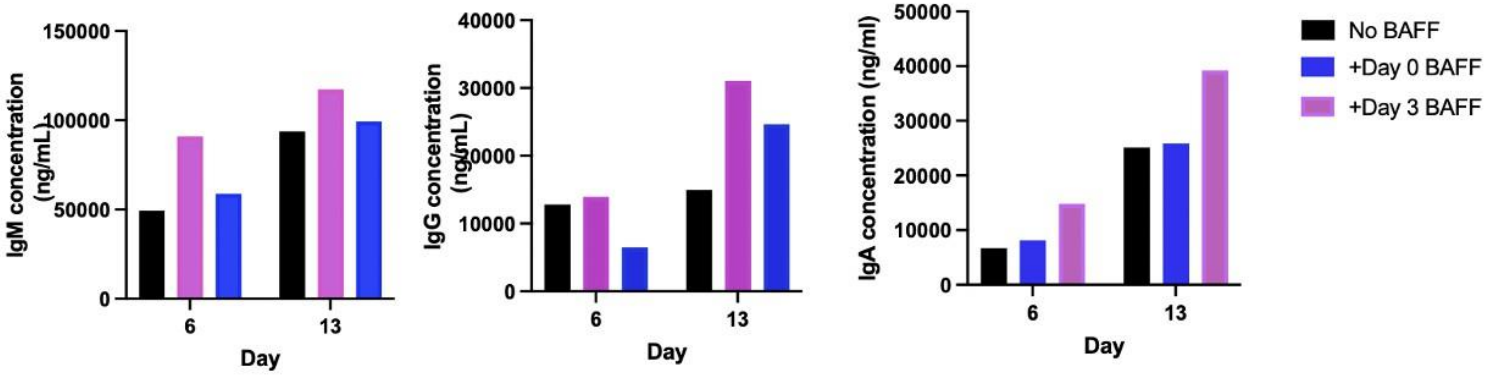

Figure 4.13: Quantification of IgM, IgG, IgA concentrations at days 6 and 13 in the representative healthy control either in the absence of BAFF or with the addition of BAFF at day 0 (D0) or day 3 (D3) under TD stimulation using CD40L of total B-cells. Supernatants from heathy control 1 total B-cells were collected at the specified time points and analysed using specific ELISA quantification kits as per the manufacturer's protocol. Values were normalised against respective control ELISA standards. Representative data is shown for one donor, and values are based on the average of three separate dilutions per sample.

Cell counts demonstrate the B-cell expanding actions of BAFF, whereby both cultures containing BAFF reach higher numbers than the culture without BAFF (Figure 4.14). In the representative HC and repeats, the trend of higher cell counts when BAFF was added at D3 versus D0 was observed. This demonstrates the utility of both the chosen 100 ng/mL concentration of BAFF and the benefit of addition at D3, supporting the literature regarding BAFF facilitating B-cell expansion, most notably when added to already-activated D3 B-cells (Zhang *et al.,* 2017).

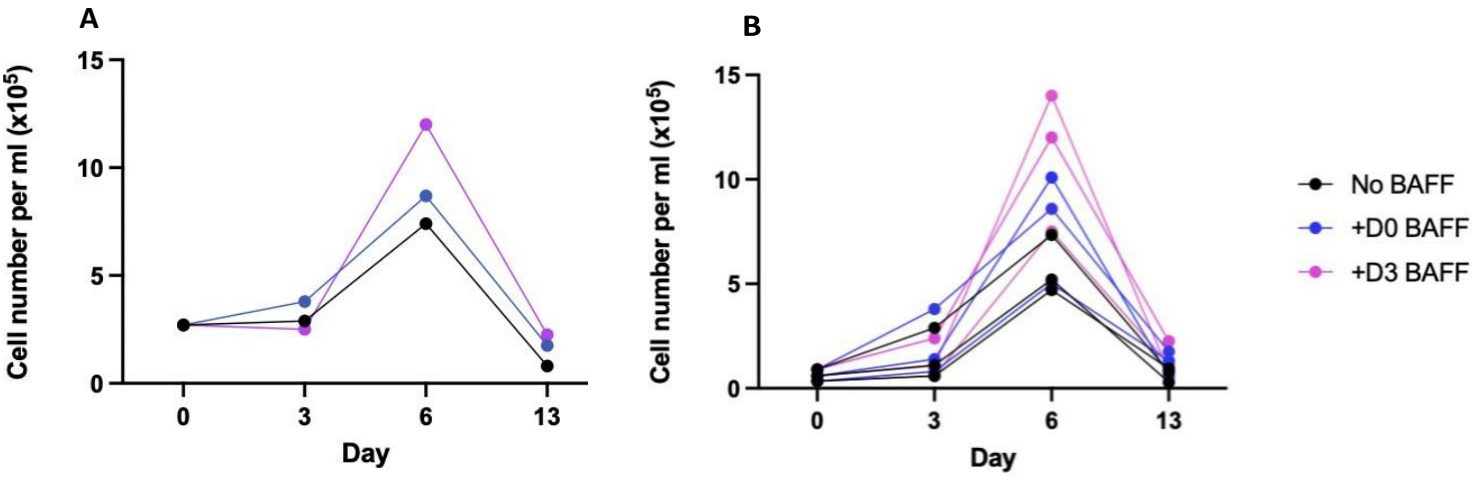

Figure 4.14: Total B-cell counts at days 0, 3, 6 and 13 in healthy control samples either in the absence of BAFF or with the addition of BAFF at day 0 (D0) or day 3 (D3) under TD stimulation using CD40L of total B-cells. Cell counts were determined manually using a haemocytometer on D0-3 and using flow cytometry CountBright absolute counting beads at later time points. Representative data for healthy control 1 (HC1) (**A**) and HC2 and HC3 replicates (**B**) demonstrate total cell counts per mL.

4.3.1 Naïve-fractioned *in vitro* B-cell differentiation with BAFF

The reduced cell input in naïve-fractioned B-cells is more comparable to antibody-deficient patients relative to inputting total B-cells. Therefore, a similar experimental setup as section 4.3 was followed using naïve B-cell fractions. Isolated naïve B-cells evidenced a purity of >94%. When BAFF was added at D3, there was an accelerated loss of BAFF-R expression, as seen in the total B-cell experiment in Figure 4.9, compared to the +D0 BAFF and no BAFF cultures (Figure 4.15), suggesting that adding BAFF to activated B-cells is likely to exert the greatest effect. Nonetheless, BAFF-R expression levelled to similar values seen in the No BAFF and +D0 BAFF cultures by D13. Similar to the total B-cell experiment, the expression of other phenotypic markers remained highly comparable across different conditions, including a consistent capacity to generate CD138+ PCs. Additionally, increased staining intensity was consistent with a higher number of CD138+ cells detected by flow cytometry, particularly in the presence of BAFF, with the most pronounced effect observed when BAFF was added at D3 (Figure 4.15).

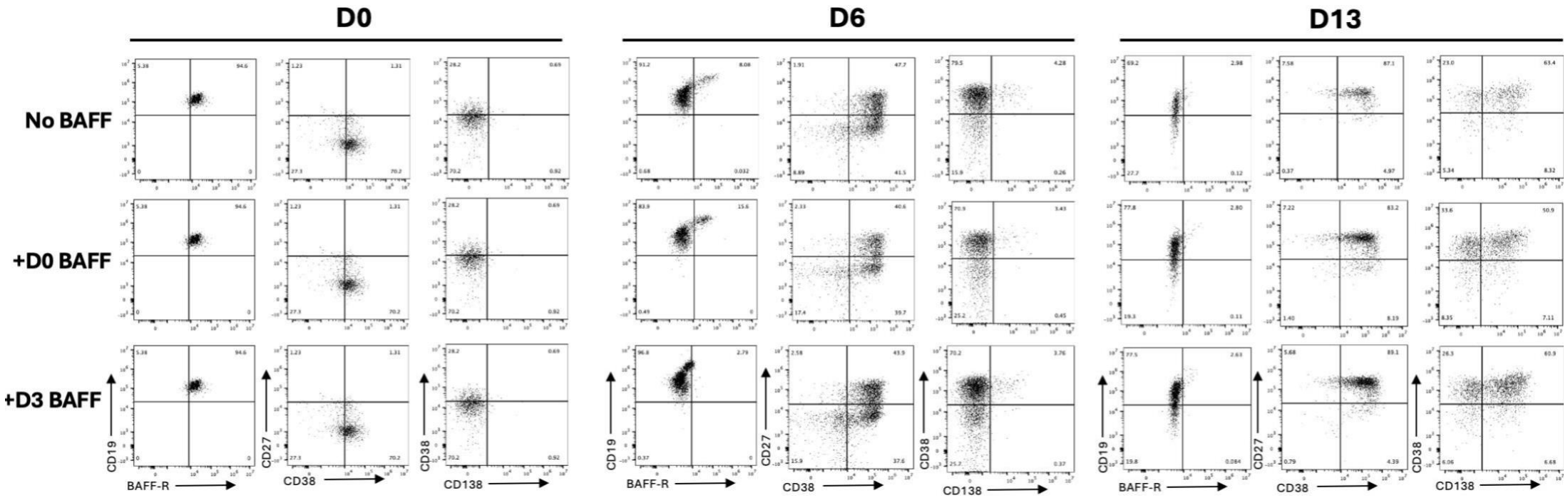

Figure 4.15: Surface immunophenotype at days 0, 6 and 13 of *in vitro* differentiated naïve-fractioned B-cells stimulated with TD conditions either in the absence of BAFF or with the addition of BAFF at day 0 (D0) or day 3 (D3). Naïve B-cells were isolated from 50 mL of healthy donor peripheral blood obtained from the same blood-donor and stimulated with $F(ab')_2$ anti- IgG/M/A and CD40L at day 0. Cytokines and supplements were added at specific time points: day 0: IL-2, IL-21; day 3: IL-2, IL-21, lipid media, amino acids (AA)**;** day 6: IL-6, IL-21, APRIL, lipid media, AA. Isolated B-cells were equally split into three conditions: No BAFF, BAFF added at D0 or BAFF added at D3. Surface staining was determined on days 0, 6 and 13. Representative data is shown for one donor.

Intracellular immunoglobulin expression profiles showed a slight decrease in class-switched isotypes by D13 when BAFF was added, most notably when introduced on D3. However, the overall expression patterns remained steady, and productive antibody secretion was observed regardless of BAFF addition at any time point (Figure 4.16), which was comparable to secreted immunoglobulin values (Figure 4.17). The increased staining intensity seen with BAFF further indicates that the presence of BAFF contributed to higher cell counts, reinforcing its role in enhancing cell proliferation rather than significantly altering differentiation profiles (Figure 4.18).

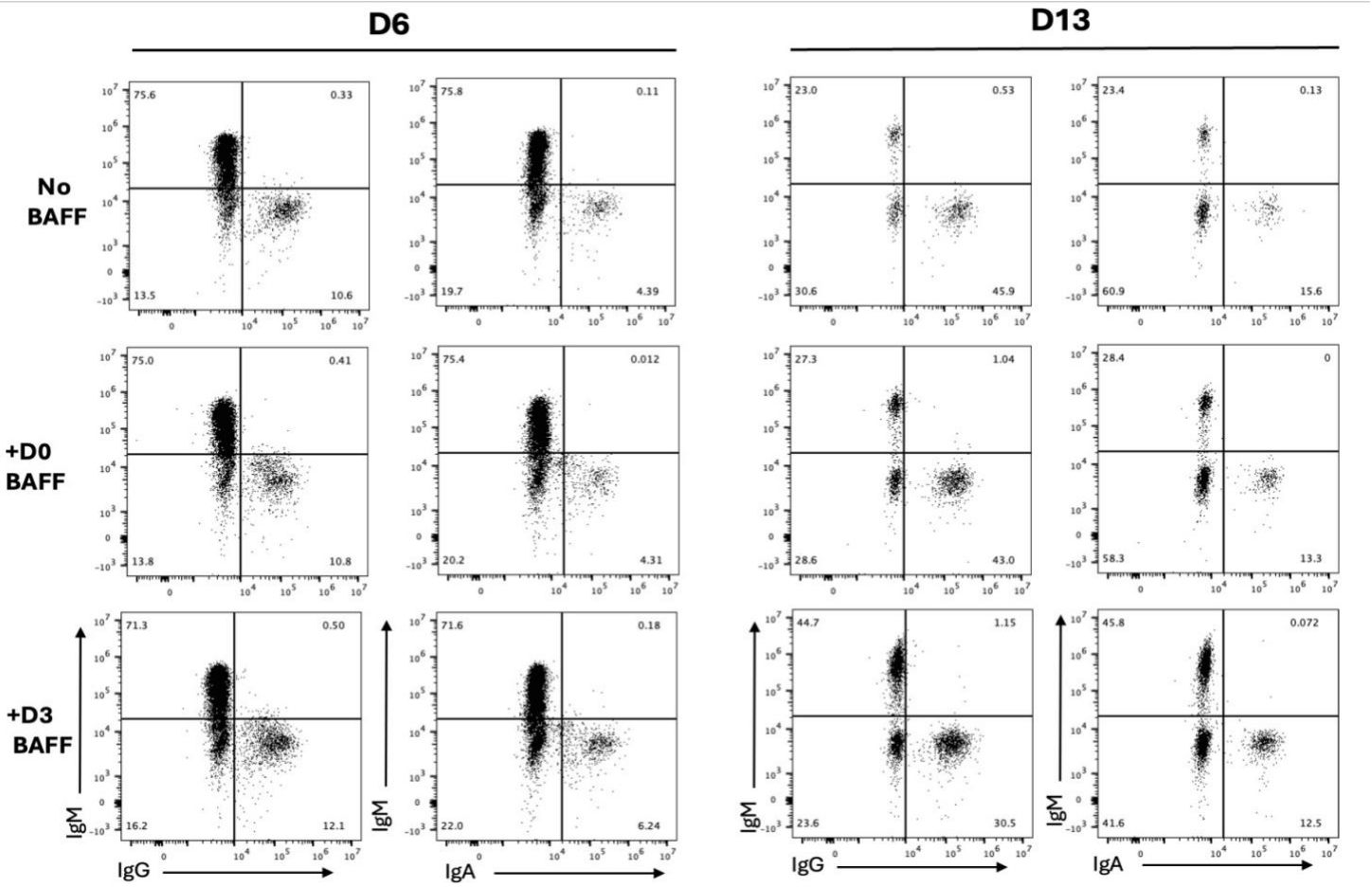

Figure 4.16: Intracellular immunophenotype at days 6 and 13 of *in vitro* differentiated naïve-fractioned B-cells stimulated with TD conditions either in the absence of BAFF or with the addition of BAFF at day 0 (D0) or day 3 (D3). Naïve B-cells were isolated from 50 mL of healthy donor peripheral blood obtained from the same blood-donor and stimulated with $F(ab')_2$ anti- IgG/M/A and CD40L at day 0. Cytokines and supplements were added at specific time points: day 0: IL-2, IL-21; day 3: IL-2, IL-21, lipid media, amino acids (AA)**;** day 6: IL-6, IL-21, APRIL, lipid media, AA. Isolated B-cells were equally split into three conditions: No BAFF, BAFF added at D0 or BAFF added at D3. Intracellular staining was determined on days 6 and 13. Representative data is shown for one donor.

Consistent with the total B-cell experiments, the naïve-only B-cell experiment mimicked the enhanced cell counts when adding BAFF to activated B-cells at D3 compared to the other conditions (Figure 4.18). This ability of +D3 BAFF to increase cell counts whilst minimally impacting differentiation prompted the decision to add 100 ng/mL BAFF at this specific timepoint in all experiments hereafter.

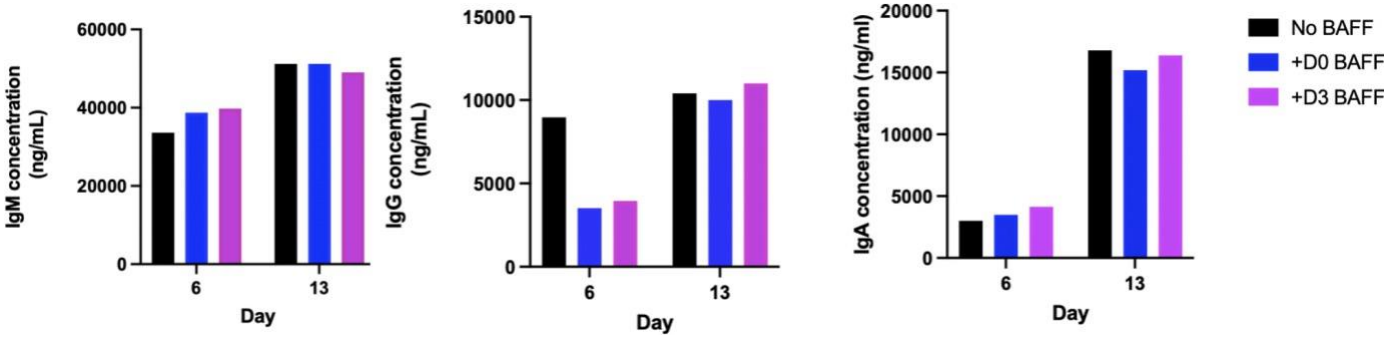

Figure 4.17: Quantification of IgM, IgG, IgA concentrations at days 6 and 13 in the representative healthy control either in the absence of BAFF or with the addition of BAFF at day 0 (D0) or day 3 (D3) under TD stimulation using CD40L in naïve B-cells. Supernatants from heathy control 1 naïve B-cells were collected at the specified time points and analysed using specific ELISA quantification kits as per the manufacturer's protocol. Values were normalised against respective control ELISA standards. Representative data is shown for one donor, and values are based on the average of three separate dilutions per sample.

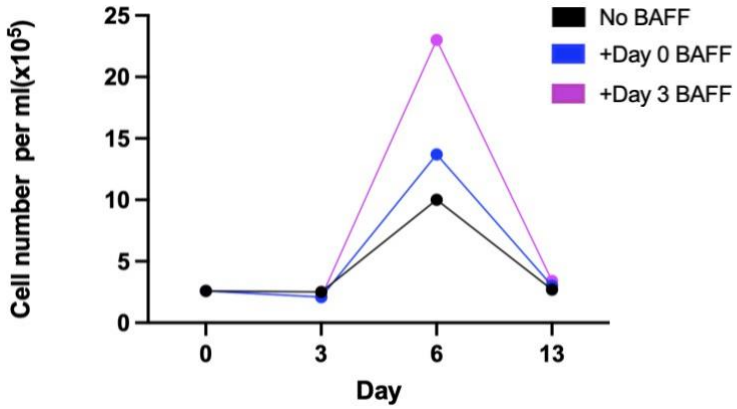

Figure 4.18: Total B-cell counts at days 0, 3, 6 and 13 in representative healthy control sample either in the absence of BAFF or with the addition of BAFF at day 0 (D0) or day 3 (D3) under TD stimulation of naïve B-cells. Cell counts were determined manually using a haemocytometer on D0-3 and using flow cytometry CountBright absolute counting beads at later time points. Data is shown for the representative healthy control.

4.4 The addition of BAFF at day 3 on low starting cell counts under TD stimulation

Preliminary data shown in chapter 4.3 suggests that incorporation of 100 ng/mL BAFF at D3 of B-cell culture, starting with plentiful cell numbers, increases D6 plasmablast production without impacting B-cell phenotypes and immunoglobulin secretion. Hence, the subsequent objective was to determine whether this trend is reciprocated in the smaller starting cell numbers generated in the 5 mL versus 10 mL versus 15 mL B-cell differentiation experiments under CD40L and R848 stimulation (see Chapter 4.5).

First, 60 mL of HC blood was obtained and split into two conditions whereby one would receive BAFF at D3 and the other would not. Each of the two conditions were thereafter divided into 15 mL, 10 mL or 5 mL fresh blood and were individually subject to B-cell isolation and differentiation as outlined in Chapter 2.3 under CD40L

stimulation (Figure 4.19). Cell counts, flow cytometry and ELISA data were generated at specific timepoints to provide clues as to whether BAFF can increase cell counts whilst minimally affecting surface and immunoglobulin profiles where limited initial cells are available, which will be likely with regards to patient samples.

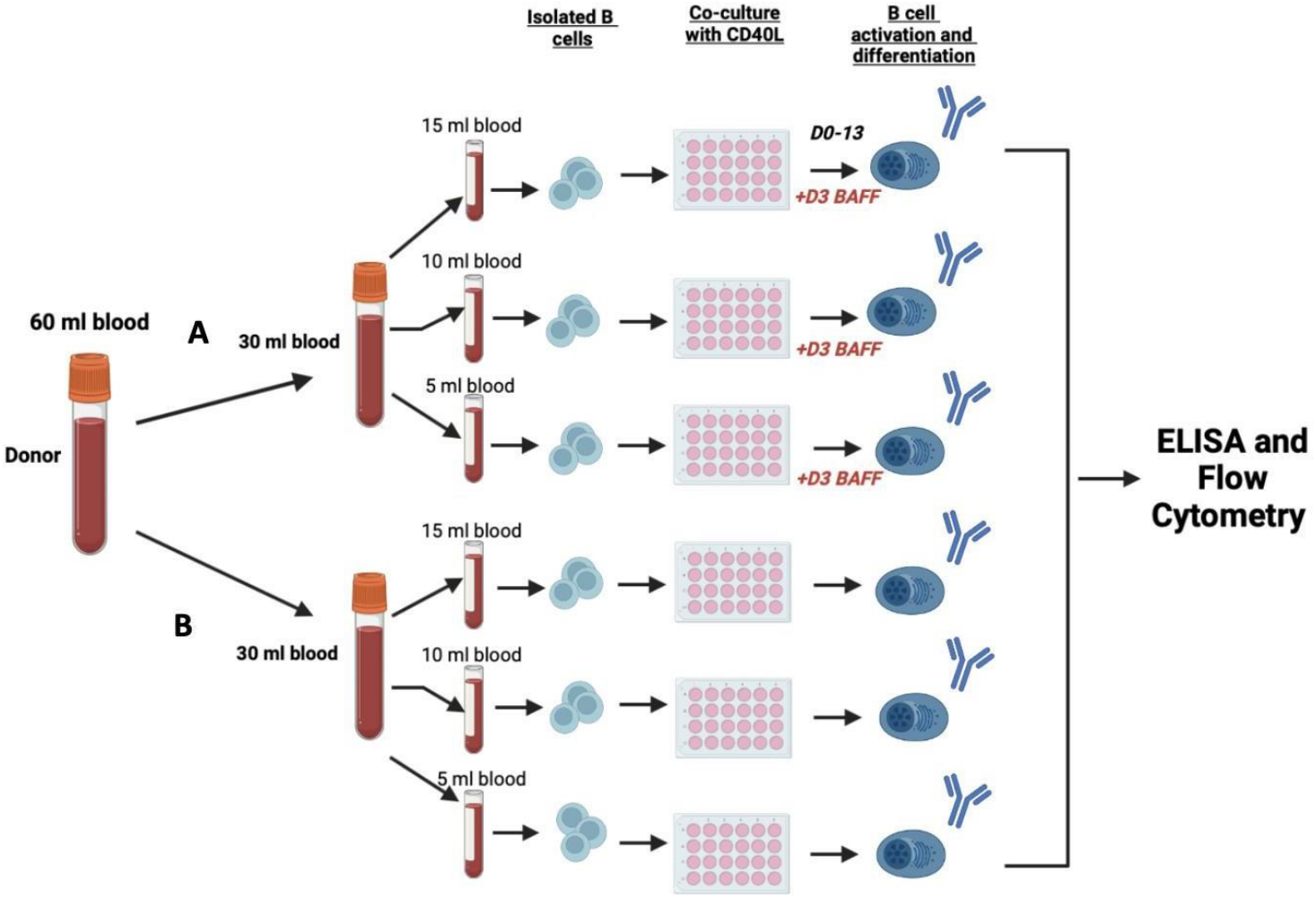

Figure 4.19: Schematic of the experimental workflow for studying the effect of adding BAFF in B-cell cultures at day 3 under TD stimulation. Blood was collected from a healthy control and split into various conditions to determine whether BAFF can increase cell counts whilst minimally affected surface and immunoglobulin profiles where limited initial cells are available.

All six D0 cultures generated purity of >96% and had overall highly comparable CD19+BAFF-R+CD27-CD38hiCD138- surface expression. Contrary to data obtained in section 4.3, the decline in BAFF-R expression at D6 was overall only marginally lower in the +D3 BAFF cultures compared to when no BAFF was added. This is likely attributed to the lower cell counts in this experiment, notably in the 5 mL cultures, whereby BAFF-R expression was higher when BAFF was not added. Furthermore, albeit marginal, all cultures without BAFF had higher relative percentages of CD38hiCD138+ PCs than those that included BAFF (Figure 4.20). Since this effect was not seen in previous data from chapter 4.3, it is likely to reflect minor differences in donors. Thus, what is conclusive, is that the addition of BAFF does not significantly affect B-cell phenotypes across differentiation timepoints, regardless of cell counts and BAFF-related conditions.

Similar to the prior BAFF experiments in chapter 4.3, only minor differences in intracellular immunoglobulin were observed with versus without the addition of BAFF (Figure 4.21). Any differences in immunoglobulin expression in BAFF versus no BAFF tended to be between the 5 mL samples, where IgM appeared to be retained at D6 and less IgG and IgA was expressed at D13 in the absence of BAFF. This was reciprocated in secreted immunoglobulin values denoted by ELISA (Figure 4.22) whereby secretion, regardless of stimulatory conditions, was highly similar. The only possible exception to this similarity, as per intracellular immunoglobulin expression in Figure 4.21, is the higher IgA expression in the 5 mL samples at D13 in addition to an overall elevated IgA expression with versus without the addition of BAFF at D13 at all starting amounts.

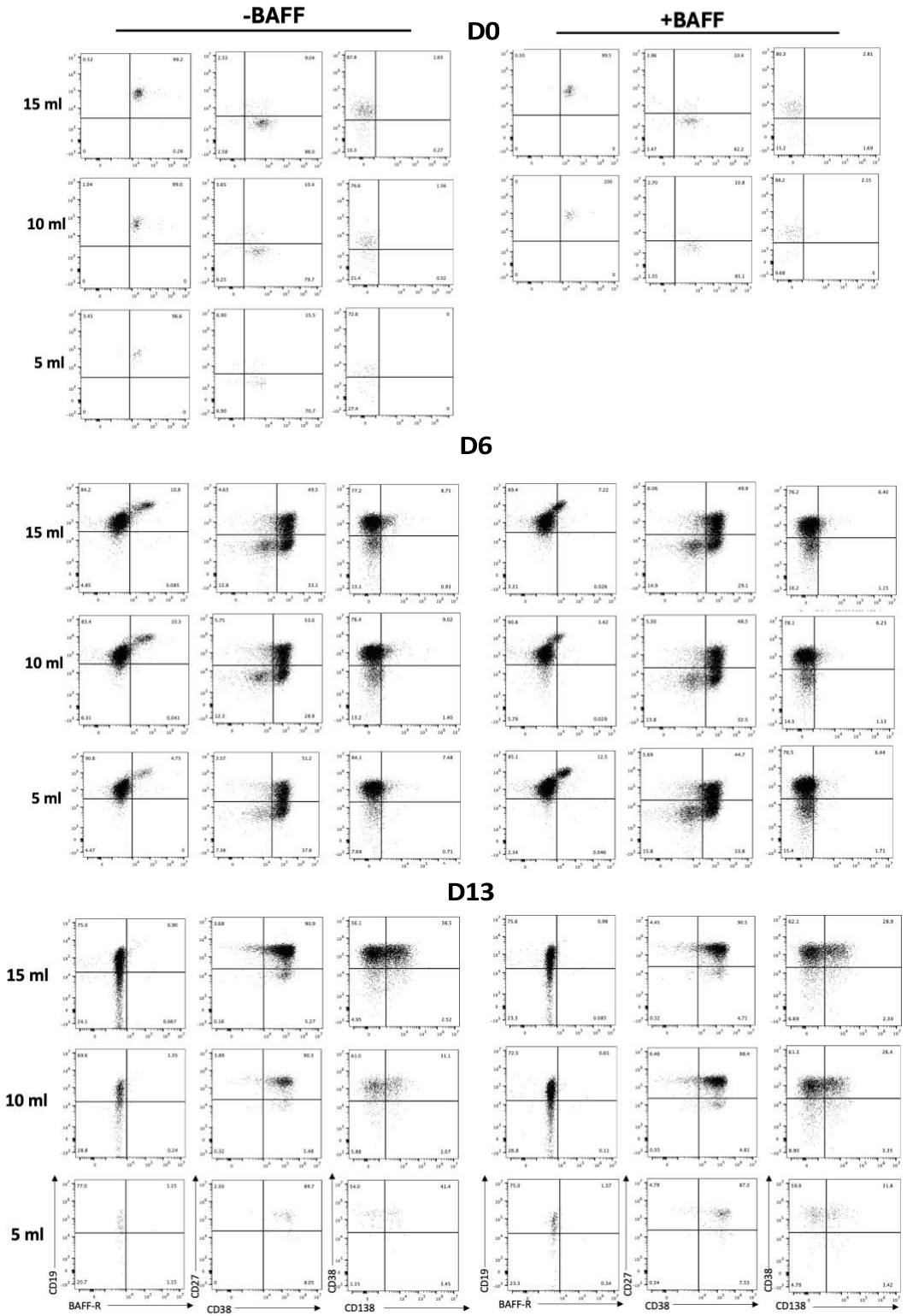

Figure 4.20: Surface phenotype at days 0, 6 and 13 (D0-13) of *in vitro* differentiated B-cells generated from either 15mL, 10 mL or 5 mL fresh healthy control blood with versus without the addition of BAFF under TD stimulation using CD40L. Total B-cells from 15, 10 and 5 mL (-BAFF) and 15, 10 and 5 mL (+BAFF) were isolated from healthy donor peripheral blood obtained from the same blood-donor and stimulated with $F(ab')_2$ anti-IgG/M/A and CD40L at day 0. Cytokines and supplements were added at specific time points: day 0: IL-2, IL-21; day 3: IL-2, IL-21, lipid media, amino acids (AA**);** day 6: IL-6, IL-21, APRIL, lipid media, AA. In cultures with BAFF, BAFF was added at D3 and removed from culture by D6. Surface staining was determined on days 0, 6 and 13. Representative data is shown for one donor. Data for D0 5mL +BAFF culture was not available.

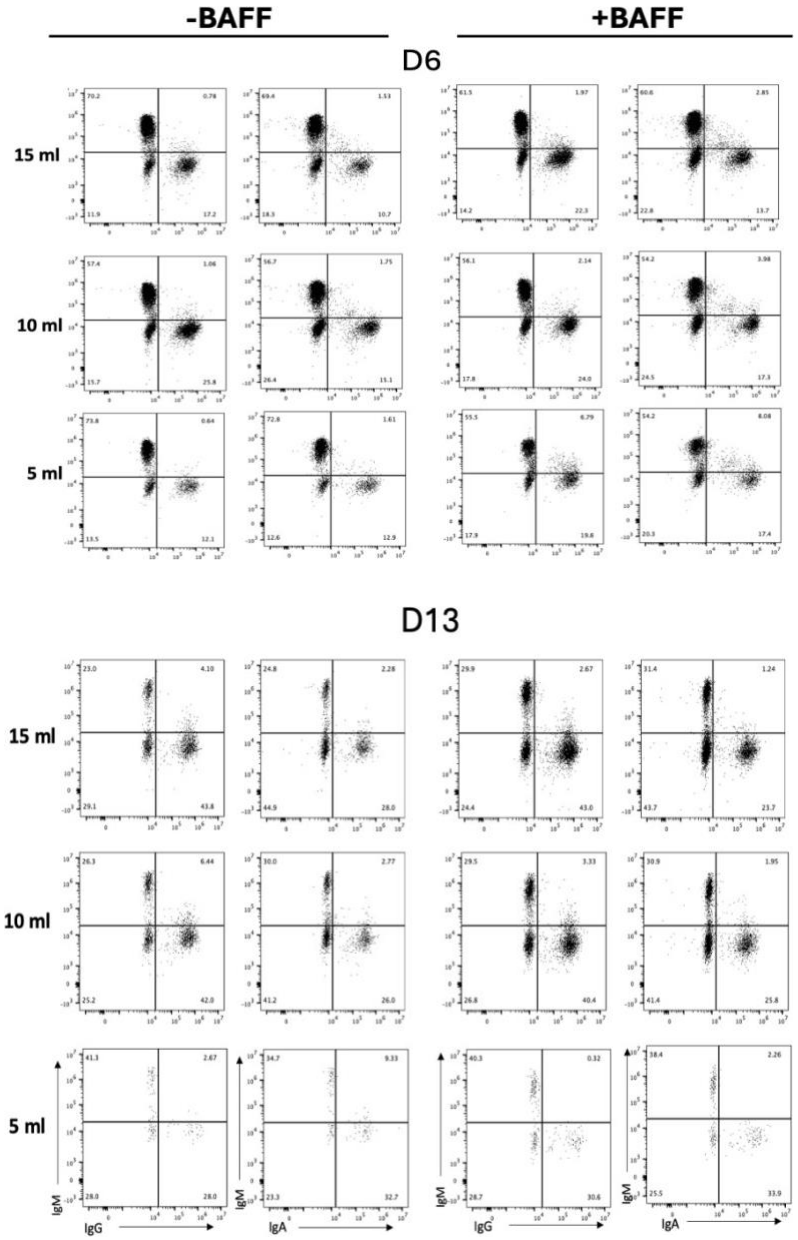

Figure 4.21: Intracellular immunophenotype at days 6 and 13 (D6-13) of *in vitro* differentiated B-cells generated from either 15 mL, 10 mL or 5 mL fresh healthy control blood with versus without the addition of BAFF under TD stimulation using CD40L. Total B-cells from 15, 10 and 5 mL (-BAFF) and 15, 10 and 5 mL (+BAFF) were isolated from healthy donor peripheral blood obtained from the same blood-donor and stimulated with F(ab')$_2$ anti-IgG/M/A and CD40L at day 0. Cytokines and supplements were added at specific time points: day 0: IL-2, IL-21; day 3: IL-2, IL-21, lipid media, amino acids (AA**);** day 6: IL-6, IL-21, APRIL, lipid media, AA. In cultures with BAFF, BAFF was added at D3 and removed from culture by D6. Intracellular staining was determined on days 6 and 13. Representative data is shown for one donor.

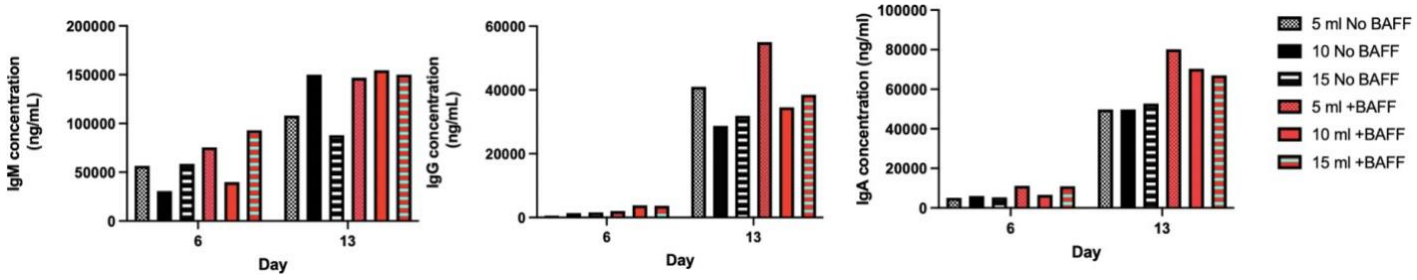

Figure 4.22: Quantification of IgM, IgG and IgA concentrations generated from either 15 mL, 10 mL or 5 mL fresh healthy control blood with versus without the addition of BAFF at days 6 and 13 in the representative healthy control under TD stimulation using CD40L. Supernatants from total B-cells were collected at the specified time points and analysed using specific ELISA quantification kits as per the manufacturer's protocol. Values were normalised against respective control ELISA standards. Representative data is shown for one donor, and values are based on the average of three separate dilutions per sample.

Across all starting amounts, the addition of BAFF at D3 notably increased the cell numbers in all three starting amounts at D6, evidencing a pro-B-cell survival effect of BAFF that is independent of cell count. This elevated cell count with the addition of BAFF was lost by D13 (Figure 4.23), suggesting BAFF preferentially exerts its effect on activated B-cells that are entering the plasmablast stage rather than promoting the development and retention of LLPCs.

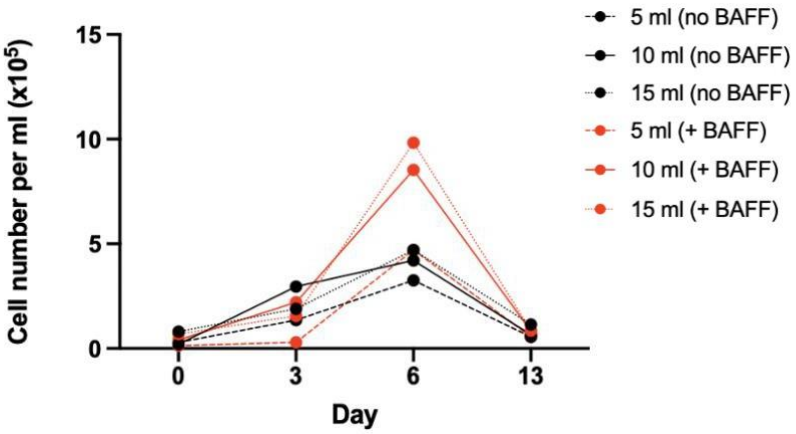

Figure 4.23: B-cell counts at days 0, 3, 6 and 13 generated from either 15 mL, 10 mL or 5 mL fresh healthy control blood with versus without the addition of BAFF in the representative healthy control under TD stimulation using CD40L. Cell counts were determined manually using a haemocytometer on D0-3 and using flow cytometry CountBright absolute counting beads at later time points. Representative data is shown for one donor.

4.5 The addition of BAFF at day 3 on low starting cell counts under TI stimulation

To assess whether the effects of BAFF addition at D3 in healthy B-cells under TD stimulation could be replicated under TI conditions, the same experiment outlined in Figure 4.19 was repeated, substituting CD40L stimulation with R848. This allowed for a direct comparison between the two stimulation pathways, providing insight into BAFF's role in enhancing B-cell survival and differentiation under TI conditions (Figure 4.24).

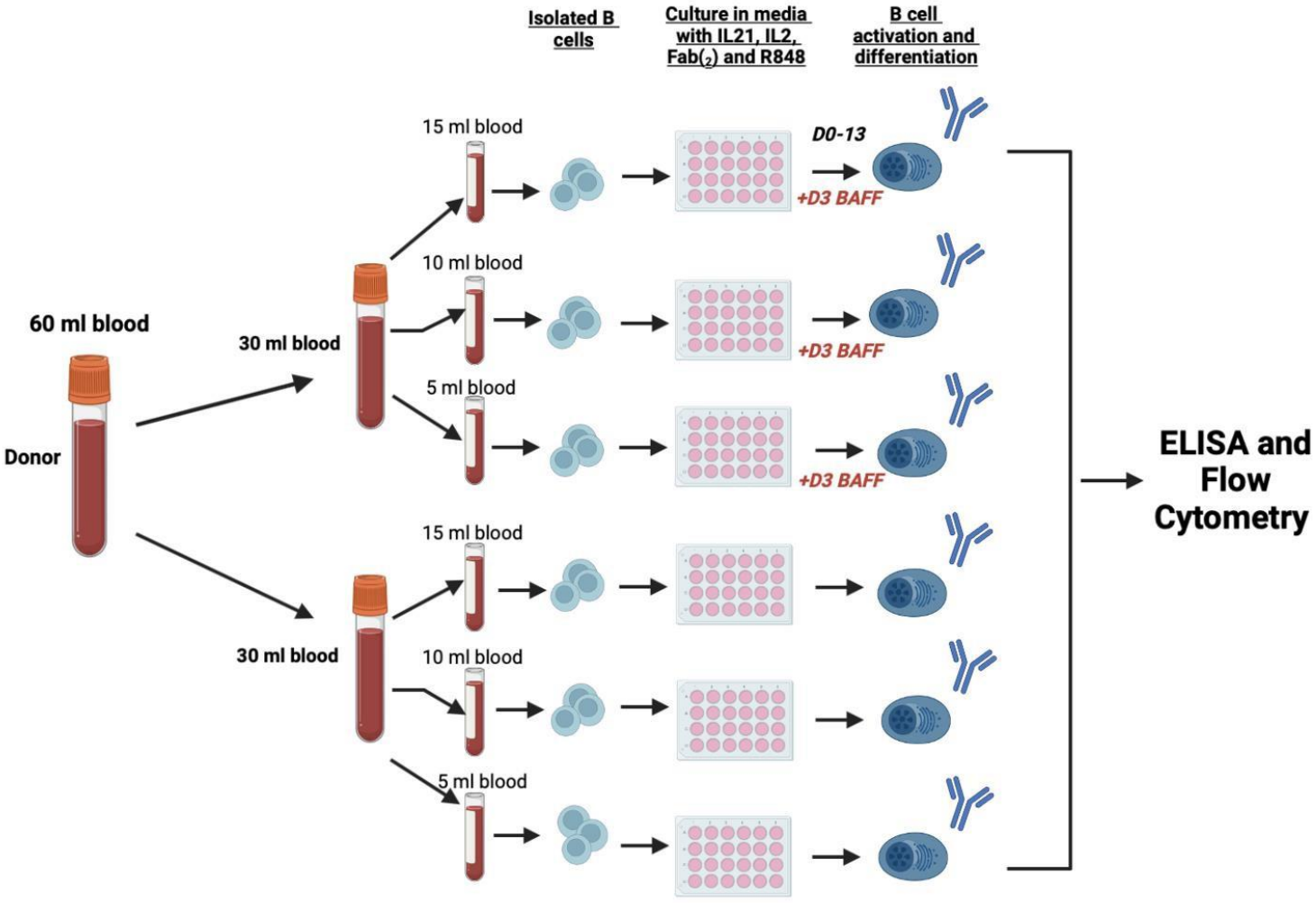

Figure 4.24: Schematic of the experimental workflow for studying the effect of adding BAFF in B-cell cultures at day 3 under TI R848 stimulation. Blood was collected from a healthy control and split into various conditions to determine whether BAFF can increase cell counts whilst minimally affecting surface and immunoglobulin profiles where limited initial cells are available.

Each condition started with pre B-cell populations, devoid of detectible contamination. However, it is important to note that the 5mL samples, both with and without BAFF, failed to yield sufficient cell numbers by D6 to continue culture to D13, resulting in the absence of data at that time-point. Similar to the outcomes observed with CD40L stimulation (chapter 4.3), phenotypic differentiation remained highly comparable regardless of BAFF addition, with visibly higher staining intensities in all conditions at D6 when BAFF was included. Notably, the relative percentage of CD138+ cells by D13 was more consistent under R848 stimulation compared to CD40L stimulation, where PC expression appeared slightly diminished. This difference may be due to slight differences in the use of BAFF in TI versus TD signalling pathways (Lau *et al.,* 2020; Mackay and Schneider, 2009). Furthermore, retention of CD19+ populations was observed at D13 in cultures with BAFF under T-cell independent R848 conditions, a phenomenon less evident in corresponding T-cell dependent CD40L stimulation experiments (Figure 4.25).
Intracellular IgM and IgA expression was remarkably consistent across both time points and starting amounts, irrespective of BAFF addition. At D6, IgG expression was notably higher, exceeding 34% in all conditions with BAFF and reaching 50% without it, potentially indicating enhanced activation. By D13, IgG levels plateaued in the absence of BAFF but continued to rise with its presence, suggesting ongoing stimulation (Figure 4.26). Secreted immunoglobulin data indicated higher IgM concentrations at D6 with BAFF, which normalised by D13, while differences in IgG and IgA concentrations remained insignificant across both time points (Figure 4.27).

In line with earlier findings, cell counts were higher at D6 with the addition of D3 BAFF across all experimental conditions, and these elevated counts were maintained in D13 samples, particularly within the 10 mL group (Figure 4.28). This experiment was designed as a preliminary investigation to determine whether the pro-survival effects of BAFF seen under TD (CD40L) stimulation could also be observed in TI conditions using R848. As subsequent patient experiments focused exclusively on CD40L-based stimulation, repetition of this assay was not pursued. Moreover, insufficient cell numbers in the R848-stimulated cultures at D6 prevented continuation through to D13, accounting for the absence of data points in the 5 mL group. Nonetheless, the results suggest that the benefits of BAFF can be translated into TI conditions, whereby B-cell counts are increased with minimal differences in surface and intracellular phenotypes.

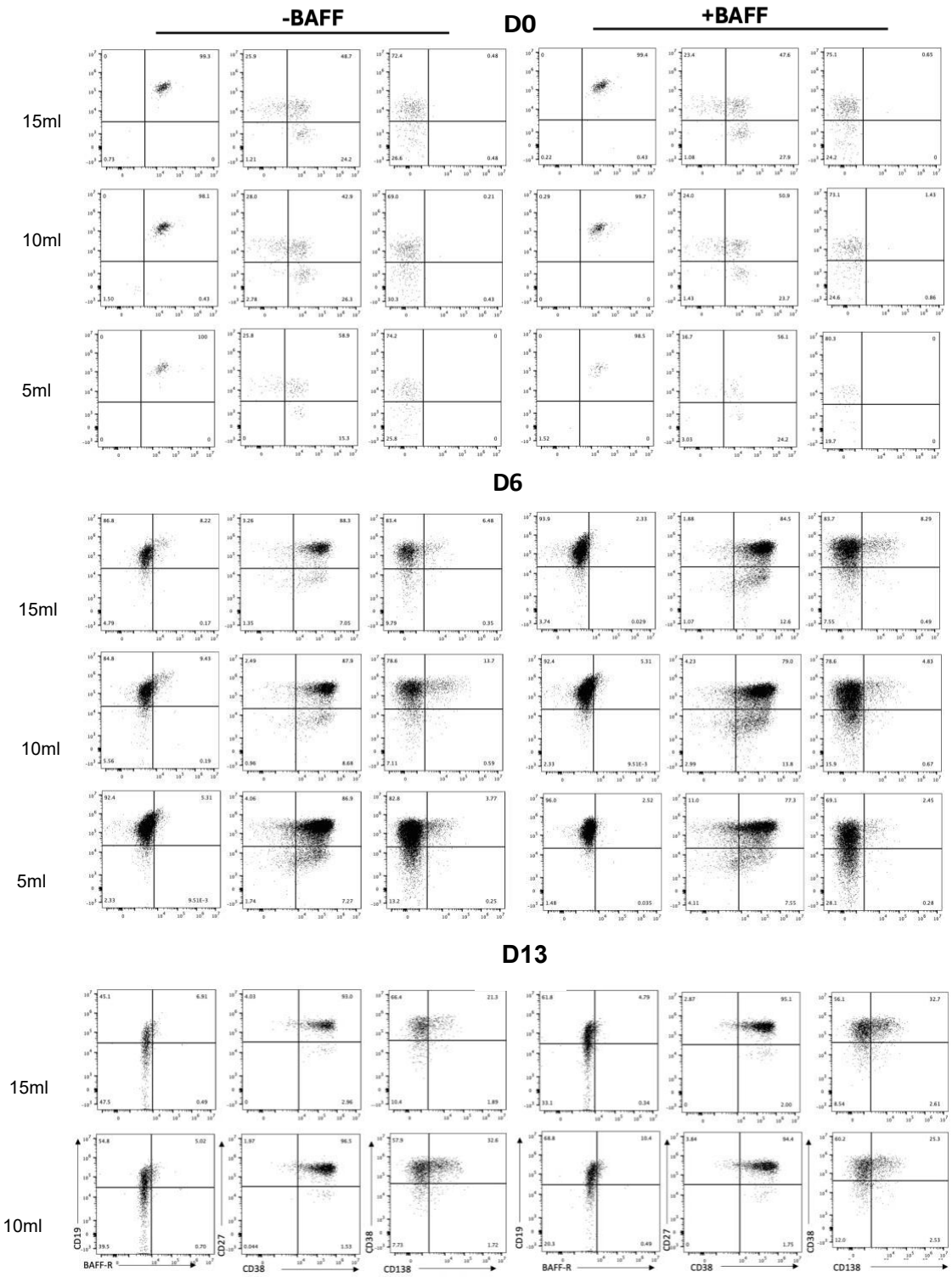

Figure 4.25: Surface phenotype at days 0, 6 and 13 (D0-13) of *in vitro* differentiated B-cells generated from either 15 mL, 10 mL or 5 mL fresh healthy control blood with versus without the addition of BAFF under TI stimulation using R848. Total B-cells from 15, 10 and 5 mL (-BAFF) and 15, 10 and 5 mL (+BAFF) were isolated from the same blood-donor and stimulated with F(ab)2 anti-IgG/M/A and R848 at day 0. Cytokines and supplements were added at specific time points: day 0: IL-2, IL-21; day 3: IL-2, IL-21, lipid media, amino acids (AA); day 6: IL-6, IL-21, APRIL, lipid media, AA. In cultures with BAFF, BAFF was added at D3 and removed from culture by D6. Surface staining was determined on days 0, 6 and 13. Representative data is shown for one donor. Data for D13 5mL -BAFF and +BAFF cultures were not available.

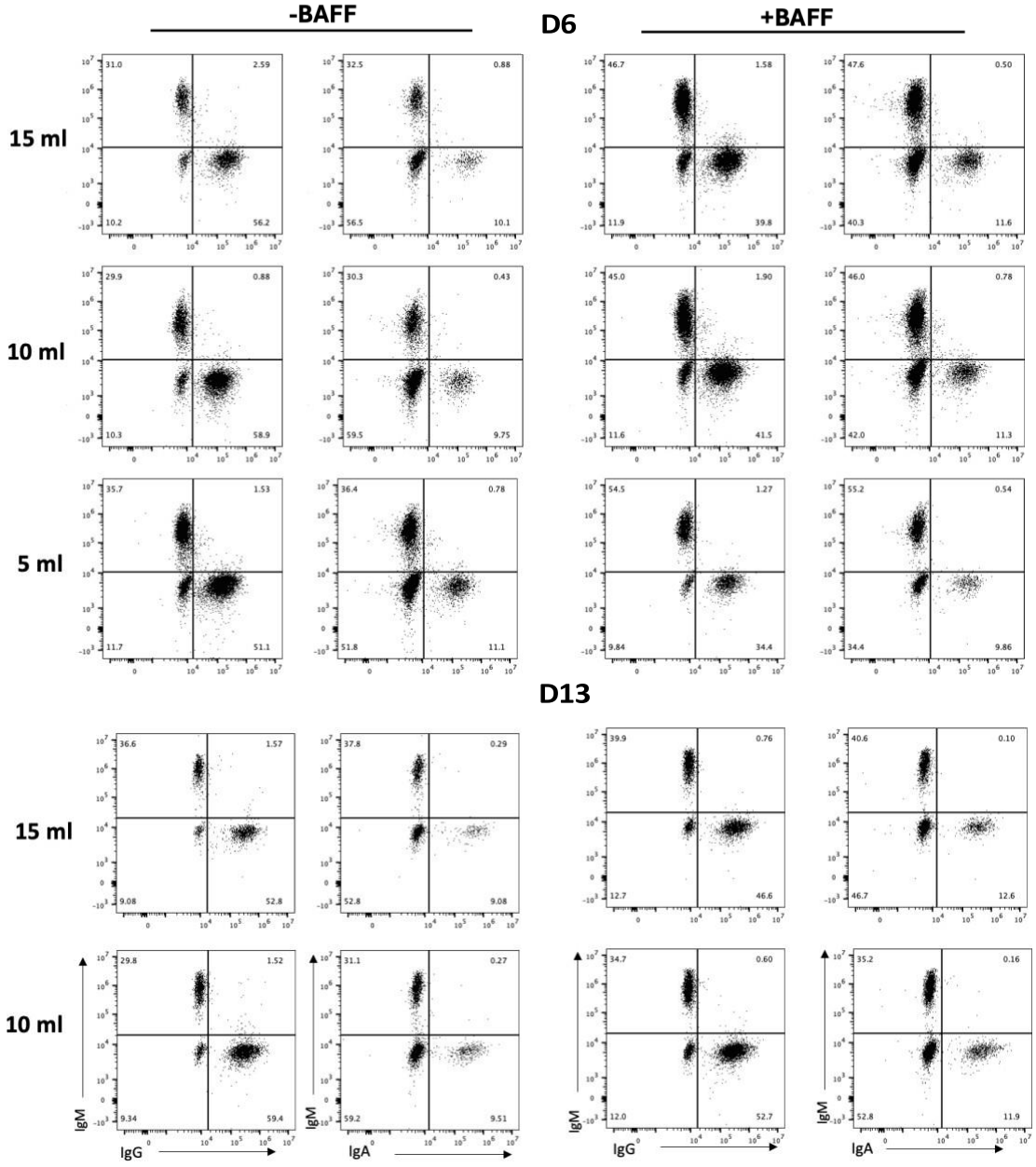

Figure 4.26: Intracellular immunophenotype at days 6 and 13 (D6-13) of *in vitro* differentiated B-cells generated from either 15mL, 10 mL or 5 mL fresh healthy control blood with versus without the addition of BAFF under TI stimulation using R848. Total B-cells from 15, 10 and 5 mL (-BAFF) and 15, 10 and 5 mL (+BAFF) were isolated from healthy donor peripheral blood obtained from the same blood-donor and stimulated with $F(ab')_2$ anti-IgG/M/A and R848 at day 0. Cytokines and supplements were added at specific time points: day 0: IL-2, IL-21; day 3: IL-2, IL-21, lipid media, amino acids (AA)**;** day 6: IL-6, IL-21, APRIL, lipid media, AA. In cultures with BAFF, BAFF was added at D3 and removed from culture by D6. Intracellular staining was determined on days 6 and 13. Representative data is shown for one donor. Data for D13 5 mL -BAFF and +BAFF cultures were not available.

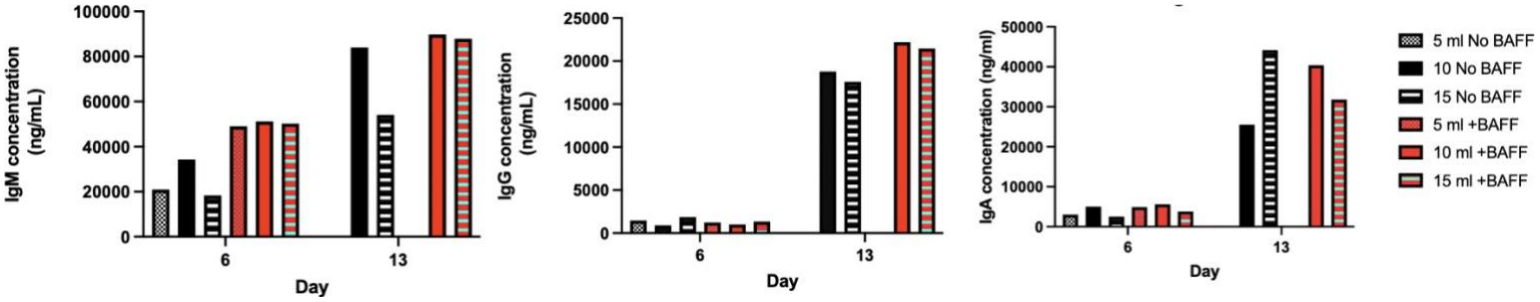

Figure 4.27: Quantification of IgM, IgG and IgA concentrations generated from either 15 mL or 10 mL or 5 mL fresh healthy control blood with versus without the addition of BAFF at day 3 during days 6 and 13 in the representative healthy control under TI stimulation using R848. Supernatants were collected at the specified time points and analysed using specific ELISA quantification kits as per the manufacturer's protocol. Values were normalised against respective control ELISA standards. Representative data is shown for one donor, and different plots under the same condition represent repeats using different dilutions (section 2.4). Data for 5 mL was not available at day 13.

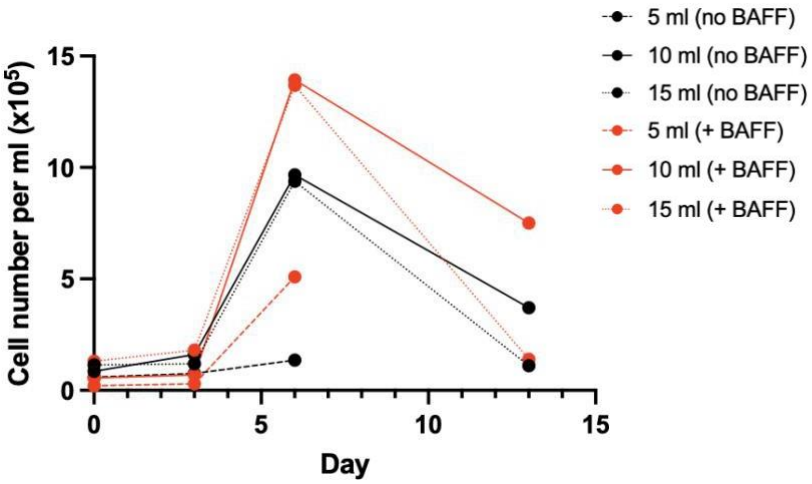

Figure 4.28: B-cell counts at days 0, 3, 6 and 13 generated from either 15 mL, 10 mL or 5 mL fresh healthy control blood with versus without the addition of BAFF at day 3 in the representative healthy control under TI stimulation using R848. Cell counts were determined manually using a haemocytometer on D0-3 and using flow cytometry CountBright absolute counting beads at later time points. Representative data is shown for one donor. Data for 5 mL was not available at day 13 due to insufficient cell numbers at day 6 for further culture.

4.6 Discussion

A critical caveat when harnessing the *in vitro* B-cell differentiation model for use in antibody deficient patients, particularly in terms of frozen samples from the COV-AD study, is the high possibility of severely reduced cell counts that could hinder analysis from isolation to PC stages. Hence, the first aim of this chapter was to closely mimic these low-cell conditions by evaluating how different starting volumes (15 mL, 10 mL and 5 mL) affect B-cell differentiation and resulting cell numbers. These findings demonstrate that B-cells can successfully differentiate into LLPCs with minimal differences in surface phenotypes, intracellular and secreted immunoglobulin profiles, regardless of the starting volume. Whilst this demonstrates the potential for studying patient B-cells using the *in vitro* system, this experimental setup mimics optimum conditions in HCs. Such conditions are likely to be harder to achieve when working with the patient samples for reasons beyond scarcity (i.e. difficulty in obtaining large volumes of blood), including freezing PBMCs and disease-related defects (Ballow, 2002; Browne *et al.,* 2024). These factors are likely to impair the ability for productive downstream analysis, underscoring the need for optimised culture conditions that can sustain B-cell viability and differentiation even when starting with minimal cell numbers and sub-optimal conditions.

To address the challenge of low B-cell viability, the potential of BAFF, a member of the TNF family known for its role in promoting B-cell survival (Mackay and Browning, 2002), was investigated. BAFF was added to the culture following TD CD40-L stimulation at different timepoints (D0 or D3) to assess its impact on B-cell differentiation and cell numbers. Results indicate that the addition of BAFF at D3 sufficiently enhanced cell counts at D6 without implicating differentiation phenotypes, demonstrating a notable pro-survival effect on B-cells when added to cultures at the D3 timepoint. The benefit of adding BAFF to activated B-cells addition is, in part, mediated by BAFF-receptor, BAFF-R, upregulation at the D3 timepoint (as well as TACI and BCMA to a lesser extent) which enhances their sensitivity to BAFF's survival signals. Since activated B-cells should express high levels of BAFF-R

(Schneider, 2005), they are more effective at responding to BAFF and promoting survival/proliferation. Additionally, by D3, B-cells have likely transitioned into a state both more responsive to and requiring additional survival signals relative to D0, thus making BAFF more beneficial after activation and able to selectively support successfully activated B-cells that require additional signals to avoid apoptosis and continue proliferating (Avery *et al.,* 2003).

The applicability of BAFF's pro-survival effects additionally translated to low starting cell counts (15 mL, 10 mL and 5 mL) when investigated under both TD CD40-L and TI R848 conditions. However, by D13 under CD40L stimulatory conditions, the advantage conferred by BAFF addition diminished, supporting the notion that BAFF primarily supports early-stage B-cell expansion and survival rather than LLPC maintenance (Mackay *et al.,* 2003). In contrast, under TI R848 stimulatory conditions, the addition of BAFF appeared to generate more cells than the non-BAFF counterpart. Whilst this could be attributed to niche-specific factors beyond activation differences, this discrepancy could also be because TI activation provides rapid but short-lived survival signals whereby BAFF may be supplementing the limited survival cues i.e. the effects of BAFF may become more pronounced/prolonged and supports B-cells that would otherwise undergo apoptosis more rapidly in the absence of T-cell help (Thompson *et al.,* 2000). Regardless, the data shown demonstrates that adding D3 BAFF to both TI and TD B-cell cultures is greatly beneficial in expanding B-cell counts, facilitating analysis up to later PC stages.

Throughout all BAFF-related experiments, there is an apparent lack of significant impact on surface phenotype or intracellular and secretory immunoglobulin expression across different conditions. This further supports the idea that BAFF's primary role is to enhance early survival and proliferation, i.e. BAFF does not directly interfere with differentiation signals (Thompson, 2001). The ability of BAFF to enhance cell counts without notably altering differentiation phenotype is seen in the literature whereby BAFF promotes immature transitional B-cell survival that in turn triggers elevated mature B-cell numbers (Batten *et al.,* 2000). The ability to promote survival has been attributed to the capability of BAFF to activate signalling pathways that inhibit apoptosis, notably the NF-κB pathway. This anti-apoptotic effect helps

maintain higher cell viability, especially under *in vitro* conditions where cell death can occur due to suboptimal nutrient and cytokine levels (Mackay *et al.,* 1999). By restricting apoptosis, BAFF enables a greater number of B-cells to survive, evident at earlier time points, when BAFF's survival-promoting effects are most needed and effective.

Collectively, the data presented in this section highlight the ability of D3 BAFF to enhance B-cell survival and proliferation *in vitro* without affecting differentiation phenotypes. Given the nature of the samples from the COV-AD study that are, in most instances, likely to give even lower initial cell counts than shown in this section, optimising the differentiation model through the addition of D3 BAFF will provide an imperative optimisation step to facilitate sufficient downstream analysis (Figure 4.29). Indeed, further optimisation approaches could also be followed to ensure robust cell counts for all downstream analysis. Applying the optimised B-cell assay to patient-derived samples would be the next step.

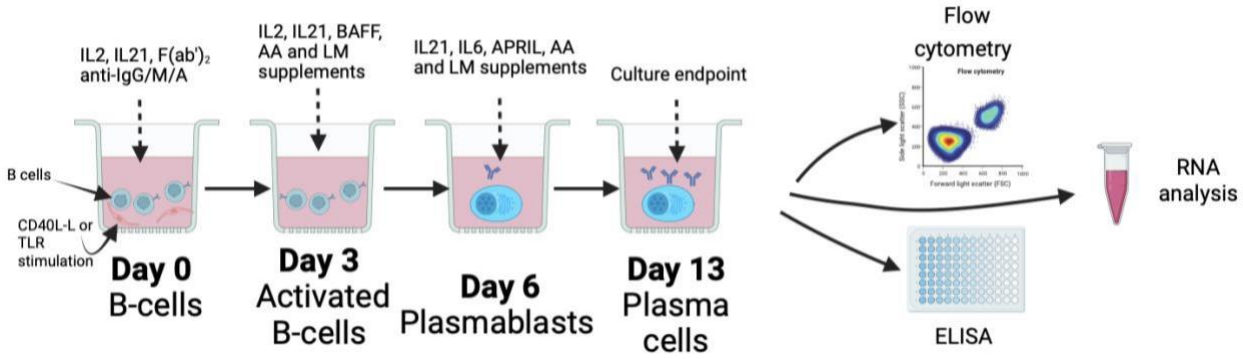

Figure 4.29: Optimised *In vitro* B-cell differentiation culture conditions. Isolated B-cells at day 0 are activated by CD40L or TLR agonist (i.e. R848) with F(ab')$_2$ anti-IgG/M/A. Corresponding stages of differentiation relative to the days are indicated, and cytokines/media requirements at each stage are stated above. Samples for flow cytometry, ELISA and RNA analysis are taken at the different stages. BAFF, B-cell activating factor; APRIL, a proliferation-inducing ligand; AA, amino acid; LM, lipid media.

Chapter 5- B-cell differentiation profiles of antibody-deficient patients enrolled in the COV-AD study

5.1 Introduction

Following the successful optimisation of the *in vitro* B-cell model for use with antibody-deficient patient samples, attention was turned to characterising B-cell differentiation profiles in these patients. This analysis aligns with the broader objectives of the COV-AD study, which aims to investigate how patients with antibody deficiencies respond to SARS-CoV-2 infection and vaccination, particularly given their heightened susceptibility to severe outcomes. A key focus of this study is to characterise the immune responses of these patients, with an emphasis on antibody production following vaccination (Shields *et al.,* 2022a; Shields *et al.,* 2022b).

Given the proven utility of the *in vitro* model in dissecting B-cell responses, it was suggested that the system could be effectively applied to COV-AD patients to study how various aspects of PC differentiation might influence a patient's ability to mount a successful immune response, or fail to do so, after SARS-CoV-2 vaccination. A successful immune response following COVID-19 vaccination is commonly defined by the presence of neutralising antibodies, primarily IgG and IgA, targeting the SARS-CoV-2 spike protein. This response includes a rise in IgG antibodies around 10-14 days post-vaccination, often reaching peak levels after the second dose. IgA responses typically appear earlier but decline more rapidly in serum. However, IgA can persist longer at mucosal surfaces, contributing to ongoing neutralising activity. Together, these antibody responses play a key role in the vaccine's protective effects by neutralising the virus and preventing infection at initial entry points (Wisnewski *et al.,* 2021; Pang *et al.,* 2021).

Studies have highlighted the significant contribution of germline-encoded BCRs to neutralising SARS-CoV-2. These antibodies, derived from conserved germline genes such as IGHV3-53 and IGHV3-6, demonstrate potent neutralisation abilities with minimal or no

SHM. Notably, Lunderberg et al. (2022) found that germline-encoded antibodies can effectively neutralise multiple SARS-CoV-2 variants, including those with mutations in the spike protein, by targeting conserved regions of the virus. This suggests that early protective antibody responses can be generated without extensive affinity maturation, providing a potential mechanism for immune responses even in antibody-deficient patients with impaired GC function. These findings are particularly relevant for understanding vaccine responses in individuals with limited SHM, as seen in some antibody-deficient conditions (Yuan *et al.,* 2020; Robbiani *et al.,* 2020; Andreano and Rappuoli, 2021).

Studying antibody responses to vaccination in COV-AD patients could provide important insights into the cellular mechanisms underlying vaccine responsiveness in antibody-deficient individuals and may also help identify biomarkers that could predict vaccine response, offering a potential tool for risk stratifying patients and personalising treatment strategies.

Accordingly, 50 frozen patient PBMC samples were selected and total B-cells were isolated from 49 of the patients who had recoverable B-cells. The patient cohort included a heterogenous group of both SARS-CoV-2 vaccine responding (*n*=35) and non-responding (*n*=14) patients with various primary (*n*=29) and secondary (*n*=20) antibody deficiencies. Samples were nationally obtained, and patients were both male and female adults aged 24-78 (Table 5.1). Previous findings from the COV-AD study primarily define non-responders based on their inadequate serological and cellular immune response following a second dose of either the approved Pfizer BioNTech (162b2) or AstraZeneca (ChAdOx1 nCoV-19) vaccine. Specifically, non-responders were defined as those with an IgGAM ratio <1.0 (optical density compared with calibrator), as measured by anti-spike glycoprotein antibody assays, around 28 days post-vaccination. This ratio provides a semi-quantitative assessment of antibody magnitude, where values greater than 1.0 are considered seropositive (Shields *et al.,* 2022a; Shields *et al.,* 2022b). Serum samples were also tested for neutralising activity using an in-house live virus neutralisation assay, which assesses the ability of antibodies to prevent virus entry into host cells. Non-responders were further defined by the absence of significant neutralising capacity. Additionally, T-cell responses were assessed using the T-SPOT®.COVID assay, with fewer than 5 spots per well indicating a negative response. A third group, termed 'true non-responders,' could be

defined as patients with IgGAM ratios below the threshold after both the second and third vaccine doses. However, for the purpose of this thesis, the classification will focus solely on responders versus non-responders, with non-responders defined as those who fail to generate a robust response to any vaccine dose.

5.1.1 Experimental setup

To distribute the workload efficiently, the differentiation of samples was performed in batches of five over ten experimental sessions. Each experimental setup included a naïve-fractioned HC obtained from approximately 5-10 mL of blood. The inclusion of a HC in each experiment was crucial to serve as a control, enabling the detection and exclusion of experimental errors or anomalies, i.e. any observed deviations in patient samples would likely be attributed to biological differences rather than technical variability. Using smaller amounts of starting blood and selecting only naïve B-cell populations was an approach to maintain as much consistency as possible between patient and HC samples. This would facilitate for cell inputs and counts to be as similar as possible, minimising any variability that could be accounted for by large differences in cell numbers or activation states. For patient samples, total B-cells were used, rather than fractionating into naïve B-cells as per controls, to better reflect the patient's natural B-cell composition.

	Overall	**Vaccine responders**	**Vaccine non-responders**
n	49	35	14
Primary antibody deficiency, *n*	29	21	8
Secondary antibody deficiency, *n*	20	14	6
Female, *n*	32	25	7
Age range (years)	24-78	24-78	31-74

Table 5.1: Characteristics of patients enrolled in the COV-AD study. Response to SARS-CoV-2 vaccination is determined post-third or fourth vaccination.

Although a total of 49 patient differentiations were conducted, this chapter will focus in detail on a selected subset of 9 patients (Table 5.2, along with a naïve-only healthy control and patients with either a known pathogenic mutation in *NFKB1* (c.447del) or a VUS *NFKB1* variant c.257A>G. In the Figures herein, HCs are represented in green, vaccine-responders in black, non-responders in red, and *NFKB1* patients in maroon. A variant of uncertain significance (VUS) refers to a genetic alteration in the *NFKB1* gene that has unclear implications for protein function and disease risk (ACGS, 2024). The inclusion of the HC is crucial for establishing baseline differentiation profiles, allowing for comparison against the patient samples to identify deviations indicative of immune dysfunction. The patients with *NFKB1* mutations serve as functional controls for flow cytometry analysis only, providing relevant insights into how variations in *NFKB1* function may influence B-cell differentiation, especially given that *NFKB1* mutations are often observed in patients with CVID (Fliegauf *et al.,* 2021). Notably, a subset of patients in the COV-AD study have been diagnosed with CVID, further emphasising the relevance of examining *NFKB1* patients in this context. This comparative approach enables a more nuanced analysis of the differentiation profiles within these groups, helping to clarify the variations that may impact immune responses. The data from the remaining patients will be included in summary figures, offering an overview of trends and patterns across the broader cohort without compromising the depth of insight gained from the detailed examination of the selected individuals. Statistical analysis was initially performed using one-way ANOVA, but as assumptions of normality and equal variance were not consistently met, the Kruskal-Wallis test was used to assess overall differences between groups, with Dunn’s test applied where appropriate to explore specific group differences.

Patient	Age	Sex	Diagnosis	Post V2 IgGAM ratio	Post V3 IgGAM ratio	Post V2 responder or non-responder
P1	63	M	CVID	3.71	6.14	Responder
P2	56	F	Secondary - HAEM	5.54	20.39	Responder
P3	62	M	CVID	1.9	6.18	Responder
P4	56	F	Secondary - RHEUM	4.47	4.56	Responder
P5	67	M	CVID	3.36	7.12	Responder
P6	38	F	Secondary - RHEUM	1.65	0.84	Non-responder
P7	34	M	CVID	0.13	N/A	Non-responder
P8	69	M	CVID	0.18	0.72	Non-responder
P9	43	M	CVID	0.31	2.18	Non-responder

Table 5.2: Patient characteristics and immune responses to vaccination. Clinical data from nine patients (P1-9), including age, sex, diagnosis, and their immune response status post-vaccination. The diagnoses include common variable immunodeficiency (CVID), and secondary immunodeficiency related to haematological (HAEM) and rheumatological (RHEUM) conditions. Post-vaccination immune response is measured by the IgG, IgA, and IgM (IgGAM) anti-spike glycoprotein ratio after the second (V2) and third (V3) vaccine doses. Patients are classified as either responders or non-responders based on their post-V2 IgGAM ratio.

5.2 B-cell proliferation capacities

The primary goal of the experiments in chapter 4 was to expand B-cell counts, given the anticipated low cell yields from patient samples in the COV-AD study. It was crucial to demonstrate the ability to generate sufficient cell numbers through to D13, as inadequate cell counts across all timepoints would impede the ability to perform comprehensive analyses.

In the representative patients (P1-P9), despite some patient-specific variability, overall B-cell counts were highly consistent with each other and with the controls at all timepoints, further evidenced by overlaps in data points (Figure 5.1A). However, data from the entire sample cohort at both the D6 and D13 timepoints revealed trends towards lower B-cell counts in both patient groups compared to controls, with non-responders displaying significantly reduced numbers at both timepoints (Figures 5.1B and 5.1C). This may suggest an intrinsic defect in B-cell survival or proliferation capacity amongst non-responders within the *in vitro* culture system. Despite this, the data also demonstrate that, with the incorporation of the modified *in vitro* differentiation system described in chapter 4, sufficient B-cells were generated to support the study of PC differentiation up to and including D13.

Furthermore, both vaccine responders (n=5) and non-responders (n=4) exhibited a typical B-cell proliferative pattern, similar to that of healthy controls (n=2) and NF-κB controls (n=2). This was characterised by an expansion of B-cells by D6 followed by a significant reduction, with only long-lived PCs persisting thereafter.

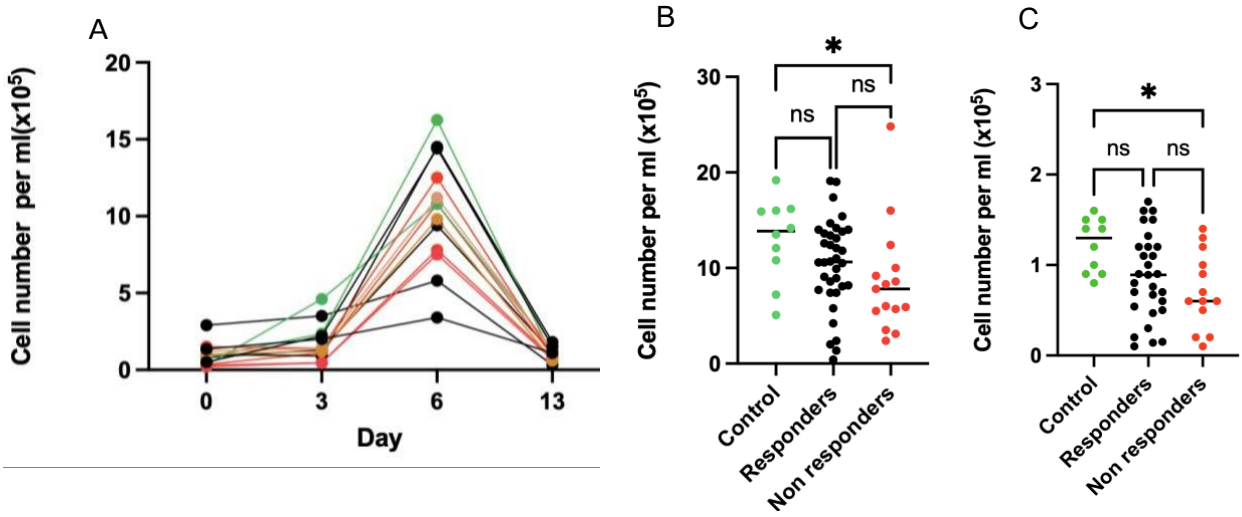

Figure 5.1: Evaluation of viable cell number in naïve controls, vaccine-responding and non-responding antibody deficient patients using the differentiation assays. A. Viable cell counts in representative controls and antibody deficient patients (P1-P9) from start to end of culture**.** HC (green), n=2; NF-κB controls (maroon), n=2; responders (black), n=5; non-responders (red), n=4. **B.** Quantification of the cell number per mL at the day 6 timepoint. **C.** Quantification of the cell number per mL at the day 13 timepoint. Healthy control (HC) naive B-cells, n= 10; Vaccine-responding patient B-cells, n=35; Vaccine non-responding patient B-cells, n=14. Significant differences were determined by one-way ANOVA or Kruskal-Wallis test with Dunn's multiple comparison, as appropriate (****p<0.0001 ***p<0.001 **p<0.01, *p<0.05).

5.3 Plasma cell generation

As expected, the representative HC displayed a typical differentiation profile, producing over 63% CD38hiCD138+ cells by D13. Vaccine-responding CVID patients and the *NFKB1* VUS patient similarly showed the anticipated CD138 expression pattern across the timepoints, though with notable variability in percentages. For example, P1 produced only 21% CD138+ cells by D13, whereas P5 generated over 75% CD138+ cells at the same timepoint and more than 9% CD138+ by D6, exceeding the levels seen in the HC (Figure 5.2).

Responding SAD patients, on the other hand, exhibited a tendency for lower CD38hi cell populations at D0 compared to the HC and CVID patients, potentially reflecting B-cell depletion, immunosuppressive treatments, or intrinsic B-cell dysfunction, all of which may impair early activation and differentiation. Nevertheless, by D6, CD38 expression in these patients appeared to return to near-normal levels. Regarding CD138 expression, the relative percentages were similarly variable. Notably, P2 showed abnormally high CD138+ expression at day 6, which normalised by D13 (Figure 5.2), possibly indicating an accelerated PC response as a compensatory mechanism to immune challenges.

Vaccine non-responders with both CVID and SAD demonstrated a typical B-cell differentiation phenotype, showing comparable ability to generate CD138+ PCs as seen in responders (Figure 5.2). This trend was observed across all differentiated patient samples (Figure 5.3), where no significant differences in CD138+ PC generation were observed at any timepoint between controls, responders, and non-responders. Any variation in CD138+ expression appeared to be driven more by the individual's antibody deficiency phenotype rather than by responder status within a specific patient subset.

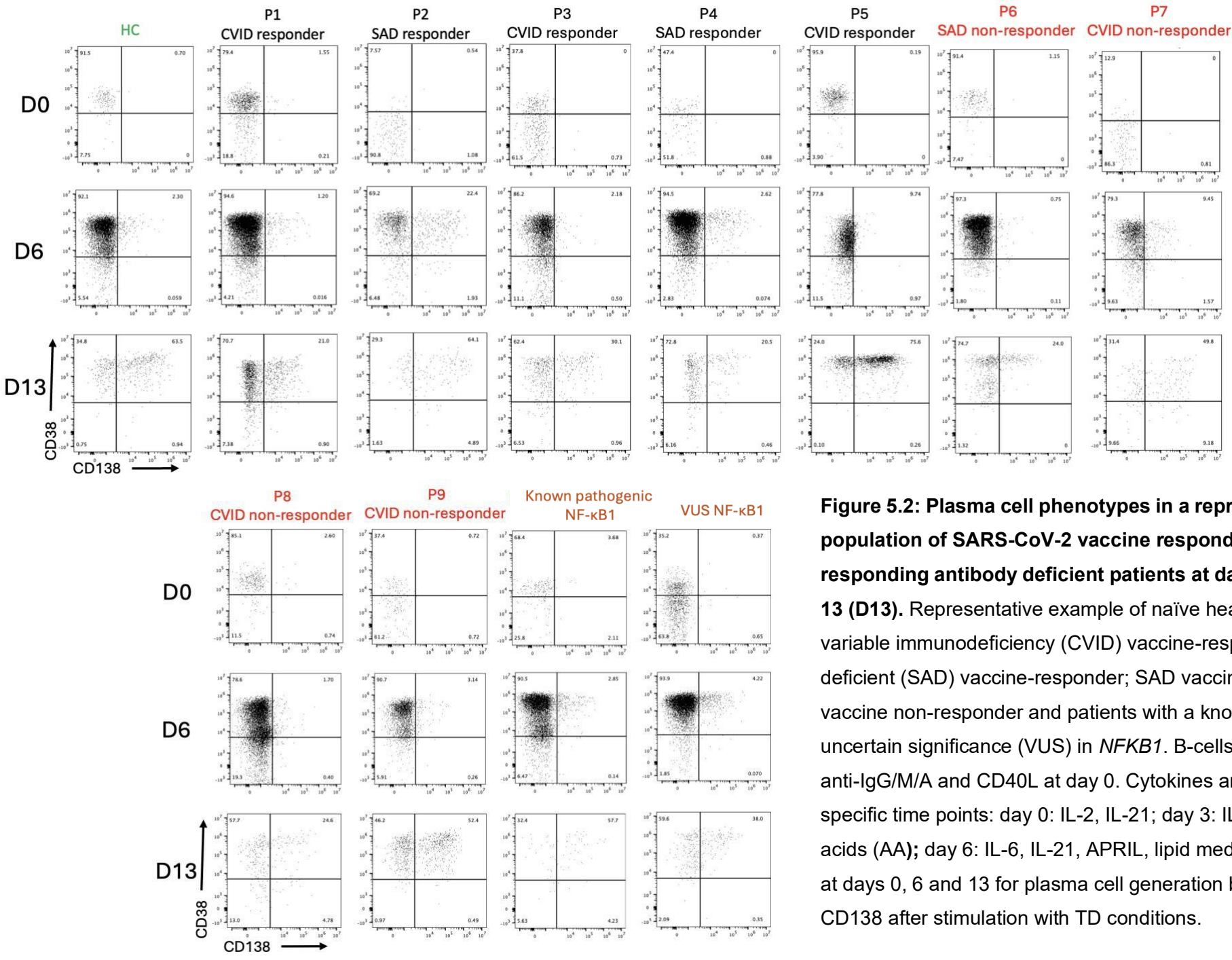

Figure 5.2: Plasma cell phenotypes in a representative heterogenous population of SARS-CoV-2 vaccine responding and vaccine non-responding antibody deficient patients at day 0 (D0), day 6 (D6) and day 13 (D13). Representative example of naïve healthy control (HC); Common variable immunodeficiency (CVID) vaccine-responder; Secondary antibody deficient (SAD) vaccine-responder; SAD vaccine non-responder and CVID vaccine non-responder and patients with a known variant and variant of uncertain significance (VUS) in *NFKB1*. B-cells were stimulated with $F(ab')_2$ anti-IgG/M/A and CD40L at day 0. Cytokines and supplements were added at specific time points: day 0: IL-2, IL-21; day 3: IL-2, IL-21, lipid media, amino acids (AA)**;** day 6: IL-6, IL-21, APRIL, lipid media, AA. B-cells were assessed at days 0, 6 and 13 for plasma cell generation by the gain of CD38 and CD138 after stimulation with TD conditions.

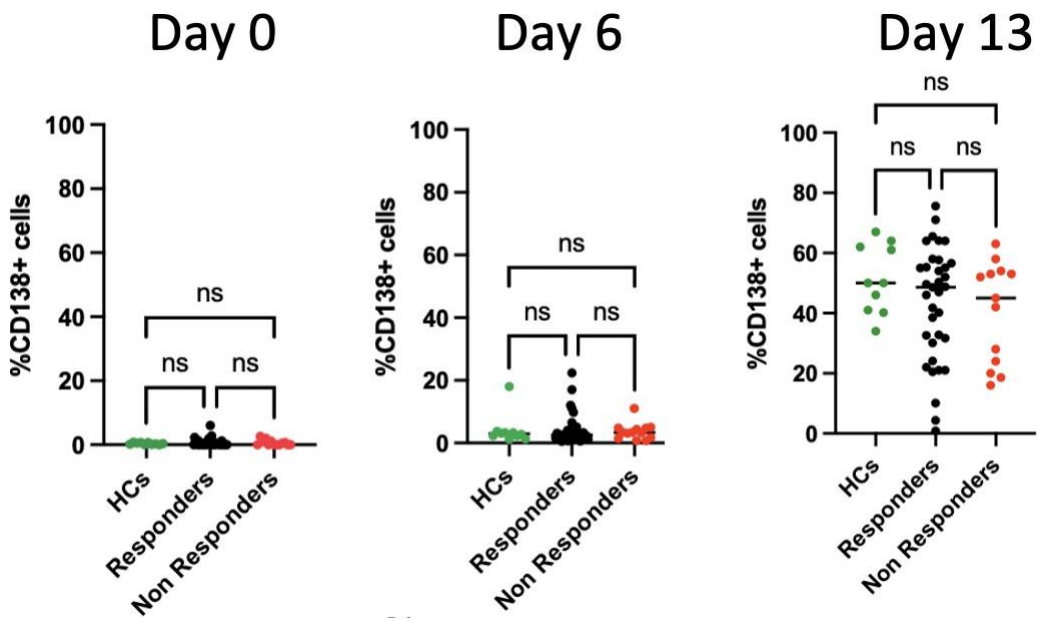

Figure 5.3: Summary of plasma cell phenotypes in a heterogenous population of antibody deficient patients. B-cells were stimulated with F(ab')$_2$ anti-IgG/M/A and CD40L at day 0. Cytokines and supplements were added at specific time points: day 0: IL-2, IL-21; day 3: IL-2, IL-21, lipid media, amino acids (AA**);** day 6: IL-6, IL-21, APRIL, lipid media, AA. Quantification of the percentage of cells expressing CD138 at the start of the assay, day 6 and day 13. Healthy control (HC) naive B-cells, n= 10; Vaccine-responding patient total B-cells, n=35; Vaccine non-responding patient total B-cells, n=14. Significant differences were determined by one-way ANOVA or Kruskal-Wallis test with Dunn's multiple comparison, as appropriate (****p<0.0001 ***p<0.001 **p<0.01, *p<0.05). Note that low cell numbers resulted in the inability to obtain certain samples at later time-points.

5.5 Plasmablast generation

The representative HC exhibited the expected gradual increase in CD27+ cells up to D13, with 95.1% of cells expressing the $CD38^{hi}$CD27+ phenotype. This trend was observed across all representative COV-AD samples and in the *NFKB1* patients, though to varying extents. While all samples demonstrated an increase in $CD38^{hi}$CD27+ populations, they showed a reduced capacity for this compared to the control, particularly at days 6 and 13, where the differences were statistically significant, most notably at D6 (Figure 5.4). The only notable deviation was P5, which displayed an atypical differentiation pattern. While P5 showed typical percentages at D6, the exceedingly high $CD38^{hi}$CD27+ expression at D13 and the abnormal phenotype make this patient distinct (Figure 5.4).

Regarding vaccine responders versus non-responders, no significant difference in the generation of $CD38^{hi}$CD27+ plasmablasts was observed, either in the representative samples or the total sample pool, for both primary and secondary antibody deficiencies (Figures 5.4 and 5.5). Therefore, while this data highlights a reduced capacity for generating $CD38^{hi}$CD27+ plasmablasts in the patient cohort (most notably in the non-responders), it also suggests that variations in plasmablast generation, similar to the patterns of PC generation discussed in chapter 5.4, are unlikely to dictate vaccine responsiveness.

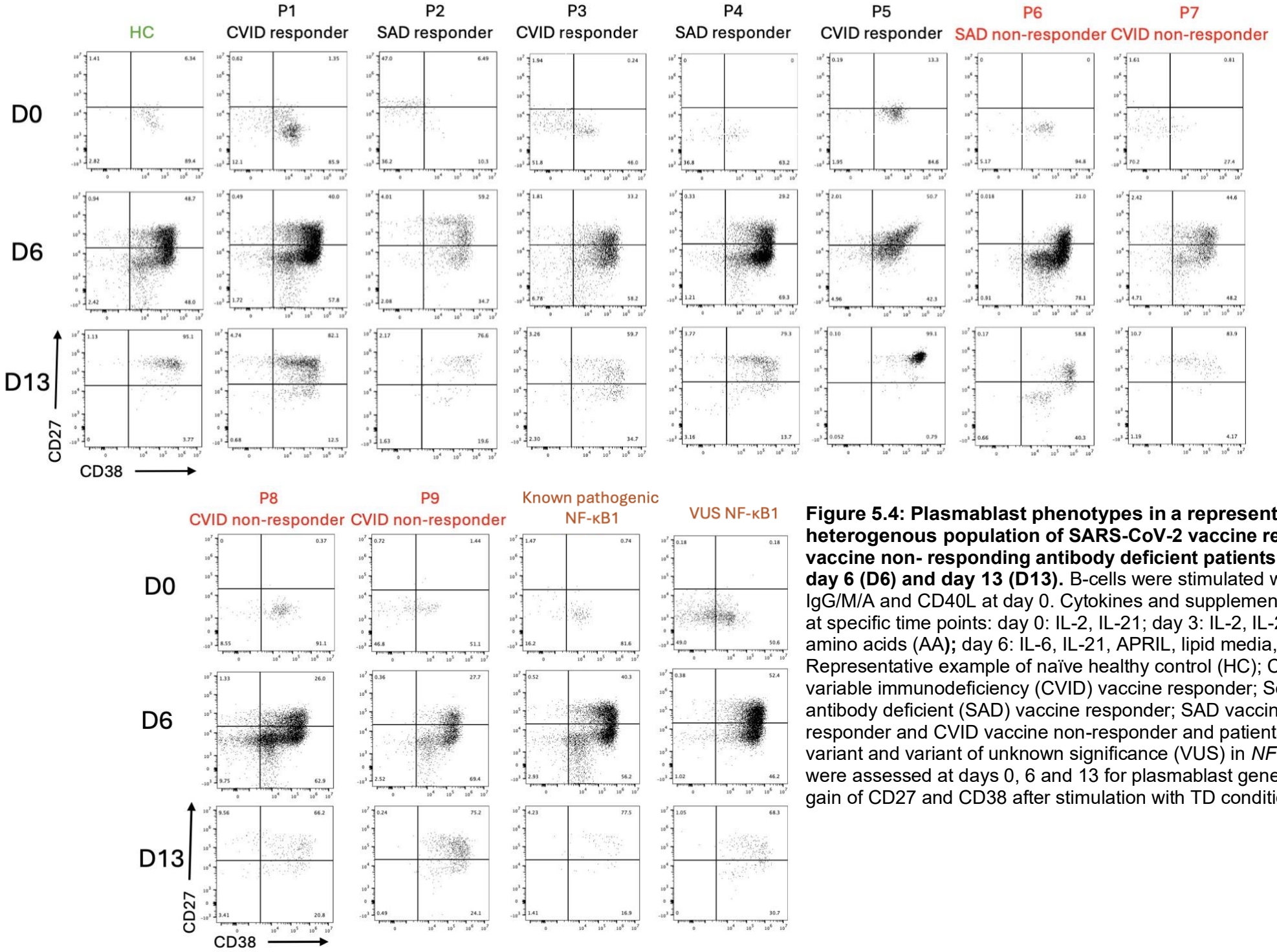

Figure 5.4: Plasmablast phenotypes in a representative heterogenous population of SARS-CoV-2 vaccine responding and vaccine non- responding antibody deficient patients at day 0 (D), day 6 (D6) and day 13 (D13). B-cells were stimulated with F(ab')$_2$ anti-IgG/M/A and CD40L at day 0. Cytokines and supplements were added at specific time points: day 0: IL-2, IL-21; day 3: IL-2, IL-21, lipid media, amino acids (AA**);** day 6: IL-6, IL-21, APRIL, lipid media, AA. Representative example of naïve healthy control (HC); Common variable immunodeficiency (CVID) vaccine responder; Secondary antibody deficient (SAD) vaccine responder; SAD vaccine non-responder and CVID vaccine non-responder and patients with a known variant and variant of unknown significance (VUS) in *NFKB1*. B-cells were assessed at days 0, 6 and 13 for plasmablast generation by the gain of CD27 and CD38 after stimulation with TD conditions.

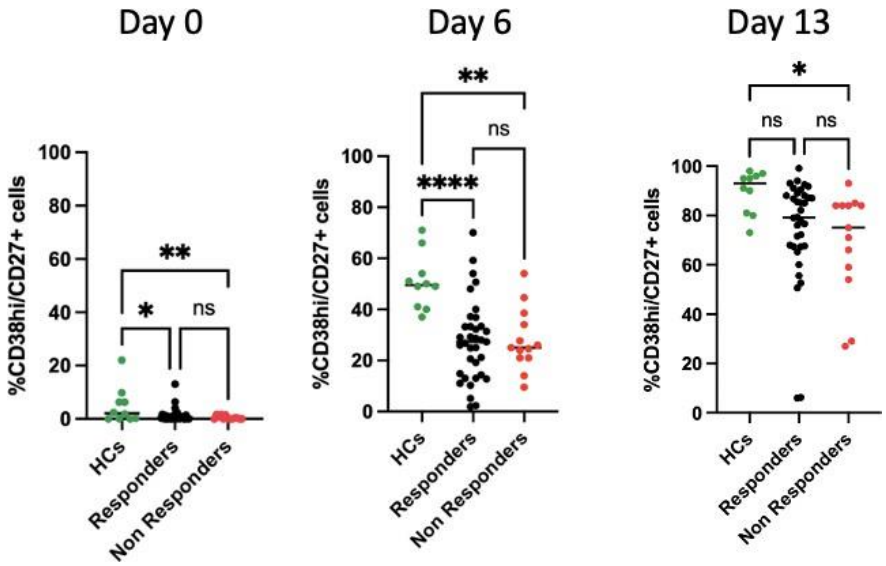

Figure 5.5: Summary of plasmablast phenotypes in a heterogenous population of antibody deficient patients. B-cells were stimulated with F(ab')$_2$ anti-IgG/M/A and CD40L at day 0. Cytokines and supplements were added at specific time points: day 0: IL-2, IL-21; day 3: IL-2, IL-21, lipid media, amino acids (AA**);** day 6: IL-6, IL-21, APRIL, lipid media, AA. Quantification of the percentage of cells expressing CD38^{hi}CD27+ at the start of the assay, day 6 and day 13. Healthy control (HC) naive B-cells, n= 10; Vaccine-responding patient total B-cells, n=35; Vaccine non-responding patient total B-cells, n=14. Significant differences were determined by one-way ANOVA or Kruskal-Wallis test with Dunn's multiple comparison, as appropriate (****p<0.0001 ***p<0.001 **p<0.01, *p<0.05). Note that low cell numbers resulted in the inability to obtain certain samples at later time-points.

5.6 Immunoglobulin expression

Thus far, the data presented in this chapter has shown that, despite phenotypic variability in the expression of PC and plasmablast markers among individual patients, these markers alone do not clearly distinguish vaccine non-responders from responders. While surface phenotypes indicate activation, they do not necessarily reflect the functional capacity of the cells to produce sufficient immunoglobulin. By definition, antibody-deficient patients have reduced or impaired antibody production, which may reflect intrinsic B-cell problems, or a lack of adequate T-cell help. However, because the reduced production of these immunoglobulins is a defining feature of antibody deficiency, it may serve as a critical factor in explaining why some individuals fail to respond effectively to COVID-19 vaccination. Differences in immunoglobulin production profiles between responders and non-responders could

provide further insight. Without adequate intracellular and secreted immunoglobulin, these cells may remain functionally deficient, contributing to poor vaccine responses, even in the presence of 'normal' surface markers. Therefore, the next objective is to examine the intracellular and secretory expression of IgM, IgG, and IgA in the patient cohort to better assess their functional capacity.

5.7 Intracellular immunoglobulin expression

The representative HC displayed a typical intracellular immunoglobulin expression profile, demonstrating effective class switching. Higher IgM expression at D6 decreased by D13, at which point IgG and IgA levels reached approximately 46% and 30%, respectively. The *NFKB1* VUS patient exhibited good IgG expression at both time points, though IgA expression was reduced. Based on the collective representative patient data, no clear distinction was observed between SAD and CVID patients. Most patients exhibited elevated IgM and reduced IgG and IgA expression at both time points, consistent with an antibody deficiency. A subset of patients (e.g., P1, P4, P6, and P8) displayed particularly high IgM expression, as evidenced by increased fluorescence. (Figure 5.6 and Figure 5.7). Across the wider cohort, IgM expression was significantly higher in non-responders compared to controls at both D6 and D13, while responders also demonstrated significantly increased IgM at D6 but only a non-significant trend towards elevated levels at D13 (Figure 5.8).

Anomalies in the IgG profile was noted in P3 and P4, with P3 demonstrating intracellular IgM, IgG, and IgA levels comparable to a HC. However, P5 showed a highly unusual phenotype, with an inability to express IgM, minimal IgA expression, and an unusually high expression of IgG (~92%) at both time points (Figure 5.6), suggesting possible dysregulation in isotype switching or a skewed immunoglobulin production pattern possibly attributed to a disorder other than the CVID.

With regard to IgG, the representative data suggested that non-responders expressed lower levels of IgG at both time points compared to responders (Figure 5.6). However, when all samples were analysed collectively (Figure 5.8), no significant difference in IgG expression between responders and non-responders

was observed at either D6 or D13, though both groups had significantly lower IgG levels compared to HCs.

IgA expression was overall lower in all representative patients compared to the control. Notably, P4 and P7 showed no IgA expression at either D6 or D13 (Figure 5.7). When considering all patient samples, non-responders had significantly reduced intracellular IgA expression by D13 compared to both controls and vaccine responders (Figure 5.8), suggesting a potential link between poor IgA production and a lack of response to the COVID vaccine.

In summary, across all patient differentiations (Figure 5.8), both vaccine responders and non-responders tended to exhibit elevated IgM expression throughout the time points. Both groups also showed significantly reduced IgG and IgA levels compared to controls at days 6 and 13, but the only isotype with a significant difference between responders and non-responders was IgA expression at D13, potentially linking IgA deficiency with poor vaccine response.

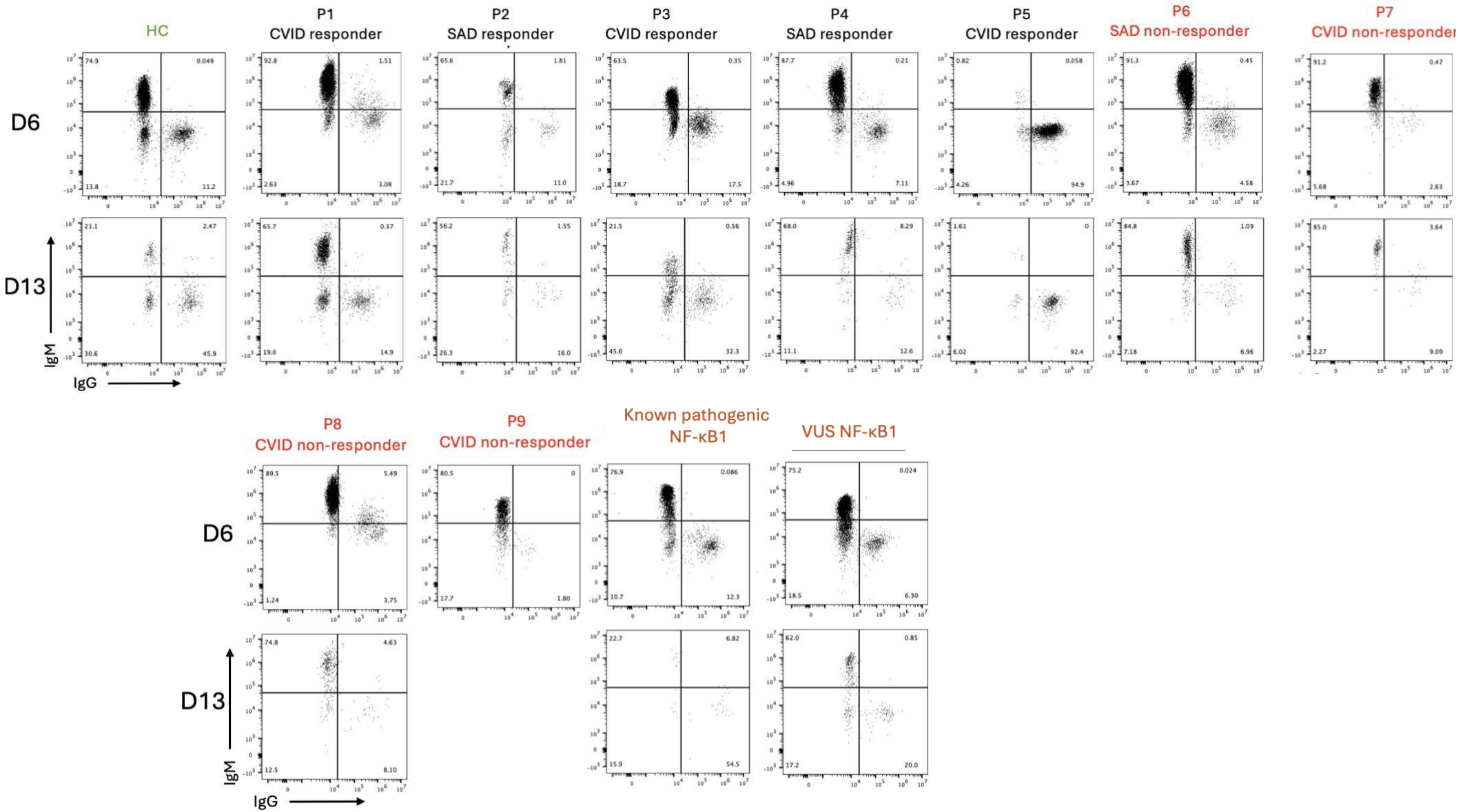

Figure 5.6: Intracellular immunoglobulin (IgM and IgG) expression in representative SARS-CoV-2 vaccine responding and vaccine non-responding antibody deficient patients at day 6 (D6) and day 13 (D13). B-cells were stimulated with F(ab')$_2$ anti-IgG/M/A and CD40L at day 0. Cytokines and supplements were added at specific time points: day 0: IL-2, IL-21; day 3: IL-2, IL-21, lipid media, amino acids (AA**);** day 6: IL-6, IL-21, APRIL, lipid media, AA. Representative example of naïve healthy control (HC); Common variable immunodeficiency (CVID) vaccine-responder; Secondary antibody deficient (SAD) vaccine-responder; SAD vaccine non-responder; CVID vaccine non-responder and patients with a known variant and variant of uncertain significance (VUS) in *NFKB1.* B-cells were assessed at days 6 and 13 for intracellular IgM and IgG expression after stimulation with TD conditions. Note that insufficient cell counts at D13 in P9 rendered analysis not possible.

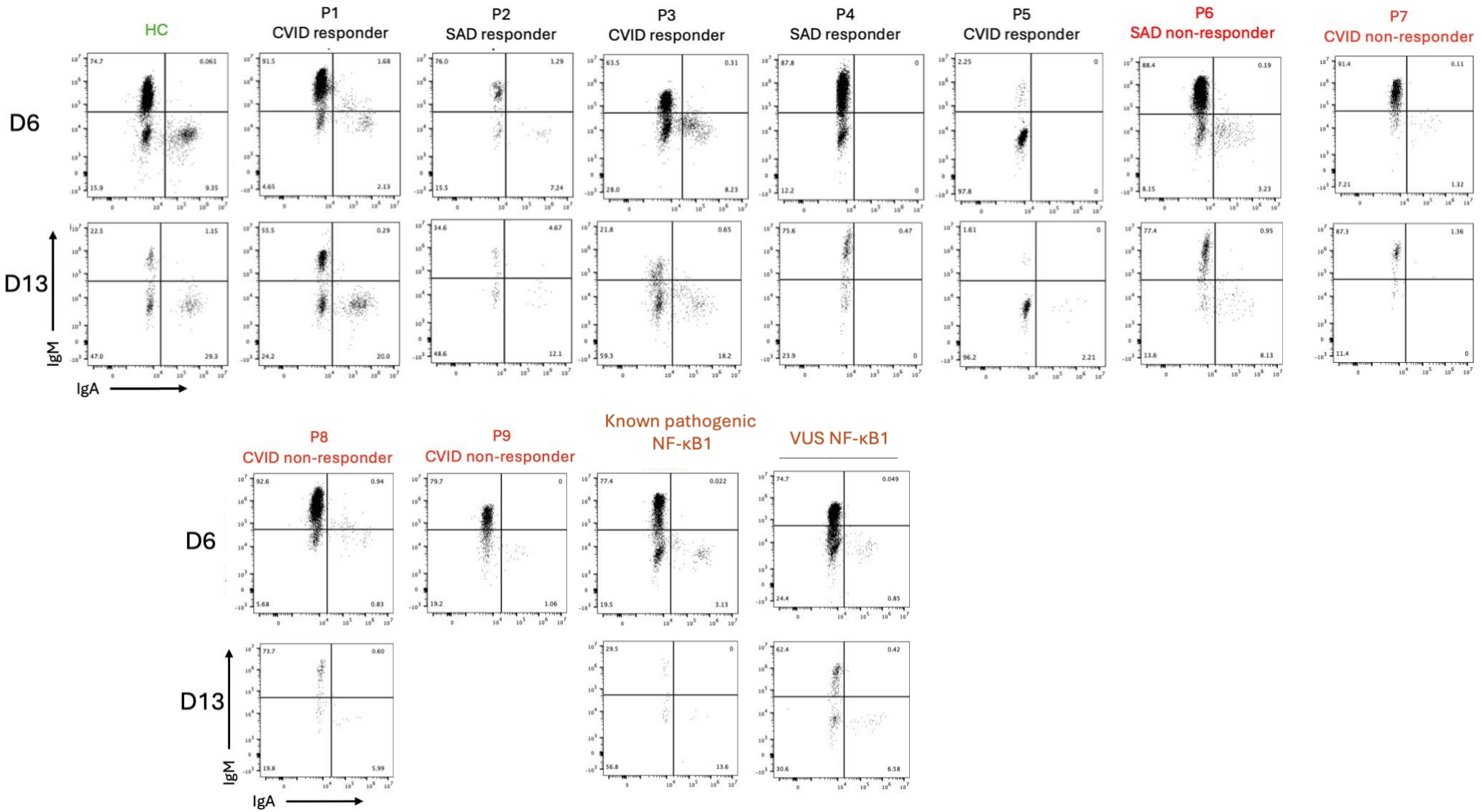

Figure 5.7: Intracellular immunoglobulin (IgM and IgA) expression in representative SARS-CoV-2 vaccine responding and vaccine non-responding antibody deficient patients at day 6 (D6) and day 13 (D13). B-cells were stimulated with F(ab')$_2$ anti-IgG/M/A and CD40L at day 0. Cytokines and supplements were added at specific time points: day 0: IL-2, IL-21; day 3: IL-2, IL-21, lipid media, amino acids (AA**);** day 6: IL-6, IL-21, APRIL, lipid media, AA. Representative example of Naïve Healthy Control (HC); Common Variable Immunodeficiency (CVID)vaccine-responder; Secondary antibody deficient (SAD) vaccine-responder; SAD vaccine non-responder; CVID vaccine non-responder and patients with a known variant and variant of uncertain significance (VUS) in *NFKB1*. B-cells were assessed at days 6 and 13 for intracellular IgM and IgG expression after stimulation with TD conditions. Note that insufficient cell counts at D13 in P9 rendered analysis not possible.

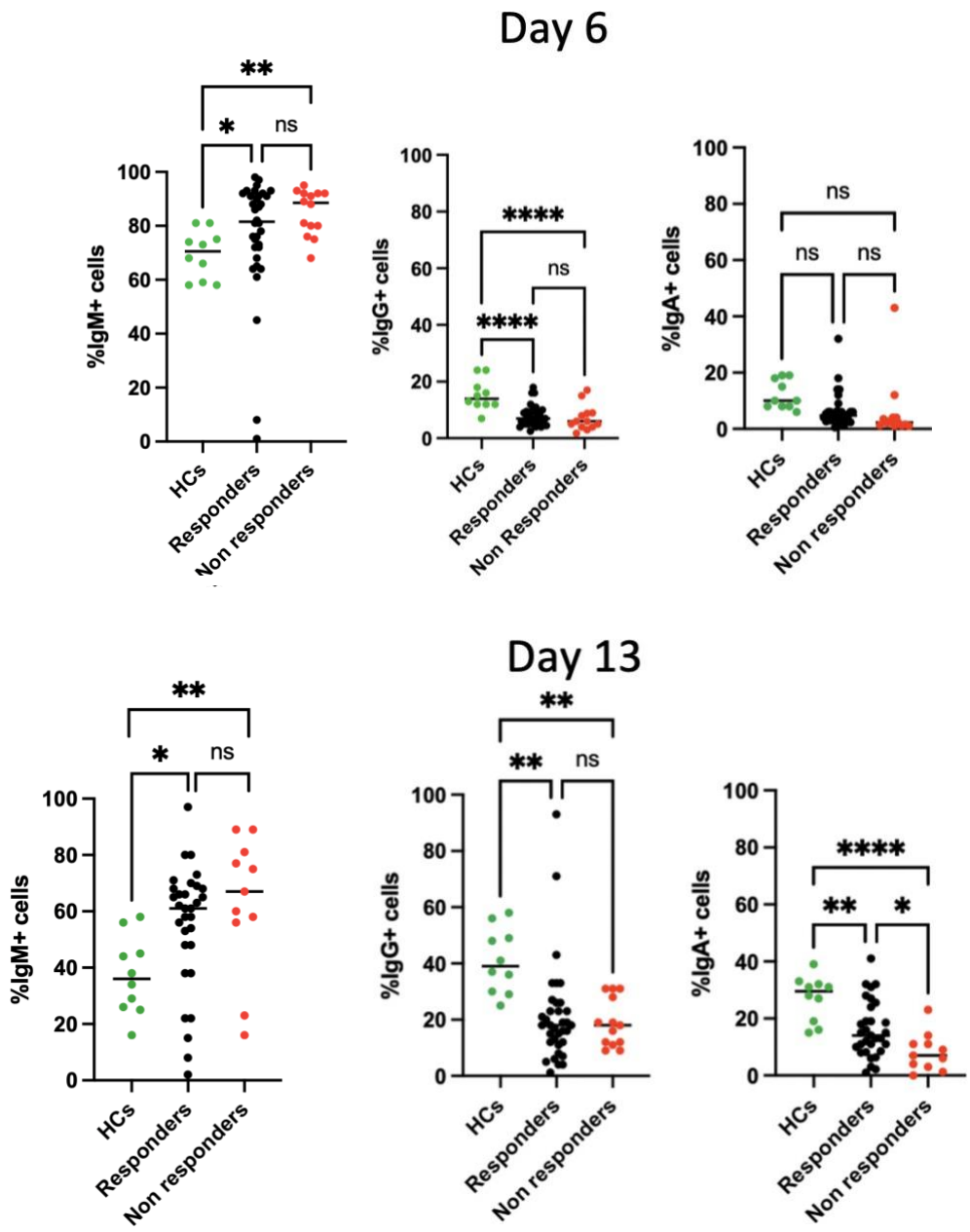

Figure 5.8: Assessment of the percentage of cells expressing IgM, IgG and IgA at days 6 and 13. B-cells were stimulated with F(ab')$_2$ anti-IgG/M/A and CD40L at day 0. Cytokines and supplements were added at specific time points: day 0: IL-2, IL-21; day 3: IL-2, IL-21, lipid media, amino acids (AA)**;** day 6: IL-6, IL-21, APRIL, lipid media, AA. Healthy control (HC) naïve B-cells, n=10; vaccine-responding patient total B-cells, n=35; vaccine non- responding patient total B-cells, n=13. Quantification of intracellular IgM, IgG and IgA expression at days 6 and 13 from representative naïve HC, Vaccine responding and vaccine non-responding patients. Significant differences were determined by one-way ANOVA or Kruskal-Wallis test with Dunn's multiple comparison, as appropriate (****p<0.0001 ***p<0.001 **p<0.01, *p<0.05). Note that low cell numbers resulted in the inability to obtain certain samples at later time-points.

5.8 Secreted immunoglobulin quantification

Immunoglobulin secretion varied across the patient cohort. In both the representative and collective HCs, IgM secretion ranged between 5,000–100,000 ng/mL at D6 and remained consistent through D13. At D6, most representative patients, including the *NFKB1* VUS control, showed IgM levels comparable to the HCs, except for P3, who had lower secretion, and P5, who secreted almost no IgM - consistent with P5's intracellular IgM phenotype in Figures 5.6 and 5.7. By D13, most patients demonstrated the consistent IgM concentration across the timepoints seen in the HC, although four patients (P1, P4, P8, and P9) demonstrated higher IgM secretion relative to HC (Figure 5.9). In the broader analysis, there was additionally trend towards higher IgM secretion in non-responders compared to responders (Figure 5.10), possibly representing an impairment in class-switching.

IgG secretion was also variable across all representative and total patient datapoints, although showed a general trend of lower IgG levels at both timepoints in COV-AD patients and the *NFKB1* VUS control compared to HCs. P5 was a notable outlier, with an exceptionally high D13 IgG level that skewed the overall results (Figure 5.9). The summary plot showed that vaccine responders had significantly lower IgG concentrations than HCs at D13, whereas non-responders exhibited IgG levels comparable to controls at the same timepoint (Figure 5.10). Unexpectedly higher IgG secretion values may reflect assay-related background interference, heterogeneity within non-responders or autoantibody production in a subset of patients. It is also possible that preferential survival or outgrowth of switched IgG+ B-cells in culture contributed to these secretory findings (King *et al.,* 2021).

In terms of IgA secretion, all representative patients, including the VUS *NFKB1* control, exhibited lower IgA levels at both timepoints compared to HCs. Similar to intracellular data, certain patients, such as P5 and P6, either secreted very little or no IgA at all (Figure 5.9). Based on the collective patient results, both vaccine responding and non-responding groups had significantly lower IgA secretion compared to controls (Figure 5.10), with non-responders showing an even greater reduction, comparable to intracellular IgA data (Figure 5.7).

Overall, immunoglobulin secretion varied across the patient cohort, influenced more by individual patient factors than by diagnosis or vaccine response. The findings revealed patterns consistent with those seen in intracellular data, with IgA being the only isotype that demonstrated significant differences in concentrations between both patient groups and HCs, likely reflecting the high prevalence of deficiencies in this isotype. However, given that only a trend was noted in lower IgA concentrations in non-responders compared to responders at D13, it is unlikely that IgA levels-or any of the other isotypes measured-can reliably predict vaccine response.

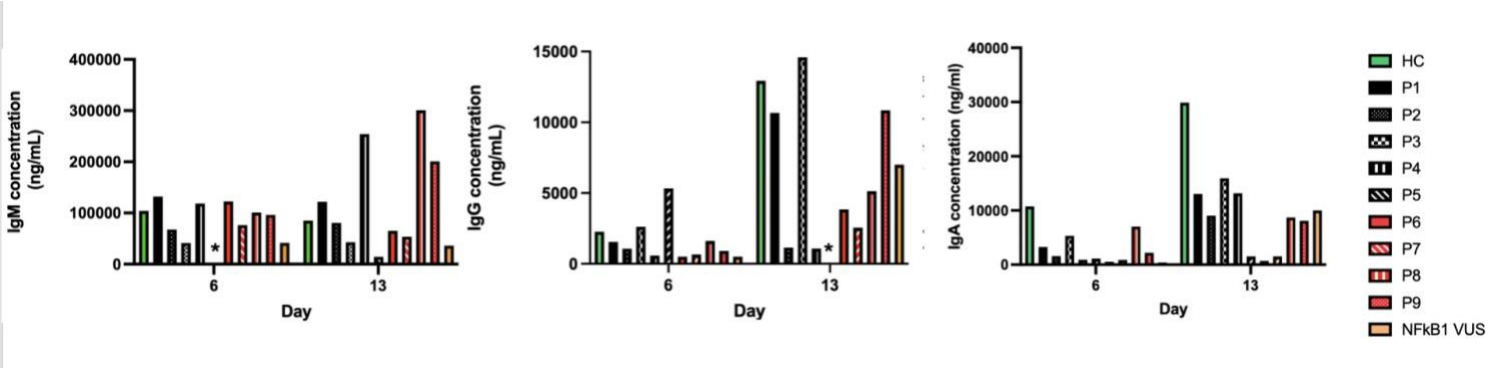

Figure 5.9: Assessment of secreted IgM, IgG and IgA at days 6 and 13 in a heterogenous cohort of antibody deficient patients (P1-P9). Representative example of Naïve Healthy Control (HC); Common Variable Immunodeficiency (CVID) vaccine-responder; Secondary antibody deficient (SAD) vaccine-responder; SAD vaccine non-responder; CVID vaccine non-responder and patient with a variant of uncertain significance (VUS) in *NFKB1*. B-cells were assessed at days 6 and 13 for secreted IgM, IgG and IgA expression after stimulation with T-dependent stimulation conditions. *Note: some values were exceptionally low (day 6 IgM, P5) or high (day 13 IgG, P5) and were not included in the Figure.

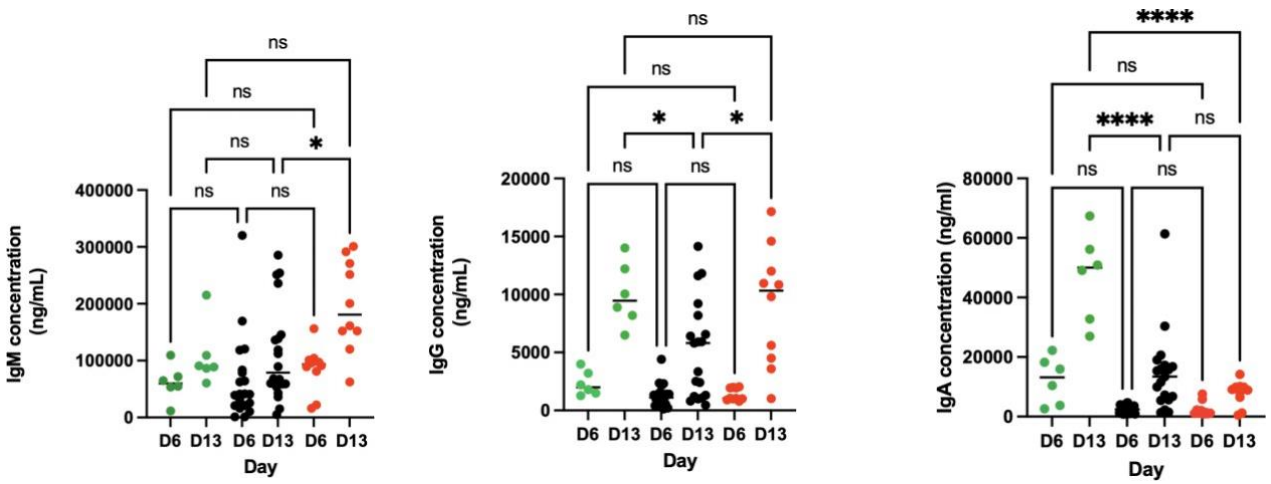

Figure 5.10: Assessment of secreted IgM, IgG and IgA at days 6 and 13 in a heterogenous cohort of antibody deficient patients. B-cells were stimulated with F(ab')$_2$ anti-IgG/M/A and CD40L at day 0. Cytokines and supplements were added at specific time points: day 0: IL-2, IL-21; day 3: IL-2, IL-21, lipid media, amino acids (AA)**;** day 6: IL-6, IL-21, APRIL, lipid media, AA. Healthy control (HC) naïve B-cells, n=6; vaccine-responding patient total B-cells, n=20; vaccine non-responding patient total B-cells, n=10. Quantification of intracellular IgM, IgG and IgA expression at days 6 and 13 from representative naïve HC, Vaccine responding and vaccine non-responding patients. Significant differences were determined by one-way ANOVA or Kruskal-Wallis test with Dunn's multiple comparison, as appropriate (****p<0.0001 ***p<0.001 **p<0.01,*p<0.05). Note that low cell numbers resulted in the inability to obtain certain samples.

5.9 Phenotypic features regulating survival

Despite the inherent variability among patients, analyses thus far have revealed no significant differences in the expansion of B-cells, generation of phenotypically identifiable antibody-secreting cells or the expression of immunoglobulin isotypes between vaccine non-responders and responders likely to predict a productive response to vaccination. These results suggest that provision of optimised differentiation and survival factors *in vitro* are sufficient to overcome in vivo limitations. If this is the case, then there may be changes in access to these factors in vivo that lead to vaccine failure. To further explore whether non-responders might

have alterations in key external regulators of the B-cell lineage, CD19 and BAFF-R expression were next investigated (Darce *et al.,* 2007; Wang *et al.,* 2012; Lau *et al.,* 2020).

In line with expected B-cell differentiation patterns, the representative HC demonstrated a homogeneous population of 100% CD19+BAFF-R+ pre-activated B-cells at D0. Consistent with the literature, BAFF-R expression declined by D6 and remained low at D13, mirroring the *in vivo* expression dynamics of BAFF-R (Smulski *et al.,* 2018). While PCs typically do not express BAFF-R, the apparent increase in expression at D13 may indicate the maturation of B-cells that have not fully differentiated into PCs but are still in stages where BAFF-R is essential for survival, such as mature naive or memory B-cells. This is exemplified in patient sample P1, which displayed 44.1% BAFF-R+ expression at D13 alongside only 21% CD138+ expression at the same time point (Figure 5.11). Alternatively, this increase could be an artifact resulting from the consistent gating strategy applied across all samples and time points.

Regarding patient samples, vaccine non-responders, P4 and the *NFKB1* VUS patient exhibited abnormally low or absent BAFF-R expression at D0 (Figure 5.11), a trend that persisted across all other patient samples (Figure 5.12). In contrast, all HCs showed expected CD19+BAFF-R+ expression near 100%, while most responders demonstrated high BAFF-R expression; however, some exhibited intermediate or low levels. Notably, all non-responders showed low or absent BAFF-R expression in pre-activated B-cells. While this marked difference in BAFF-R expression did not extend to time points beyond D0 (Figure 5.12), there was a trend suggesting slightly higher BAFF-R expression at D6 in non-responders relative to responders and controls, potentially indicating a delayed BAFF-R response in certain patients.

Thus, the data regarding CD19 and BAFF-R expression strongly correlate with vaccine response, highlighting a significant relationship between BAFF-R expression in pre-activated B-cells and the ability to mount an effective immune response. Additionally, the presence of a subset of vaccine responders exhibiting similar low BAFF-R expression raises intriguing questions about whether these individuals may have a predisposition to impaired vaccine responses, suggesting that BAFF-R could potentially serve as a biomarker for predicting responses to the SARS-CoV-2

vaccine.

The reduced BAFF-R expression observed may reflect impaired B-cell survival, as BAFF-R-mediated signalling is crucial for maintaining mature B-cell homeostasis and promoting cell survival in both naïve and memory compartments (Mackay *et al.,* 2003; Cancro, 2009). Furthermore, diminished BAFF-R expression could limit responsiveness to BAFF-dependent differentiation signals, potentially restricting the generation of antibody-secreting cells or memory B-cells following stimulation (Thompson*,* 2001; Mackay *et al.,* 2003). This may partly explain the reduced immunogenicity observed in non-responders, although the lack of associated abnormalities in responders with low BAFF-R expression suggests additional factors are likely involved.

It should be noted, however, that responders with low/absent BAFF-R expression did not trend towards borderline IgGAM values nor did they share any other known distinguishing features.

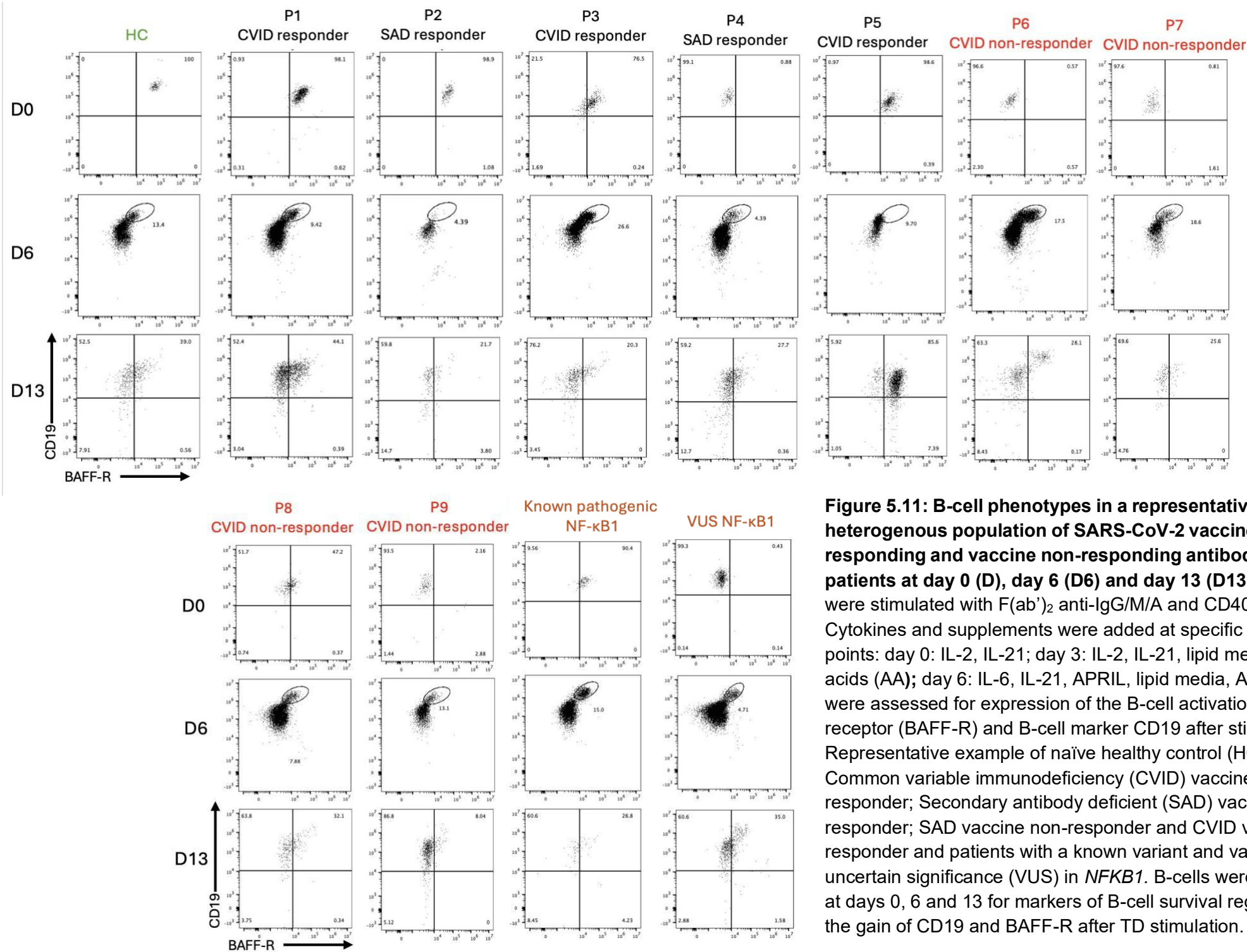

Figure 5.11: B-cell phenotypes in a representative heterogenous population of SARS-CoV-2 vaccine responding and vaccine non-responding antibody deficient patients at day 0 (D), day 6 (D6) and day 13 (D13). B-cells were stimulated with F(ab')$_2$ anti-IgG/M/A and CD40L at day 0. Cytokines and supplements were added at specific time points: day 0: IL-2, IL-21; day 3: IL-2, IL-21, lipid media, amino acids (AA**);** day 6: IL-6, IL-21, APRIL, lipid media, AA. B-cells were assessed for expression of the B-cell activation factor-receptor (BAFF-R) and B-cell marker CD19 after stimulation. Representative example of naïve healthy control (HC); Common variable immunodeficiency (CVID) vaccine-responder; Secondary antibody deficient (SAD) vaccine-responder; SAD vaccine non-responder and CVID vaccine non-responder and patients with a known variant and variant of uncertain significance (VUS) in *NFKB1.* B-cells were assessed at days 0, 6 and 13 for markers of B-cell survival regulators by the gain of CD19 and BAFF-R after TD stimulation.

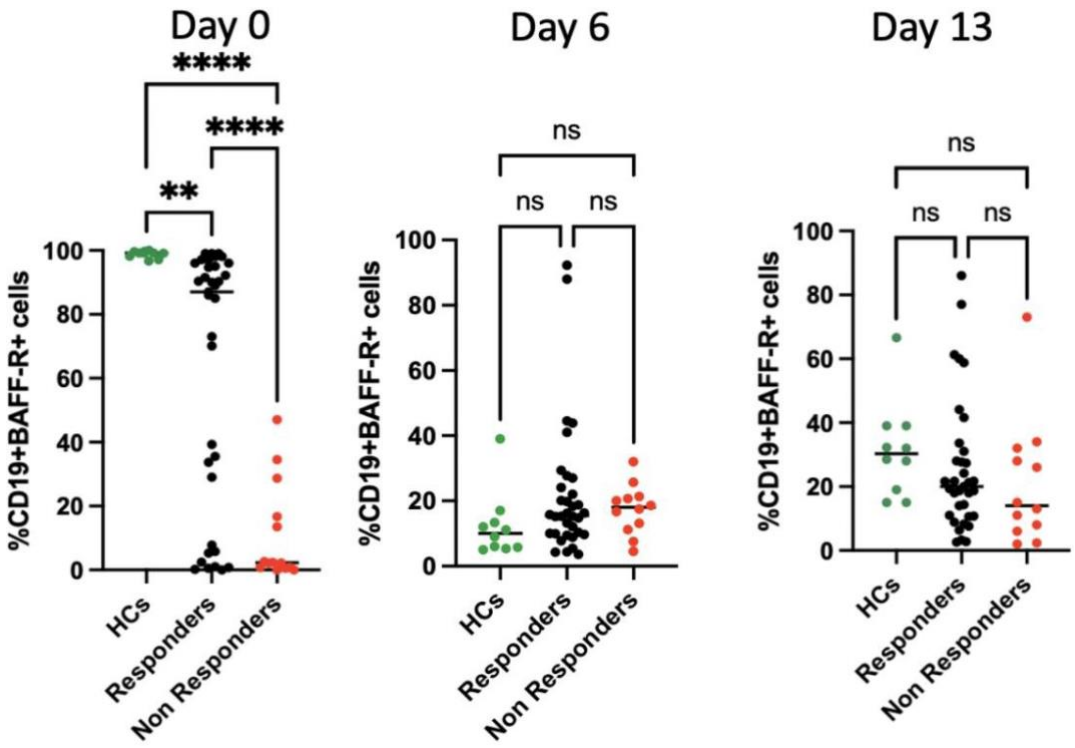

Figure 5.12: Summary of CD19+BAFF-R+ phenotypes in a heterogenous population of antibody deficient patients. B-cells were stimulated with F(ab')$_2$ anti-IgG/M/A and CD40L at day 0. Cytokines and supplements were added at specific time points: day 0: IL-2, IL-21; day 3: IL-2, IL-21, lipid media, amino acids (AA**);** day 6: IL-6, IL-21, APRIL, lipid media, AA. Quantification of the percentage of cells expressing the B-cell activation factor-receptor (BAFF-R) and B-cell marker CD19 at the start of the assay, day 6 and day 13 after stimulation with TD conditions. HC naive B-cells, n= 10; Vaccine-responding patient total B-cells, n=35; Vaccine non-responding patient total B-cells, n=14. Significant differences were determined by one-way ANOVA or Kruskal-Wallis test with Dunn's multiple comparison, as appropriate (****p<0.0001 ***p<0.001 **p<0.01*p<0.05). Note that low cell numbers resulted in the inability to obtain certain samples at later time-points.

.

5.10 Expression of the *TNFRSF13C* gene

Due to the striking differences in BAFF-R expression observed at the D0 timepoint, samples were next collected at this stage to explore whether RNA expression could shed light on whether impaired transcription of the BAFF-R-encoding gene, *TNFRSF13C,* contributes to the abnormal surface expression phenotype. Patients selected for RNA-seq represented a diverse group of vaccine responders and non-responders with CVID or SAD diagnoses, covering a range of BAFF-R surface expression levels at D0. Selection was also dependent on the availability of sufficient B-cell numbers, as cell yields are typically limited at this early timepoint. These samples contained adequate material for both phenotypic analyses, as described in previous chapters, and RNA-seq analysis. For consistency, low surface BAFF-R expression was defined as 50% or lower relative to healthy controls.

RNA-seq data revealed that *TNFRSF13C* expression was high in representative HCs and reduced in both non-responders and responders with low BAFF-R surface expression at D0 (Figure 5.13). This suggests that in some cases, reduced BAFF-R surface expression may be mirrored by lower transcript levels.
However, *TNFRSF13C* expression was unexpectedly variable among responders with high surface BAFF-R levels (Figure 5.13), implying that additional regulatory factors (i.e. compensatory mechanisms, post-transcriptional modifications, or heterogeneity within the responder group) may influence its expression. These differences also reflect the limitations of grouping CVID and SAD patients together in analyses, hinting at the value of more refined patient stratification in future studies.

Taken together, RNA-seq data suggest that while reduced *TNFRSF13C* expression may partially explain low surface BAFF-R expression in some patients, it is unlikely to account for the entirety of the phenotype, particularly in cases where RNA levels appear unchanged. This raises the possibility that post-translational modifications, altered receptor trafficking, or increased receptor degradation could be contributing to the abnormal surface expression (Yoshinage and Takeuchi, 2019). To investigate other potential mechanisms influencing the observed BAFF-R phenotype, subsequent work in this Chapter will focus on exploring other surface-level mechanisms that might underpin these findings.

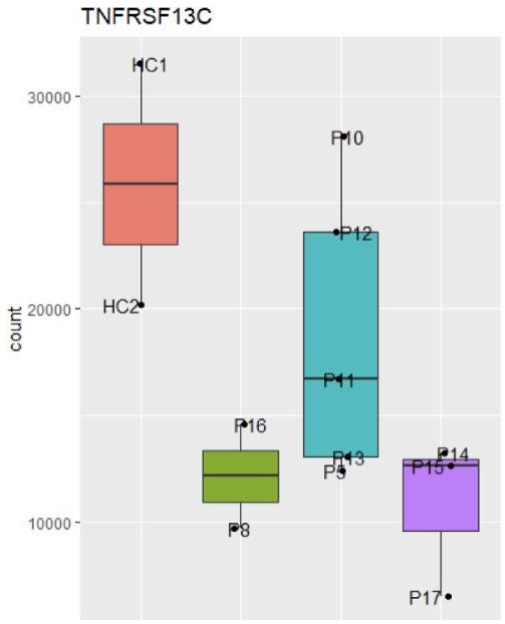

Figure 5.13: Boxplot showing the expression of the BAFF-R encoding gene, *TNFRSF13C,* in a cohort of vaccine responding and non-responding antibody deficient patients and healthy controls (HC). RNA from B-cells was isolated at day 0, and COV-AD samples were divided into those who responded to COVID-19 vaccination and evidenced high surface expression of BAFF-R at day 0 (n=5), those who responded to vaccination and evidenced low surface expression of BAFF-R at day 0 (n=3) and those who did not respond to vaccination and evidenced low surface expression of BAFF-R at day 0 (n=2). Samples were additionally compared relative to naïve-fractioned HC comparators taken at the day 0 time point (n=2).

5.11 Surface expression of BAFF-R, TACI and BCMA

Data from chapter 5.9 demonstrated a correlation between vaccine responsiveness and BAFF-R expression in pre-activated B-cells, revealing that subsets of antibody-deficient patients have reduced BAFF-R expression, a finding that was not consistently accounted for reduced *TNFRSF13C* gene expression. Published literature has associated BAFF-R deficiency with antibody deficiency, demonstrating that CVID patients can exhibit reduced BAFF-R expression, which inversely correlated with serum BAFF levels, and elevated expression of TACI (Transmembrane Activator and CAML Interactor), particularly in patients with splenomegaly (Barbosa *et al.,* 2014).
Whilst BAFF-R is primarily responsible for B-cell survival, TACI regulates immunoglobulin class switching and PC generation (Salzer *et al.,* 2005). Alongside BCMA (B-cell Maturation Antigen), which also supports PC survival, these receptors interact with BAFF and APRIL (Vincent *et al.,* 2013). In cases of impaired BAFF-R expression, TACI and BCMA may compensate for impaired BAFF-R expression in response to elevated BAFF levels.

Given this, the next objective was to investigate whether findings from this study, such as elevated serum BAFF and compensatory TACI upregulation, were evident in the COV-AD patient samples. Initially, the focus was on the surface expression of BAFF-R, TACI, and BCMA in B-cells from various HCs, responders, and non-responders at days 0, 6, and 13 to observe potential receptor-level compensatory mechanisms. A random subset of patients was selected for initial analysis to preserve cells from the representative patients for further downstream experiments.

Both HCs showed the anticipated profile: BAFF-R downregulated and TACI/BCMA upregulated as B-cells differentiated into PCs (Smulski *et al.,* 2018). As per Figures 5.11 and 5.12, non-responders and some responders showed reduced BAFF-R at D0, which normalised by D6. Minor differences in TACI and BCMA expression were observed, but these did not correlate with reduced BAFF-R (Figure 5.14), suggesting no clear compensatory role (i.e. for TACI) in these patients.

Finally, to rule out the possibility that low BAFF-R expression at D0 was due to elevated serum BAFF levels, as reported in previous studies (Barbosa *et al.,* 2014), serum TNFRSF13 levels were analysed, using data generated by Adrian Shields, University of Birmingham (Figure 5.15). No significant differences were found, ruling out this hypothesis and confirming that serum BAFF does not explain the impaired BAFF-R expression seen in non-responding and certain responding patients.

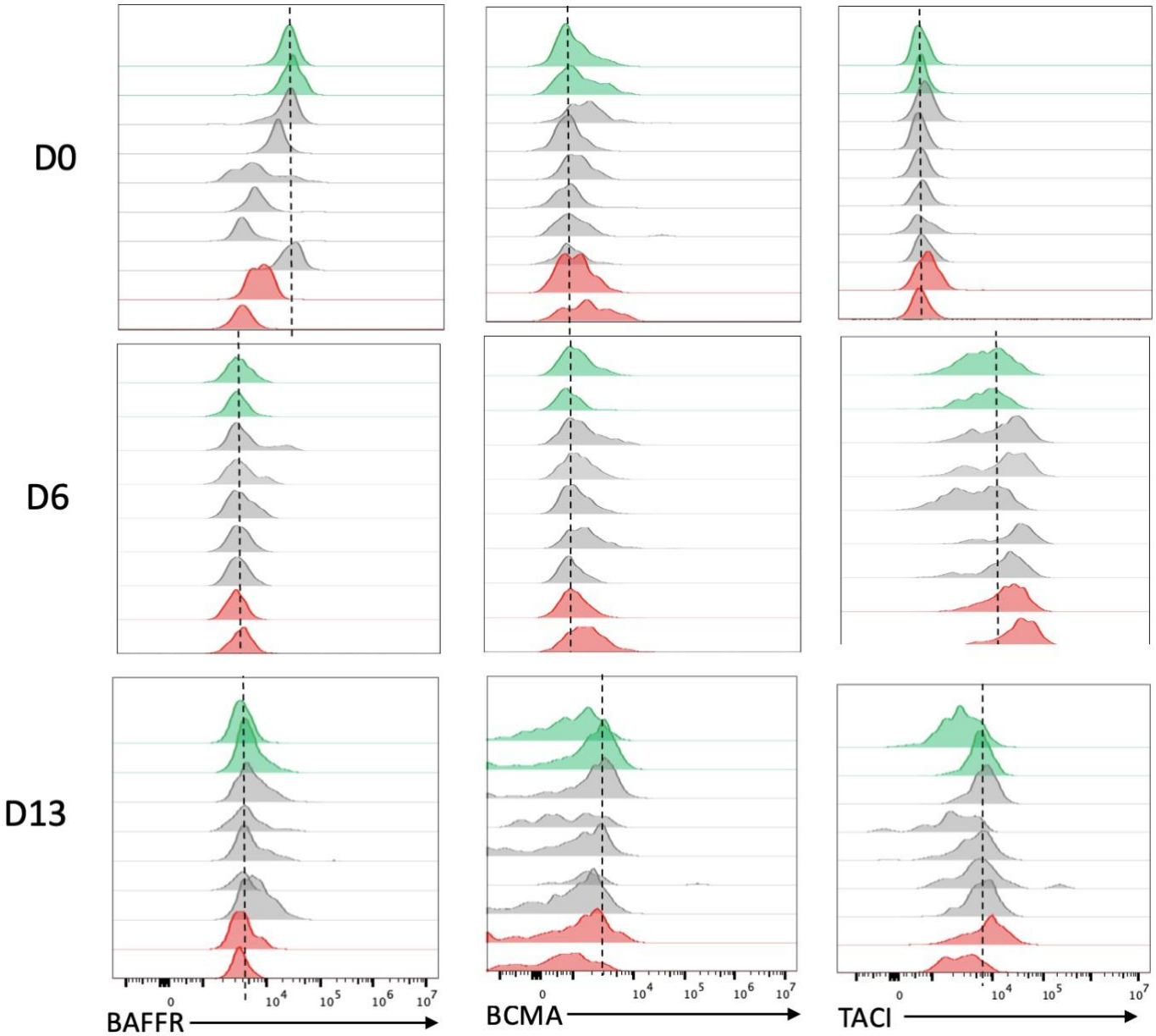

Figure 5.14: Surface expression of the B-cell activation factor receptor (BAFF-R), B-cell maturation antigen (BCMA) and the transmembrane activator and CAML interactor (TACI) receptors in healthy controls, SARS-CoV-2 vaccine responding and non-responding antibody deficient patients at days 0 (D0), 6 (D6) and 13 (D13) following stimulation with T-dependent stimulation conditions. Green histogram plots indicate healthy controls, grey indicates responding patients and red indicates non-responding patients.

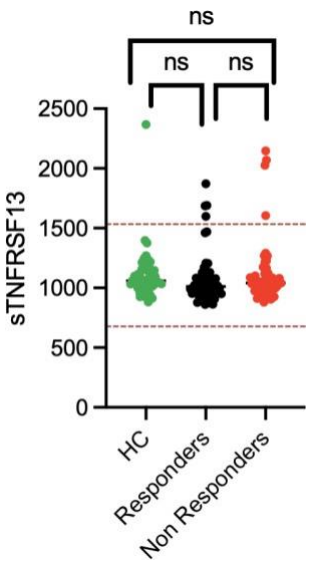

Figure 5.15: Soluble levels of the Tumour Necrosis Factor Receptor Superfamily member 13 (sTNFRSF13) in Healthy controls (HCs), SARS-CoV-2 vaccine-responding and non-responding antibody deficient patients. Serum was taken 1-2 months post second vaccination. Significant differences were determined by one-way ANOVA (****p<0.0001 ***p<0.001 **p<0.01, *p<0.05).

5.11 Discussion

The COVID-19 pandemic exposed the global vulnerability to a novel pathogen, creating an unprecedented sense of uncertainty. It was only with the rollout of vaccination programmes that many began to feel more protected. However, these vaccines also highlighted a critical issue: some individuals, particularly those with antibody deficiencies, remained just as vulnerable due to their inability to mount an adequate immune response. The COV-AD study addresses this gap by investigating the impact of COVID-19 on individuals with antibody deficiencies, with a key focus on vaccine efficacy in this patient population (Shields *et al.,* 2022a; Shields *et al.,* 2022b). This chapter utilised the optimised *in vitro* B-cell differentiation system (Chapter 2.3) to conduct a preliminary investigation into the intrinsic capacity of patient B-cells to generate functional plasma cells in selected vaccine responders and non-responders enrolled in the COV-AD study, potentially aiding in the risk stratification of the most vulnerable patients.

Before examining the differentiation phenotypes in the patients, cell counts were assessed throughout the culture. Notably, the data demonstrated consistent B-cell numbers across both patient groups and HCs, indicating that B-cell proliferation is not impaired and is therefore unlikely to contribute to the observed vaccine responses in these patients. While this finding may contrast with previous studies suggesting that non-responders exhibit reduced B-cell numbers (Puissant-Librano *et al.,* 2014), it aligns with other research indicating that patients with various antibody deficiencies may experience reductions in antibody production while maintaining intact B-cell proliferation capabilities (Vale and Schroeder, 2010).

The formation of PCs, as indicated by CD138+ expression, is crucial for an effective immune response to antigens and vaccines. Thus, investigating CD138+ PCs provides valuable insights into whether non-responders fail to generate adequate PCs, potentially explaining their poor vaccine responses. Data presented here revealed no significant difference in the generation of CD138+ PCs between responders and non-responders by D13, suggesting that the intrinsic capacity to generate PCs is not impaired in non-responders. Whilst this finding may contradict the assumption that non-responders exhibit reduced PC formation, the observation from previous reports that most patients with PC dyscrasias demonstrated good response to COVID-19 vaccinations strongly suggests that insufficient PC generation is not the sole factor contributing to impaired vaccine response (Shah *et al.,* 2022). Thus, the variability in CD138+ generation observed in this study, particularly at D13, can likely be attributed to the heterogeneity among the patients. The lower-than-expected CD138+ expression in some individuals may be linked to their specific diagnoses, as some may indeed have underlying PC dyscrasias (Setiadi and Sheikine, 2019; Kawano *et al.,* 2012).

At the opposite end of the spectrum, higher than anticipated CD138+ expression at D13 was observed in P5, indicating a highly dysregulated PC response. This elevated expression may suggest an enhanced activation of PCs in response to additional underlying immune dysregulation (Sharma *et al.,* 2018). Consequently, while phenotypic analysis of CD138+ plasma cell expression does not distinguish between vaccine responders and non-responders, it remains a valuable tool for

identifying individuals who may require close monitoring or further clinical investigation for potential PC abnormalities.

After assessing PC generation in patient samples, plasmablast production ($CD27^{+}CD38^{hi}$ cells) was subsequently evaluated, revealing reduced levels in both patient groups at days 6 and 13, with notably lower numbers among vaccine non-responders. This pattern suggests that impaired plasmablast differentiation is a common feature among antibody-deficient patients, being especially pronounced in those with poor vaccine responses. Published literature has made associations between abnormal plasmablast generation and COVID-19 disease severity, suggesting correlations to levels of BAFF, IL10 and IL4 (Schultheiß *et al.,* 2021). Accordingly, it could be hypothesised that the reduced plasmablast generation observed, most notably in non-responders, may correlate with the low or absent D0 BAFF-R expression. However, since the representative data indicate no link between BAFF-R expression and plasmablast numbers, this explanation in unlikely. Instead, the reduced plasmablast levels may more plausibly stem from each patient in the heterogenous cohort's specific antibody deficiency and its impact on critical B-cell signalling pathways required for activation and differentiation. This could relate to defects in B-cell signalling pathways, possibly leading to impaired activation and differentiation capabilities due to altered cytokine environments and intrinsic signalling mechanisms (Fekrvand *et al.,* 2022). Regardless, plasmablast data here showed no significant differences in $CD27^{+}CD38^{hi}$ expression between the vaccine response groups, indicating that this marker alone is not a reliable predictor of COVID-19 vaccine response.

The analysis of intracellular and secreted immunoglobulin production revealed notable differences in expression across controls, vaccine responders, and non-responders, though these differences did not always reach statistical significance. In line with existing literature, most patients exhibited reduced intracellular IgG and IgA expression, with compensatory increases in IgM, a pattern commonly observed in individuals with antibody deficiencies (Catanzaro *et al.,* 2019; Agarwal and Cunningham-Rundles, 2007). This trend was particularly pronounced in patients with

SAD, who, due to immunosuppressive treatments, can experience more pronounced hypogammaglobinaemia compared to PAD patients, where intrinsic B-cell defects are present (Ponsford *et al.,* 2019).

Additionally, secondary conditions like chronic infections or malignancies may lead to compensatory IgM increases. For instance, patients with multiple myeloma or nephrotic syndrome may show elevated IgM levels as part of their immune response to infections or due to disease-induced dysregulation in B-cell function and cytokine production (Bogner and Pecher, 2013). Dysgammaglobinaemia characterised by low IgG and high IgM is a known immune profile in such conditions, further complicating the immune response (El Mashad *et al.,* 2017).

Low or absent intracellular and/or secretory IgG or IgA expression may reflect defects in class switch recombination. This was seen most noticeably in the context of IgA in patients 4, 5 and 7 whereby there was minimal or absent IgA expression. Such patients could have defects in CSR pathways, particularly those involving transforming growth factor-beta (TGF-β), which is essential for IgA production (Asano *et al.,* 2004). The possibility that selective IgA deficiency, the most common primary immunodeficiency, exacerbates IgA impairment in patients with other antibody deficiencies cannot be ruled out. Notably, at D13, vaccine non-responders exhibited significantly lower intracellular IgA compared to controls and responders, a trend that persisted at the secretory level as well.

While the differences in IgA expression may indicate differential immune responses to vaccination, studies have shown that certain vaccines, such as COVID-19 mRNA vaccines, can elicit strong IgG responses with weaker IgA production. Tang *et al*. reported that the mRNA vaccine induces robust systemic IgG responses but limited IgA production, potentially explaining why non-responders maintain IgG levels but show reduced IgA (Tan *et al.,* 2024). This differential stimulation of immune pathways could contribute to the overall reduced IgA levels observed in non-responders, despite no significant differences in IgG.

Additionally, the presence of chronic infections or underlying immunological conditions that may be present in vaccine non-responders can further complicate the antibody response. Chronic inflammatory states can lead to dysregulation of the immune system, which may preferentially support IgG production while suppressing

IgA synthesis (Hopp and Niebur, 2022). For example, in patients with CVID, it has been observed that while IgG levels may remain stable, IgA levels can be significantly lower, reflecting the underlying immunological dysfunction that could be used as a prognostic tool for predicting vaccine responses (Pulvirenti *et al.,* 2020).

When comparing overall *in vitro* immunoglobulin production between controls and vaccine response groups, it is it is evident that non-responders tend to have elevated IgM, reduced intracellular IgG, and markedly lower IgA at all time points. However, the only statistically significant difference between groups was the lower intracellular IgA at D13. Given that some responders, such as P4 and P5, also exhibited minimal IgA expression, relying on IgA as a predictor of vaccine response may not be valid in this context. Further research into alternative biomarkers may provide better predictive value for immune response efficacy in these patients.

Expanding on the abnormal $CD38^{+}CD138^{+}$ and $CD27^{+}CD38^{hi}$ phenotypes observed in P5, notable abnormalities were also identified in their immunoglobulin profile. IgM and IgA were marginally expressed, while IgG levels were abnormally elevated, reaching over 94% by D6. The rarity and severity of this immunophenotype prompted further investigation into the patient's clinical history, revealing that P6 was receiving IgRT, azithromycin, and various cardiac medications, in addition to having a diagnosis of Chronic Lymphocytic Leukaemia (CLL) alongside CVID.

CLL, a B-cell malignancy, can lead to immune dysregulation, promoting abnormal B-cell activity and altering immunoglobulin production, potentially driving the increase in IgG and CD138+ while suppressing IgM and IgA synthesis (Cerutti *et al.,* 2002). The high IgG and near absent IgM level in P5 may be attributed to a rare case of class-switched IgG CLL, where ongoing CSR occurs within a subset of the CLL clone (Cerutti *et al.,* 2002; Klein and Dalla-Favera, 2005). This rare IgG-expressing CLL phenotype suggests a possible origin from more antigen-experienced, memory-like B-cells rather than naïve B-cells, which may contribute to the patient's highly abnormal phenotype and immune dysregulation (Klein *et al.,* 2001).

Additionally, the aberrant immunoglobulin profile raises the possibility that, beyond CLL and CVID, other autoimmune phenomena- such as autoimmune cytopenia- may be contributing to the immune dysregulation. This could trigger excessive B-cell activation and the production of autoantibodies (Podjasek and Abraham, 2012;

Upton, 2015). Some CLL B-cells may recognise autoantigens, leading to autoantibody secretion and possibly contributing to the complex phenotype observed in P5 (García-Muñoz *et al*., 2012).

Further investigation, including sequencing or more detailed immunophenotyping, could be beneficial in understanding the interplay of these factors and whether this patient's CVID diagnosis is compounded by autoantibody production. This case highlights the value of the *in vitro* system for identifying patients who require more in-depth study, potentially reconsidering whether ongoing IgRT is necessary or if alternative therapeutic approaches are warranted based on their complex clinical presentation.

A striking difference in BAFF-R expression was observed between vaccine responders and non-responders, with all non-responders and a subset of responders showing absent or very low BAFF-R expression at D0.

RNA expression analysis has been widely utilised in the context of primary immunodeficiencies and in understanding differential vaccine responses to uncover gene-level anomalies that provide critical insights into immune system dysfunction and reveal diagnostic targets that traditional DNA sequencing might miss (Lye et al., 2019; Van Schouwenburg et al., 2015; Santos-Rebouças et al., 2024; Haralambieva et al., 2024). Therefore, applying RNA-seq to isolated B-cells from various primary and secondary antibody deficient COV-AD patients at D0 could provide valuable mechanistic insights into the gene-level basis of this observation.

TNFRSF13C, which encodes the BAFF-R protein, exhibited reduced RNA expression in non-responders and in some patients with low surface BAFF-R expression. This reduction aligns with the flow cytometry showing diminished or absent BAFF-R on the surface of B-cells in these groups. A plausible explanation for this reduced RNA expression could be impaired transcriptional regulation, potentially driven by epigenetic factors affecting the promoter or enhancer regions of *TNFRSF13C* (Warnatz *et al.,* 2009). However, it is unlikely attributed to genetic mutations, as variants in receptors related to BAFF signalling pathways (such as BAFF-R, TACI and BCMA), which are occasionally identified in CVID patients, were not detected in the individuals studied. Moreover, even if such mutations were present in isolated cases, they would not explain the abnormal BAFF-R phenotype observed in SAD patients, who are unlikely to carry pathogenic variants in these

genes.

Interestingly, some responders with normal surface BAFF-R expression also exhibited similarly low *TNFRSF13C* RNA levels, suggesting a complex interplay between RNA levels and protein expression. Post-transcriptional mechanisms, including mRNA stability, translation efficiency, and protein turnover, might account for these discrepancies (Yoshinage and Takeuchi, 2019). For example, RNA degradation or translational inefficiency might destabilise transcripts without directly impacting protein abundance, possibly explaining why low RNA expression does not always correlate with reduced surface expression (Gallego Romero *et al.,* 2014; Li *et al.,* 2020; Agarwal and Kelley, 2022). Furthermore, protein turnover influenced by cellular degradation pathways may allow sufficient surface expression despite low RNA levels, since mechanisms such as the ubiquitin-proteasome system and autophagy can stabilise proteins (Li *et al.,* 2022). These pathways regulate protein stability and degradation, ensuring that proteins can be maintained on the surface of cells despite reduced transcriptional activity, contributing to discrepancies between RNA and protein expression (Li *et al.,* 2020).

Another plausible explanation for the low or absent BAFF-R expression in pre-activated B-cells is elevated circulating BAFF, which is well-documented in CVID patients and patients with B-cell malignancies. Increased BAFF signalling through BAFF-R could lead to downregulation of the receptor to prevent overactivation of B-cells (Kreuzaler *et al.,* 2012). This phenomenon has been observed in autoimmune diseases where high BAFF levels correlate with reduced BAFF-R expression (Matharu *et al.,* 2013; Jacobs *et al.,* 2016). Additionally, elevated serum BAFF and reduced BAFF-R expression in memory B-cells have also been linked with HIV-positive non-responders to the H1N1/09 vaccination, further supporting the connection between impaired vaccine responses, low BAFF-R expression and high BAFF levels (Pallikkuth *et al.,* 2011). In response to elevated BAFF, compensatory overexpression of TACI or BCMA may occur to mitigate excessive BAFF signalling (Barbosa *et al.,* 2014).

To investigate this, surface expression levels of BAFF-R, TACI and BCMA were measured across HCs, responders and non-responders, in addition to referring to already-obtained serum BAFF-R levels. This data indicated that neither excessive serum BAFF levels nor compensatory receptor changes explain the aberrant BAFF-R expression at D0. Serum BAFF levels were normal in all patients, suggesting that reduced expression was not solely due to chronically raised BAFF levels, however this possibility could not be excluded with certainty.

While serum BAFF levels appeared normal across patients, one potential explanation for the impaired BAFF-R staining could be masking of the receptor by its ligand. It has previously been shown that BAFF receptors are difficult to detect with specific antibodies when bound to BAFF, as ligand engagement may obscure the antibody-binding epitope (Smulski *et al.,* 2017). However, as BAFF serum concentrations were comparable across all patients in this work, it seems unlikely that receptor masking alone accounts for the observed reduction in BAFF-R staining. If ligand-induced masking were responsible, variation in BAFF levels would be expected to correlate with receptor detection, which was not observed. This makes it more plausible that intrinsic alterations in receptor expression, stability, or regulation at the cell surface contribute to this phenotype.

Another potential mechanism involves receptor shedding, where membrane-bound receptors like BAFF-R are cleaved by metalloproteinases, such as ADAM10 and ADAM17, leading to decreased surface expression. Dysregulation of this shedding process could account for the observed reduction in BAFF-R expression (Smulski *et al.,* 2017). Overactivation of this shedding mechanism could result in significantly lower BAFF-R levels on B-cell surfaces, impairing signalling and contributing to the phenotypic variability observed among patients.

BAFF-R expression is regulated by a complex network of immune signals, including pro-inflammatory cytokines, which can modulate BAFF-R levels and influence B-cell activation and vaccine response (Yuan *et al.,* 2010). Disruption of BAFF-R signalling, whether due to low BAFF availability or imbalances in the BAFF-BAFF-R axis, impairs B-cell function, leading to suboptimal antibody production post-vaccination. A notable study on rheumatoid arthritis therapy demonstrated significant reductions in BAFF-R expression following B-cell depletion, despite stable serum BAFF levels (de la Torre *et al.,* 2010). This reduction was linked to increased CSR and post-translational modifications of BAFF-R, suggesting that lower BAFF-R levels on newly

generated B-cells may reduce their survival potential, favouring B-cell populations capable of undergoing productive, but not antigen-specific, differentiation.

Given that this mechanism could parallel what is observed in data presented in this chapter, RNA analysis at D0 could provide crucial insights into the underlying molecular processes. Additionally, investigating the clonality of B-cells at later time points may reveal patterns in B-cell differentiation and activation that contribute to the impaired BAFF-R expression in non-responders. Identifying gene signatures associated with BAFF-R regulation in these patients could illuminate key regulatory pathways involved in this phenotype and provide further clues to their poor vaccine responses.

This chapter highlights the invaluable applications of the *in vitro* B-cell differentiation system in studying immune responses among antibody-deficient patients, underscoring its potential as a risk-stratification tool. Notably, the variability in BAFF-R expression observed in non-responders suggests the possibility of using BAFF-R as a biomarker for predicting vaccine responses universally. However, this observation raises several critical questions, particularly regarding the underlying mechanisms driving the observed phenotype. It remains to be determined whether intermediate or low BAFF-R expression in responders predisposes these patients to poorer or less effective antibody responses to vaccinations. Additionally, the implications of these findings for other vaccines warrant exploration, especially in the context of future pandemics. To establish the reliability of BAFF-R as a predictive biomarker, further investigation is essential.

Chapter 6 - BCR repertoire analysis

6.1 Introduction

The previous chapter underscored the promising applications of the *in vitro* B-cell differentiation system in elucidating B-cell intrinsic immune response variability in antibody-deficient patients, with BAFF-R expression emerging as a potentially valuable biomarker for vaccine responsiveness. This variability highlighted the need to understand underlying mechanisms, including the association between BAFF-R levels and immune competence, as well as its potential as a universal predictor for vaccine efficacy. The findings raised critical questions regarding the influence of BAFF-R expression on B-cell functionality and the consistency of these effects across different vaccines - a line of inquiry that could hold substantial implications for both current and future immunisation strategies.

In an attempt to further delve into the utility of the *in vitro* system in characterising antibody responses in antibody-deficient patients, this chapter will explore B-cell receptor (BCR) analysis in COV-AD patients. Sequencing the BCR repertoire at D13 will facilitate characterisation of the diversity and clonality of B-cell populations, metrics that might reveal differences in the immune potential of vaccine responders versus non-responders.

6.2 BCR repertoire

The B-cell receptor (BCR) repertoire represents the diversity and specificity of the adaptive immune response, encompassing the unique set of immunoglobulin sequences that allow B-cells to recognise a vast array of antigens. BCR diversity arises from V (D) J recombination, where variable (V), diversity (D), and joining (J) gene segments undergo rearrangement to create unique BCR sequences on individual B-cells (Tonegawa, 1983). This process is complemented by somatic hypermutation and clonal expansion in response to antigen exposure, enabling further diversification and adaptation (Chapter 1.2). Collectively, these mechanisms

generate a vast array of BCR specificities that are crucial for robust immune responses (Alt *et.,* 1992; Schatz *et al.,* 2011).

Examining the BCR repertoire provides critical insights into immune system function, as diversity within the repertoire is often linked to enhanced immune defence and adaptability against infections and vaccines (Soto *et al.,* 2019a; Yaari and Kleinstein, 2015). However, in patients with antibody deficiencies, the BCR repertoire may exhibit restricted diversity, reduced clonal expansion or other alterations that could impair immune effectiveness (Roskin *et al.,* 2015). Hence, BCR repertoire sequencing has emerged as a powerful tool for understanding immune capacity in both healthy and immunocompromised populations (Zheng *et al.,* 2022).

Herein, BCR repertoire analysis was performed on D13 samples, capturing B-cell responses at an advanced stage of *in vitro* differentiation. This timepoint allows for the assessment of diversity and clonality patterns that may distinguish vaccine non-responders from responders. Previous studies of BCR repertoire analysis in patients with antibody deficiencies, such as CVID, have yielded mixed results, likely reflecting the heterogeneity of the disease. While some studies show no significant differences in BCR characteristics between controls and patients (Ijspeert *et al.,* 2016), others have observed notable alterations in diversity or clonal expansion (Roskin *et al.,* 2015; Ghraichy *et al.,* 2018).

In the context of vaccination, BCR repertoire studies have revealed that younger individuals tend to elicit stronger immune responses to vaccines like yellow fever, in comparison to middle-aged individuals (Davydov *et al.,* 2018). Furthermore, immune responses in healthy individuals to the SARS-CoV-2 vaccination have been characterised, evidencing the differential effect of the vaccine on BCR repertoire development (Kotagiri *et al.,* 2022). However, it remains unclear whether distinct differences in the BCR repertoire exist between vaccine responders and non-responders, particularly in populations with antibody deficiencies and in the context of SARS-CoV-2 vaccination. Previous research suggests that increased BCR diversity typically correlates with broader antigen recognition and more effective immune responses, while reduced diversity or high clonality can signal impaired immune function (Friedman *et al.,* 2016; Rubelt *et al.,* 2016). Hence, this analysis aims to identify BCR characteristics linked to variability in the immune responses of

antibody deficient patients, shedding light on immune dysregulation and vaccine efficacy among COV-AD patients.

6.2.1 BCR repertoire workflow

RNA was extracted from samples collected at the D13 timepoint derived from differentiated non-fractionated B-cells of vaccine responders and non-responders, as well as from CVID and SAD patients. Additionally, a naïve-enriched HC sample from the same timepoint was also analysed. For the purposes of this study, patients P3, P4, P5, P8, and P9 (Table 5.2) will serve as representative cases. cDNA was synthesised from the extracted RNA and amplified using specific primers targeting the V and J regions of the immunoglobulin heavy chain variable region. PCR products were subsequently barcoded with Nextera™ Index primers. The indexed samples were then sequenced, and the resulting fastq files were processed using MiXCR v.4.6.0 and Immunarch software. The fastq files were split into two reads per sample: R1 and R2. R1 covers the region from framework region 1 (FR1) to the start of the complementarity-determining region 3 (CDR3), while R2 spans from FR4 through the end of CDR3 and into the beginning of FR2 (Figure 6.1). This methodology allows for a comprehensive analysis of the BCR repertoire and its diversity, aiding in the understanding of immune responses in both responders and non-responders.

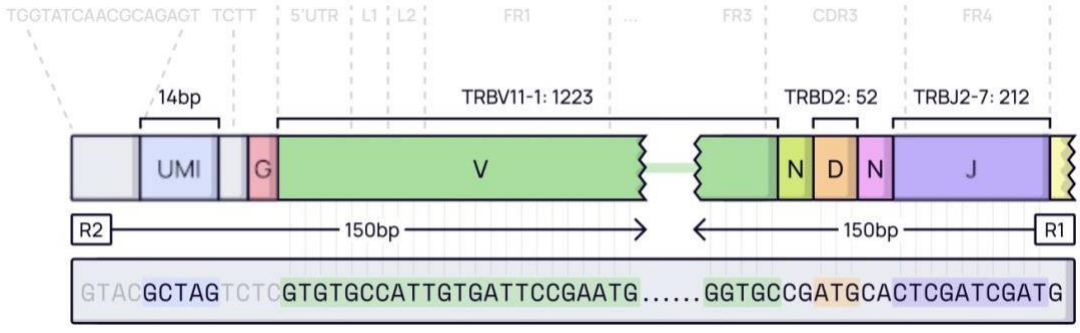

Figure 6.1: Schematic representation of read map using VDJ primers. Within V (D) J regions are framework regions (FR) and complementary-determining (CD) regions. Two read files, R1 and R2 were used to generate pair-end sequencing data, with R1 representing the forward read of the V(D)J region and R2 representing the reverse read. Taken from https://mixcr.com/mixcr/reference/overview-analysis-overview/#upstream-analysis-steps.

6.3 Alignments

Sequencing files were loaded into the MiXCR platform and quality checks against a reference gene segment databases were first determined to confirm the efficiency of sequence alignment of each sample. Productive alignment was demonstrated by over 90% successful alignment rate in all representative samples and control. A small percentage of reads in the samples showed an absence of hits, most noticeably J hits (Figure 6.2), however the high percentage of efficient alignment confirmed confidence in the quality of all samples.

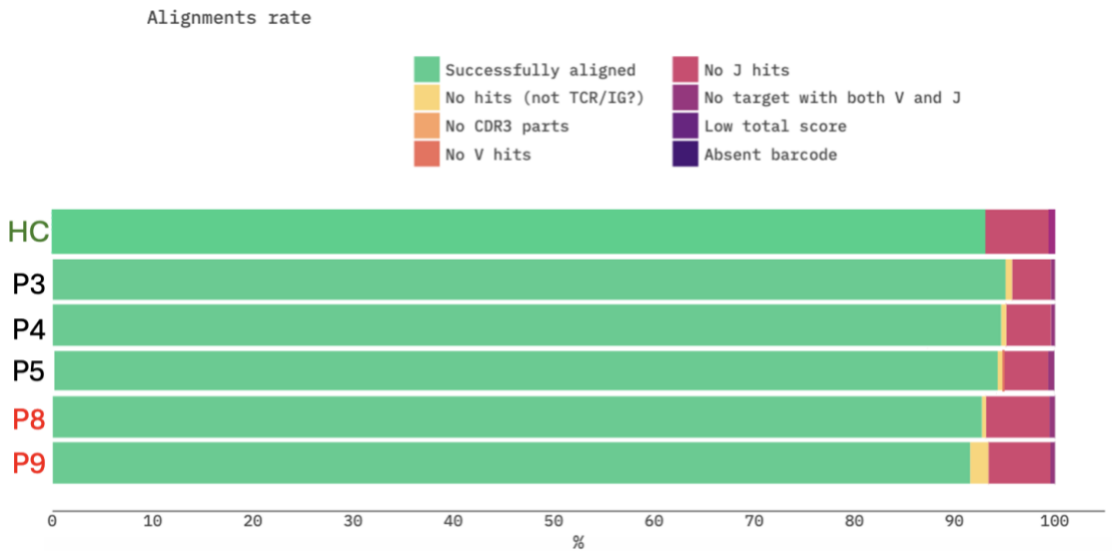

Figure 6.2: Alignment rates of COV-AD patients (P3, P4, P5, P8 and P9) and healthy control (HC) samples. Sequenced BCR amplicons were derived from RNA extracted from a representative naïve-fractioned HC (green), SARS-CoV-2 vaccine responding (black) and non-responding (red) antibody deficient patient cells at day 13 of *in vitro* differentiation.

6.4 Chain usage

After evaluating successful sequence alignments, clonal usage can confirm whether the primers effectively targeted the correct regions of the VDJ segments. Analysis of chain usage showed that the heavy chain (IGH) appeared in over 95% of aligned reads, indicating high primer efficiency (Figure 6.3).

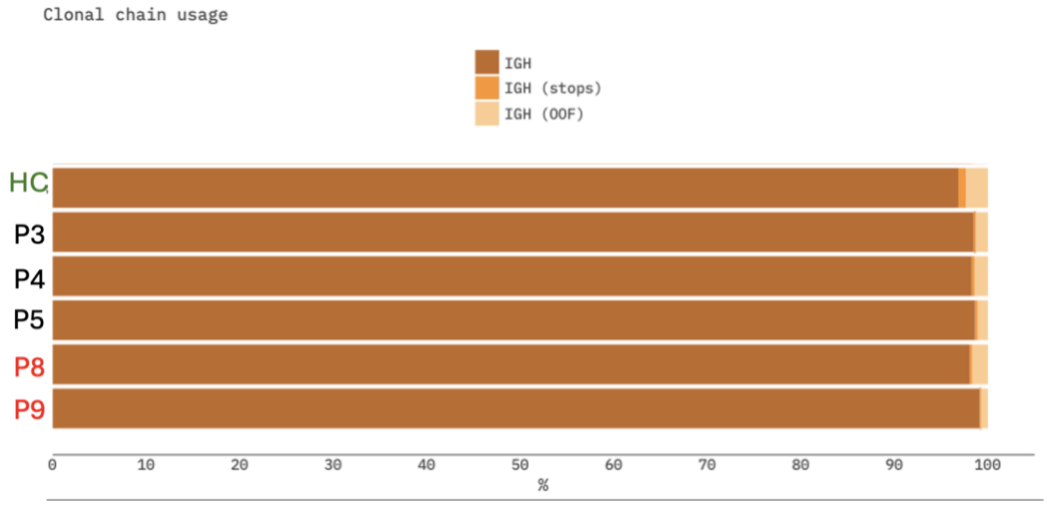

Figure 6.3: Chain abundance in COV-AD patients (P3, P4, P5, P8 and P9) and healthy control (HC) samples. Sequenced BCR amplicons were derived from RNA extracted from a representative naïve-fractioned HC (green), SARS-CoV-2 vaccine responding (black) and non-responding (red) antibody deficient patient B-cells at day 13 of *in vitro* differentiation.

6.5 Clonotypes

The high alignment and chain usage quality in the sequencing data justified continued analysis, enabling the assessment of clonal populations using the MiXCR output in Immunarch for clonotype visualisation. The HC displayed a high number of unique clonotypes, indicating a broad and diverse BCR repertoire typical of an intact immune system, capable of recognising various antigens (Roskin *et al.,* 2015) and consistent with the use of a polyclonal stimulus to initiate *in vitro* differentiation (Cocco *et al.,* 2012). In contrast, all patient samples, particularly P3 and P5, showed

lower numbers of unique clonotypes (Figure 6.4A), suggesting reduced clonal diversity (Schlegel *et al.,* 2024) regardless of vaccine response status or type of antibody deficiency. Clonotypes grouped by relative abundance revealed that while the HC had a range of small, medium, and large clonotypes, responders showed a notable proportion of hyperexpanded clonotypes (Figure 6.4B). Since patient samples were collected following the third or fourth vaccination, this hyperexpansion in responders may reflect successful clonal responses to vaccination (Laserson *et al.,* 2014; Fraley *et al.,* 2022), which were absent in non-responders and the HC, who had not recently received vaccination against SARS-CoV-2. Analysis of rare clonal proportions further supports this finding, as vaccine responders exhibited a higher representation of high-frequency clonotypes (notably within the 101-MAX category) compared to non-responders and the HC (Figure 6.4C). This pattern is indicative of effective clonal expansion following recent vaccination, likely reflecting a strong antigen-specific immune response (Laserson *et al.,* 2014; Fraley *et al.,* 2022).

Together, the clonotype analysis demonstrates that vaccine responders show robust clonal expansion and diversity, reflecting a strong immune response to vaccination. In contrast, non-responders and the HC exhibit limited expansion, suggesting impaired vaccine response in non-responders and a lack of recent conspicuous antigen exposure in the HC. This highlights the link between clonotypic diversity and immune competence.

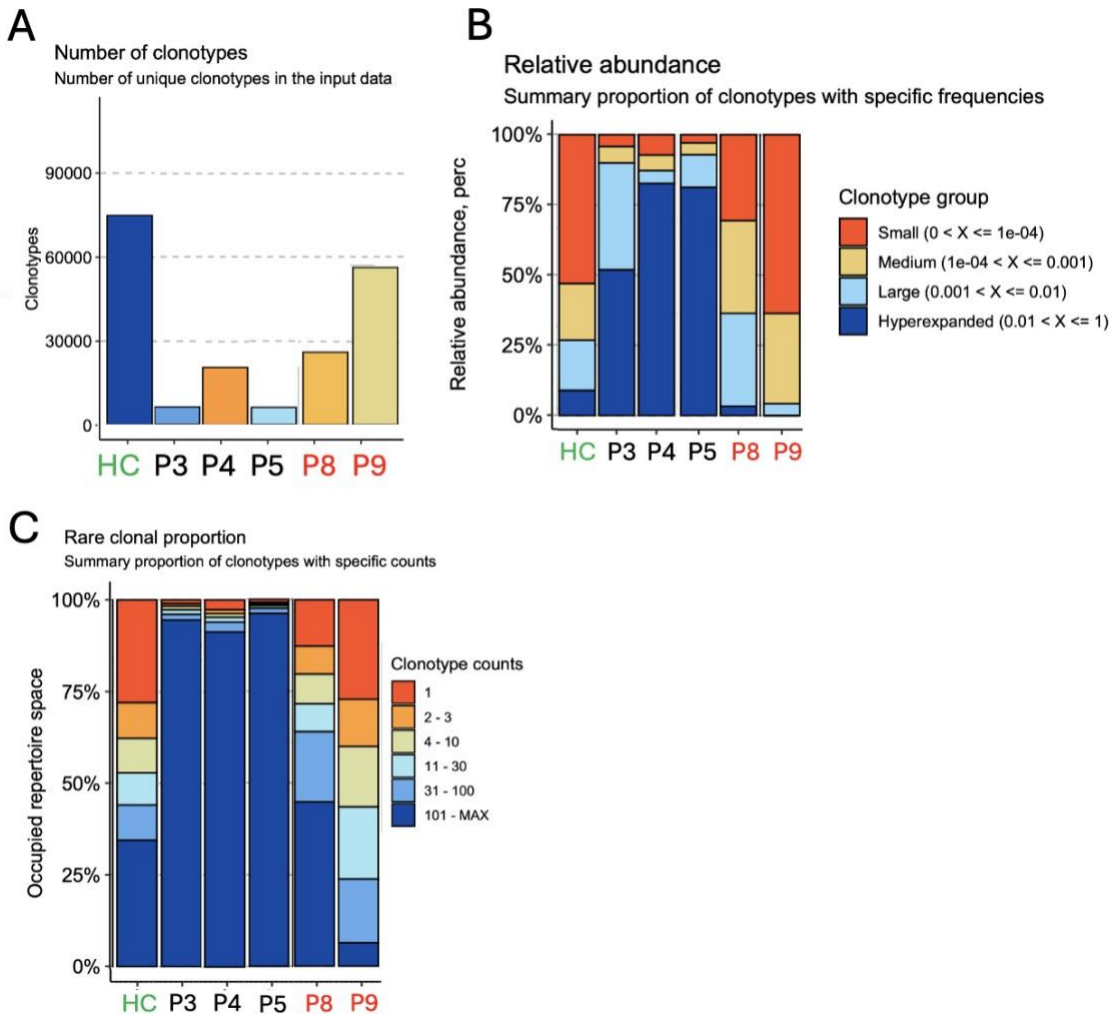

Figure 6.4: Clonotype proportions and abundance in COV-AD patients (P3, P4, P5, P8 and P9) and healthy control (HC) samples. Sequenced BCR amplicons were derived from RNA extracted from a representative HC (green), SARS-CoV-2 vaccine responding (black) and non-responding (red) antibody deficient patient B-cells at day 13 of *in vitro* differentiation. Analysis was performed using MiXCR software and the R package Immunarch. **A**: Number of clonotypes. **B:** Relative abundance of clonotypes. **C**: Rare clonal proportion.

6.6 V and J gene usage

Since the diversity of the BCR repertoire is largely attributed to V (D) J recombination, the analysis of V and J gene usage provides insight into the diversity and selection processes of the BCR repertoire (Schlegel *et al.,* 2024). Examining V and J gene segment facilitates understanding as to how different combinations contribute to antigen recognition and specificity. In immune responses, certain V and J genes may be preferentially used, reflecting an adaptive response to antigen exposure or a predisposition based on genetic background. Hence, the next objective was to compare V and J gene usage between the HC and antibody-deficient patients, highlighting patterns associated with immune competence and response to vaccination. Post-analysis of MiXCR data was performed to generate tables detailing the specific V and J gene segments utilised by each clone. These results were then visualised as bar charts, illustrating the frequency of each V and J gene segment across samples to reveal patterns of gene usage.

6.6.1 V gene usage

BCRs and antibodies rely on a diverse set of V gene segments to recognise a wide range of antigens. In humans, there are 7 VH gene families (Rees, 2020), and VH3 usage has been documented as the predominant subgroup (Wang *et al.,* 2022). This finding was recapitulated in this study, whereby the HC and most patient samples demonstrated highest abundance of *IGV3* (Figure 6.5). *IGHV3* was particularly overrepresented in P5, likely reflecting the high-risk nature of this patient's additional CLL diagnosis (Ghia *et al.,* 2008). P3, P8, and P9 exhibited higher *IGHV4* abundance compared to the control and other patients (Figure 6.5), consistent with existing literature that identifies *IGHV4* as the second most frequent VH gene family (Ghia *et al.,* 2008).

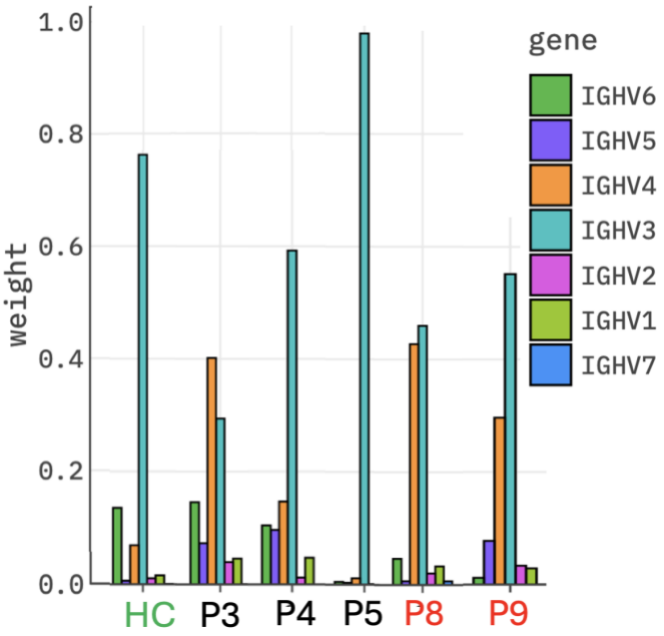

Figure 6.5: Usage of the V gene segments in COV-AD patients (P3, P4, P5, P8 and P9) and healthy control (HC) samples. Sequenced BCR amplicons were derived from RNA extracted from a representative healthy control (green), SARS-CoV-2 vaccine responding (black) and non-responding (red) antibody deficient patient B-cells at day 13 of *in vitro* differentiation. Weight indicates the frequency of the specified gene segment.

6.6.2 J gene usage

Among the seven J gene families, *IGHJ4* is typically the most frequently observed, while *IGHJ2* and *IGHJ1* are found at the lowest frequencies (Shi *et al.,* 2020). Consistent with this, *IGHJ4* was highly abundant in both the HC and all patient samples, except for P5 (Figure 6.6). The unusually high expression of *IGHJ6* in P5 likely reflects characteristics specific to the CLL pathology rather than an antibody deficiency (Datta and Jumaa, 2022; Agathangelidis *et al.,* 2012).

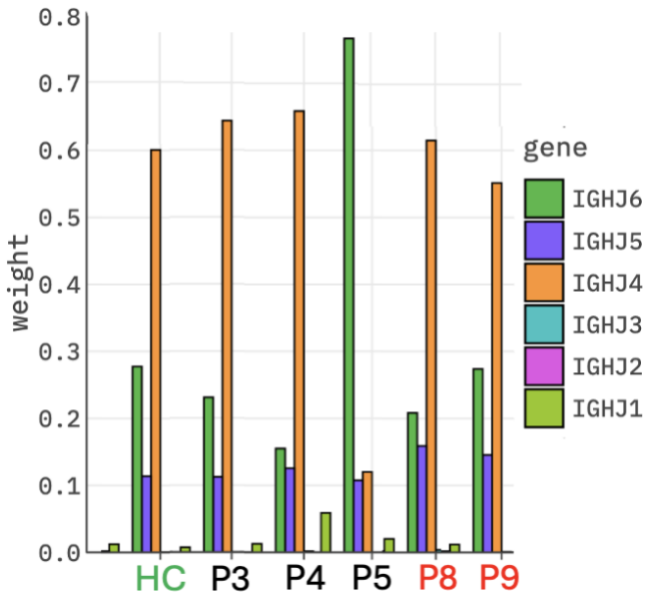

Figure 6.6: Usage of the J gene segments in COV-AD patients (P3, P4, P5, P8 and P9) and healthy control (HC) samples. Sequenced BCR amplicons were derived from RNA extracted from a representative healthy control (green), SARS-CoV-2 vaccine responding (black) and non-responding (red) antibody deficient patient B-cells at day 13 of *in vitro* differentiation. Weight indicates the frequency of the specified gene segment.

6.7 V and J segment combinations

The human immune repertoire relies on the extensive combination of V(D)J segments to create the diverse array of antibodies necessary for identifying and combating numerous pathogens. It was therefore thought that antibody-deficient patients may have disruptions in V or J segment usage which may limit their diversity or functionality of the antibody repertoire. By comparing V and J gene segment combinations in HC and antibody-deficient patients, it could be possible to better understand how these patterns may differ and how certain segment pairings might correlate with immune deficiency and dysregulation (IJspeert *et al.,* 2017). Using an online visualisation tool (https://mk.bcgsc.ca/tableviewer/visualize/), Circos plots were generated to illustrate V-J connections, offering insights into potential biases or gaps in segment usage that may contribute to antibody deficiency. In the HC, there

was a broad and balanced spread of V-J connections across the circle, with arcs linking various V and J segments relatively evenly (Figure 6.7). This pattern is indicative of a diverse and functional antibody repertoire, allowing for a wide range of antigen recognition. Patient samples similarly showed a relatively diverse range of V-J pairings, although some combinational links appear different between all patients (except P5) and the HC which might suggest a functional yet mildly restricted repertoire. P4, a SAD responder, had fewer V-J combinations with certain segments appearing more dominant (Figure 6.7), indicating a more focused but still functional repertoire that allowed for a positive vaccine response.

P5 displayed a highly restricted pattern, with dense connections concentrated within fewer V-J pairings, suggesting limited recombination events or clonal expansions (Figure 6.7). This restricted diversity may still permit a vaccine response but hints at underlying immune dysregulation most likely attributed to the CLL (IJspeert *et al.,* 2017). Notably, this observation is reminiscent of results obtained using Waldenström macroglobulinemia (WM) cells, another B-cell malignancy, as the starting population, where similarly restricted diversity and clonal expansions were reported following activation (Shrimpton *et al.,* 2020).

The non-responders demonstrated a high number of combinations and seemingly diverse V-J pairings (Figure 6.7). Despite this apparent diversity, these two samples displayed a pattern that is similar to each other, more so than the other samples in the representative cohort. While this pattern could suggest a reliance on a limited set of recurring and possibly redundant V-J pairings in non-responders, it is more likely that there is no true functional difference between responders and non-responders, and a larger sample cohort is needed to clarify this distinction.

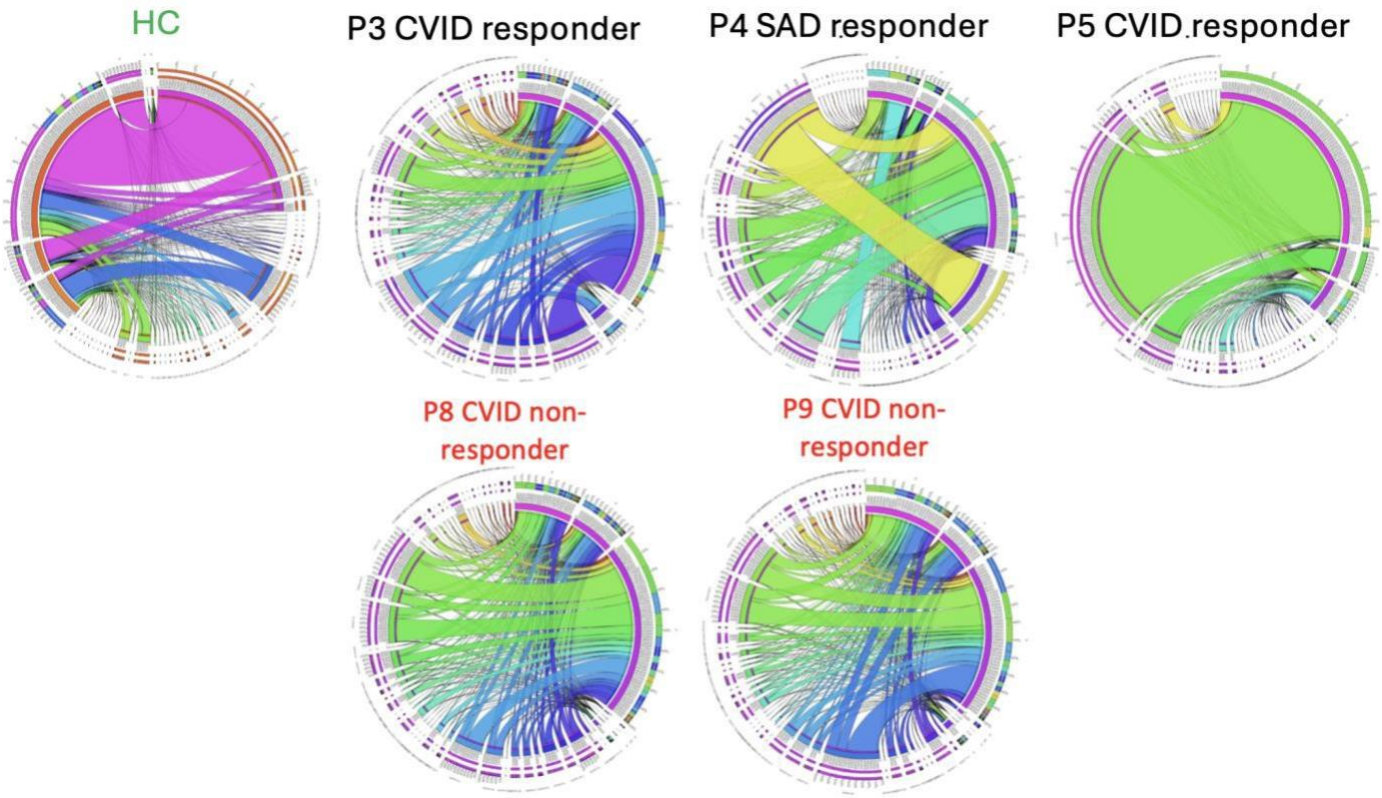

Figure 6.7: V and J gene combinations in COV-AD patients (P3, P4, P5, P8 and P9) and healthy control (HC) samples. Sequenced B-cell receptor (BCR) amplicons were derived from RNA extracted from a representative healthy control (green), SARS-CoV-2 vaccine responding (black) and non-responding (red) antibody deficient patient B-cells at day 13 of *in vitro* differentiation. Each plot represents the clonal distribution of BCR sequences within individual patients. The arc length corresponds to the relative frequencies of V of J gene segments used, and the ribbon width depicts relative connection frequencies of each clonotype within the sample. Colours indicate different clonotypes, allowing for visual comparison of diversity and clonality across samples.

6.8 CDR3 characteristics

The CDR3 region is the most variable region of the BCR and is crucial for antigen recognition, due to its direct interaction with the antigen's epitope (Xu and Davis, 2000). Studies have shown that variation in CDR3 characteristics can affect immune responses, particularly in the context of vaccine efficacy (Wong *et al.,* 2022). For instance, alteration in the CDR3 sequence composition have been observed in individuals with certain immunodeficiencies (Roskin *et al.,* 2016). By analysing the hydrophobicity, charge and length distribution of CDR3 in the HC and patient cohort, it might be possible to uncover potential patterns or abnormalities that may

contribute to vaccine non-responsiveness in antibody deficient patients.
The characteristics of the CDR3 region were analysed using MiXCR for BCR repertoire profiling. All patient samples exhibited negatively charged CDR3 regions, with the HC sample showing the most negative charge, consistent with a repertoire that favours non-autoreactive B cells (Figure 6.8A). An exception was observed in P8, who displayed a positively charged CDR3 region- a trait often associated with increased self-reactivity, which could hint at underlying immune dysregulation or reduced tolerance possibly contributing to the impaired vaccine response (Wardemann, 2003).

CDR3 length was next examined in the representative cohort. The HC and both responding patients, except the abnormal responder P5, showed a shorter CDR3 length, supporting the expected pattern. However, the two non-responders and P5 exhibited notably longer CDR3 regions (Figure 6.8B), possibly indicating a higher risk of autoreactivity that may distinguish patients with additional immune impairments (Bashford-Rogers *et al.,* 2018).

The final CDR3 characteristic analysed was hydrophobicity, which typically converges near a neutral value of zero; lower values are considered hydrophilic, and higher values indicate hydrophobicity. The HC and P8 showed values close to zero, suggesting a balanced hydrophobicity profile, while P3, P4, and P9 exhibited slightly elevated hydrophobic CDR3 regions, and P5 displayed a more hydrophilic CDR3 (Figure 6.8C). These variations may reflect differences in antigen-binding affinities or immune repertoire diversity across the cohort but are likely impacted by individual immune selection pressures, which may influence autoreactivity (Ghraichy *et al.,* 2018)

Analysis of CDR3 characteristics in the representative patient cohort reveals trends suggesting differences between patients and controls, including a distinction in CDR3 length between vaccine responders and non-responders. However, given the considerable variability in the studied characteristics among patients and the limited sample size, these findings should be interpreted with caution. Sequencing additional samples would be necessary to confidently confirm whether these observed differences are statistically significant.

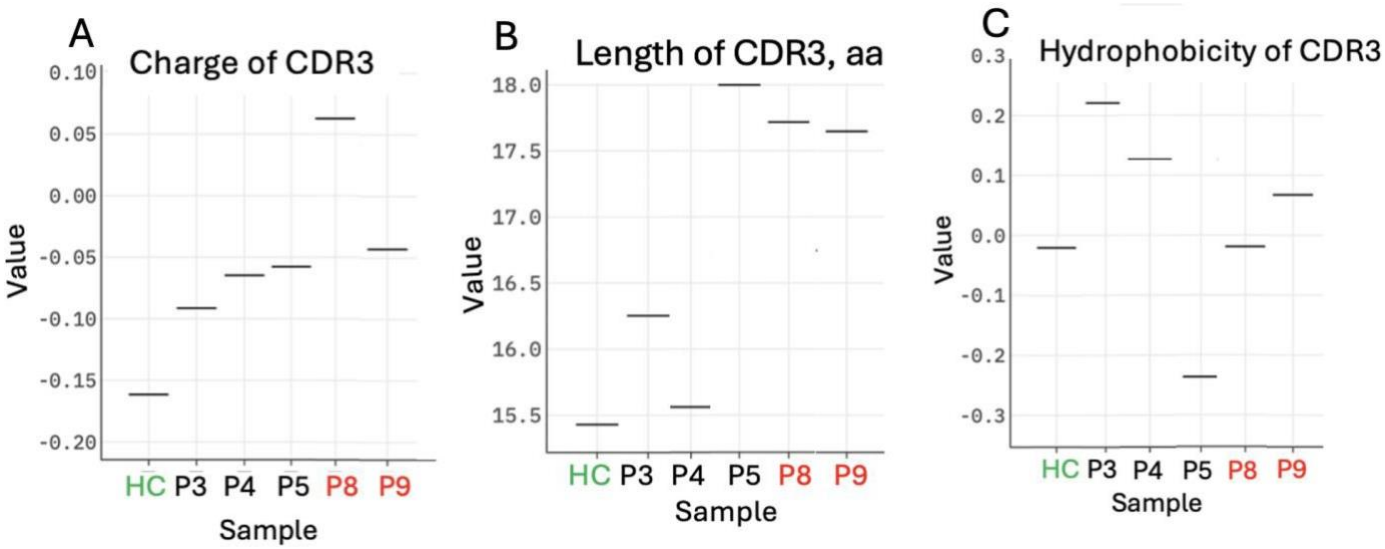

Figure 6.8: CDR3 characteristics in COV-AD patients (P3, P4, P5, P8 and P9) and healthy control (HC) samples. Sequenced BCR amplicons were derived from RNA extracted from a representative healthy control (green), SARS-CoV-2 vaccine responding (black) and non-responding (red) antibody deficient patient B-cells at day 13 of *in vitro* differentiation. **A**: Charge of CDR3 region. **B**: Amino acid (aa) length of CDR3 region. **C**: Hydrophobicity of CDR3 region. Statistical significance was evaluated using the Wilcoxon test, p= -1.00.

6.9 Discussion

The incorporation of BCR repertoire analysis has proved a useful tool in facilitating understanding of immune dysfunction in antibody-deficient patients, who have been previously shown to exhibit limited diversity in their antibody response (Roskin *et al.,* 2015; Soto *et al.,* 2019b). In healthy individuals, diverse BCR repertoires allows broad antigen recognition, but antibody-deficient patients may show restricted repertoires or abnormal clonal expansion, limiting effective immunity (Roskin *et al.,* 2015; Ghraichy *et al.,* 2018). Therefore, this approach may provide insights into the

mechanisms underlying poor vaccine responses and highlights potential markers of immune competence in immunodeficient populations.

In this chapter, BCR repertoire analysis was performed on five samples from antibody-deficient patients, with a focus on distinguishing between vaccine responders (P3, P4, and P5) and non-responders (P7 and P8). After confirming the quality of the samples, clonal populations were assessed, revealing differences in BCR diversity and clonal expansion across the samples. One finding was the significantly reduced number of unique clonotypes in all patient samples compared to the HC. Healthy adult naive B-cell populations typically exhibit millions of unique clonotypes, as seen in the HC, which is expected given the high diversity inherent in the naive BCR repertoire (Soto *et al.,* 2019b; Greiff *et al.,* 2017). Moreover, the observation of a high number of clonotypes in the HC aligns with previously published data under similar conditions, where polyclonal stimulation without selective pressure promotes the presence of a diverse range of clonotypes (Cocco *et al.,* 2012). However, with regards to the patient samples, it remains unclear whether the *in vitro* conditions may be promoting the expansion or survival of particular clones, despite the use of polyclonal stimuli. This raises the question of whether clonotypic observations in patients are reflecting the true repertoire or are skewed by the experimental setup. In this context, it could be useful to address this by comparing the BCR repertoire before and after differentiation to determine if the same degree of diversity is maintained or if there is evidence for the outgrowth/survival of specific clones. Another possible explanation for the differences in clonotypic features across all samples could be individual variations in responses to stimuli, such as BAFF, which may promote broader B-cell activation in HCs, thereby enhancing clonotypic diversity (Mackay and Schneider, 2009). Experimental factors, such as sequencing errors or artifacts, could also contribute to an overestimation of diversity (Yaari and Kleinstein, 2015). Incorporating additional control samples would strengthen the reference and increase confidence in the observed trends. Nonetheless, based on the representative data, antibody-deficient patients exhibit a reduced number of unique clonotypes, irrespective of vaccine response.

Clonotype analysis based on relative abundance revealed distinct patterns between groups. The HC exhibited a diverse mix of small, medium, and large clonotypes,

while vaccine responders displayed a significant proportion of hyperexpanded clonotypes. This may reflect successful clonal responses to vaccination (Laserson *et al.,* 2014; Fraley *et al.,* 2022; Lopes de Assis *et al.,* 2023), since hyperexpansion was absent in both non-responders and the HC. Confirmation of this hypothesis in future experiments could be achieved using COVID-specific ELISAs of D13 supernatants.

Further analysis of rare clonal proportions reinforced this finding, with responders showing a higher frequency of high-abundance clonotypes, particularly within the 101-MAX category, indicative of effective clonal expansion in response to vaccination. In the case of the HC, who had not been recently vaccinated, clonal expansion was limited to low-level activation driven by normal immune system maintenance, which is typically triggered by BCR signalling through low-affinity antigens (Hershberg and Luning Prak, 2015). This background expansion is minimal and does not involve the large-scale clonal proliferation seen after stimulation by infection of vaccination (Hershberg and Luning Prak, 2015). On the other hand, the reduced expansion of specific clonotypes in vaccine non-responders could suggest issues with immune tolerance or insufficient T-cell help - critical factors for optimal B-cell activation and differentiation (Frasca *et al.,* 2016; Malvey *et al.,* 1998). However, the observation of reduced clonal expansion in non-responders at the D13 timepoint is speculative and supporting literature is minimal. Hence, it would be important to include a recently vaccinated HC sample for direct comparison in order to draw more definitive conclusions. Such a comparison would help determine whether the reduced clonal expansion in non-responders is specifically linked to their immune response to vaccination or reflects broader underlying immunological differences.

The next aspect of the BCR repertoire analysed was V and J gene usage. Most samples, including HC, showed a predominance of the *IGHV3* gene, consistent with its role as the most common VH subgroup (Wang *et al.,* 2022). However, unlike the HC, all patients-irrespective of vaccine response (except P5) - displayed higher than expected *IGHV4* levels. *IGHV4* is frequently associated with autoreactivity (Schickel *et al.,* 2017), which has been observed in several autoimmune and immunodeficient conditions (Costagliola *et al.,* 2021). Elevated *IGHV4* levels have been linked to autoreactivity, a feature that has been associated with severe COVID-19 infection (Woodruff *et al.,* 2022). The shift towards *IGHV4* could also result from antigen pressure, leading to CDR3 somatic hypermutation (Hirokawa *et al.,* 2019), which

may represent an interesting avenue for further investigation in the context of vaccine response.

Unsurprisingly, the only patient exhibiting an anomaly in *IGHV* usage was P5, who showed a notable overrepresentation of *IGHV3*. This is likely attributable to the patient's CLL diagnosis, which is probably a rare and clinically distinct subset of CLL (Ghia et al., 2008; Bomben *et al.,* 2010). This suggests a disease-specific alteration in the BCR repertoire, rather than a deficiency-related change.

Similarly, regarding J gene usage, the overrepresentation of *IGHJ6* in P5 likely reflects the patient's unique CLL diagnosis (Datta and Jumaa, 2022; Agathangelidis *et al.,* 2012). In contrast, analysis of the J gene usage in the remaining samples revealed highly consistent patterns, with *IGHJ4* being the most frequently observed in all samples (except P5), which aligns with the literature (Shi *et al.,* 2020). These findings suggest that V and J gene usage patterns reflect both adaptive responses and individual health conditions, offering insights into the differences between immune-competent and antibody-deficient individuals rather than vaccine responders versus non-responders.

Given the large number of possible V-J gene segment combinations required to recognise a vast array of pathogens, it was suggested that antibody-deficient patients, particularly vaccine non-responders, might exhibit restricted diversity in V-J gene segment combinations, potentially limiting their ability to elicit a sufficient immune response. Patient samples displayed a similar range of V-J pairings to the HC, with connections broadly distributed, indicating the preservation of immunoglobulin gene usage and diversity within the antibody repertoire. This finding aligns with previous work which notes similar patterns, even in antibody deficient patients with severe clinical phenotypes (Ghraichy *et al.,* 2018). This suggests that, at least at the level of V-J recombination, the repertoire in patients, particularly non-responders, may not be inherently restricted. However, it remains possible that functional limitations in immune responses arise from other factors, such as signalling defects or impaired maturation processes, rather than a lack of diversity in V-J combinations (Ghraichy *et al.,* 2018). It was also noted that the two representative non-responders exhibited combinational patterns most similar to each

other, possibly suggesting a shared underlying effect in their repertoires. However, this is speculative and may not represent a true functional difference. The similarities observed could simply be due to the limited sample size, and further investigation with more patient samples would be necessary to clarify whether this pattern reflects a meaningful distinction or if it is an artifact of the data.

The final analysis of the BCR repertoire was looking at CDR3 characteristics. Existing studies on CDR3 metrics in antibody deficient patients show conflicting results (Ghraichy *et al.,* 2018; IJspeert *et al.,* 2016), likely due to the extensive heterogeneity of immunodeficiencies (i.e. CVID). Nonetheless, this analysis aimed to identify any distinctive CDR3 features within our patient cohort, particularly between vaccine responders and non-responders, to investigate if specific trends might correlate with vaccine response outcomes.

In agreement with published literature on mature B-cell subsets (Kaplinsky *et al.,* 2014), all samples in the cohort exhibited negatively charged CDR3 regions, with the HC showing the most negative charge. This likely reflects selection against autoreactive B cells, a process that favours more negatively charged CDR3s in mature B cells (Kaplinsky *et al.,* 2014). The only patient to deviate from the negatively charged CDR3 was P8, possibly suggesting low specificity and the presence of autoreactive and polyreactive BCRs (Rabia *et al.,* 2018; Wardemann, 2003).

The average CDR3 length of the BCR repertoire typically decreases after antigen exposure (Galson *et al.,* 2015), and shorter CDR3 lengths are associated with reduced autoreactivity (Wardemann, 2003), which is critical for avoiding self-reactive immune responses. However, patients with CVID, particularly in clinically severe cases, often show trends towards longer CDR3 lengths compared to healthy individuals (Roskin *et al.,* 2015), potentially contributing to an increased prevalence of autoimmunity. This association between longer CDR3 lengths and autoreactivity may reflect a reduced negative selection against self-reactive B-cells (Roskin *et al.,* 2015). Data presented here recapitulate the findings from Roskin et al. (2015), whereby those with probable more clinically severe phenotypes (i.e. P5 and the vaccine non-responders) demonstrated longer CDR3 lengths. P5 aside, this could suggest that vaccine non-responders have a higher risk of autoreactivity. To

determine whether longer CDR3 lengths consistently differentiate non-responders, additional data from a larger cohort would be essential. Sequencing more samples from both patient and HCs could help clarify if this pattern is consistent, potentially strengthening the link between CDR3 length and vaccine response. Such data could also address current discrepancies in findings across studies, further illuminating how characteristics of the BCR repertoire may relate to immune function and vaccine responsiveness in antibody-deficient patients.

Collectively, the BCR repertoire analysis in this study revealed no overall distinguishable differences in immune diversity or clonal expansion between representative COV-AD patients, particularly when comparing vaccine responders and non-responders. While trends such as longer CDR3 regions in non-responders and varied V and J gene segment usage were observed, these findings align with some literature on immunodeficient populations, they should be interpreted with caution, as they represent preliminary trends rather than definitive conclusions. Given the limited sample size, observed patterns in clonal expansion and CDR3 characteristics should be considered suggestive rather than conclusive. However, the analysis does show the potential of BCR repertoire sequencing to identify particularly vulnerable patients, such as P5, and could be used alongside other risk stratification-approaches, though this may be more applicable outside an immunodeficiency setting. Further BCR repertoire analysis, incorporating methodologies such as repertoire profiling across different timepoints or high-throughput sequencing, could provide deeper insights into the evolution of B-cell responses following vaccination and the mechanisms underlying impaired immune responses in antibody-deficient patients. In particular, integrating repertoire data with complementary immunophenotyping, functional assays, and sequencing-based approaches may help to better characterise patient subgroups and inform future strategies for personalised management in this population.

Concluding remarks

The vulnerability of antibody-deficient patients to severe infections, notably COVID-19, highlights the critical need to deepen our understanding of the immune dysfunctions underlying these deficiencies. Despite widespread vaccination efforts, many individuals with antibody deficiencies continue to face a heightened risk of poor outcomes due to their impaired capacity to generate adequate immune responses. This issue remains especially pertinent in the context of the COVID-19 pandemic and the emergence of new variants, as well as other infectious diseases that continue to threaten immunocompromised populations. Addressing these challenges is paramount to developing targeted therapeutic strategies and ensuring equitable healthcare outcomes for these vulnerable groups.

This thesis represents a novel *in vitro* investigation into the B-cell profiles of antibody-deficient patients, aiming to assess their contributions to vaccine responsiveness in the context of COVID-19. By optimising an established B-cell differentiation model (Cocco *et al.,* 2012; Stephenson *et al.,* 2019; Stephenson *et al.,* 2021) to accommodate patient cells with low cell counts, this work demonstrates the unique ability of this system to profile heterogeneous antibody-deficient patients on an individual basis. This approach provides invaluable information on their B-cell biology, offering critical insights into their immune functionality and potential vaccine responsiveness. Furthermore, it has shed light on the mechanisms underlying vaccine non-responsiveness in these patients, paving the way for future studies to refine therapeutic strategies and improve vaccination outcomes in this vulnerable population.

While the findings show some minor differences that likely reflect patient heterogeneity, rather than intrinsic differences in the vaccine response, both groups, vaccine responders and non-responders, were able to differentiate into antibody-secreting plasma cells following T-dependent CD40-L stimulation. However, among the key findings of this thesis, the most significant was the identification of impaired or absent BAFF-R expression at day 0 as a central factor contributing to vaccine non-responsiveness. Data from this study revealed a notable reduction or complete

absence of BAFF-R expression in vaccine non-responders, and even in a subset of responders, suggesting that BAFF-R dysfunction may play a pivotal role in modulating the immune response.

The initial hypothesis that reduced surface BAFF-R expression might be explained by transcriptional abnormalities in its encoding gene, *TNFRSF13C*, was not supported by the RNA expression data. Notably, some vaccine responders with normal or high surface BAFF-R expression displayed similarly low *TNFRSF13C* transcript levels to those with reduced surface expression, indicating that mRNA levels alone do not account for the observed variability. This prompted further investigation into potential compensatory upregulation of alternative receptors such as TACI or BCMA, in addition to serum level, but neither circulating BAFF concentrations nor patterns of surface receptor staining provided a clear causal link. These findings suggest that factors downstream of transcription, such as post-transcriptional modifications, receptor shedding, or altered protein trafficking, likely play a more significant role in regulating surface BAFF-R availability and influencing immune outcomes (Smulski *et al.,* 2017; Mihalcik *et al.,* 2010).

The reduction in BAFF-R surface expression is likely driven by a complex interplay of post-transcriptional, genetic, epigenetic, and environmental factors (Gibney and Nolan, 2010; Martínez-Cano *et al.,* 2019; Hedrich and Tsokos, 2011). Collectively, these findings suggest that BAFF-R dysfunction, whether through transcriptional or post- transcriptional alterations, plays a critical role in impaired vaccine responses in antibody-deficient patients. Notably, this thesis identifies a novel biomarker, BAFF-R expression in preactivated B-cells, as a potential tool to risk-stratify patients who are unlikely to respond to vaccination against COVID-19 and potentially other infections. This insight is both clinically significant and economically relevant, as it opens avenues to address the barriers preventing effective vaccine responses in these individuals.

Interestingly, the relevance of impairments in the BAFF/BAFF-R axis on COVID-19 vaccine efficacy can be backed up by a recent publication that demonstrates an association between heightened extrafollicular B-cell activity and anti-BAFF therapy with inferior responses to COVID-19 vaccines (Faliti *et al.,* 2024). This study highlights how disruptions in BAFF signalling pathways can negatively impact B-cell survival and differentiation. These findings align with the data presented in this

thesis, as they underscore the critical role of the BAFF/BAFF-R axis in shaping effective immune responses. The potential link between reduced BAFF-R expression and extrafollicular B-cell dysregulation further supports the hypothesis that altered BAFF-R function, whether through diminished expression or defective signalling, plays a central role in vaccine non-responsiveness in antibody-deficient patients.

BAFF-R-related findings from this thesis may also have direct relevance to IgRT, since BAFF-R dysfunction could serve as a marker to identify patients who may benefit from more aggressive or tailored IgRT regimens. Given that IgRT aims to restore functional antibody levels (Sil *et al.,* 2024), understanding the role of BAFF-R in B-cell activation and differentiation could help in determining which patients are more likely to respond to IgRT, and how their B-cell biology might affect their long-term immune functionality (Le pottier *et al.,* 2007). In particular, patients with impaired BAFF-R expression could potentially require a more personalised IgRT approach, or closer monitoring, to achieve optimal protection against infections (Le pottier *et al.,* 2007). Identifying these patients early could guide therapeutic decisions, enabling clinicians to tailor IgRT treatment more effectively based on the patient's immune dysfunction profile.

Refining this *in vitro* plasma cell differentiation model will enable more rapid assessments of BAFF-R levels and other key biomarkers, thereby improving its potential as a practical tool for risk stratification in clinical settings, particularly for predicting vaccine response. However, the current data linking impaired BAFF-R expression to impaired vaccine response is limited, highlighting the need for more mechanistic studies to elucidate why this phenotype continually occurs and what it might mean for patient outcomes. Understanding these mechanisms is critical for refining therapeutic interventions. Future studies could investigate key aspects such as the signalling pathways downstream of BAFF-R, the role of receptor shedding or trafficking in vaccine responses, and how BAFF-R dysfunction affects long-term immunity. Techniques such as gene editing, single-cell RNA-seq, and proteomics could provide valuable insights into these processes.

Furthermore, applying a large-scale BAFF-R risk stratification approach to a broad cohort of antibody-deficient patients could validate the utility of this biomarker and identify trends across different patient populations. Expanding these investigations to

include responses to vaccines beyond COVID-19 may also reveal broader relevance, potentially aiding in efforts to address future pandemics. By combining mechanistic data with large-scale clinical applications, this research could inform strategies to optimise vaccine efficacy, improve clinical outcomes, and enhance risk stratification for IgRT interventions in vulnerable populations.

References

1. Absolute Antibody (2018) *Antibody Isotypes & Subtypes | Absolute antibody*. https://absoluteantibody.com/antibody-resources/antibody-overview/antibody-isotypes-subtypes/.
2. Agarwal, S. and Cunningham-Rundles, C. (2007). Assessment and clinical interpretation of reduced IgG values. *Annals of Allergy, Asthma & Immunology*, [online] 99(3), pp.281–283. doi:https://doi.org/10.1016/s1081-1206(10)60665-5.
3. Agarwal, V. and Kelley, D.R. (2022). The genetic and biochemical determinants of mRNA degradation rates in mammals. *Genome Biology*, 23(1). doi:https://doi.org/10.1186/s13059-022-02811-x.
4. Agathangelidis, A., Nikos Darzentas, Hadzidimitriou, A., Brochet, X., Murray, F., Yan, X.-J., Davis, Z., Gastel-Mol, V., Tresoldi, C., Chiu, C.Y., Cahill, N., Véronique Giudicelli, Tichy, B., Lone Bredo Pedersen, Letizia Foroni, Bonello, L., Janus, A., Smedby, K.E., Anagnostopoulos, A. and Hélène Merle-Béral (2012). Stereotyped B-cell receptors in one-third of chronic lymphocytic leukemia: a molecular classification with implications for targeted therapies. 119(19), pp.4467–4475. doi:https://doi.org/10.1182/blood-2011-11-393694.
5. Agostini, C., Blau, I.-W., Kimby, E. and Plesner, T. (2016). Prophylactic immunoglobulin therapy in secondary immune deficiency – an expert opinion. *Expert Review of Clinical Immunology*, 12(9), pp.921–926. doi:https://doi.org/10.1080/1744666x.2016.1208085.
6. Akalu, Y.T. and Bogunovic, D. (2023). Inborn errors of immunity: an expanding universe of disease and genetic architecture. *Nature Reviews Genetics* [Preprint]. https://doi.org/10.1038/s41576-023-00656-z.
7. Akkaya, M. and Kwak, K. (2019). B cell memory: building two walls of protection against pathogens,' *Nature Reviews Immunology*, 20(4), pp. 229–238. https://doi.org/10.1038/s41577-019-0244-2.
8. Alt, F. W., Blackwell, T. K., & Yancopoulos, G. D. (1992). Immunoglobulin gene rearrangement in developing lymphocytes: Mechanism and regulation. *Annual Review of Immunology*, 10, 217-238.
9. Alt, F.W., Yancopoulos, G.D., T. Keith Blackwell, Wood, C.M., Thomas, E., Boss, M., Coffman, R.L., Rosenberg, N., Susumu Tonegawa and Baltimore, D. (1984). Ordered rearrangement of immunoglobulin heavy chain variable region segments. *The EMBO Journal*, 3(6), pp.1209–1219. doi:https://doi.org/10.1002/j.1460-2075.1984.tb01955.x.
10. Ameratunga, R., Leung, E., Woon, S.-T., Lea, E., Allan, C., Chan, L., Longhurst, H., Steele, R., Snell, R. and Lehnert, K. (2023). Challenges for

gene editing in common variable immunodeficiency disorders: Current and future prospects. *Clinical Immunology*, [online] p.109854. doi:https://doi.org/10.1016/j.clim.2023.109854.

11. Ameratunga, R., Woon, S.T., Gillis, D., Koopmans, W. and Steele, R. (2014). New diagnostic criteria for common variable immune deficiency (CVID), which may assist with decisions to treat with intravenous or subcutaneous immunoglobulin. *Pediatric Hematology/Oncology and Immunopathology*, 13(4), pp.21–35.
12. Ammann, E.M., Haskins, C.B., Fillman, K.M., Ritter, R.L., Gu, X., Winiecki, S.K., Carnahan, R.M., Torner, J.C., Fireman, B.H., Jones, M.P. and Chrischilles, E.A. (2016). Intravenous immune globulin and thromboembolic adverse events: A systematic review and meta-analysis of RCTs. *American Journal of Hematology*, 91(6), pp.594–605. doi:https://doi.org/10.1002/ajh.24358.
13. Arpin, C., Banchereau, J. and Liu, Y.-J. (1997). Memory B Cells Are Biased Towards Terminal Differentiation: A Strategy That May Prevent Repertoire Freezing. *Journal of Experimental Medicine*, 186(6), pp.931–940. doi:https://doi.org/10.1084/jem.186.6.931.
14. ASANO, T., KANEKO, H., TERADA, T., KASAHARA, Y., FUKAO, T., KASAHARA, K. and KONDO, N. (2004). Molecular analysis of B-cell differentiation in selective or partial IgA deficiency. *Clinical and Experimental Immunology*, 136(2), pp.284–290. doi:https://doi.org/10.1111/j.1365-2249.2004.02440.x.
15. Andreano, E., & Rappuoli, R. (2021). Immunodominant antibody germlines in COVID-19. *Journal of Experimental Medicine*, 218(5), e20210281. https://doi.org/10.1084/jem.20210281
16. Avery, D.T., Kalled, S.L., Ellyard, J.I., Ambrose, C., Bixler, S.A., Thien, M., Brink, R., Mackay, F., Hodgkin, P.D. and Tangye, S.G. (2003). BAFF selectively enhances the survival of plasmablasts generated from human memory B cells. *The Journal of Clinical Investigation*, [online] 112(2), pp.286–297. doi:https://doi.org/10.1172/JCI18025.
17. Ballow, M. (2002). Primary immunodeficiency disorders: Antibody deficiency. *Journal of Allergy and Clinical Immunology*, [online] 109(4), pp.581–591. doi:https://doi.org/10.1067/mai.2002.122466.
18. Ballow, M. (2023). 'The Use of Prophylactic Antibiotics in Antibody Deficiencies' [PowerPoint presentation]. Immune Deficiency Foundation. Available at: https://primaryimmune.org/sites/default/files/FOR%20WEB%20-%20Prophylactic%20Antibiotics%20PI.pdf (Accessed: 1 April 2024).
19. Banchereau, J., de Paoli, P., Valle, A., Garcia, E. and Rousset, F. (1991). Long-term human B cell lines dependent on interleukin-4 and antibody to CD40. *Science*, 251(4989), pp.70–72. doi:https://doi.org/10.1126/science.1702555.
20. Barbosa, R.R., Silva, S.L., Silva, S.P., Melo, A.C., M. Conceição Pereira-Santos, Barata, J.T., Lennart Hammarström, Marília Cascalho and Sousa,

A.E. (2014). Reduced BAFF-R and Increased TACI Expression in Common Variable Immunodeficiency. *Journal of Clinical Immunology*, 34(5), pp.573–583. doi:https://doi.org/10.1007/s10875-014-0047-y.

21. Barnes, E., Goodyear, C.S., Willicombe, M., Gaskell, C., Siebert, S., Silva, Murray, S.M., Rea, D., Snowden, J.A., Carroll, M.W., Pirrie, S., Bowden, S., Dunachie, S., Richter, A., Lim, Z., Satsangi, J., Cook, G., Pope, A., Hughes, A. and Harrison, M. (2023). SARS-CoV-2-specific immune responses and clinical outcomes after COVID-19 vaccination in patients with immune-suppressive disease. *Nature Medicine*, 29(7), pp.1760–1774. doi:https://doi.org/10.1038/s41591-023-02414-4.
22. Bassing, C., Swat, W. and Alt, F. (2002). The mechanism and regulation of chromosomal V(D)J recombination. *Cell*, 109(2).
23. Batten, M., Groom, J.R., Cachero, T.G., Qian, F., Schneider, P., Tschopp, J., Browning, J.L. and Mackay, F. (2000). Baff Mediates Survival of Peripheral Immature B Lymphocytes. *Journal of Experimental Medicine*, 192(10), pp.1453–1466. doi:https://doi.org/10.1084/jem.192.10.1453.
24. Bayry, J., Ahmed, E.A., Toscano-Rivero, D., Vonniessen, N., Genest, G., Cohen, C.G., Dembele, M., Kaveri, S.V. and Mazer, B.D. (2023). Intravenous Immunoglobulin: Mechanism of Action in Autoimmune and Inflammatory Conditions. *The Journal of Allergy and Clinical Immunology: In Practice*, [online] 11(6), pp.1688–1697. doi:https://doi.org/10.1016/j.jaip.2023.04.002.
25. Beauté, J., Levy, P., Millet, V., Debré, M., Dudoit, Y., Le Mignot, L., Tajahmady, A., Thomas, C., Suarez, F., Pellier, I., Hermine, O., Aladjidi, N., Mahlaoui, N. and Fischer, A. (2009). Economic evaluation of immunoglobulin replacement in patients with primary antibody deficiencies. *Clinical & Experimental Immunology*, 160(2), pp.240–245. doi:https://doi.org/10.1111/j.1365-2249.2009.04079.x.
26. Benjamini, Y. and Hochberg, Y. (1995). Controlling the False Discovery Rate: A Practical and Powerful Approach to Multiple Testing. *Journal of the Royal Statistical Society: Series B (Methodological)*, 57(1), pp.289–300. doi:https://doi.org/10.1111/j.2517-6161.1995.tb02031.x.

27. Bernasconi, N.L., Onai, N. and Lanzavecchia, A. (2003). A role for Toll-like receptors in acquired immunity: up-regulation of TLR9 by BCR triggering in naive B cells and constitutive expression in memory B cells. *Blood*, 101(11), pp.4500–4504. doi:https://doi.org/10.1182/blood-2002-11-3569.
28. Bogner, E. and Pecher, G. (2013). Pattern of the Epitope-Specific IgG/IgM Response against Human Cytomegalovirus in Patients with Multiple Myeloma. *Clinical and Vaccine Immunology*, 20(8), pp.1298–1304. doi:https://doi.org/10.1128/cvi.00317-13.
29. Bomben, R., Dal-Bo, M., Benedetti, D., Capello, D., Forconi, F., Marconi, D., Bertoni, F., Maffei, R., Laurenti, L., Rossi, D., Ilaria, M., Luciano, F., Sozzi, E., Ilaria Cattarossi, Antonella Zucchetto, Francesca Maria Rossi, Pietro Bulian, Zucca, E., Nicoloso, M.S. and Degan, M. (2010). Expression of Mutated *IGHV3-23* Genes in Chronic Lymphocytic Leukemia Identifies a Disease Subset with Peculiar Clinical and Biological Features. *Clinical cancer research*, 16(2), pp.620–628. doi:https://doi.org/10.1158/1078-0432.ccr-09-1638.
30. Bonet, M., C., Waser, N., Cheng, K., Tzivelekis, S., Edgar, J.D.M. and Sánchez-Ramón, S. (2020). A systematic literature review of the effects of immunoglobulin replacement therapy on the burden of secondary immunodeficiency diseases associated with hematological malignancies and stem cell transplants. *Expert review of clinical immunology*, [online] 16(9), pp.911–921. doi:https://doi.org/10.1080/1744666X.2020.1807328.
31. Bonilla, F.A., Barlan, I., Chapel, H., Costa-Carvalho, B.T., Cunningham-Rundles, C., de la Morena, M.T., Espinosa-Rosales, F.J., Hammarström, L., Nonoyama, S., Quinti, I., Routes, J.M., Tang, M.L.K. and Warnatz, K. (2016). International Consensus Document (ICON): Common Variable Immunodeficiency Disorders. *The journal of allergy and clinical immunology. In practice*, [online] 4(1), pp.38–59. doi:https://doi.org/10.1016/j.jaip.2015.07.025.
32. Borsutzky, S., Cazac, B.B., RoesJ. and GuzmánC.A. (2004). TGF-β Receptor Signaling Is Critical for Mucosal IgA Responses. *The Journal of Immunology*, 173(5), pp.3305–3309. doi:https://doi.org/10.4049/jimmunol.173.5.3305.
33. Boughton, B.J., Jackson, N., Lim, S and Smith, N (1995). Randomized trial of intravenous immunoglobulin prophylaxis for patients with chronic lymphocytic leukaemia and secondary hypogammaglobulinaemia. *Clinical and Laboratory Haematology*, 17(1), pp. 75–80. https://doi.org/10.1111/j.1365-2257.1995.tb00322.x.

34. Browne, D.J., Miller, C.M. and Doolan, D.L. (2024). Technical pitfalls when collecting, cryopreserving, thawing, and stimulating human T-cells. *Frontiers in immunology*, 15. doi:https://doi.org/10.3389/fimmu.2024.1382192.

35. Calame, K., Lin, K. and Tunyaplin, C. (2003). Regulatory Mechanisms that Determine the Development and Function of Plasma Cells. *Annual Review of Immunology*, 21(1), pp. 205–230. https://doi.org/10.1146/annurev.immunol.21.120601.141138.

36. Cano, R.L.E. and Lopera, H.D.E. (2013). *Introduction to T and B lymphocytes*. https://www.ncbi.nlm.nih.gov/books/NBK459471/.

37. Cancro, M.P. (2009). Signalling crosstalk in B cells: managing worth and need. *Nature Reviews Immunology*, 9(9), pp.657–661. doi:https://doi.org/10.1038/nri2621.

38. Carotta, S., Holmes, M., Pridans, C. and Nutt, S.L. (2006). Pax5 Maintains Cellular Identity by Repressing Gene Expression Throughout B Cell Differentiation. *Cell Cycle*, 5(21), pp.2452–2456. doi:https://doi.org/10.4161/cc.5.21.3396.

39. Carotta, S., Willis, S.N., Jhagvaral Hasbold, Inouye, M., Swee, Emslie, D., Light, A., Chopin, M., Shi, W., Wang, H., Morse, H.C., Tarlinton, D.M., Corcoran, L.M., Hodgkin, P.D. and Nutt, S.L. (2014). The transcription factors IRF8 and PU.1 negatively regulate plasma cell differentiation. *Journal of Experimental Medicine*, 211(11), pp.2169–2181. doi:https://doi.org/10.1084/jem.20140425.

40. Carsetti, R. (2000). The Development of B Cells in the Bone Marrow Is Controlled by the Balance between Cell-Autonomous Mechanisms and Signals from the Microenvironment. *Journal of Experimental Medicine*, 191(1), pp. 5–8.

41. Cascalho, M and Platt, J.L. (2021). TNFRSF13B Diversification Fueled by B Cell Responses to Environmental Challenges—A Hypothesis. *Frontiers in Immunology*, 12. doi:https://doi.org/10.3389/fimmu.2021.634544.

42. Catanzaro, J.R., Strauss, J.D., Bielecka, A., Porto, A.F., Lobo, F.M., Urban, A., Schofield, W.B. and Palm, N.W. (2019). IgA-deficient humans exhibit gut microbiota dysbiosis despite secretion of compensatory IgM. *Scientific Reports*, 9(1). doi:https://doi.org/10.1038/s41598-019-49923-2.

43. Cerutti, A., Cols, M. and Puga, I. (2013). Marginal zone B cells: virtues of innate-like antibody-producing lymphocytes. *Nature Reviews Immunology*, 13(2), pp. 118–132. https://doi.org/10.1038/nri3383.

44. Cerutti, A., Zan, H., Kim, E.C., Shah, S., Schattner, E.J., SchafferA. and Casali, P. (2002). Ongoing In Vivo Immunoglobulin Class Switch DNA Recombination in Chronic Lymphocytic Leukemia B Cells. *The Journal of Immunology*, [online] 169(11), pp.6594–6603. doi:https://doi.org/10.4049/jimmunol.169.11.6594.

45. Chang, L., Gardner, L., House, C., Daly, C., Allsopp, A., Roiz, D., Shaw, M.-A. and Hopkins, P.M. (2023). Comparison of Transcriptomic Changes in Survivors of Exertional Heat Illness with Malignant Hyperthermia Susceptible Patients. *International journal of molecular sciences*, 24(22), pp.16124–16124. doi:https://doi.org/10.3390/ijms242216124.

46. Chapel, H., M. Dicato, Gamm, H., Brennan, V., Ries, F., Bunch, C. and Lee, M. (1994). Immunoglobulin replacement in patients with chronic lymphocytic leukaemia: a comparison of two dose regimes. *British Journal of Haematology*, 88(1), pp.209–212. doi:https://doi.org/10.1111/j.1365-2141.1994.tb05002.x.

47. Chaudhuri, J. and Alt, F.W. (2004). Class-switch recombination: interplay of transcription, DNA deamination and DNA repair. *Nature Reviews Immunology*, 4(7), pp. 541–552. https://doi.org/10.1038/nri1395.

48. Chen, E.Y., Tan, C.M., Kou, Y., Duan, Q., Wang, Z., Meirelles, G., Clark, N.R. and Ma'ayan, A. (2013). Enrichr: interactive and collaborative HTML5 gene list enrichment analysis tool. *BMC Bioinformatics*, 14(1), p.128. doi:https://doi.org/10.1186/1471-2105-14-128.

49. Chi, X., Li, Y. and Qui, X. (2020). V(D)J recombination, somatic hypermutation and class switch recombination of immunoglobulins: Mechanism and regulation. *Immunology*, 160(3), pp. 233–247.

50. Christie, S.M., Fijen, C. and Rothenberg, E. (2022). V(D)J Recombination: Recent insights in formation of the recombinase complex and recruitment of DNA repair machinery. *Frontiers in Cell and Developmental Biology*, 10. https://doi.org/10.3389/fcell.2022.886718.

51. Chung, J.B., Silverman, M. and Monroe, J.G. (2003). Transitional B cells: step by step towards immune competence. *Trends in Immunology*, 24(6), pp.342–348. doi:https://doi.org/10.1016/s1471-4906(03)00119-4.

52. Cobaleda, C., Schebesta, A., Delogu, A. and Busslinger, M. (2007). Pax5: the guardian of B cell identity and function. *Nature Immunology*, [online] 8(5), pp.463–470. doi:https://doi.org/10.1038/ni1454.

53. Cocco, M., Stephenson, S., Care, M.A., Newton, D., Barnes, N.A., Davison, A., Rawstron, A., Westhead, D.R., Doody, G.M. and Tooze, R.M. (2012). *In vitro* Generation of Long-lived Human Plasma Cells. *The Journal of Immunology*, [online] 189(12), pp.5773–5785. doi:https://doi.org/10.4049/jimmunol.1103720.

54. Cock, P.J.A., Fields, C.J., Goto, N., Heuer, M.L. and Rice, P.M. (2010). The Sanger FASTQ file format for sequences with quality scores, and the Solexa/Illumina FASTQ variants. *Nucleic Acids Research*, [online] 38(6), pp.1767–1771. doi:https://doi.org/10.1093/nar/gkp1137.

55. Collins, A.M. and Watson, C.T. (2018). Immunoglobulin light chain gene rearrangements, receptor editing and the development of a Self-Tolerant antibody repertoire. *Frontiers in Immunology*, 9. https://doi.org/10.3389/fimmu.2018.02249.

56. Costagliola, G., Cappelli, S. and Consolini, R. (2021). Autoimmunity in Primary Immunodeficiency Disorders: An Updated Review on Pathogenic and Clinical Implications. *Journal of Clinical Medicine*, 10(20), p.4729. doi:https://doi.org/10.3390/jcm10204729.

57. Cunningham-Rundles, C. (2012). The many faces of common variable immunodeficiency. *Hematology American Society Hematology Education Program*, 2012(1), pp. 301–305. https://doi.org/10.1182/asheducation.v2012.1.301.3798316.

58. Darce, J.R., Arendt, B.K., Wu, X. and Jelinek, D.F. (2007). Regulated Expression of BAFF-Binding Receptors during Human B Cell Differentiation. *The Journal of Immunology*, 179(11), pp.7276–7286. doi:https://doi.org/10.4049/jimmunol.179.11.7276.

59. Datta, M. and Jumaa, H. (2022). Immunoglobulin Gene Sequence as an Inherited and Acquired Risk Factor for Chronic Lymphocytic Leukemia. *Cancers*, [online] 14(13), pp.3045–3045. doi:https://doi.org/10.3390/cancers14133045.

60. Davydov, A.N., Obraztsova, A.S., Lebedin, M.Y., Turchaninova, M.A., Staroverov, D.B., Merzlyak, E.M., Sharonov, G.V., Kladova, O., Shugay, M., Britanova, O.V. and Chudakov, D.M. (2018). Comparative Analysis of B-Cell Receptor Repertoires Induced by Live Yellow Fever Vaccine in Young and Middle-Age Donors. *Frontiers in Immunology*, 9. doi:https://doi.org/10.3389/fimmu.2018.02309.

61. De la Torre, I., Moura, R.A., Leandro, M., Edwards, J. and Cambridge, G. (2010). B-cell-activating factor receptor expression on naive and memory B cells: relationship with relapse in patients with rheumatoid arthritis following B-cell depletion therapy. *Annals of the Rheumatic Diseases*, 69(12), pp.2181–2188. doi:https://doi.org/10.1136/ard.2010.131326.

62. De Silva, N.S. and Klein, U. (2015). Dynamics of B cells in germinal centres. *Nature Reviews Immunology*, [online] 15(3), pp.137–148. doi:https://doi.org/10.1038/nri3804.

63. De Sousa-Pereira, P. and Woof, J.M. (2019). IGA: Structure, Function, and Developability. *Antibodies*, 8(4), p. 57. https://doi.org/10.3390/antib8040057.

Deenick, E.K., Avery, D.T., Chan, A., Berglund, L.J., Ives, M.L., Moens, L., Stoddard, J.L., Bustamante, J., Boisson-Dupuis, S., Tsumura, M., Kobayashi, M., Arkwright, P.D., Averbuch, D., Engelhard, D., Roesler, J., Peake, J., Wong, M., Adelstein, S., Choo, S. and Smart, J.M. (2013). Naive and memory human B cells have distinct requirements for STAT3 activation to differentiate

into antibody-secreting plasma cells. *The Journal of Experimental Medicine*, 210(12), pp.2739–2753. doi:https://doi.org/10.1084/jem.20130323.

64. Del Pino Molina, Torres, M., O Pernía, Pena, R.R., Ibanez, I. and Granados, E.L. (2020). Defective Bcl-2 expression in memory B cells from common variable immunodeficiency patients. *Clinical & Experimental Immunology*, 203(3), pp.341–350. doi:https://doi.org/10.1111/cei.13522.

65. Demirdağ, Y.Y. and Gupta, S. (2021). Update on infections in primary antibody deficiencies. *Frontiers in Immunology*, 12. https://doi.org/10.3389/fimmu.2021.634181.

66. Dhalla, F., Lucas, M., Schuh, A., Bhole, M., Jain, R., Patel, S.Y., Misbah, S. and Chapel, H. (2014). Antibody Deficiency Secondary to Chronic Lymphocytic Leukemia: Should Patients be Treated with Prophylactic Replacement Immunoglobulin? *Journal of Clinical Immunology*, 34(3), pp.277–282. doi:https://doi.org/10.1007/s10875-014-9995-5.

67. Dienz, O. *et al.* (2009). The induction of antibody production by IL-6 is indirectly mediated by IL-21 produced by CD4+ T cells. *Journal of Experimental Medicine*, 206(1), pp. 69–78. https://doi.org/10.1084/jem.20081571.

68. DiLillo, D.J., Weinberg, J.B., Yoshizaki, A., Horikawa, M., Bryant, J.M., Iwata, Y., Matsushita, T., Matta, K.M., Chen, Y., Venturi, G.M., Russo, G., Gockerman, J.P., Moore, J.O., Diehl, L.F., Volkheimer, A.D., Friedman, D.R., Lanasa, M.C., Hall, R.P. and Tedder, T.F. (2012). Chronic lymphocytic leukemia and regulatory B cells share IL-10 competence and immunosuppressive function. *Leukemia*, [online] 27(1), pp.170–182. doi:https://doi.org/10.1038/leu.2012.165.

69. Dobin, A., Davis, C.A., Schlesinger, F., Drenkow, J., Zaleski, C., Jha, S., Batut, P., Chaisson, M. and Gingeras, T.R. (2012). STAR: ultrafast universal RNA-seq aligner. *Bioinformatics*, 29(1), pp.15–21. doi:https://doi.org/10.1093/bioinformatics/bts635.

70. Driessen, G.J., Zelm, van, Martin, Hartwig, N.G., Trip, M., Adilia Warris, Esther de Vries, Barendregt, B.H., Pico, I., Hop, W., Jacques and van (2011). B-cell replication history and somatic hypermutation status identify distinct pathophysiological backgrounds in common variable immunodeficiency. *Blood*, 118(26), pp.6814–6823. doi:https://doi.org/10.1182/blood-2011-06-361881.

71. Duraisingham, S.S., Buckland, M., Dempster, J., Lorenzo, L., Grigoriadou, S. and Longhurst, H.J. (2014). Primary vs. Secondary Antibody Deficiency: Clinical Features and Infection Outcomes of Immunoglobulin Replacement. *PLoS ONE*, 9(6), p.e100324. doi:https://doi.org/10.1371/journal.pone.0100324.
72. Durandy, A., Kracker, S. and Fischer, A. (2013). Primary antibody deficiencies. *Nature Reviews Immunology*, 13(7), pp. 519–533. https://doi.org/10.1038/nri3466.
73. Durandy, A., Peron, S., Taubenheim, N. and Fischer, A. (2006). Activation-induced cytidine deaminase: structure–function relationship as based on the study of mutants. *Human Mutation*, 27(12), pp.1185–1191. doi:https://doi.org/10.1002/humu.20414.
74. El Mashad, G., El Hady, S and Abdelnaby, S. (2017). *Immunoglobulin G and M levels in childhood nephrotic syndrome: two centers Egyptian study*. [online] Ephysician.ir. Available at: https://www.ephysician.ir/index.php/browse-issues/2017/2/588-3728 [Accessed 8 Oct. 2024].
75. Elgueta, R., Benson, M.J., de Vries, V.C., Wasiuk, A., Guo, Y. and Noelle, R.J. (2009). Molecular mechanism and function of CD40/CD40L engagement in the immune system. *Immunological Reviews*, [online] 229(1), pp.152–172. doi:https://doi.org/10.1111/j.1600-065x.2009.00782.x.
76. Ellyard, J.I., Avery, D.T., Phan, T.G., Hare, N.J., Hodgkin, P.D. and Tangye, S.G. (2004). Antigen-selected, immunoglobulin-secreting cells persist in human spleen and bone marrow. *Blood*, 103(10), pp.3805–3812. doi:https://doi.org/10.1182/blood-2003-09-3109.
77. EMA (2018). *Core summary of product characteristics for human normal intravenous adminstration (IVIg)- European Medicines Agency*. [online] European Medicines Agency. Available at: https://www.ema.europa.eu/en/core-summary-product-characteristics-human-normal-immunoglobulin-intravenous-administration-ivig-scientific-guideline [accessed 12 July 2022].
78. *European Society for Immunodeficiencies* (2024). Diseases and Genes [Database]. Available at https://esid.org/Working-Parties/Registry-Working-Party/ESID-Registry/List-of-diseases-and-genes (Accessed 4 April 2024).
79. Faliti, C.E., Van, T.T.P., Anam, F.A., Cheedarla, N., Williams, M.E., Mishra, A.K., Usman, S.Y., Woodruff, M.C., Kraker, G., Runnstrom, M.C., Kyu, S., Sanz, D., Ahmed, H., Ghimire, M., Morrison-Porter, A., Quehl, H., Haddad, N.S., Chen, W., Cheedarla, S and Neish, A.S (2024). Disease-associated B-

cells and immune endotypes shape adaptive immune responses to SARS-CoV-2 mRNA vaccination in human SLE. *Nature Immunology*. [online] doi:https://doi.org/10.1038/s41590-024-02010-9.

80. Fekrvand, S., Khanmohammadi, S., Abolhassani, H and Yazdani, R (2022). B- and T-Cell Subset Abnormalities in Monogenic Common Variable Immunodeficiency. *Frontiers in Immunology*, 13. doi:https://doi.org/10.3389/fimmu.2022.912826.

81. Fell, V.L. and Schild-Poulter, C. (2015). The Ku heterodimer: Function in DNA repair and beyond. *Mutation Research/Reviews in Mutation Research*, 763, pp. 15–29. https://doi.org/10.1016/j.mrrev.2014.06.002.

82. Fernandez, N.F., Gundersen, G.W., Rahman, A., Grimes, M.L., Rikova, K., Hornbeck, P. and Ma'ayan, A. (2017). Clustergrammer, a web-based heatmap visualization and analysis tool for high-dimensional biological data. *Scientific Data*, 4(1). doi:https://doi.org/10.1038/sdata.2017.151.

83. Fliegauf, M., Kruger, R., Steiner, S., Hanitsch, L., Buchel, S., Wahn, V., von Bernuth, H and Grimbacher, B (2021). A Pathogenic Missense Variant in *NFKB1* Causes Common Variable Immunodeficiency Due to Detrimental Protein Damage [online]. *Frontiers in Immunology*. **12.**

84. Forconi, F. and Moss, P. (2015). Perturbation of the normal immune system in patients with CLL. *Blood*, 126(5), pp. 573–581. https://doi.org/10.1182/blood-2015-03-567388.

85. Fraley, E.R., Santosh Khanal, Pierce, S., LeMaster, C., McLennan, R., Pastinen, T. and Bradley, T. (2022). Effects of Prior Infection with SARS-CoV-2 on B Cell Receptor Repertoire Response during Vaccination. *Vaccines*, [online] 10(9), pp.1477–1477. doi:https://doi.org/10.3390/vaccines10091477.

86. Frasca, D., Diaz, A., Romero, M. and Blomberg, B.B. (2016). The generation of memory B cells is maintained, but the antibody response is not, in the elderly after repeated influenza immunizations. *Vaccine*, 34(25), pp.2834–2840. doi:https://doi.org/10.1016/j.vaccine.2016.04.023.

87. Friedman, N., Shen-Orr, S. S., & Gaujoux, R. (2016). Defining B-cell immune fitness trajectories through high-throughput B-cell receptor sequencing. *PNAS*, 113(30), E4333-E4342.

88. Galson, J.D., Trück, J., Fowler, A., Clutterbuck, E.A., Münz, M., Cerundolo, V., Reinhard, C., van der Most, R., Pollard, A.J., Lunter, G. and Kelly, D.F. (2015). Analysis of B Cell Repertoire Dynamics Following Hepatitis B Vaccination in Humans, and Enrichment of Vaccine-specific Antibody Sequences. *EBioMedicine*, 2(12), pp.2070–2079. doi:https://doi.org/10.1016/j.ebiom.2015.11.034.

89. Gallego Romero, I., Pai, A.A., Tung, J. and Gilad, Y. (2014). RNA-seq: impact of RNA degradation on transcript quantification. *BMC Biology*, 12(1), p.42. doi:https://doi.org/10.1186/1741-7007-12-42.

90. García-Muñoz, R., Roldan Galiacho, V. and Llorente, L. (2012). Immunological aspects in chronic lymphocytic leukemia (CLL)

development. *Annals of Hematology*, 91(7), pp.981–996. doi:https://doi.org/10.1007/s00277-012-1460-z.

91. Geisberger, R., Lamers, M.C. and Achatz, G. (2006). The riddle of the dual expression of IgM and IgD. *Immunology*, 118(4), pp. 429–437. https://doi.org/10.1111/j.1365-2567.2006.02386.x.

92. Gereige, J. and Maglione, P.J. (2019). Current understanding and recent developments in common variable immunodeficiency associated autoimmunity. *Frontiers in Immunology*, 10. https://doi.org/10.3389/fimmu.2019.02753.

93. Ghia, E.M., Jain, S., Widhopf, G.F., Rassenti, L.Z., Keating, M.J., Wierda, W.G., Gribben, J.G., Brown, J.R., Rai, K.R., Byrd, J.C., Kay, N.E., Greaves, A.W. and Kipps, T.J. (2008). Use of IGHV3–21 in chronic lymphocytic leukemia is associated with high-risk disease and reflects antigen-driven, post–germinal center leukemogenic selection. *Blood*, 111(10), pp.5101–5108. doi:https://doi.org/10.1182/blood-2007-12-130229.

94. Ghraichy, M., Galson, J.D., Kelly, D.F. and Johannes Trück (2018). B-cell receptor repertoire sequencing in patients with primary immunodeficiency: a review. 153(2), pp.145–160. doi:https://doi.org/10.1111/imm.12865.

95. Gilmore, T.D. and Gerondakis, S. (2011). The c-Rel Transcription Factor in Development and Disease. *Genes & Cancer*, 2(7), pp.695–711. doi:https://doi.org/10.1177/1947601911421925.

96. Good, K.L. and Tangye, S.G. (2007). Decreased expression of Kruppel-like factors in memory B cells induces the rapid response typical of secondary antibody responses. *Proceedings of the National Academy of Sciences of the United States of America*, [online] 104(33), pp.13420–5. doi:https://doi.org/10.1073/pnas.0703872104.

97. Good, K.L., Avery, D.T. and Tangye, S.G. (2009). Resting Human Memory B Cells Are Intrinsically Programmed for Enhanced Survival and Responsiveness to Diverse Stimuli Compared to Naive B Cells. *Journal of Immunology*, [online] 182(2), pp.890–901. doi:https://doi.org/10.4049/jimmunol.182.2.890.

98. Graham, T.G.W., Walter, J.C. and Loparo, J.J. (2016). Two-Stage Synapsis of DNA Ends during Non-homologous End Joining. *Molecular Cell*, 61(6), pp. 850–858. https://doi.org/10.1016/j.molcel.2016.02.010.

99. Greiff, V., Menzel, U., Miho, E., Weber, C., Riedel, R., Cook, S., Valai, A., Lopes, T., Radbruch, A., Winkler, T.H. and Reddy, S.T. (2017). Systems Analysis Reveals High Genetic and Antigen-Driven Predetermination of Antibody Repertoires throughout B Cell Development. *Cell Reports*, [online] 19(7), pp.1467–1478. doi:https://doi.org/10.1016/j.celrep.2017.04.054

100. Griffiths, H., Brennan, V., Lea, J., Bunch, C., Lee, M. and Chapel, H. (1989). Crossover study of immunoglobulin replacement therapy in patients with low-grade B-cell tumors. *Blood*, 73(2), pp.366–368. doi:https://doi.org/10.1182/blood.v73.2.366.366.

101. Guldenpfennig, C., Teixeiro, E. and Daniels, M. (2023). NF-κB ’s contribution to B cell fate decisions. *Frontiers in immunology*, 14. doi:https://doi.org/10.3389/fimmu.2023.1214095.

102. Gutzeit, C., Chen, K. and Cerutti, A. (2018). The enigmatic function of IgD: some answers at last. *European Journal of Immunology*, 48(7), pp. 1101–1113. https://doi.org/10.1002/eji.201646547.

103. Hamblin, A. and Hamblin, T.J. (2008). The immunodeficiency of chronic lymphocytic leukaemia. *British Medical Bulletin*, 87(1), pp. 49–62. https://doi.org/10.1093/bmb/ldn034.

104. Harriman, G.R., Kunimoto, D.Y., Elliott, J.F., Paetkau, V. and Strober, W. (1988). The role of IL-5 in IgA B cell differentiation. *Journal of Immunology (Baltimore, Md.: 1950)*, [online] 140(9), pp.3033–3039. Available at: https://pubmed.ncbi.nlm.nih.gov/3258891/.

105. Hedrich, C.M. and Tsokos, G.C. (2011). Epigenetic mechanisms in systemic lupus erythematosus and other autoimmune diseases. *Trends in Molecular Medicine*, 17(12), pp.714–724. doi:https://doi.org/10.1016/j.molmed.2011.07.005.

106. Hernandez, N., Bucciol, G., Moens, L., Le Pen, J., Shahrooei, M., Goudouris, E., Shirkani, A., Changi-Ashtiani, M., Rokni-Zadeh, H., Sayar, E.H., Reisli, I., Lefevre-Utile, A., Zijlmans, D., Jurado, A., Pholien, R., Drutman, S., Belkaya, S., Cobat, A., Boudewijns, R. and Jochmans, D. (2019). Inherited IFNAR1 deficiency in otherwise healthy patients with adverse reaction to measles and yellow fever live vaccines. *Journal of Experimental Medicine*, 216(9), pp.2057–2070. doi:https://doi.org/10.1084/jem.20182295.

107. Herriot, R. and Sewell, W.A. (2008). Antibody deficiency. *Journal of Clinical Pathology*, 61(9), pp. 994–1000. https://doi.org/10.1136/jcp.2007.051177.

108. Hershberg, U. and Luning Prak, E.T. (2015). The analysis of clonal expansions in normal and autoimmune B cell repertoires. *Philosophical Transactions of the Royal Society B: Biological Sciences*, 370(1676), p.20140239. doi:https://doi.org/10.1098/rstb.2014.0239.

109. Heyne, H.O., Karjalainen, J., Karczewski, K.J., Lemmelä, S.M., Zhou, W., Havulinna, A.S., Kurki, M., Rehm, H.L., Palotie, A. and Daly, M.J. (2023). Mono- and biallelic variant effects on disease at biobank scale. *Nature*,

613(7944), pp.519–525. doi:https://doi.org/10.1038/s41586-022-05420-7.

110. Hirokawa, M., Fujishima, N., Togashi, M., Saga, A., Omokawa, A., Saga, T., Moritoki, Y., Ueki, S., Takahashi, N., Kitaura, K. and Suzuki, R. (2019). High-throughput sequencing of IgG B-cell receptors reveals frequent usage of the rearranged IGHV4–28/IGHJ4 gene in primary immune thrombocytopenia. *Scientific Reports*, 9(1). doi:https://doi.org/10.1038/s41598-019-45264-2.

111. Honjo, T., Kinoshita, K. and Muramatsu, M. (2002). Molecular Mechanism of Class Switch Recombination: Linkage with Somatic Hypermutation. *Annual Review of Immunology*, 20(1), pp. 165–196. https://doi.org/10.1146/annurev.immunol.20.090501.112049.

112. Hopp, R.J. and Niebur, H.B. (2022). Persistent Hyper IgA as a Marker of Immune Deficiency: A Case Report. *Antibodies*, 11(2), p.30. doi:https://doi.org/10.3390/antib11020030.

113. Horikawa, K., Martin, S.W., Pogue, S.L., Silver, K., Peng, K., Kiyoshi Takatsu and Goodnow, C.C. (2007). Enhancement and suppression of signaling by the conserved tail of IgG memory–type B cell antigen receptors. *The Journal of experimental medicine*, 204(4), pp.759–769. doi:https://doi.org/10.1084/jem.20061923.

114. Huang, D.W., Sherman, B.T. and Lempicki, R.A. (2009). Bioinformatics enrichment tools: paths toward the comprehensive functional analysis of large gene lists. Nucleic Acids Research, 37 (1), pp. 1-13. doi:https://doi.org/10.1093/nar/gkn923.Ijspeert H, Van Schouwenburg PA, Van Zessen D, Pico-Knijnenburg I, Driessen GJ, Stubbs AP, et al. Evaluation of the antigen-experienced B-cell receptor repertoire in healthy children and adults. Front Immunol. (2016) 7:410. 10.3389/fimmu.2016.00410

115. IJspeert, H., van Schouwenburg, P.A., van Zessen, D., Pico-Knijnenburg, I., Stubbs, A.P. and van der Burg, M. (2017). Antigen Receptor Galaxy: A User-Friendly, Web-Based Tool for Analysis and Visualization of T and B Cell Receptor Repertoire Data. *The Journal of Immunology*, 198(10), pp.4156–4165. doi:https://doi.org/10.4049/jimmunol.1601921.

116. Immunodeficiency UK (2023) *COVID-19 research update - Immunodeficiency UK*. https://www.immunodeficiencyuk.org/resources/research/covid19researchupdate/.

117. Inoue, M., Uchida, Y., Makoto Edagawa, Hirata, M., Jun Mitamura, Miyamoto, D., Kenji Taketani, Sekine, S., Junya Kawauchi and Kitajima, S. (2018). The stress response gene ATF3 is a direct target of the Wnt/β-catenin pathway and inhibits the invasion and migration of HCT116 human colorectal cancer cells. *PloS one*, 13(7), pp.e0194160–e0194160. doi:https://doi.org/10.1371/journal.pone.0194160.

118. Inoue, R., Kondo, N., Kobayashi, Y., Fukutomi, O. and Orii, T. (1995). IgG2 deficiency associated with defects in production of interferon-gamma; comparison with common variable immunodeficiency. *Scandinavian journal of immunology*, [online] 41(2), pp.130–4. doi:https://doi.org/10.1111/j.1365-3083.1995.tb03544.x.

119. Jacobs, H.M., Thouvenel, C.D., Leach, S., Tanvi Arkatkar, Metzler, G., Scharping, N.E., Kolhatkar, N.S., Rawlings, D.J. and Jackson, S.W. (2016). Cutting Edge: BAFF Promotes Autoantibody Production via TACI-Dependent Activation of Transitional B Cells. *The Journal of Immunology*, [online] 196(9), pp.3525–3531. doi:https://doi.org/10.4049/jimmunol.1600017.x

120. Jacobson, R.M., Ovsyannikova, I.G., Vierkant, R.A., Pankratz, V.S. and Poland, G.A. (2011). Human leukocyte antigen associations with humoral and cellular immunity following a second dose of measles-containing vaccine: persistence, dampening, and extinction of associations found after a first dose. *Vaccine*, [online] 29(45), pp.7982–91. doi:https://doi.org/10.1016/j.vaccine.2011.08.060.

121. Jak, M., Mous, R., Remmerswaal, E.B.M., Spijker, R., Jaspers, A., Yagüe, A., Eldering, E., Van Lier, R.A.W. and Van Oers, M.H.J. (2009). Enhanced formation and survival of CD4+ CD25hi Foxp3+ T-cells in chronic lymphocytic leukemia. *Leukemia & lymphoma*, [online] 50(5), pp.788–801. doi:https://doi.org/10.1080/10428190902803677.

122. Jeurissen, A., Ceuppens, J.L. and Bossuyt, X. (2004). T lymphocyte dependence of the antibody response to 'T lymphocyte independent type 2' antigens. *Immunology*, 111(1), pp. 1–7. https://doi.org/10.1111/j.1365-2567.2004.01775.x.

123. Jolles, S., Chapel, H. and Litzman, J. (2017). When to initiate immunoglobulin replacement therapy (IGRT) in antibody deficiency: a practical approach. *Clinical and Experimental Immunology*, 188(3), pp. 333–341. https://doi.org/10.1111/cei.12915.

124. Jolles, S., Mauricette Michallet, Agostini, C., Albert, M.H., Edgar, Ria, R., Livio Trentin and Lévy, V. (2021). Treating secondary antibody deficiency in patients with haematological malignancy: European expert consensus. *European Journal of Haematology*, 106(4), pp.439–449. doi:https://doi.org/10.1111/ejh.13580.

125. Jurlander, J., Geisler, C.H. and Hansen, M. (1994). Treatment of hypogammaglobulinemia in chronic lymphocytic leukaemia by low-dose intravenous gammaglobulin. *European Journal of Haematology*, 53(2), pp. 114–118. https://doi.org/10.1111/j.1600-0609.1994.tb01874.x.

126. Kaplinsky, J., Li, A., Sun, A., Coffre, M., Koralov, S.B. and Arnaout, R. (2014). Antibody repertoire deep sequencing reveals antigen-independent

selection in maturing B cells. *Proceedings of the National Academy of Sciences*, 111(25). doi:https://doi.org/10.1073/pnas.1403278111.

127. Kawano, Y., Fujiwara, S., Wada, N., Izaki, M., Yuki, H., Okuno, Y., Iyama, K., Yamasaki, H., Sakai, A., Mitsuya, H. and Hata, H. (2012). Multiple myeloma cells expressing low levels of CD138 have an immature phenotype and reduced sensitivity to lenalidomide. *International Journal of Oncology*, [online] 41(3), pp.876–884. doi:https://doi.org/10.3892/ijo.2012.1545.

128. Kawasaki, T. and Kawai, T. (2014). Toll-Like Receptor Signaling Pathways,' *Frontiers in Immunology*, 5. https://doi.org/10.3389/fimmu.2014.00461.

129. Khan, W.N. (2009). B Cell Receptor and BAFF Receptor Signaling Regulation of B Cell Homeostasis. *The Journal of Immunology*, 183(6), pp.3561–3567. doi:https://doi.org/10.4049/jimmunol.0800933.

130. Khatri, P., Sirota, M. and Butte, A.J. (2012). Ten Years of Pathway Analysis: Current Approaches and Outstanding Challenges. *PLoS. Computational Biology*, [online] 8(2), p.e1002375. doi:https://doi.org/10.1371/journal.pcbi.1002375.

131. King, H.W., Orban, N., Riches, J.C., Clear, A.J., Warnes, G., Teichmann, S.A. and James, L.K. (2021). Single-cell analysis of human B cell maturation predicts how antibody class switching shapes selection dynamics. *Science Immunology*, [online] 6(56). doi:https://doi.org/10.1126/sciimmunol.abe6291.

132. Klein, U. and R. Dalla-Favera (2005). New Insights into the Phenotype and Cell Derivation of B Cell Chronic Lymphocytic Leukemia. *Springer eBooks*, pp.31–49. doi:https://doi.org/10.1007/3-540-29933-5_3.

133. Klein, U., Tu, Y., Stolovitzky, G.A., Mattioli, M., Cattoretti, G., HussonH., Freedman, A., Inghirami, G., Cro, L., Baldini, L., Neri, A., Califano, A. and Dalla-Favera, R. (2001). Gene Expression Profiling of B Cell Chronic Lymphocytic Leukemia Reveals a Homogeneous Phenotype Related to Memory B Cells. *Journal of Experimental Medicine*, 194(11), pp.1625–1638. doi:https://doi.org/10.1084/jem.194.11.1625.

134. Kohn, L.A. and Kohn, D.B. (2021). Gene therapies for primary immune deficiencies. *Frontiers in Immunology*, 12. https://doi.org/10.3389/fimmu.2021.648951.

135. Kotagiri, P., Mescia, F., Rae, W.M., Bergamaschi, L., Tuong, Z.K., Turner, L., Hunter, K., Gerber, P.P., Hosmillo, M., Hess, C., Clatworthy, M.R., Goodfellow, I.G., Matheson, N.J., McKinney, E.F., Wills, M.R., Gupta, R.K., Bradley, J.R., Bashford-Rogers, R.J.M., Lyons, P.A. and Smith, K.G.C. (2022). B cell receptor repertoire kinetics after SARS-CoV-2 infection and vaccination. *Cell Reports*, [online] 38(7), p.110393. doi:https://doi.org/10.1016/j.celrep.2022.110393.

136. Kreuzaler, M., Rauch, M., Salzer, U., Birmelin, J., Rizzi, M., Grimbacher, B., Plebani, A., Lougaris, V., Quinti, I., Thon, V., Litzman, J., Schlesier, M., Warnatz, K., Thiel, J., Rolink, A.G. and Eibel, H. (2012). Soluble

BAFF levels inversely correlate with peripheral B cell numbers and the expression of BAFF receptors. *Journal of Immunology (Baltimore, Md.: 1950)*, [online] 188(1), pp.497–503. doi:https://doi.org/10.4049/jimmunol.1102321.

137. Kular, D., Chis Ster, I., Sarnowski, A., Lioudaki, E., Braide-Azikiwe, D.C.B., Ford, M.L., Makanjuola, D., Rankin, A., Cairns, H., Popoola, J., Cole, N., Phanish, M., Hull, R., Swift, P.A. and Banerjee, D. (2020). The Characteristics, Dynamics, and the Risk of Death in COVID-19 Positive Dialysis Patients in London, UK. *Kidney360*, [online] 1(11), pp.1226–1243. doi:https://doi.org/10.34067/KID.0004502020.

138. Kuraoka, M., T. Matt Holl, Liao, D., Womble, M., Cain, D.W., Reynolds, A.E. and Kelsoe, G. (2011). Activation-induced cytidine deaminase mediates central tolerance in B cells. *Proceedings of the National Academy of Sciences of the United States of America*, 108(28), pp.11560–11565. doi:https://doi.org/10.1073/pnas.1102571108.

139. Laserson, U., Vigneault, F., Gadala-Maria, D., Yaari, G., Uduman, M., Heiden, J.A.V., Kelton, W., Jung, S.T., Liu, Y., Laserson, J., Chari, R., Lee, J.-H., Bachelet, I., Hickey, B., Lieberman-Aiden, E., Hanczaruk, B., Simen, B.B., Egholm, M., Koller, D. and Georgiou, G. (2014). High-resolution antibody dynamics of vaccine-induced immune responses. *Proceedings of the National Academy of Sciences*, [online] 111(13), pp.4928–4933. doi:https://doi.org/10.1073/pnas.1323862111.

140. Lau, A.W.Y., Turner, V.M., Bourne, K., Hermes, J.R., Chan, T.D. and Brink, R. (2020). BAFFR controls early memory B cell responses but is dispensable for germinal center function. *Journal of Experimental Medicine*, 218(2). doi:https://doi.org/10.1084/jem.20191167.

141. LeBien, T.W. and Tedder, T.F. (2008). B lymphocytes: how they develop and function. *Blood*, 112(5), pp. 1570–1580. https://doi.org/10.1182/blood- 2008-02-078071.

142. Lee, H.C. (2006). Structure and enzymatic functions of human CD38. *Molecular Medicine*, 12(11–12), pp. 317–323. https://doi.org/10.2119/2006-00086.lee.

143. Legendre, P., Chahwan, D., Marjanovic, Z., Vignon, M., Hermine, O., Lortholary, O., Morelle, G., Darrodes, M., Kahn, J.-E., Ouzegdouh, M., Chaibi, P., Montestruc, F., Caumont-Prim, A., Le Jouan, M., Hassani, Y., Godeau, B., Durand-Zaleski, I. and Mouthon, L. (2020). Utilization of intravenous or subcutaneous immunoglobulins in secondary immune deficiency (ULTIMATE): A retrospective multicenter study. *Clinical immunology (Orlando, Fla.)*, [online] 215, p.108419. doi:https://doi.org/10.1016/j.clim.2020.108419.

144. Le pottier, L., Bendaoud, B., Dueymes, M., Daridon, C., Youinou, P., Shoenfeld, Y. and Pers, J. (2007). BAFF, a New Target for Intravenous

Immunoglobulin in Autoimmunity and Cancer. *Journal of Clinical Immunology*, 27(3), pp.257–265. doi:https://doi.org/10.1007/s10875-007-9082-2.

145. Li, J., Zhang, Y., Yang, C. and Rong, R. (2020). Discrepant mRNA and Protein Expression in Immune Cells. [online] 21(8), pp.560–563. doi:https://doi.org/10.2174/1389202921999200716103758.

146. Li, X.-Y., Corvino, D., Nowlan, B., Aguilera, A.R., Ng, S.S., Braun, M., Cillo, A.R., Bald, T., Smyth, M.J. and Engwerda, C.R. (2022). NKG7 Is Required for Optimal Antitumor T-cell Immunity. *Cancer Immunology Research*, [online] 10(2), pp.154–161. doi:https://doi.org/10.1158/2326- 6066.CIR-20-0649.

147. Liao, Y., Smyth, G.K. and Shi, W. (2013). featureCounts: an efficient general purpose program for assigning sequence reads to genomic features. *Bioinformatics*, 30(7), pp.923–930. doi:https://doi.org/10.1093/bioinformatics/btt656.

148. Lightman, S.M., Utley, A. and Lee, K.P. (2019). Survival of Long-Lived Plasma Cells (LLPC): Piecing Together the Puzzle. *Frontiers in Immunology*, 10. doi:https://doi.org/10.3389/fimmu.2019.00965.

149. Lindquist, R.L., Raluca Niesner and Hauser, A.E. (2019). In the Right Place, at the Right Time: Spatiotemporal Conditions Determining Plasma Cell Survival and Function. *Frontiers in Immunology*, 10. doi:https://doi.org/10.3389/fimmu.2019.00788.

150. Liu, Y., Barthélémy, C., Odette de Bouteiller, Arpin, C., Durand, I. and Banchereau, J. (1995). Memory B cells from human tonsils colonize mucosal epithelium and directly present antigen to T cells by Rapid Up-Regulation of B7-1 and B7-2. *Immunity*, 2(3), pp.239–248. doi:https://doi.org/10.1016/1074-7613(95)90048-9.

151. Liu, Z., Liang, Q., Ren, Y., Guo, C., Ge, X., Wang, L., Cheng, Q., Luo, P., Zhang, Y. and Han, X. (2023). Immunosenescence: molecular mechanisms and diseases. *Signal Transduction and Targeted Therapy*, [online] 8(1), pp.1–16. doi:https://doi.org/10.1038/s41392-023-01451-2.

152. Lopes de Assis, F., Hoehn, K.B., Zhang, X., Kardava, L., Smith, C.D., Omar El Merhebi, Buckner, C.M., Krittin Trihemasava, Wang, W., Seamon, C.A., Chen, V., Schaughency, P., Cheung, F., Martins, A.J., Chiang, C.-I., Li, Y., Tsang, J.S., Chun, T.-W., Kleinstein, S.H. and Moir, S. (2023). Tracking B cell responses to the SARS-CoV-2 mRNA-1273 vaccine. 42(7), pp.112780– 112780. doi:https://doi.org/10.1016/j.celrep.2023.112780.

153. Love, M.I., Huber, W. and Anders, S. (2014). Moderated estimation of fold change and dispersion for RNA-seq data with DESeq2. *Genome Biology*, 15(12), p.550.

154. Lunderberg, J. M., Dutta, S., Collier, A.-R. Y., Lee, J.-S., Hsu, Y.-M., Wang, Q., Zheng, W., Hao, S., Zhang, H., Feng, L., Robson, S. C., Gao, W., & Riedel, S. (2022). Pan-neutralizing, germline-encoded antibodies against SARS-CoV-2: Addressing the long-term problem of escape variants. *Frontiers in Immunology*, 13, 1032574. https://doi.org/10.3389/fimmu.2022.1032574

155. Lye, J.J., Williams, A. and Baralle, D. (2019). Exploring the RNA Gap for Improving Diagnostic Yield in Primary Immunodeficiencies. *Frontiers in Genetics*, 10. doi:https://doi.org/10.3389/fgene.2019.01204.

156. Macalla, D., Wallace, D., Zhang, Y., Ghattas, H., Asquith, B., de Larda, C., Worth, A., Panayiotakopoulos, G., Griggin, G., Tough, D and Beverley, P (2005). B-cell kinetics in humans: rapid turnover of peripheral blood memory cells. *Blood*, 105(9), pp.3633–3640. doi:https://doi.org/10.1182/blood-2004-09-3740.

157. Mackay, F. and Browning, J.L. (2002). BAFF: a fundamental survival factor for B cells. *Nature reviews. Immunology*, [online] 2(7), pp.465–75. doi:https://doi.org/10.1038/nri844.

158. Mackay, F. and Schneider, P. (2009). Cracking the BAFF code. *Nature Reviews Immunology*, 9(7), pp.491–502. doi:https://doi.org/10.1038/nri2572.

159. Mackay, F., Huston, W.M., Lawton, P., Ambrose, C., Manfred Baetscher, Schneider, P., Tschopp, J. and Browning, J.L. (1999). Mice Transgenic for Baff Develop Lymphocytic Disorders along with Autoimmune Manifestations. *Journal of Experimental Medicine*, 190(11), pp.1697–1710. doi:https://doi.org/10.1084/jem.190.11.1697.

160. Mackay, F., Schneider, P., Rennert, P.D. and Browning, J.L. (2003). BAFF and APRIL: A Tutorial on B Cell Survival. *Annual Review of Immunology*, 21(1), pp.231–264. doi:https://doi.org/10.1146/annurev.immunol.21.120601.141152.

161. Maglione, P.J., Gyimesi, G., Cols, M., Radigan, L., Ko, H.M., Weinberger, T., Lee, B.H., Grasset, E.K., Rahman, A.H., Cerutti, A. and Cunningham-Rundles, C. (2019). BAFF-driven B cell hyperplasia underlies lung disease in common variable immunodeficiency. *JCI Insight*, 4(5). doi:https://doi.org/10.1172/jci.insight.122728.

162. Mallick, R., Divino, V., Smith, B.D., Jolles, S., DeKoven, M. and Vinh, D.C. (2021). Infections in secondary immunodeficiency patients treated with Privigen®or Hizentra®: a retrospective US administrative claims study in patients with hematological malignancies. *Leukemia & lymphoma/Leukemia and lymphoma*, 62(14), pp.3463–3473. doi:https://doi.org/10.1080/10428194.2021.1961233.

163. Malvey, E.-N., Jenkins, M.K. and Mueller, D.L. (1998). Peripheral Immune Tolerance Blocks Clonal Expansion but Fails to Prevent the Differentiation of Th1 Cells. *The Journal of Immunology*, 161(5), pp.2168–2177. doi:https://doi.org/10.4049/jimmunol.161.5.2168.

164. Marshall, J.S., Warrington, R., Watson, W. and Kim, H.L. (2018). An

Introduction to Immunology and Immunopathology. *Allergy, Asthma & Clinical Immunology*, 14(S2). doi:https://doi.org/10.1186/s13223-018-0278-1.

165. Marsman, C., Verhoeven, D., Koers, J., Rispens, T., Anja ten Brinke, Ham, van and Kuijpers, T.W. (2022). Optimized Protocols for In-Vitro T-Cell-Dependent and T-Cell-Independent Activation for B-Cell Differentiation Studies Using Limited Cells. *Frontiers in Immunology*, 13. doi:https://doi.org/10.3389/fimmu.2022.815449.

166. Martin, M. (2011). Cutadapt removes adapter sequences from high-throughput sequencing reads. *EMBnet.journal*, [online] 17(1), p.10. doi:https://doi.org/10.14806/ej.17.1.200.

167. Martínez-Cano, J., Campos-Sánchez, E. and Cobaleda, C. (2019). Epigenetic Priming in Immunodeficiencies. *Frontiers in Cell and Developmental Biology*, 7. doi:https://doi.org/10.3389/fcell.2019.00125.

168. Matharu, K., Zarember, K.A., Marciano, B.E., Kuhns, D.B., Spalding, C., Garofalo, M., Dimaggio, T., Estwick, T., Huang, C.-Y., Fink, D., Priel, D.L., Fleisher, T.A., Holland, S.M., Malech, H.L. and Gallin, J.I. (2013). B-Cell Activating Factor (BAFF) is elevated in Chronic Granulomatous Disease. *Clinical immunology (Orlando, Fla.)*, [online] 148(2), p.258. doi:https://doi.org/10.1016/j.clim.2013.05.007.

169. McCarron, M.J., Park, P.W. and Fooksman, D.R. (2017). CD138 mediates selection of mature plasma cells by regulating their survival. *Blood*, 129(20), pp. 2749–2759. https://doi.org/10.1182/blood-2017-01-761643.

170. Meyts, I., Bousfiha, A., Duff, C., Singh, S., Lau, Y.L., Condino-Neto, A., Bezrodnik, L., Ali, A., Adeli, M. and Drabwell, J. (2020). Primary Immunodeficiencies: A Decade of Progress and a Promising Future. *Frontiers in Immunology*, [online] 11, p.625753. doi:https://doi.org/10.3389/fimmu.2020.625753.

171. Mihalcik, S.A., Tschumper, R.C. and Jelinek, D.F. (2010). Transcriptional and post-transcriptional mechanisms of BAFF-receptor dysregulation in human B lineage malignancies . *Cell Cycle*, 9(24), pp.4884–4892. doi:https://doi.org/10.4161/cc.9.24.14156.

172. Milito, C., Pulvirenti, F., Cinetto, F., Vassilios Lougaris, Annarosa Soresina, Pecoraro, A., Vultaggio, A., Carrabba, M., Lassandro, G., Alessandro Plebani, Spadaro, G., Matucci, A., Fabio, G., Rosa Maria Dellepiane, Martire, B., Agostini, C., Damiano Abeni, Stefano Tabolli and Quinti, I. (2019). Double-blind, placebo-controlled, randomized trial on low-dose azithromycin prophylaxis in patients with primary antibody deficiencies. *The Journal of Allergy and Clinical Immunology*, 144(2), pp.584-593.e7. doi:https://doi.org/10.1016/j.jaci.2019.01.051.

173. Milota, T., Smetanova, J. and Bartunkova, J. (2023). Clinical Outcome of Coronavirus Disease 2019 in patients with primary antibody

deficiencies. *Pathogens*, 12(1).

174. Minnich, M., Tagoh, H., Bönelt, P., Axelsson, E., Fischer, M., Cebolla, B., Tarakhovsky, A., Nutt, S.L., Jaritz, M. and Busslinger, M. (2016). Multifunctional role of the transcription factor Blimp-1 in coordinating plasma cell differentiation. *Nature Immunology*, 17(3), pp.331–343. doi:https://doi.org/10.1038/ni.3349.

175. Moens, L., Kane, A. and Tangye, S.G. (2016). Naïve and memory B cells exhibit distinct biochemical responses following BCR engagement. *Immunology and Cell Biology*, 94(8), pp.774–786. doi:https://doi.org/10.1038/icb.2016.41.

176. Molica, S., Musto, P., Chiurazzi, F., Specchia, G., Brugiatelli, M., Cicoira, L., Levato, D., Nobile, F., Carotenuto, M., Liso, V. and Rotoli, B. (1996). Prophylaxis against infections with low-dose intravenous immunoglobulins (IVIG) in chronic lymphocytic leukemia. Results of a crossover study. *Haematologica*, [online] 81(2), pp.121–6. Available at: https://pubmed.ncbi.nlm.nih.gov/8641639/.

177. Muramatsu, M., Kinoshita, K., Fagarasan, S., Yamada, S., Shinkai, Y. and Honjo, T. (2000). Class switch recombination and hypermutation require activation-induced cytidine deaminase (AID), a potential RNA editing enzyme. *Cell*, [online] 102(5), pp.553–563. doi:https://doi.org/10.1016/s0092-8674(00)00078-7.

178. Murphy, K.M., Weaver, C. and Janeway, C. (2017) *Janeway's immunobiology: Ninth International Student Edition*. 9th edn. Garland Science.

179. Murray, P.D., McKenzie, D.T., Swain, S.L. and Kagnoff, M.F. (1987). Interleukin 5 and interleukin 4 produced by Peyer's patch T cells selectively enhance immunoglobulin A expression. *Journal of immunology (Baltimore, Md. : 1950)*, [online] 139(8), pp.2669–74. Available at: https://pubmed.ncbi.nlm.nih.gov/3498768/.

180. Na, I K., Buckland, M., Agostini, C., David, J., Friman, V., Mauricette Michallet, Sánchez-Ramón, S., Scheibenbogen, C. and Quinti, I. (2019). Current clinical practice and challenges in the management of secondary immunodeficiency in hematological malignancies. *European Journal of Haematology*, 102(6), pp.447–456. doi:https://doi.org/10.1111/ejh.13223.

187. Newman, R (2021). B cells. https://www.immunology.org/public-information/bitesized-immunology/cells/b-cells (Accessed: May 28, 2024).

188. Nguyen, T.V., Pawlikowska, P., Firlej, V., Rosselli, F. and Aoufouchi, S. (2016). V(D)J recombination process and the Pre-B to immature B-cells transition are altered in Fanca −/− mice. *Scientific Reports*, [online] 6(1), pp.1–11. doi:https://doi.org/10.1038/srep36906.

181. Nutt, S.L., Heavey, B., Rolink, A.G. and Busslinger, M. (1999). Commitment to the B-lymphoid lineage depends on the transcription factor Pax5. *Nature*, 402(6763supp), pp.14–20. doi:https://doi.org/10.1038/35005514.

182. Nutt, S.L., Hodgkin, P.D., Tarlinton, D.M. and Corcoran, L.M. (2015). The generation of antibody-secreting plasma cells. *Nature Reviews Immunology*, 15(3), pp.160–171. doi:https://doi.org/10.1038/nri3795.

183. Nutt, S.L., Taubenheim, N., Hasbold, J., Corcoran, L.M. and Hodgkin, P.D. (2011). The genetic network controlling plasma cell differentiation. *Seminars in Immunology*, 23(5), pp.341–349. doi:https://doi.org/10.1016/j.smim.2011.08.010.

184. Ochiai, K., Maienschein-Cline, M., Simonetti, G., Chen, J., Rosenthal, R., Brink, R., Chong, A.S., Klein, U., Dinner, A.R., Singh, H. and Sciammas, R. (2013). Transcriptional Regulation of Germinal Center B and Plasma Cell Fates by Dynamical Control of IRF4. *Immunity*, [online] 38(5), pp.918–929. doi:https://doi.org/10.1016/j.immuni.2013.04.009.

185. Oettinger, M., Schatz, D., Gorka, C. and Baltimore, D. (1990). RAG-1 and RAG-2, adjacent genes that synergistically activate V(D)J recombination. *Science*, 248(4962), pp.1517–1523. doi:https://doi.org/10.1126/science.2360047.

186. Ono, M., Bolland, S., Tempst, P. and Ravetch, J.V. (1996). Role of the inositol phosphatase SHIP in negative regulation of the immune system by the receptor FeγRIIB. 383(6597), pp.263–266. doi:https://doi.org/10.1038/383263a0.

187. Ovsyannikova, I.G., Pankratz, V.S., Larrabee, B.R., Jacobson, R.M. and Poland, G.A. (2014). HLA genotypes and rubella vaccine immune response: Additional evidence. *Vaccine*, 32(33), pp.4206–4213. doi:https://doi.org/10.1016/j.vaccine.2014.04.091.

188. Oxford University Hospitals NHS Trust (no date) *Immunoglobulins - Immunology laboratory*. https://www.ouh.nhs.uk/immunology/diagnostic-tests/tests-catalogue/immunoglobulins.aspx#:~:text=Reference%20range%2Funits,IgM%200.4%20%2D%202.5g%2FL (Accessed: March 31, 2024).

189. Pabst, O. (2012). New concepts in the generation and functions of IgA. *Nature Reviews Immunology*, 12(12), pp.821–832. doi:https://doi.org/10.1038/nri3322.

190. Pabst, O. and Slack, E. (2019). IgA and the intestinal microbiota: the importance of being specific. *Mucosal Immunology*, 13(1), pp.12–21. doi:https://doi.org/10.1038/s41385-019-0227-4.

191. Pallikkuth, S., Kanthikeel, S.P., Silva, S.Y., Fischl, M., Pahwa, R. and

Pahwa, S. (2011). Innate immune defects correlate with failure of antibody responses to H1N1/09 vaccine in HIV-infected patients. *Journal of Allergy and Clinical Immunology*, 128(6), pp.1279–1285. doi:https://doi.org/10.1016/j.jaci.2011.05.033.

192. Pang, N.Y.-L., Pang, A.S.-R., Chow, V.T. and Wang, D.-Y. (2021). Understanding neutralising antibodies against SARS-CoV-2 and their implications in clinical practice. *Military Medical Research*, 8(1). doi:https://doi.org/10.1186/s40779-021-00342-3.

193. Papavasiliou, F.N. and Schatz, D.G. (2002). Somatic hypermutation of immunoglobulin genes. *Cell*, 109(2), pp. S35–S44. https://doi.org/10.1016/s0092-8674(02)00706-7.

194. Parker, D.C. (1993). T Cell-Dependent B cell activation. *Annual Review of Immunology*, 11(1), pp. 331–360. https://doi.org/10.1146/annurev.iy.11.040193.001555.

195. Paydas, S. (2019). Management of adverse effects/toxicity of ibrutinib. *Critical Reviews in Oncology/Hematology*, 136, pp. 56–63.

196. Piqueras, B., Lavenu-Bombled, C., Galicier, L., F.Bergeron-Van Der Cruyssen, L. Mouthon, Chevret, S., Debré, P., Schmitt, C. and Oksenhendler, E. (2003). Common Variable Immunodeficiency Patient Classification Based on Impaired B Cell Memory Differentiation Correlates with Clinical Aspects. *Journal of Clinical Immunology*, 23(5), pp. 385–400. https://doi.org/10.1023/a:1025373601374.

197. Podjasek, J.C. and Abraham, R.S. (2012). Autoimmune Cytopenias In Common Variable Immunodeficiency. *Frontiers in Immunology*, 3. doi:https://doi.org/10.3389/fimmu.2012.00189.

198. Poeck, H., Wagner, M., Battiany, J., Rothenfusser, S., Wellisch, D., Hornung, V., Bernd Jahrsdörfer, Giese, T., Endres, S. and Hartmann, G. (2004). Plasmacytoid dendritic cells, antigen, and CpG-C license human B cells for plasma cell differentiation and immunoglobulin production in the absence of T-cell help. 103(8), pp.3058–3064. doi:https://doi.org/10.1182/blood-2003-08-2972

199. Pone, E.J., Zhang, J., Mai, T., White, C.A., Li, G., Sakakura, J.K., Patel, P.J., Al-Qahtani, A., Zan, H., Xu, Z. and Casali, P. (2012). BCR-signalling synergizes with TLR-signalling for induction of AID and immunoglobulin class-switching through the non-canonical NF-κB pathway. *Nature Communications*, [online] 3(1). doi:https://doi.org/10.1038/ncomms1769.

200. Ponsford, M., Castle, D., Tahir, T., Robinson, R., Wade, W., Steven, R., Bramhall, K., Moody, M., Carne, E., Ford, C., Farewell, D., Williams, P., El-Shanawany, T. and Jolles, S. (2019). Clozapine is associated with secondary

antibody deficiency. *The British Journal of Psychiatry*, [online] 214(2), pp.83–89. doi:https://doi.org/10.1192/bjp.2018.152.

201. Public Health England (2020). Disparities in the risk and outcomes of COVID-19. Available at: https://assets.publishing.service.gov.uk/media/5f328354d3bf7f1b12a7023a/Disparities_in_the_risk_and_outcomes_of_COVID_August_2020_update.pdf (Accessed: 1 April 2024).

202. Puissant-Lubrano B., Rostaing L., Kamar N., Abbal M., Fort M., Blancher A (2014). Impact of rituximab therapy on response to tetanus toxoid vaccination in kidney-transplant patients. *Experimental and clinical transplantation : official journal of the Middle East Society for Organ Transplantation*, [online] 8(1). Available at: https://pubmed.ncbi.nlm.nih.gov/20199367/ [Accessed 7 Oct. 2024].

203. Pulvirenti, F., Milito, C., Cavaliere, F.M., Mezzaroma, I., Cinetto, F. and Quinti, I. (2020). IGA Antibody Induced by Immunization With Pneumococcal Polysaccharides Is a Prognostic Tool in Common Variable Immune Deficiencies. *Frontiers in Immunology*, 11. doi:https://doi.org/10.3389/fimmu.2020.01283.

204. Rabia, L.A., Zhang, Y., Ludwig, S.D., Julian, M.C. and Tessier, P.M. (2018). Net charge of antibody complementarity-determining regions is a key predictor of specificity. *Protein Engineering, Design and Selection*, 31(11), pp.409–418. doi:https://doi.org/10.1093/protein/gzz002.

205. Rees, A.R. (2020). Understanding the human antibody repertoire. *mAbs*, 12(1), p.1729683. doi:https://doi.org/10.1080/19420862.2020.1729683.

206. Reimold, A.M., Iwakoshi, N.N., Manis, J., Vallabhajosyula, P., Szomolanyi-Tsuda, E., Gravallese, E.M., Friend, D., Grusby, M.J., Alt, F. and Glimcher, L.H. (2001). Plasma cell differentiation requires the transcription factor XBP-1. *Nature*, 412(6844), pp.300–307. doi:https://doi.org/10.1038/35085509.

207. Reljić, R., Wagner, S.D., Peakman, L.J. and Fearon, D.T. (2000). Suppression of Signal Transducer and Activator of Transcription 3–Dependent B Lymphocyte Terminal Differentiation by Bcl-6. *Journal of Experimental Medicine*, 192(12), pp.1841–1848. doi:https://doi.org/10.1084/jem.192.12.1841.

208. Resnick, E.S., Moshier, E.L., Godbold, J.H. and Cunningham-Rundles, C. (2011). Morbidity and mortality in common variable immune deficiency over 4 decades. *Blood*, [online] 119(7), pp.1650–1657. doi:https://doi.org/10.1182/blood-2011-09-377945.

209. Revy, P., Muto, T., Levy, Y., Geissmann, F., Plebani, A., Sanal, O., Catalan, N., Forveille, M., Dufourcq-Lagelouse, R., Gennery, A., Tezcan, I., Ersoy, F., Kayserili, H., Ugazio, A.G., Brousse, N., Muramatsu, M., Notarangelo, L.D., Kinoshita, K., Honjo, T. and Fischer, A. (2000). Activation-

Induced Cytidine Deaminase (AID) Deficiency Causes the Autosomal Recessive Form of the Hyper-IgM Syndrome (HIGM2). *Cell*, [online] 102(5), pp.565–575. doi:https://doi.org/10.1016/S0092-8674(00)00079-9.

210. Robbiani, D. F., Gaebler, C., Muecksch, F., Lorenzi, J. C. C., Wang, Z., Cho, A., Agudelo, M., Barnes, C. O., Gazumyan, A., Finkin, S., Hägglöf, T., Oliveira, T. Y., Viant, C., Hurley, A., Hoffmann, H. H., Millard, K. G., Kost, R. G., Cipolla, M., Gordon, K., ... Nussenzweig, M. C. (2020). Convergent antibody responses to SARS-CoV-2 in convalescent individuals. *Nature*, 584(7821), 437–442. https://doi.org/10.1038/s41586-020-2456-9

211. Rodríguez-Ubreva, J., Arutyunyan, A., Marc Jan Bonder, Lucía Del Pino-Molina, Clark, S.J., Carlos, Garcia-Alonso, L., Handfield, L.-F., Ciudad, L., Andrés-León, E., Krueger, F., Francesc Català-Moll, Rodríguez-Cortez, V.C., Polanski, K., Lira Mamanova, Stijn van Dongen, Vladimir Yu. Kiselev, Martínez-Saavedra, M.T., Heyn, H. and Martín, J. (2022). Single-cell Atlas of common variable immunodeficiency shows germinal center-associated epigenetic dysregulation in B-cell responses. *Nature Communications*, 13(1). doi:https://doi.org/10.1038/s41467-022-29450-x.

212. Rolink AG., Tschopp J., Schneider P., Melchers F (2024). BAFF is a survival and maturation factor for mouse B cells. *European journal of immunology*, [online] 32(7). doi:https://doi.org/10.1002/1521-4141(200207)32:7%3C2004::AID-IMMU2004%3E3.0.CO;2-5.

213. Roskin, K.M., Simchoni, N., Liu, Y., Lee, J.-Y., Seo, K., Hoh, R.A.,

214. Pham, T., Park, J.H., Furman, D., Dekker, C.L., Davis, M.M., James, J.A., Nadeau, K.C., Cunningham-Rundles, C. and Boyd, S.D. (2015). IgH sequences in common variable immune deficiency reveal altered B cell development and selection. *Science translational medicine*, [online] 7(302), p.302ra135. doi:https://doi.org/10.1126/scitranslmed.aab1216

215. Roth, K., Oehme, L., Zehentmeier, S., Zhang, Y., Niesner, R. and Hauser, A.E. (2013). Tracking plasma cell differentiation and survival. *Cytometry Part A*, 85(1), pp.15–24. doi:https://doi.org/10.1002/cyto.a.22355.

216. Rubelt, F., Sievert, V., Knaust, F., Langmann, C., Glanville, J., & Milholland, B. (2016). Characterization of human antibody repertoires through high-throughput sequencing: from phage display to deep sequencing. *mAbs*, 8(6), 1060-1070.

217. Ruschel, M. a. P. and Vaqar, S. (2023). *Common Variable Immunodeficiency*. https://www.ncbi.nlm.nih.gov/books/NBK549787/.

218. Salzer, U., Chapel, H.M., Webster, A.D.B., Pan-Hammarström, Q., Schmitt-Graeff, A., Schlesier, M., Peter, H.H., Rockstroh, J.K., Schneider, P., Schäffer, A.A., Hammarström, L. and Grimbacher, B. (2005). Mutations in TNFRSF13B encoding TACI are associated with common variable immunodeficiency in humans. *Nature Genetics*, 37(8), pp.820–828. doi:https://doi.org/10.1038/ng1600.

219. Sampalo, A. and Brieva, J.A. (2002). Humoral immunodeficiency in

chronic lymphocytic leukemia: Role of CD95/CD95L in tumoral damage and escape. *Leukemia & Lymphoma*, 43(4), pp. 881–884. https://doi.org/10.1080/10428190290017033.

220. Sanderson, R.D., Sneed, T.B., Young, L.A., Sullivan, G.L. and Lander, A.D. (1992). Adhesion of B lymphoid (MPC-11) cells to type I collagen is mediated by integral membrane proteoglycan, syndecan. *The Journal of Immunology*, 148(12), pp.3902–3911. doi:https://doi.org/10.4049/jimmunol.148.12.3902.

221. Sanz, I., Wei, C., Jenks, S.A., Cashman, K.S., Tipton, C., Woodruff, M.C., Hom, J. and Lee, F.E.-H. (2019). Challenges and Opportunities for Consistent Classification of Human B Cell and Plasma Cell Populations. *Frontiers in Immunology*, 10. doi:https://doi.org/10.3389/fimmu.2019.02458.

222. Schatz, D. G., & Swanson, P. C. (2011). V(D)J recombination: Mechanisms of initiation. *Annual Review of Genetics*, 45, 167-202.

223. Schatz, D.G., Oettinger, M.A. and Baltimore, D. (1989). The V(D)J recombination activating gene, RAG-1. *Cell*, 59(6), pp. 1035–1048. https://doi.org/10.1016/0092-8674(89)90760-5.

224. Schebesta, A., McManus, S., Salvagiotto, G., Delogu, A., Busslinger, G.A. and Busslinger, M. (2007). Transcription Factor Pax5 Activates the Chromatin of Key Genes Involved in B Cell Signaling, Adhesion, Migration, and Immune Function. *Immunity*, 27(1), pp.49–63. doi:https://doi.org/10.1016/j.immuni.2007.05.019.

225. Schickel, J.-N., Salomé Glauzy, Ng, Y.-S., Chamberlain, N., Massad, C., Isnardi, I., Katz, N., Uzel, G., Holland, S.M., Picard, C., Puel, A., Casanova, J.-L. and Meffre, E. (2017). Self-reactive VH4-34–expressing IgG B cells recognize commensal bacteria. *The Journal of Experimental Medicine*, [online] 214(7), pp.1991–2003. doi:https://doi.org/10.1084/jem.20160201.

226. Schlegel, B., Morikone, M., Mu, F., Tang, W.-Y., Kohanbash, G. and Dhivyaa Rajasundaram (2024). bcRflow: a Nextflow pipeline for characterizing B cell receptor repertoires from non-targeted transcriptomic data. *NAR Genomics and Bioinformatics*, 6(4). doi:https://doi.org/10.1093/nargab/lqae137.

227. Schmid, V.K., Khadour, A., Ahmed, N., Brandl, C., Nitschke, L., Rajewsky, K., Jumaa, H. and Hobeika, E. (2022). B cell receptor antigen receptor expression and phosphatidylinositol 3-kinase signaling regulate genesis and maintenance of mouse chronic lymphocytic leukemia. *Haematologica*. doi:https://doi.org/10.3324/haematol.2021.279924.

228. Schneider, P. (2005). The role of APRIL and BAFF in lymphocyte activation. *Current Opinion in Immunology*, 17(3), pp.282–289. doi:https://doi.org/10.1016/j.coi.2005.04.005.

229. Schroeder, H. and Cavacini, L. (2010). Structure and Function of

Immunoglobulins. *Journal of Allergy and Clinical Immunology*, 125(202).

230. Schultheiß, C., Paschold, L., Willscher, E., Donjete Simnica, Wöstemeier, A., Franziska Muscate, Wass, M., Eisenmann, S., Jochen Dutzmann, Gernot Keyßer, Gagliani, N. and Binder, M. (2021). Maturation trajectories and transcriptional landscape of plasmablasts and autoreactive B cells in COVID-19. *iScience*, 24(11), pp.103325–103325. doi:https://doi.org/10.1016/j.isci.2021.103325.

231. Setiadi, A.F. and Sheikine, Y. (2019). CD138-negative plasma cell myeloma: a diagnostic challenge and a unique entity. *BMJ Case Reports*, 12(11), p.e232233. doi:https://doi.org/10.1136/bcr-2019-232233.

232. Shaffer, A.L., Lin, K.-I., Kuo, T.C., Yu, X., Hurt, E.M., Rosenwald, A., Giltnane, J.M., Yang, L., Zhao, H., Calame, K. and Staudt, L.M. (2002). Blimp- 1 Orchestrates Plasma Cell Differentiation by Extinguishing the Mature B Cell Gene Expression Program. *Immunity*, 17(1), pp.51–62. doi:https://doi.org/10.1016/s1074-7613(02)00335-7

233. Shah, M., Gabel, A., Beers, S., Gratian Salaru, Lin, Y. and Cooper, D. (2022). COVID-19 Vaccine Responses in Patients With Plasma Cell Dyscrasias After Complete Vaccination. *Clinical Lymphoma, Myeloma & Leukemia*, 22(5), pp.e321–e326. doi:https://doi.org/10.1016/j.clmL.2021.11.001.

234. Sharma, M., Tyagi, S., Tripathi, P. and Seth, T. (2018). Syndecan-1 (sCD138) levels in chronic lymphocytic leukemia: clinical and hematological correlations. *Blood Research*, 53(3), p.205. doi:https://doi.org/10.5045/br.2018.53.3.205.

235. Shi, B., Dong, X., Ma, Q., Sun, S., Ma, L., Yu, J., Wang, X., Pan, J., He, X., Su, D. and Yao, X. (2020). The Usage of Human IGHJ Genes Follows a Particular Non-random Selection: The Recombination Signal Sequence May Affect the Usage of Human IGHJ Genes. *Frontiers in Genetics*, 11. doi:https://doi.org/10.3389/fgene.2020.524413.

236. Shields, A., Faustini, S., Hill, H.J., Al-Taei, S., Tanner, C., Ashford, F., *et al.* (2022b). Increased Seroprevalence and Improved Antibody Responses Following Third Primary SARS-CoV-2 Immunisation: An Update From the COV-AD Study. *Frontiers in Immunology*, 13. https://doi.org/10.3389/fimmu.2022.912571.

237. Shields, A., Faustini, S., Hill, H.J., Al-Taei, S., Tanner, C., Walder, S., *et al.* (2022a). SARS-CoV-2 Vaccine Responses in Individuals with Antibody Deficiency: Findings from the COV-AD Study. *Journal of Clinical Immunology*, 42(5), pp. 923–934. https://doi.org/10.1007/s10875-022-01231-7.

238. Shields, A., Venkatachalam, S., Shafeek, S., Paneesha, S., Ford, M., Sheeran, T., Kelly, M., Qureshi, I., Salhan, B., Karim, F et al (2022c). SARS-CoV-2 vaccine responses following CD20-depletion treatment in patients with haematological and rheumatological disease: a West Midlands Research Consortium study. *Clinical and Experimental Immunology*. **207** (1), 3-10.

239. Shields, A.M., Burns, S.O., Savic, S. and Richter, A.G. (2021). COVID-

19 in patients with primary and secondary immunodeficiency: The United Kingdom experience. *The Journal of Allergy and Clinical Immunology*, [online] 147(3), pp.870-875.e1. doi:https://doi.org/10.1016/j.jaci.2020.12.620.

240. Shinnakasu, R., Inoue, T., Kometani, K., Moriyama, S., Adachi, Y., Nakayama, M., Takahashi, Y., Fukuyama, H., Okada, T. and Kurosaki, T. (2016). Regulated selection of germinal-center cells into the memory B cell compartment. *Nature Immunology*, 17(7), pp.861–869. doi:https://doi.org/10.1038/ni.3460.

241. Shrimpton, J., Care, M.A., Carmichael, J., Walker, K., Evans, P., Evans, C., de Tute, R., Owen, R., Tooze, R.M. and Doody, G.M. (2020). TLR-mediated activation of Waldenström macroglobulinemia B cells reveals an uncoupling from plasma cell differentiation. *Blood advances*, [online] 4(12), pp.2821–2836. doi:https://doi.org/10.1182/bloodadvances.2019001279.

242. Sil, A., Basu, S., Joshi, V., Rakesh Kumar Pilania, Sangeetha Siniah, Suri, D., Rawat, A. and Singh, S. (2024). Immunoglobulin replacement therapies in inborn errors of immunity: a review. *Frontiers in Pediatrics*, 12. doi:https://doi.org/10.3389/fped.2024.1368755.

243. Simchoni, N. and Cunningham-Rundles, C. (2015). TLR7- and TLR9-Responsive Human B Cells Share Phenotypic and Genetic Characteristics. *The Journal of Immunology*, 194(7), pp.3035–3044. doi:https://doi.org/10.4049/jimmunol.1402690.

244. Simons, B.D. and Karin, O. (2024). Tuning of plasma cell lifespan by competition explains the longevity and heterogeneity of antibody persistence. *Immunity*, [online] 57(3), pp.600-611.e6. doi:https://doi.org/10.1016/j.immuni.2024.02.005.

245. Sims, G., Ettinger, R., Shirota, Y., Yarboro, C., Illei, G and Lipsky, P (2005). Identification and characterization of circulating human transitional B cells. *Blood*, 105(11), pp. 4390–4398. https://doi.org/10.1182/blood-2004-11-4284.

246. Sklenar, I., Schiffman, G., V. Jønsson, Verhoef, G., H. Birgens, M. Boogaerts, Ferrant, A., Christensen, B.E., H. Hasle, A. Drivsholm, Pedersen, R., N.A. Peterslund, Christensen, K.D., Hansen, N.E., J. Nikoskelainen, Lahtinen, R., Gardiner, D., Towse, G., S. Taesch and T. Jørgensen (1993). Effect of Various Doses of Intravenous Polyclonal IgG on in vivo Levels of 12 Pneumococcal Antibodies in Patients with Chronic Lymphocytic Leukaemia and Multiple Myeloma. *Oncology*, 50(6), pp.466–477. doi:https://doi.org/10.1159/000227231.

247. Smith, M.R. (2003). Rituximab (monoclonal anti-CD20 antibody): mechanisms of action and resistance. *Oncogene*, 22(47), pp. 7359–7368. https://doi.org/10.1038/sj.onc.1206939.

248. Smulski, C.R. and Eibel, H. (2018). BAFF and BAFF-Receptor in B Cell Selection and Survival. *Frontiers in Immunology*, 9. doi:https://doi.org/10.3389/fimmu.2018.02285.

249. Smulski, C.R., Kury, P., Seidel, L.M., Staiger, H.S., Edinger, A., Willen, L., Seidl, M., Hess, H.-D., Salzer, U., Rolink, A.G., Rizzi, M., Schneider, P. and Eibel, H. (2017). BAFF- and TACI-Dependent Processing of BAFFR by ADAM Proteases Regulates the Survival of B Cells. 18(9), pp.2189–2202. doi:https://doi.org/10.1016/j.celrep.2017.02.005

250. Snapper, C.M., Finkelman, F.D. and Paul, W.E. (1988). Regulation of IGG1 and IGE production by Interleukin 4. *Immunological Reviews*, 102(1), pp. 51–75. https://doi.org/10.1111/j.1600-065x.1988.tb00741.x.

251. Snapper, C.M., McIntyre, T.M., Mandler, R., Pecanha, L.M., Finkelman, F.D., Lees, A and Mond, J.J (1992). Induction of IgG3 secretion by interferon gamma: a model for T cell- independent class switching in response to T cell-independent type 2 antigens. *Journal of Experimental Medicine*, [online] 175(5), pp.1367–1371. doi:https://doi.org/10.1084/jem.175.5.1367.

252. Soto, C., Bombardi, R. G., Branchizio, A., & Costa, M. R. (2019a). High-throughput sequencing of the antibody repertoire in health and disease*. Immunity*, 50(2), 211-223.

253. Soto, C., Bombardi, R. G., Branchizio, A., Kose, N., Matta, P., Sevy, A. M., Sinkovits, R. S., & Crowe, J. E. (2019b). High frequency of shared clonotypes in human B cell receptor repertoires. *Nature*, 574(7779), 98–102.

254. Spegarova, S., J., Lawless, D., Mohamad, S.M.B., Engelhardt, K.R., Doody, G., Shrimpton, J., Rensing-Ehl, A., Ehl, S., Rieux-Laucat, F., Cargo, C., Griffin, H., Mikulasova, A., Acres, M., Morgan, N.V., Poulter, J.A., Sheridan, E.G., Chetcuti, P., O'Riordan, S., Anwar, R. and Carter, C.R. (2020). GermLine TET2 loss of function causes childhood immunodeficiency and lymphoma. *Blood*, [online] 136(9), pp.1055–1066. doi:https://doi.org/10.1182/blood.2020005844.

255. Srivastava, S. and Wood, P. (2016). Secondary antibody deficiency – causes and approach to diagnosis. *Clinical Medicine*, 16(6), pp. 571–576. https://doi.org/10.7861/clinmedicine.16-6-571.

256. States, D.J., Walseth, T.F. and Lee, H.C. (1992). Similarities in amino acid sequences of Aplysia ADP-ribosyl cyclase and human lymphocyte antigen CD38. *Trends in Biochemical Sciences*, 17(12), p. 495. https://doi.org/10.1016/0968-0004(92)90337-9.

257. Stebegg, M., Kumar, S.D., Silva-Cayetano, A., Fonseca, V.R., Linterman, M.A. and Graca, L. (2018). Regulation of the Germinal Center Response. *Frontiers in Immunology*, [online] 9, p.2469.

doi:https://doi.org/10.3389/fimmu.2018.02469.

258. Stephenson, S., Care, M.A., Doody, G.M. and Tooze, R.M. (2022). APRIL Drives a Coordinated but Diverse Response as a Foundation for Plasma Cell Longevity. *The Journal of Immunology*, 209(5), pp.926–937. doi:https://doi.org/10.4049/jimmunol.2100623.

259. Stephenson, S., Care, M.A., Fan, I., Alexandre Zougman, Westhead, D.R., Doody, G.M. and Tooze, R. (2019). Growth Factor–like Gene Regulation Is Separable from Survival and Maturation in Antibody-Secreting Cells. *Journal of Immunology*, 202(4), pp.1287–1300. doi:https://doi.org/10.4049/jimmunol.1801407.

260. Sterlin, D., Mathian, A., Miyara, M., Mohr, A., Anna, F., Claër, L., Quentric, P., Fadlallah, J., Devilliers, H., Ghillani, P., Gunn, C., Hockett, R., Mudumba, S., Guihot, A., Luyt, C.-E., Mayaux, J., Beurton, A., Fourati, S., Bruel, T. and Schwartz, O. (2021). IgA dominates the early neutralizing antibody response to SARS-CoV-2. *Science Translational Medicine*, [online] 13(577). doi:https://doi.org/10.1126/scitranslmed.abd2223.

261. Stewart, A., Ng, J.C.-F., Wallis, G., Tsioligka, V., Fraternali, F. and Dunn-Walters, D.K. (2021). Single-Cell Transcriptomic Analyses Define Distinct Peripheral B Cell Subsets and Discrete Development Pathways. *Frontiers in Immunology*, 12. doi:https://doi.org/10.3389/fimmu.2021.602539.

262. Stiehm, E.R. (2013). Adverse Effects of Human Immunoglobulin Therapy. *Transfusion Medicine Reviews*, 27(3), pp.171–178. doi:https://doi.org/10.1016/j.tmrv.2013.05.004.

263. Sun, D., Heimall, J., Greenhawt, M., Bunin, N., Shaker, M. and Romberg, N. (2021). Cost Utility of Lifelong Immunoglobulin Replacement Therapy vs Hematopoietic Stem Cell Transplant to Treat Agammaglobulinemia. *JAMA Pediatrics*, [online] 176(2), pp.176–176. doi:https://doi.org/10.1001/jamapediatrics.2021.4583.

264. Takasawa, S., Tohgo, A., Noguchi, N., Koguma, T., Nata, K., Sugimoto, T., Yonekura, H. and Okamoto, H. (1993). Synthesis and hydrolysis of cyclic ADP-ribose by human leukocyte antigen CD38 and inhibition of the hydrolysis by ATP. *The Journal of biological chemistry*, [online] 268(35), pp.26052–4. Available at: https://pubmed.ncbi.nlm.nih.gov/8253715/.

265. Tan, Y., Boribong, B., Swank, Z., Demokritou, M., Luban, M., Fasano, A., Du, M., Wolf, R., Griffiths, J., Shultz, J., Borgerg, E., Chalise, S., Gonzalez, W., Walt, D., Yonker, L and Horwitz, B (2024). COVID-19 mRNA vaccines induce robust levels of IgG but limited amounts of IgA within the oronasopharynx of young children [online]. [preprint]. Available from doi: https://doi.org/10.1101/2024.04.15.24305767

266. Tangye, S.G., Al-Herz, W., Bousfiha, A., Chatila, T., Cunningham-Rundles, C., Etzioni, A., Franco, J.L., Holland, S.M., Klein, C., Morio, T., Ochs, H.D., Oksenhendler, E., Picard, C., Puck, J., Torgerson, T.R., Casanova, J.-L. and Sullivan, K.E. (2020). Human Inborn Errors of Immunity: 2019 Update on the Classification from the International Union of Immunological Societies Expert Committee. *Journal of Clinical Immunology*, 40(1), pp.24–64. doi:https://doi.org/10.1007/s10875-019-00737-x.

267. Tangye, S.G., Al-Herz, W., Bousfiha, A., Cunningham-Rundles, C., Franco, J.L., Holland, S.M., Klein, C., Morio, T., Oksenhendler, E., Picard, C., Puel, A., Puck, J., Seppänen, M.R.J., Somech, R., Su, H.C., Sullivan, K.E., Torgerson, T.R. and Meyts, I. (2022). Human Inborn Errors of Immunity: 2022 Update on the Classification from the International Union of Immunological Societies Expert Committee. *Journal of Clinical Immunology*. doi:https://doi.org/10.1007/s10875-022-01289-3.

268. Tangye, S.G., Avery, D.T., Deenick, E.K. and Hodgkin, P.D. (2003). Intrinsic Differences in the Proliferation of Naive and Memory Human B Cells as a Mechanism for Enhanced Secondary Immune Responses. *The Journal of Immunology*, 170(2), pp.686–694. doi:https://doi.org/10.4049/jimmunol.170.2.686.

269. Tangye, S.G., Liu, Y.-J., Aversa, G., Phillips, J.H. and de Vries, J.E. (1998). Identification of Functional Human Splenic Memory B Cells by Expression of CD148 and CD27. *Journal of Experimental Medicine*, 188(9), pp.1691–1703. doi:https://doi.org/10.1084/jem.188.9.1691.

270. Taylor, J.J., Pape, K.A. and Jenkins, M.K. (2012). A germinal center– independent pathway generates unswitched memory B cells early in the primary response. *Journal of Experimental Medicine*, 209(3), pp. 597–606. https://doi.org/10.1084/jem.20111696.

271. Tedder, T.F. and Engel, P. (1994). CD20: a regulator of cell-cycle progression of B lymphocytes. *Immunology Today*, 15(9), pp. 450–454. https://doi.org/10.1016/0167-5699(94)90276-3.

272. Tellier, J., Ilariya Tarasova, Nie, J., Smillie, C.S., Fedele, P.L., Cao, W.H.J., Groom, J.R., Belz, G.T., Bhattacharya, D., Smyth, G.K. and Nutt, S.L. (2024). Unraveling the diversity and functions of tissue-resident plasma cells. *Nature Immunology*, [online] 25(2), pp.330–342. doi:https://doi.org/10.1038/s41590-023-01712-w.

273. Thien, M., Phan, T.G., Gardam, S., Amesbury, M., Basten, A., Mackay, F. and Brink, R. (2004). Excess BAFF Rescues Self-Reactive B Cells from Peripheral Deletion and Allows Them to Enter Forbidden Follicular and Marginal Zone Niches. *Immunity*, 20(6), pp.785–798. doi:https://doi.org/10.1016/j.immuni.2004.05.010

189. Thompson, J.S. (2001). BAFF-R, a Newly Identified TNF Receptor That Specifically Interacts with BAFF. *Science*, 293(5537), pp.2108–2111. doi:https://doi.org/10.1126/science.1061965.

190. Thompson, J.S., Schneider, P., Kalled, S.L., Wang, L., Lefevre, E.A., Cachero, T.G., MacKay, F., Bixler, S.A., Zafari, M., Liu, Z.-Y., Woodcock, S.A., Qian, F., Batten, M., Madry, C., Richard, Y., Benjamin, C.D., Browning, J.L., Tsapis, A., Tschopp, J. and Ambrose, C. (2000). Baff Binds to the Tumor Necrosis Factor Receptor–Like Molecule B Cell Maturation Antigen and Is Important for Maintaining the Peripheral B Cell Population. *Journal of Experimental Medicine*, 192(1), pp.129–136. doi:https://doi.org/10.1084/jem.192.1.129.

191. Tinhofer, I., Marschitz, I., Kos, M., Henn, T., Egle, A., Villunger, A. and Greil, R. (1998). Differential Sensitivity of CD4+ and CD8+T Lymphocytes to the Killing Efficacy of Fas (Apo-1/CD95) Ligand+ Tumor Cells in B Chronic Lymphocytic Leukemia. *Blood*, 91(11), pp.4273–4281. doi:https://doi.org/10.1182/blood.v91.11.4273.

192. Tonegawa, S. (1983). Somatic generation of antibody diversity. *Nature*, 302(5909), 575–581.

193. Tsubata, T. and Reth, M. (1990). The Products of Pre-B Cell-specific Genes (λ5 and V preB) and the Immunoglobulin μ Chain Form a Complex That Is Transported onto the Cell Surface. *Journal of Experimental Medicine*, 172, pp. 973–976.

194. UK Practice Guidelines for Variant Classification. (2024). *ACGS Best Practise Guidelines for Variant Classification in Rare Disease 2024*. Association for Clinical Genetic Science (ACGS). Available at: https://www.acgs.uk.com/media/12533/uk-practice-guidelines-for-variant-classification-v12-2024.pdf (Accessed: 1 October 2024).

195. Unger, S., Seidl, M., Schmitt-Graeff, A., Böhm, J., Schrenk, K., Wehr, C., Goldacker, S., Dräger, R., Gärtner, B.C., Fisch, P., Werner, M. and Warnatz, K. (2014). Ill-Defined Germinal Centers and Severely Reduced Plasma Cells are Histological Hallmarks of Lymphadenopathy in Patients with Common Variable Immunodeficiency. *Journal of Clinical Immunology*, 34(6), pp.615–626. doi:https://doi.org/10.1007/s10875-014-0052-1.

196. Upton, J. (2015). Immunodeficiencies with hypergammaglobulinemia: a review. *LymphoSign Journal*, 2(2), pp.57–73. doi:https://doi.org/10.14785/lpsn-2014-0019.

274. Vacca, A., Melaccio, A., Sportelli, A., Solimando, A.G., Dammacco, F. and Ria, R. (2018). Subcutaneous immunoglobulins in patients with multiple myeloma and secondary hypogammaglobulinemia: a randomized trial. *Clinical Immunology*, [online] 191, pp.110–115. doi:https://doi.org/10.1016/j.clim.2017.11.014.

275. Vale, A.M. and Schroeder, H.W. (2010). Clinical Consequences of Defects in B cell Development. *The Journal of allergy and clinical immunology*, [online] 125(4), pp.778–787.

doi:https://doi.org/10.1016/j.jaci.2010.02.018.

276. Van Dongen, J.J.M., Langerak, A.W., Brüggemann, M., Evans, P.A.S., Hummel, M., Lavender, F.L., Delabesse, E., Davi, F., Schuuring, E., García- sa, R., van Krieken, J.H.J.M., Droese, J., González, D., Bastard, C., White, H.E., Spaargaren, M., González, M., Parreira, A., Smith, J.L. and Morgan,
G.J. (2003). Design and standardization of PCR primers and protocols for detection of clonal immunoglobulin and T-cell receptor gene recombinations in suspect lymphoproliferations: Report of the BIOMED-2 Concerted Action BMH4-CT98-3936. *Leukemia*, 17(12), pp.2257–2317. doi:https://doi.org/10.1038/sj.leu.2403202.

277. Varughese, T., Taur, Y., Cohen, N., Palomba, M.L., Seo, S.K., Hohl, T.M. and Redelman-Sidi, G. (2018). Serious Infections in Patients Receiving Ibrutinib for Treatment of Lymphoid Cancer. *Clinical Infectious Diseases: An Official Publication of the Infectious Diseases Society of America*, [online] 67(5), pp.687–692. doi:https://doi.org/10.1093/cid/ciy175.

278. Victora, G.D., Schwickert, T.A., Fooksman, D.R., Kamphorst, A.O., Meyer-Hermann, M., Dustin, M.L. and Nussenzweig, M.C. (2010). Germinal center dynamics revealed by multiphoton microscopy with a photoactivatable fluorescent reporter. *Cell*, [online] 143(4), pp.592–605. doi:https://doi.org/10.1016/j.cell.2010.10.032.

279. Vidarsson, G., Dekkers, G. and Rispens, T. (2014). IGG subclasses and allotypes: From structure to effector functions. *Frontiers in Immunology*, 5. https://doi.org/10.3389/fimmu.2014.00520.

280. Vigorito, E., Perks, K.L., Abreu-Goodger, C., Bunting, S., Xiang, Z., Kohlhaas, S., Das, P.P., Miska, E.A., Rodriguez, A., Bradley, A., Smith, K.G.C., Rada, C., Enright, A.J., Toellner, K.-M., MacLennan, I.C.M. and Turner, M. (2007). microRNA-155 Regulates the Generation of Immunoglobulin Class-Switched Plasma Cells. *Immunity*, [online] 27(6), pp.847–859. doi:https://doi.org/10.1016/j.immuni.2007.10.009

281. Vincent, F.B., Saulep-Easton, D., Figgett, W.A., Fairfax, K.A. and Mackay, F. (2013). The BAFF/APRIL system: Emerging functions beyond B cell biology and autoimmunity. *Cytokine & Growth Factor Reviews*, [online] 24(3), pp.203–215. doi:https://doi.org/10.1016/j.cytogfr.2013.04.003.

282. Vos, Q., Lees, A., Wu, Z., Snapper, C and Mond, JJ (2000). B-cell activation by T-cell-independent type 2 antigens as an integral part of the humoral immune response to pathogenic microorganisms. *Immunological Reviews*, 176(1), pp.154–170. doi:https://doi.org/10.1034/j.1600-065x.2000.00607.x.

283. Walker, K., Mistry, A., Watson, C.M., Nadat, F., O'Callaghan, E., Care, M., Crinnion, L.A., Arumugakani, G., Bonthron, D.T., Carter, C., Doody, G.M.

and Savic, S. (2023). Inherited CD19 Deficiency Does Not Impair Plasma Cell Formation or Response to CXCL12. *Journal of Clinical Immunology*, 43(7), pp.1543–1556. doi:https://doi.org/10.1007/s10875-023-01511-w.

284. Wang, J., Yan, Y., Xiong, W., Song, G., Wang, Y., Zhao, J., Jia, Y., Li, C., Yu, Z., Yu, Y., Chen, J., Jiao, Y., Wang, T., Lyu, R., Li, Q., Ma, Y., Liu, W., Zou, D., An, G. and Sun, Q. (2022). Landscape of immunoglobulin heavy chain gene repertoire and its clinical relevance to LPL/WM. *Blood Advances*, [online] 6(13), pp.4049–4059. doi:https://doi.org/10.1182/bloodadvances.2022007279.

285. Wang, K., Wei, G. and Liu, D. (2012). CD19: a biomarker for B cell development, lymphoma diagnosis and therapy. *Experimental Hematology & Oncology*, [online] 1(1), p.36. doi:https://doi.org/10.1186/2162-3619-1-36.

286. Wardemann, H. (2003). Predominant Autoantibody Production by Early Human B Cell Precursors. *Science*, 301(5638), pp.1374–1377. doi:https://doi.org/10.1126/science.1086907.

287. Warnatz, K., Denz, A., Dräger, R., Braun, M., Groth, C., Wolff-Vorbeck, G., Eibel, H., Schlesier, M. and Peter, H.H. (2002). Severe deficiency of switched memory B cells (CD27+IgM−IgD−) in subgroups of patients with common variable immunodeficiency: a new approach to classify a heterogeneous disease. *Blood*, [online] 99(5), pp.1544–1551. doi:https://doi.org/10.1182/blood.V99.5.1544.

288. Warnatz, K., Salzer, U., Rizzi, M., Fischer, B., Gutenberger, S., Joachim Böhm, Kienzler, A.-K., Qiang Pan-Hammarström, Lennart Hammarström, Mirzokhid Rakhmanov, Schlesier, M., Bodo Grimbacher, Peter, H.-H. and Eibel, H. (2009). B-cell activating factor receptor deficiency is associated with an adult-onset antibody deficiency syndrome in humans. 106(33), pp.13945–13950. doi:https://doi.org/10.1073/pnas.0903543106

289. Wehr, C., Kivioja, T., Schmitt, C., Ferry, B., Witte, T., Eren, E., Vlkova, M., Hernandez, M., Detkova, D., Bos, P.R., Poerksen, G., von Bernuth, H., Baumann, U., Goldacker, S., Gutenberger, S., Schlesier, M., Bergeron-van der Cruyssen, F., Le Garff, M., Debré, P. and Jacobs, R. (2008). The EUROclass trial: defining subgroups in common variable immunodeficiency. *Blood*, [online] 111(1), pp.77–85. doi:https://doi.org/10.1182/blood-2007-06-091744.

290. Wilmore, J.R., Gaudette, B.T., Gómez, D., Rosenthal, R., Reiser, S.J., Meng, W., Rosenfeld, A.M., Eline and Allman, D. (2021). IgA Plasma Cells Are Long-Lived Residents of Gut and Bone Marrow That Express Isotype- and Tissue-Specific Gene Expression Patterns. 12. doi:https://doi.org/10.3389/fimmu.2021.791095.

291. Winkler, T. and Mårtensson, I. (2018). The role of the Pre-B cell receptor in B cell development, repertoire selection, and tolerance. *Frontiers in Immunology*, 9. https://doi.org/10.3389/fimmu.2018.02423.

292. Wisnewski, A.V., Campillo Luna, J. and Redlich, C.A. (2021). Human IgG and IgA responses to COVID-19 mRNA vaccines. *PLOS ONE*, 16(6), p.e0249499. doi:https://doi.org/10.1371/journal.pone.0249499.

293. Wong, M.K., Liu, J.T., Budylowksi, P., Yue, F.Y., Li, Z., Rini, J.M., Carlyle, J.R., Zia, A., Ostrowski, M. and Martin, A. (2022). Convergent CDR3 homology amongst Spike-specific antibody responses in convalescent COVID-19 subjects receiving the BNT162b2 vaccine. *Clinical Immunology*, [online] 237, p.108963. doi:https://doi.org/10.1016/j.clim.2022.108963.

294. Wood, P. (2009). Primary antibody deficiencies: recognition, clinical diagnosis and referral of patients. *Clinical Medicine*, 9(6), pp. 595–599. https://doi.org/10.7861/clinmedicine.9-6-595.

295. Woodruff, M.C., Ramonell, R.P., Haddad, N.S., Anam, F., Rudolph, M.E., Walker, T., Truong, A.D., Dixit, A.N., Han, J.E., Mónica Cabrera-Mora, Runnstrom, M., Bugrovsky, R., Hom, J., Connolly, E.C., Igor Albizua, Vidhi Javia, Cashman, K.S., Nguyen, D.C., Kyu, S. and Saini, A. (2022). Dysregulated naive B cells and de novo autoreactivity in severe COVID-19. *Nature*, 611(7934), pp.139–147. doi:https://doi.org/10.1038/s41586-022-05273-0.

296. Wu, B., Rice, L., Shrimpton, J., Lawless, D., Walker, K., Carter, C., McKeown, L., Anwar, R., Doody, G.M., Srikanth, S., Gwack, Y. and Savic, S. (2021). Biallelic mutations in calcium release activated channel regulator 2A (CRACR2A) cause a primary immunodeficiency disorder. *eLife*, 10. doi:https://doi.org/10.7554/elife.72559.

197. Xie, X., Shrimpton, J., Doody, G.M., Conaghan, P.G. and Ponchel, F. (2021). B-cell capacity for differentiation changes with age. *Aging Cell*, 20(4). doi:https://doi.org/10.1111/acel.13341.

198. Xu, J.L. and Davis, M.M. (2000). Diversity in the CDR3 Region of VH Is Sufficient for Most Antibody Specificities. *Immunity*, 13(1), pp.37–45. doi:https://doi.org/10.1016/s1074-7613(00)00006-6.

199. Yaari, G. and Kleinstein, S.H. (2015). Practical guidelines for B-cell receptor repertoire sequencing analysis. *Genome Medicine*, 7(1). doi:https://doi.org/10.1186/s13073-015-0243-2.

200. Yoshinaga, M. and Takeuchi, O. (2019). Post-transcriptional control of immune responses and its potential application. *Clinical & Translational Immunology*, 8(6). doi:https://doi.org/10.1002/cti2.1063.

188. Yu, J.E. (2023). New primary immunodeficiencies 2023 update. *Current Opinion in Pediatrics*, 36(1), pp. 112–123. https://doi.org/10.1097/mop.0000000000001315.

189. Yuan, H., Wang, Y., Wu, X., Wang, H., Pu, J., Ding, W., Wang, M., Shen, X., Cong, H., Zhang, L., Zhang, M. and Ju, S. (2010). Characterization of the 5′-Flanking Region and Regulation of Transcription of Human BAFF-R Gene. *DNA and Cell Biology*, 29(3), pp.133–139.

doi:https://doi.org/10.1089/dna.2009.0927.

190. Yue, X., Bai, C., Xie, D., Ma, T. and Zhou, P.-K. (2020). DNA-PKcs: A Multi-Faceted Player in DNA Damage Response. *Frontiers in Genetics*, [online] 11, p.607428. doi:https://doi.org/10.3389/fgene.2020.607428.

191. Yuseff, M.-I., Pierobon, P., Reversat, A. and Lennon-Duménil, A.-M. (2013). How B cells capture, process and present antigens: a crucial role for cell polarity. *Nature Reviews Immunology*, [online] 13(7), pp.475–486. doi:https://doi.org/10.1038/nri3469.

192. Zhang, F., Shu, J.-L., Li, Y., Wu, Y.-J., Zhang, X.-Z., Han, L., Tang, X.-Y., Wang, C., Wang, Q.-T., Chen, J.-Y., Chang, Y., Wu, H.-X., Zhang, L.-L. and Wei, W. (2017). CP-25, a Novel Anti-inflammatory and Immunomodulatory Drug, Inhibits the Functions of Activated Human B Cells through Regulating BAFF and TNF-alpha Signaling and Comparative Efficacy with Biological Agents. *Frontiers in Pharmacology*, 8. doi:https://doi.org/10.3389/fphar.2017.00933.

193. Zhao, J.C., Li, X., Guo, M., Yu, J. and Yan, C. (2016). The common stress responsive transcription factor ATF3 binds genomic sites enriched with p300 and H3K27ac for transcriptional regulation. 17(1). doi:https://doi.org/10.1186/s12864-016-2664-8.

194. Zheng, B., Yang, Y., Chen, L., Wu, M. and Zhou, S. (2022). B-cell receptor repertoire sequencing: Deeper digging into the mechanisms and clinical aspects of immune-mediated diseases. *iScience*, [online] 25(10), p.105002. doi:https://doi.org/10.1016/j.isci.2022.105002.

195. Zhou, L.-J., Ord, David, C., Omori, SidneA. and Tedder, ThomasF. (1992). Structure of the genes encoding the CD19 antigen of human and mouse B lymphocytes. *Immunogenetics*, 35(2). doi:https://doi.org/10.1007/bf00189519